UNIVERSIDADE FEDERAL DE PERNAMBUCO
CENTRO DE BIOCIÊNCIAS
DEPARTAMENTO DE GENÉTICA
PROGRAMA DE PÓS-GRADUAÇÃO EM GENÉTICA

LÍVIA DO VALE MARTINS

MAPEAMENTO COMPARATIVO ENTRE ESPÉCIES DE *VIGNA* SAVI E *PHASEOLUS VULGARIS* L. MEDIANTE BAC- E OLIGO-FISH

Recife
2020

LÍVIA DO VALE MARTINS

MAPEAMENTO COMPARATIVO ENTRE ESPÉCIES DE *VIGNA* SAVI E *PHASEOLUS VULGARIS* L. MEDIANTE BAC- E OLIGO-FISH

Tese apresentada ao Programa de Pós-Graduação em Genética da Universidade Federal de Pernambuco, como requisito parcial para a obtenção do título de doutora em Genética.

Área de concentração: Evolução.

Orientadora: Profª. Drª. Ana Christina Brasileiro-Vidal

Coorientadoras: Profª. Drª. Andrea Pedrosa-Harand
Profª. Drª. Lidiane de Lima Feitoza

.

Recife

2020

Catalogação na fonte:
Bibliotecária Claudina Queiroz, CRB4/1752

Martins, Lívia do Vale
Mapeamento comparativo entre espécies de *Vigna savi* e *Phasolus vulgaris* L. Mediante BAC- e oligo-FISH / Lívia do Vale Martins - 2020.
143 folhas: il., fig., tab.

Orientadora: Ana Christina Brasileiro-Vidal
Coorientadoras: Andrea Pedrosa-Harand
Lidiane de Lima Feitoza
Tese (doutorado) – Universidade Federal de Pernambuco. Centro de Biociências. Programa de Pós-Graduação em Genética. Recife, 2020.

Inclui referências e apêndices.

1. Feijão 2. *Genética vegetal* 3. Citogenética
I. Brasileiro-Vidal, Ana Cristina (Orientadora) II. Pedrosa-Harand, Andrea (Coorientadora) III. Feitoza, Lidiane de Lima (Coorientadora) IV.Título

581.35 CDD (22.ed.) UFPE/CB-2020-199

LÍVIA DO VALE MARTINS

MAPEAMENTO COMPARATIVO ENTRE ESPÉCIES DE *VIGNA* SAVI E *PHASEOLUS VULGARIS* L. MEDIANTE BAC- E OLIGO-FISH

Tese apresentada ao Programa de Pós-Graduação em Genética da Universidade Federal de Pernambuco, como requisito parcial para a obtenção do título de doutora em Genética.

Aprovada em 19/02/2020.

BANCA EXAMINADORA

_____
Profª. Drª. Ana Christina Brasileiro-Vidal (Orientadora)
Universidade Federal de Pernambuco

_____
Profª. Drª. Ana Maria Benko-Iseppon (Examinadora Interna)
Universidade Federal de Pernambuco

_____
Drª. Mariana Alejandra Baez (Examinadora Externa)
Universidade Federal de Pernambuco

_____
Prof. Dr. Luiz Gustavo Rodrigues Souza (Examinador Externo)
Universidade Federal de Pernambuco

_____
Prof. Dr. Reginaldo de Carvalho (Examinador Externo)
Universidade Federal Rural de Pernambuco

AGRADECIMENTOS

A Deus, energia superior que nos rege, por colocar em minha vida pessoas essenciais ao meu constante crescimento pessoal e profissional;

À Universidade Federal de Pernambuco e ao Programa de Pós-Graduação em Genética, pela oportunidade de ingresso ao doutorado acadêmico;

À CAPES, pela concessão das bolsas de estudos no Brasil e no exterior;

Aos meus pais, Aníbal e Lúcia, aos meus irmãos, Ismar e Lígia, e aos meus sobrinhos, Pedro e Theo, pelo laço familiar eterno e por me mostrarem o real significado das palavras família, amor incondicional e amizade. Obrigada pelo suporte diário e pelos exemplos de união, força e caráter;

À minha orientadora Prof[a.] Dr[a]. Ana Christina Brasileiro Vidal, pela impecável orientação, pelo aprendizado, pela oportunidade de crescimento profissional e pela amizade. Você é um exemplo de integridade, coerência e excelência profissional, sem perder o lado humano e positivo da vida;

Ao meu orientador estrangeiro, Prof. Dr. Jiming Jiang, pela oportunidade divisora de águas que me foi dada, pela confiança, pelas críticas construtivas e por me incentivar a buscar o melhor, sempre;

À minha coorientadora Prof[a.] Dr[a.] Andrea Pedrosa Harand, pelo exemplo profissional, pelos ensinamentos e por modificar e expandir o meu olhar acerca da pesquisa científica;

À minha coorientadora Lidiane de Lima Feitoza, por me introduzir à citogenética, por exigir de mim o melhor, por sua amizade e por sempre acreditar em mim;

À Prof[a.] Dr[a.] Ana Maria Benko Iseppon, pelo suporte e incentivo à pesquisa e à vida acadêmica e por ser um grande exemplo profissional e ético para todos nós;

Á minha segunda família, Artemisa, Anita, Carol, Jéssica Bárbara, Jéssica Resende e à nossa agregada, Mari Firmino. Obrigada pela amizade, companheirismo e risadas e, principalmente, pela união, irmandade e pelo laço criado durante esses 4 anos. Eu não conseguiria sem vocês;

Ao grupo de Citogenética do LGBV, especialmente às minhas amigas e companheiras de trabalho, Fernanda e Rafa, por todo o aprendizado compartilhado e pela grande equipe que nos tornamos. Eu não conseguiria sem vocês. Á Manu,

Geyse, Sibelle, Victor e Marcos, com quem, apesar de não ter trabalhado diretamente, sempre se fizeram presentes;

Ao meu colega de trabalho e amigo, Guilherme, por repassar todo o seu conhecimento a mim, pelo companheirismo, por vibrar com minhas vitórias, por estar sempre presente, do primeiro ao último dia da minha estada em Michigan;

Aos meus amigos e colegas de trabalho do Laboratório de Citogenética da UFPE e da Universidade do Estado de Michigan, em especial, ao Will, Joelson, Lynn e Sarah, pelo acolhimento durante esses anos. Obrigada por suavizarem a rotina estressante e cansativa da pós-graduação em momentos de leveza e riso;

Aos meus amigos de longa e recente data que estão espalhados pelo Brasil e no mundo, em especial, à minha amiga de infância, Andrea. Obrigada por não tornarem a distância física um empecilho, pelas risadas, pelos momentos e viagens inesquecíveis, e por contribuírem com o que sou hoje;

Finalmente, agradeço a todos que, direta ou indiretamente, contribuíram para a finalização desse ciclo.

*“*Para ser grande, sê inteiro: nada teu exagera ou exclui. Sê todo em cada coisa. Põe quanto és no mínimo que fazes. Assim em cada lago a lua toda brilha, porque alta vive” (PESSOA, 1933).

RESUMO

A família Leguminosae compreende um grupo de plantas de distribuição cosmopolita e de grande importância socioeconômica mundial, com destaque para os feijões pertencentes aos gêneros *Vigna* e *Phaseolus*. Para uma melhor compreensão da evolução cromossômica entre os gêneros, mapas físicos para *V. angularis* (*Va*) e *V. aconitilofia* (*Vac*), subgênero *Ceratotropis*, foram construídos e comparados a *V. unguiculata* (*Vu*, subgênero *Vigna*) e *P. vulgaris* (*Pv*). BACs de *Vu*, *Pv* e DNAs ribossomais foram mapeados nos 11 pares cromossômicos dessas espécies. Além disso, sondas de pintura oligo-específicas foram desenvolvidas para *Pv*2 e *Pv*3, dois dos cromossomos mais envolvidos em rearranjos entre *Vu* e *Pv*, e hibridizadas nos ortólogos de *Va* e *Vu*. O mapeamento comparativo revelou alta conservação de macrossintenia envolvendo cinco cromossomos (6, 7, 9, 10 e 11) de *Vigna* sp. e *Pv*. Duas translocações recíprocas (cromossomos 2 e 3; 1 e 8) foram confirmadas entre espécies de *Vigna* e *Pv* (~9,7 milhões de anos de divergência). Duas inversões (2 e 4) e uma translocação (1 e 5) ocorreram após a separação dos subgêneros *Ceratotropis* e *Vigna* (3,6 milhões de anos). Diferentes oligopinturas para os cromossomos 2 e 3 de *Va* e *Vu* foram observadas, com diferentes pontos de quebra confirmados para *Va*2 e *Vu*2. Ambas as espécies de *Vigna* compartilham macrorearranjos cromossômicos similares quanto a *Pv*: uma translocação (2 e 3) e uma inversão (3). A análise de sintenia revelou inversões e/ou transposições adicionais nas regiões pericentroméricas dos cromossomos 2 e 3, sendo considerados *hotspots* de rearranjos cromossômicos dentro e entre gêneros. Para o cromossomo 2, um evento de reposicionamento de centrômero é proposto durante a evolução de *Vigna*. O mapeamento BAC- e oligo-FISH forneceu informações detalhadas acerca da macrossintenia e evolução cromossômica entre e dentro *Vigna* e *Phaseolus*, fornecendo subsídios para futuros estudos evolutivos dessas leguminosas economicamente importantes.

Palavras-chave: BAC-FISH. Evolução. Oligopinturas. Rearranjos cromossômicos. Sintenia.

ABSTRACT

The Leguminosae family comprises a group of plants worldwide distributed with great socioeconomic importance, highlighting the beans belonging to *Vigna* and *Phaseolus* genera. To a better understanding of the chromosome evolution between genera, we established the physical mapping of *V. angularis* (*Va*) and *V. aconitifolia* (*Vac)*, both belonging to *Ceratotropis* subgenus, and compared with *V. unguiculata* (*Vu*, *Vigna* subgenus) and *P. vulgaris* (*Pv*). We comparatively mapped *Vu* and *Pv* BACs, and ribosomal DNA probes to the 11 chromosome pairs of each species. Furthermore, we developed oligo-based painting probes for *Pv*2 and *Pv*3, the two of the chromosomes most involved in rearrangements between *Vu* and *Pv* and hybridized on *Va* and *Vu* orthologs. Our comparative mapping revealed high conservation of synteny involving five chromosomes (6, 7, 9, 10 and 11) among *Vigna* species and *Pv*. Two reciprocal translocations (chromosomes 2 and 3; 1 and 8) were confirmed among *Vigna* species and *Pv* (~9.7 million years of divergence). Two inversions (2 and 4) and one translocation (1 and 5) have occurred after *Ceratotropis* e *Vigna* subgenera separation (3.6 million years). We observed distinct oligopainting patterns for chromosomes 2 and 3 of *Va* and *Vu*, with different breakpoints confirmed for *Va*2 and *Vu*2. Both *Vigna* species shared similar major chromosomal rearrangements with *Pv*: one translocation (2 and 3) and one inversion (3). The synteny analysis revealed additional inversions and/or transpositions in the pericentromeric regions of chromosomes 2 and 3, being considered as *hotspots* of chromosomal rearrangements within and between genera. We propose a centromere repositioning event for chromosome 2 during *Vigna* evolution. Our BAC- and oligo-FISH mapping provided detailed information about the macrosynteny and chromosome evolution between and within *Vigna* and *Phaseolus*, providing aids for future evolutionary studies of these economically important legumes.

Keywords: BAC-FISH. Evolution. Oligopainting. Chromosomal rearrangements. Sinteny.

LISTRA DE FIGURAS

Revisão de Literatura

Artigo 1

LISTA DE TABELAS

Artigo 1

LISTA DE ABREVIATURAS E SIGLAS

5-Mc	5-Methylcytosine; 5-Metilcitosina
8-HQ	8-Hydroxyquinoline; 8-Hidroxiquinoleína
A - T	Adenina – Timina
AFLP	Amplified Fragment Length Polymorphism; Polimorfismo de Comprimento de Fragmento Amplificado
APG	The Angiosperm Phylogeny Group; Grupo de Filogenia das Angiospermas
BAC	Bacterial Artificial Chromosome; Cromossomo Artificial de Bactéria
Bc	BAC clone; Clone de BAC
BESs	BAC-End Sequences; Sequências Terminais de BACs
Bngs	Bean genomic clones; Clones genômicos de feijões
bp/ pb	Base pair; Pares de bases
BSA	Bovine Serum Albumin; Albumina de Soro Bovino
C	DNA content; Conteúdo de DNA
CAPES	Coordenação de Aperfeiçoamento de Pessoal de Nível Superior
cM	Centimorgan
CMA	Chromomycin A_3; Cromomicina A_3
CNPq	Conselho Nacional de Desenvolvimento Científico e Tecnológico
CP/ PC	Chromosome Painting; Pintura Cromossômica
cv.	Cultivar
Cy3	Cyanine 3; Cianina 3
DAPI	4’,6-diamidino-2-phenylindole; 4’,6-diamidino-2-fenilindol
DNA	Desoxiribonucleic Acid; Ácido Desoxirribonucleico

DNAr	Ribosomal DNA; DNA ribossomal
dsDNA	double stranded DNA; DNA fita dupla
dUTP	deoxyuridine Triphosphate; Desoxiuridina Trifosfato
Embrapa	Empresa Brasileira de Pesquisa Agropecuária
EST	Expressed Sequence Tag; Etiqueta de Sequência Expressa
FACEPE	Fundação de Amparo à Ciência e Tecnologia do Estado de Pernambuco
FAO	Food and Agriculture Organization; Organização das Nações Unidas para Agricultura e Alimentação
FISH	Fluorescen*t In Situ* Hybridization*;* Hibridização *In Situ* Fluorescente
FITC	Fluorecein Isotiocianate; Fluoresceína Isotiocianato
G - C	Guanina – Citosina
GISH	Genomic *In Situ* Hybridization*;* Hibridização Genômica *In Situ*
ha	Hectares
HC	Heterocromatina Constitutiva
IBM	Intermated B73 x Mo17; Linhagens Endogâmicas Recombinantes entre B73 x Mo17
IGS	Intergenic Spacer; Espaçador Intergênico
IPA	Instituto Agronômico de Pernambuco
IPK	Leibniz Institute of Plant Genetics and Crop Plant Research; Instituto de Pesquisa de Genética de Plantas Cultivadas em Leibniz
ITS	Internal Transcribed Spacer; Espaçador Interno Transcrito
kb	Kilobases; quilobases
kg	Kilograms; quilogramas

LG/ GL	Linkage Group; Grupo de Ligação
LPGW	Legume Phylogeny Working Group
Ma	Milhões de anos
LTR	Long Terminal Repeat; Longa Repetição Terminal
Matk	Cloroplastidial maturase K gene; gene cloroplastidial maturase K
Mb	Megabase pair; Mega pares de bases
mM	Millimolar
Mya	Million years ago; Milhões de anos atrás
µm	micrometer; micrômetro
ng	nanogram; nanograma
NG	Next Generation; Nova Geração
NGS	Next Generation Sequencing; Sequenciamento de Nova Geração
oligos	oligonucleotides; oligonucleotídeos
PAV	Presence/ Abscence Variation; Presença/ Ausência de Variação
Pv	*Phaseolus vulgaris*
QTLs	Quantitative Trait *Loci; Loci* de Características Quantitativas
RAPD	Random Amplified Polymorphic DNA; Fragmento de DNA Amplificado ao Acaso
rbcL	ribulose-bisphosphate carboxylase gene; gene da ribulose-bifosfato carboxilase
RFLP	Restriction Fragment Length Polymorphism; Polimorfismo de Comprimento de Fragmento de Restrição
RGA	Resistance Gene Analog; Gene Análogo de rResistência
RIL	Recombinant Inbred Line; Linhagem Endogâmica Recombinante
RONs	Regiões Organizadoras de Nucléolo
SMRT	Single-Molecule Real-Time sequencing; Sequenciamento de Molécula Simples em Tempo Real

SNPs	Single Nucleotide Polymorphisms; Polimorifsmos de Nucleotideo Único
SSC	Citric acid–Sodium Citrate buffer; Tampão Citrato de Sódio-Salino
ssDNA	single stranded DNA; DNA fita simples
SSR	Simple Sequence Repeat; Sequência Curta Repetida
t	tonelada métrica
TRITC	Tetramethylrhodamine; Tetramethylrhodamina
trnK	chloroplast gene/ intergenic spacer; marcador molecular cloroplastidial intrônico
USDA	United States Department of Agriculture; Departamento de Agricultura dos Estados Unidos
Va	*Vigna angularis*
Vac	*Vigna aconitifolia*
Vu	*Vigna unguiculata*
WGS	Whole Genome Sequencing; Sequenciamento do Genoma Total
YACs	Yeast Artificial Chromosome; Cromossomo Artificial de Levedura

SUMÁRIO

1 INTRODUÇÃO

Vigna Savi e *Phaseolus* L. apresentam espécies de ampla distribuição e de grande importância socioeconômica mundial. *Phaseolus vulgaris* L. (feijão comum) é a espécie de maior importância econômica do gênero. Em *Vigna*, destacam-se: *V. angularis* (Willd.) Ohwi & H. Ohashi (feijão adzuki) e *V. aconitifolia* (Jacq.) Maréchal (feijão-traça), de origem asiática, subgênero *Ceratotropis*; e *V. ungiculata* (L.) Walp (feijão-caupi), de origem africana, subgênero *Vigna*. Atualmente, essas espécies possuem mapas genéticos e/ou genomas sequenciados e disponíveis, com exceção de *V. aconitifolia,* cujo sequenciamento do genoma está em progresso.

A disponibilidade do genoma montado, suportada pelos mapas genéticos prévios, acelerou os estudos genômicos comparativos na subtribo Phaseolinae. Nesse contexto, a técnica de BAC-FISH (Hibridização *In Situ* Fluorescente de Cromossomos Artificiais de Bactérias) tem se mostrado uma ferramenta valiosa para estudos de macrossintenia, de evolução cromossômica e de organização genômica entre as espécies desses gêneros. Além disso, a pintura cromossômica baseada na síntese *de novo* de milhares de oligonucleotídeos (oligos) utilizados como sondas em FISH (Oligo-FISH) tem permitido a identificação de cromossomos/rearranjos cromossômicos de maneira mais precisa e eficaz. Ambas as técnicas permitem identificar os principais rearranjos cromossômicos entre grupos e espécies relacionadas, inferindo acerca dos seus processos evolutivos.

Em *Phaseolus*, o primeiro mapa citogenético foi descrito para *P. vulgaris,* mediante abordagem BAC-FISH. Posteriormente, esse mapa foi comparado a outras espécies do gênero, como *P. lunatus* L., *P. microcarpus* Mart. e *P. leptostachyus* Benth (Bonifácio et *al.*, 2012; Almeida e Pedrosa-Harand, 2013; Fonsêca e Pedrosa-Harand, 2013; Fonsêca et *al.,* 2016). De maneira geral, foi observado um alto grau de macrossintenia dentro do gênero, com exceção da comparação entre *P. vulgaris e P. leptostachyus* (2*n* = 20), em que foram observadas diversas translocações provavelmente relacionadas a eventos de disploidia descendente e instabilidade cariotípica em *P. leptostachyus.*

Já em *Vigna*, essa abordagem é restrita à comparação ente *V. unguiculata* e *P. vulgaris*, sendo identificados cinco cromossomos (1, 2, 3, 5 e 8) envolvidos em inversões, translocações e duplicações que estão relacionados à divergência evolutiva entre essas espécies (~9,7 milhões de anos atrás). Quando comparado a

outros grupos de plantas de importância econômica, a análise comparativa em *Vigna* é escassa e limitada à *V. unguiculata* (subgênero *Vigna*), não sendo possível inferir sobre a diversificação cromossômica entre as demais espécies pertencentes ao gênero. Por outro lado, a pintura cromossômica baseada em oligo-FISH já tem sido reportada em plantas socioeconomicamente importantes, como pepino, morango, batata, arroz, *Poplus,* cana-de-açúcar, banana, milho, trigo, algodão e *Citrus*.

A fim de expandir o conhecimento sobre a organização e a evolução cariotípica dentro de *Vigna*, mapas citogenéticos foram construídos para as espécies asiáticas *V. aconitifolia* e *V. angularis*. Para isso, BACs de *V. unguiculata* e de *P. vulgaris* e DNAs ribossomais 5 e 35S foram utilizados para mapear comparativamente os 11 pares cromossômicos dessas espécies. Além disso, foram desenvolvidas pela primeira vez em leguminosas, sondas de pinturas oligo-específicas para os cromossomos 2 e 3 de *P. vulgaris* (*Pv*2 e *Pv*3), previamente identificados como dois dos cromossomos mais envolvidos em rearranjos em relação à *V. unguiculata.* O mapeamento BAC- e Oligo- FISH comparativo permitiu inferir sobre os rearranjos cromossômicos (inversões, translocações e duplicação) relacionados à divergência entre espécies de *Vigna* e *P. vulgaris* (há 9,7 milhões de anos) e entre os subgêneros *Ceratotropis* e *Vigna* (há 3,6 milhões de anos), contribuindo para um maior entendimento acerca da história evolutiva dos feijões dos gêneros *Vigna* e *Phaseolus.*

1.1 OBJETIVOS

1.1.1 OBJETIVO GERAL

Realizar um mapeamento genômico comparativo entre três espécies pertencentes ao gênero *Vigna e Phaseolus vulgaris*, a fim de compreender melhor a organização genômica, macrossintenia e evolução cariotípica na subtribo Phaseolinae.

1.1.2 OBJETIVOS ESPECÍFICOS

1. Construir um mapa BAC-FISH comparativo para os 11 pares cromossômicos de *V. aconitifolia* e *V. angularis,* utilizando BACs de *V. unguiculata* e *P. vulgaris* como sondas, além de sondas de DNAr 5 e 35S.
2. Identificar as relações de macrossintenia e os principais rearranjos cromossômicos relacionados à divergência evolutiva entre *V. aconitifolia, V. angularis, V. unguiculata* e *P. vulgaris,* mediante BAC-FISH, e comparar aos dados prévios da literatura.
3. Detalhar os principais rearranjos envolvendo os cromossomos 2 e 3 de *V. angularis, V. unguiculata* e *P. vulgaris,* mediante pintura cromossômica baseada em oligo-FISH e análise de sintenia de sequência.
4. Identificar os cromossomos portadores de DNAr 5S e 35S nas espécies *V. aconitifolia* e *V. angularis,* e compará-los às espécies previamente descritas na literatura, inferindo acerca da diversidade e evolução desses sítios na subtribo Phaseolinae.
5. Compreender os padrões e tendências carioevolutivas entre as espécies analisadas, a fim de traçar um perfil evolutivo completo entre as espécies da subtribo Phaseolinae.

2 REVISÃO DE LITERATURA

2.1 A FAMÍLIA LEGUMINOSAE JUSS.: TAXONOMIA E ASPECTOS BIOLÓGICOS

De acordo com o sistema APG III (The Angiosperm Phylogeny Group, 2009), a família Leguminosae (Fabaceae L.) é um grupo monofilético que está incluído no Reino Plantae, Divisão Magnoliophyta, Classe Magnoliopsida e Ordem Fabales. É a terceira maior família de angiospermas em número de espécies (atrás apenas das famílias Orchidaceae Juss. e Asteraceae L.), com representantes de grande importância socioeconômica mundial (Lewis *et al*., 2005).

As espécies pertencentes a essa família, reconhecidas pela presença de frutos do tipo legume, constituem um grupo com ampla distribuição geográfica, com formas herbáceas, arbustivas ou arbóreas, perenes ou anuais (Doyle e Luckow, 2003). É um grupo bastante diverso genética e morfologicamente, variando de simples espécies diploides autógamas a complexos poliploides de polinização cruzada (Choi *et al*., 2004). Classificadas em 36 tribos, 727 gêneros e com cerca de 20.000 espécies, as leguminosas desempenham um papel fundamental na nutrição humana e animal e apresentam grande impacto na agricultura e no meio ambiente (Lewis *et al*., 2005; Gepts *et al*., 2005).

Atualmente, uma nova classificação proposta pelo LPGW (Legume Phylogeny Working Group, 2017), baseada em trabalhos prévios e nas análises filogenéticas recentes mediante marcador molecular cloroplastidial *matK,* divide essa família em seis subfamílias: Duparquetioideae, Cercidoideae, Detarioideae, Dialioideae, Caesalpinioideae (com a antiga subfamília Mimosoidae incluída) e Papilionoideae. Essa última é a maior (com cerca de 14 mil espécies), mais diversa e amplamente distribuída das subfamílias, sendo dividida em dois clados principais: as leguminosas temperadas pertencentes ao clado Galegoid (ou Hologalegina); e as leguminosas tropicais pertencentes ao clado Phaseoloid (Wojciechowski, 2003). Dentro primeiro clado, além das leguminosas-modelo *Lotus japonicus* (Regel) K. Larsen. e *Medicago truncatula* Gaertn, pioneiras no sequenciamento do genoma do grupo, também se destacam espécies economicamente relevantes, como a ervilha, a lentilha, o feijão-fava e o grão-de-bico (Sato *et al*., 2008; Schmutz *et al*., 2010; Young *et al*., 2011; Cannon *et al*., 2013; Gupta *et al*., 2014).

As leguminosas pertencentes ao clado Phaseoloid constituem, por sua vez, cerca de 2 mil espécies, agrupadas em 114 gêneros, com amplo destaque e importância, como a soja e os feijões pertencentes aos gêneros *Vigna* Savi e *Phaseolus* L., que estão inseridos na tribo Phaseoleae, subtribo Phaseolinae (Lewis *et al*. 2005). Ambos os gêneros possuem espécies majoritariamente herbáceas, autógamas, e com ampla distribuição e adaptação. Ainda, os feijões *Vigna* e *Phaseolus* são considerados colheitas de cobertura, por reduzirem a erosão do solo e aumentarem a sua fertilidade, além de serem espécies fixadoras de nitrogênio atmosférico do solo, por meio da associação simbiótica com as bactérias *Rhizobium* (Tani *et al*., 2017).

2.2. OS FEIJÕES *VIGNA* E *PHASEOLUS VULGARIS* L.

2.2.1 Filogenia, origem, domesticação e distribuição

Análises filogenéticas baseadas em marcadores morfológicos, bioquímicos e moleculares (de DNA nuclear, cloroplastidial e mitocondrial) são aplicadas em estudos de diversidade genética e na inferência de relações evolutivas entre espécies (Judd *et al*., 2009). Estudos filogenéticos baseados em três marcadores cloroplastidiais (*rbcL, trnL*-F e regiões *trnK/ matK*) sugerem que o clado Phaseoloid divergiu das demais angiospermas há cerca de 60 milhões de anos (Ma), de acordo com a escala de tempo evolutiva estimada de Liu *et al.* (2013). Estudos envolvendo a variação de sequências ribossomais nucleares ITS/5.8S e/ou marcadores moleculares cloroplastidiais intrônicos *trnK, matK* e *rbcL* sugerem, por sua vez, que os gêneros *Vigna* e *Phaseolus* divergiram há cerca de 9,7 Ma (Delgado-Salinas et al., 2011).

O gênero *Phaseolus* é um grupo monofilético de origem Mesoamericana, representado por espécies majoritariamente difundidas nos Andes e nas Américas Central e do Sul, sendo o México seu principal centro de diversidade (com 90% das espécies distribuídas), enquanto a Europa e o Brasil são considerados centros de diversificação secundários do grupo (Mercado-Ruaro *et al*., 2009; Lioi e Piergiovanni, 2015). Esse gênero é composto por cerca de 75 espécies subagrupadas em dois clados maiores e divididos em oito grupos, sendo: Pauciflorius, Pedicellatus e Tuerckheimii pertencentes ao clado A; e Filiformis, Leptostachyus, Lunatus,

Polystachios e Vulgaris pertencentes ao clado B. Pelo menos sete eventos independentes de domesticação ocorreram dentro do gênero, o que gerou o isolamento reprodutivo de cinco espécies domesticadas: *P. acutifolius* A. Gray, *P. coccineus* L., *P polyanthus* Greeman, *P. lunatus* L. e *P. vulgaris* L., sendo as duas últimas de maior destaque mundial (Delgado-Salinas *et al*., 2006; Bitocchi *et al*., 2017).

Phaseolus vulgaris (feijão-comum), a principal espécie econômica do gênero, pertence ao clado B, grupo Vulgaris, considerado o grupo mais antigo do gênero, que divergiu dos demais há cerca de 4 Ma. Como sugerido por Gepts (1998) e Delgado-Salinas *et al.* (2006), *P. vulgaris* apresenta dois *pools* gênicos principais que divergiram há cerca de 87 mil anos: um Mesoamericano (do México até o Norte da América do Sul) e um Andino (região central e sul da América do Sul), os quais foram domesticados de maneira paralela e independente devido a barreiras geográficas e/ou incompatibilidade sexual durante seu isolamento reprodutivo. Esses dois *pools* gênicos sofreram diferentes adaptações que refletiram, por sua vez, em características morfológicas, bioquímicas e moleculares distintas, como diferenças no tamanho da semente e conteúdo de proteína faseolina (Ariani *et al*., 2018; Gioia *et al*., 2019). Ainda, há um terceiro *pool* gênico de populações selvagens existentes no Norte do Peru, Equador e em uma faixa estreita da cordilheira dos Andes, que possui frequências alélicas únicas e presença exclusiva de proteínas do grupo faseolina I (revisado por Bitocchi *et al*., 2017).

O gênero *Vigna* possui, por sua vez, origem parafilética e tem como possível centro de origem a África. É amplamente distribuído e domesticado em regiões pantropicais, especialmente em seu centro de origem, além das Américas Central, do Sul e Ásia (Delgado-Salinas *et al*., 2011; Freire-Filho *et al*., 2011). Esse gênero compreende cerca de 100 espécies (sendo 10 domesticadas), divididas em cinco subgêneros: um de origem americana (*Lasiospron*), um de origem asiática (*Ceratotropis*) e três de origem africana (*Vigna, Haydonia* e *Plectrotropis*). Os subgêneros africanos e asiáticos são considerados grupos monofiléticos, com divergência aproximada de 3,6 Ma (Delgado-Salinas *et al.,*2011).

O subgênero asiático *Ceratotropi*s contém 21 espécies divididas em três subgrupos (Angulares, Aconitifoliae e Ceratotropis), com destaque para as espécies *V. angularis* (feijão adzuki, subgrupo Angulares) e *V. aconitifolia* (feijão-traça, subgrupo Aconitifoliae), distribuídas e cultivadas majoritariamente no Leste Asiático e na Índia, respectivamente (Delgado-Salinas *et al*., 2011; She *et al*., 2015). O parente

selvagem de *V. angularis* e seu possível progenitor, *V. angularis* (Willd.) Ohwi et Ohashi var. *nipponensis,* cresce amplamente no Leste Asiático, sendo a China o seu provável centro de origem e domesticação (Kaga *et al*., 2008).

Já o subgênero africano *Vigna* contém 31 espécies divididas em seis seções (*Catiang, Comosae, Liebrechtsia, Macrodontae, Reticulatae* e *Vigna*), sendo a espécie domesticada *V. unguiculata* (feijão-caupi, seção *Catiang*) de maior importância econômica, especialmente na África e no Nordeste Brasileiro (Isemura *et al*., 2007; Delgado-Salinas *et al*., 2011; Boukar *et al.*, 2016). *Vigna unguiculata* subsp. *dekindtiana* (Harms.) Verd., forma perene existente apenas na África, é considerada o progenitor selvagem do feijão-caupi (Lush e Evans, 1981).

A Figura 1 representa uma filogenia simplificada entre os gêneros *Vigna* e *Phaseolus* e entre os subgêneros *Ceratotoropis* e *Vigna* e os tempos de divergência estimados (em Ma), com destaque para as espécies-alvo estudadas.

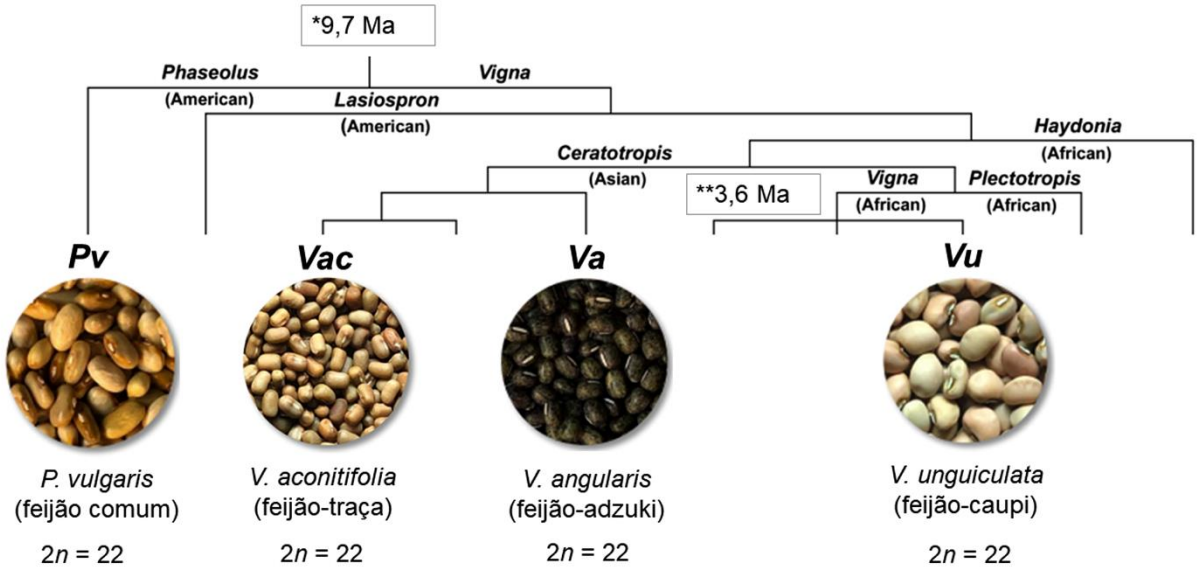

Figura 1. Filogenia entre os gêneros *Vigna* e *Phaseolus* (modificada de Delgado-Salinas *et al*., 2011), identificando os tempos de divergência entre gêneros (*) e subgêneros de *Vigna* (**), com destaque para as espécies *P. vulgaris* (*Pv), V. aconitifolia* (*Vac*), *V. angularis* (*Va*) e *V. unguiculata* (*Vu*). Todas as espécies apresentam conjunto cromossômico 2*n* = 2x = 22.

2.2.2 Segurança nutricional, social e econômica

Os feijões *Vigna* e *Phaseolus* são uma importante fonte nutricional, com cerca de 30% de proteínas presentes nos seus grãos, além de serem ricos em carboidratos, ácido fólico e sais minerais, como zinco, cálcio, magnésio e fósforo, dentre outros

(USDA, 2015). São amplamente adaptados, de ciclo de vida curto, de fácil produção e de alto consumo, especialmente em países em desenvolvimento. Esses feijões constituem a principal fonte de subsistência para a população de baixa renda, devido ao seu alto valor proteico, além de serem uma fonte geradora de emprego e renda para as famílias carentes (Boukar *et al*., 2016).

O feijão comum é uma das leguminosas de grãos com maior consumo ao redor do mundo em termos de rendimento total e área cultivada, apresentando um papel importante na alimentação em países em desenvolvimento da África e das Américas Central e do Sul (citado por Gioia *et al*., 2019). Dados mais recentes disponibilizados pela da FAO (Organização das Nações Unidas para Agricultura e Alimentação), relativos ao ano de 2018, indicam que a sua produção mundial foi estimada em cerca de 55 milhões de toneladas métricas (t) (FAO, 2020). Em 2018, o Brasil foi considerado o principal produtor de grãos de feijão comum com alta qualidade fisiológica, com produção em cerca de 3,5 milhões de toneladas (t) e produtividade média de 1.100 kg/ ha, sendo o estado de Goiás responsável por 37% da sua produção (Embrapa, 2019).

O feijão-caupi é, por sua vez, adaptado a solos ácidos, arenosos e pobres em nutrientes e, consequentemente, apresenta um bom desenvolvimento em regiões áridas e semiáridas, especialmente na África Subsaariana e no Nordeste brasileiro. O feijão-caupi destaca-se por ser particularmente tolerante à seca e a temperaturas elevadas, o que o torna uma espécie-alvo para programas de melhoramento genético do gênero (Boukar *et al*., 2016; 2019). Globalmente, a produção dessa leguminosa foi, em 2018, de cerca de 7,2 milhões de t em uma área de 12 milhões de ha (FAO, 2020). A África Subsaariana é a principal produtora de feijão-caupi a nível global, com produção em cerca de 4,5 milhões de t (62,5 %), sendo a Nigéria o maior país produtor, com 2,2 milhões de t (30,5%), seguida do Níger (15%) (Saka *et al*., 2018; Boukar *et al.,* 2019).

O Brasil ocupa o terceiro lugar de maior produção e consumo do feijão-caupi, com 12% da produção mundial. Segundo a Embrapa (Empresa Brasileira de Pesquisa Agropecuária, 2019), a produção brasileira para essa cultura foi, em 2018, de 740 mil t com produtividade de 466 kg/ha, o que gerou cerca de 1,5 milhão de empregos diretos nos últimos anos. O Nordeste brasileiro foi responsável por mais da metade da sua produção (~66%), sendo o estado de Pernambuco responsável por 375 kg/ ha da produtividade brasileira. Esses dados ratificam a relevância dessa espécie para a

geração de renda e como fonte de subsistência no país, bem como confirmam a sua participação na culinária tradicional e local do Nordeste brasileiro (Freire-Filho *et al*., 2011).

Dentre os feijões pertencentes ao subgênero asiático *Ceratotropis*, o feijão adzuki (*V. angularis*) e o feijão-traça (*V. aconitifolia*) destacam-se por apresentarem cultivo e produção limitada ao Leste Asiático e Índia, respectivamente (Mukai e Sato, 2011). O feijão adzuki é um ingrediente tradicional da culinária asiática e, devido ao seu gosto adocicado, é bastante utilizado no preparo de sobremesas e tortas. Sua produtividade, restrita à China, Japão, Coreia e Taiwan, foi de cerca de 2 t/ ha, para o ano de 2014 (Yousif *et al*., 2003; Lestari *et al*., 2014; Kang *et al.*, 2015; Rawal e Navarro et *al.,* 2019). O feijão adzuki e feijão-traça destacam-se por apresentar um menor teor de gordura (3%) e maior teor de carboidratos (68%) em relação às demais espécies de *Vigna*, além de *V. aconitifolia* também ser considerada uma espécie resistente à seca (Boukar *et al*. 2016). Na Índia, a produção de *V. aconitifolia* foi de cerca de 1,5 milhões de ha, com produtividade de até 0,4 milhão t/ha, para o ano de 2010 (FAO, 2015; Rawal e Navarro et *al.,* 2019). Dados mais recentes da produção global para o feijão adzuki e feijão-traça não foram, contudo, atualizados pela FAO. Nas Américas e no Brasil, essas leguminosas asiáticas são pouco conhecidas e divulgadas, não havendo dados disponíveis relativos à sua produção em território brasileiro (Gohara *et al*., 2016).

Essas espécies, juntamente com as espécies selvagens pouco exploradas e negligenciadas de *Vigna*, apresentam um papel fundamental na diversificação e sustentabilidade ambiental, especialmente frente a novos e urgentes desafios, como as mudanças climáticas. Assim, é necessário um maior conhecimento acerca da genômica evolutiva e da diversidade genética desse grupo. Ferramentas genéticas, genômicas e citogenéticas apresentam, portanto, um papel fundamental no desenvolvimento de cultivares resistentes a fatores bióticos e abióticos e com características morfoagronômicas de interesse para os programas de melhoramento genético de espécies de *Vigna* e *Phaseolus.*

2.3 MAPAS GENÉTICOS EM LEGUMINOSAS

Diante da sua reconhecida importância nutricional e alimentar no mundo e visando o desenvolvimento de espécies com maior rendimento e resistência a

estresses bióticos e abióticos, pesquisas genômicas têm sido voltadas ao melhoramento genético, fornecendo novas perspectivas para produção de variedades superiores de leguminosas (Varshney *et al*., 2005; 2010).

Nesse contexto, mapas genéticos ou de ligação, baseados nas distâncias relativas das frequências de recombinação entre genes, são abordagens genéticas clássicas que permitem a localização de regiões gênicas de interesse, sendo ferramentas-chave para o melhoramento genético. A funcionalidade de um mapa genético está diretamente associada à sua densidade (quanto maior sua saturação, maior sua resolução) e à presença de genes de interesse e de genes importantes para a montagem do sequenciamento de uma espécie (Liu *et al.,* 2016). Atualmente, as novas tecnologias de genômica e transcriptômica fornecem suporte para estudos de diversidade entre genomas de espécies relacionadas com o uso de diversos tipos de marcadores moleculares, viabilizando a obtenção de mapas genéticos supersaturados que permitem localizar genes e QTLs (Quantitative Trait *Loci; Loci* de Características Quantitativas) associados a características morfoagronômicas de interesse, além de estudos comparativos de sintenia entre espécies, contribuindo para o entendimento acerca da evolução dos genomas de plantas (Lucas *et al*., 2011; Andargie *et al*., 2013; Polanco *et al*., 2019).

Em leguminosas, a partir do desenvolvimento de mapas genéticos consenso com alta densidade de SNPs (Single Nucleotide Polymorphisms; Polimorfismos de Nucleotídeo Único), ocorreu um avanço nas suas pesquisas genéticas que possibilitaram a criação de bibliotecas de BACs, bibliotecas das extremidades terminais de BACs (BAC-End Sequences, BESs) e o alinhamento e a integração de mapas genéticos e físicos entre espécies relacionadas, como *M. truncatula, L. japonicus*, *Glycine max* (L.) Merr, espécies do gênero *Arachis* L. e os feijões *Vigna e Phaseolus,* permitindo estimatimar a sintenia e colinearidade entre essas espécies (Ellis *et al*., 1992; Winter *et al*., 2000; Sandal *et al*., 2002; Hougaard *et al*., 2008; Muchero *et al*., 2009; Millan *et al*., 2010; Lucas *et al*., 2011; 2013).

Em *P. vulgaris*, o primeiro mapa genético foi baseado em marcadores moleculares RFLP (Retriction Fragment Length Polymorphism; Polimorfismo de Comprimento de Fragmento de Restrição) conhecidos como *Bngs (*Bean genomic clones; Clones genômicos de feijões), que permitiram identificar os 11 grupos de ligação de *P. vulgaris* (Vallejos *et al*., 1992). Posteriormente, diferentes mapas genéticos baseados em diversos marcadores, como RAPD (Random Amplified

Polymorphic DNA; Fragmento de DNA Amplificado ao Acaso), EST-SSR (Expressed Sequence Tag; Etiqueta de Sequência Expressa - Simple Sequence Repeat; Sequência Curta Repetida), AFLP (Amplified Fragment Lenght Polymorphism; Polimorfismo de Comprimento de Fragmento Amplificado) e RGA (Resistance Analog Gene; Gene Análogo de Resistência) foram construídos e integrados a um mapa genético consenso para o feijão comum, permitindo caracterizar genes e identificar QTLs associados à resistência à antracnose e à ferrugem, bem como quantidade de fibras, deiscência da vagem e rendimento dos grãos do feijão comum, identificados nos seus respectivos grupos de ligação (Yu *et al.*, 2000; Blair *et al.*, 2003; Hanai *et al*., 2010; Galeano *et al*., 2011; Koinange *et al.*, 2015; Mier e Teran *et al.*, 2019; Parker *et al.*, 2020).

Em *Vigna*, diversas espécies possuem mapas genéticos disponíveis, como: *V. mungo* (L.) Hepper, *V. umbellata* (Thunb.) Ohwi & H.Ohashi, *V. unguiculata* subsp. *sesquipedialis* (L.) Verdc., *V. radiata* (L.) R. Wilczek, *V. marina* (Burm.) Merrill, *Vigna vexillata* (L.) A. Rich. e *V. subterranea* (L.) Verdc (Chaitieng *et al*., 2006; Isemura *et al*., 2010; Xu *et al*., 2011; Chankaew *et al*., 2014; Marubodee *et al*., 2015; Ho *et al*., 2017).

O primeiro mapa genético para o feijão-caupi foi publicado por Menéndez *et al*. (1997), utilizando marcadores RAPD, RFLP e AFLP. Posteriormente, Quédraogo *et al*. (2002) geraram um novo mapa que identificou os 11 grupos de ligação dessa espécie, além de utilizarem marcadores associados a genes de resistência. Muchero *et al*. (2009) e Lucas *et al*. (2011) utilizaram 928 e 1.107 SNPs, respectivamente, para a construção de um mapa do feijão-caupi com dados adicionais, incluindo a identificação de QTLs e de diversidade genética dessa espécie e sua comparação com *M. trunculatula* e *G. max.* Recentemente, Muñoz-Amatriaín *et al*. (2017) produziram um mapa genético consenso supersaturado (com cerca de 38 mil SNPs) entre 36 acessos de *V. unguiculata* que foram alinhados ao genoma da linhagem homozigota melhorada IT97K-499-35. Esse mapa genético permitiu a ancoragem de 100 Mb do genoma dessa espécie, que forneceu suporte para o futuro sequenciamento do genoma do feijão-caupi (Lonardi *et al*., 2019). Adicionalmente, Lo *et al.* (2018), analisaram 215 linhagens endogâmicas recombinantes (RILs) derivadas do cruzamento entre acessos selvagens e domesticados do feijão-caupi e identificaram 16 QTLs associados a nove características relacionadas aos processos de domesticação dessa espécie, como quebra e tamanho da vagem, tempo de

florescimento, largura e tamanho da folha, incluindo um grupo de QTLs, presente no GL8, que está relacionado ao aumento dos órgãos da planta.

Para *V. angularis*, o primeiro mapa genético foi publicado por Han *et al*. (2005), utilizando em conjunto, cerca de mil marcadores SSRs, AFLPs e RFLPs para sua construção. Posteriormente, Wang *et al*. (2015) construíram mapas genéticos baseados em SSRs entre populações selvagens e cultivadas do feijão adkuzi (*V. nepalensis* x *V. angularis* var. *angularis* e *V. angularis* var. *nipponensis* x *V. angularis* var. *angularis*). Esses dados permitiram identificar translocações recíprocas entre os grupos de ligação (LG) 4 e 6 das espécies selvagens em relação às domesticadas (confirmadas por BAC-FISH utilizando sondas dos LG4 e LG6), fornecendo uma maior compreensão acerca da história filogeográfica e dos processos de domesticação dos feijões adkuzi cultivados. Ainda, Liu *et al.* (2016) e Li *et al.* (2017) construíram mapas genéticos baseados em SSRs, AFLPs, RFLPs e SNPs e identificaram, respectivamente, 8 e 11 QTLs e seus respectivos GL associados ao tempo de florescimento de *V. angularis.*

Yundaeng *et al*. (2019) construíram, por sua vez, um mapa genético consenso em 188 acessos cultivados e selvagens de *V. aconitifolia*. 169 *loci* de marcadores SSR (do total dos 1644 previamente selecionados) e três marcadores morfológicos (*Sdcbm, Lfs* e *Sdtl*) foram usados para saturar os 11 grupos de ligação da espécie. No total, 50 QTLs foram associados a 17 características, como hábito de crescimento, absorção de água, tamanho de órgãos e dormência de sementes. Ainda, QTLs associados a processos domesticação dessa espécie foram identificados ao longo dos grupos de ligação de *V. aconitifolia*. Além disso, os autores analisaram as relações de sintenia e colinearidade entre os grupos de ligação de *V. aconitifolia* com outras espécies de *Vigna*, como *V. angularis*, *V. unguiculata*, *V. radiata* e V*. umbellata*, fornecendo suporte para estudos de melhoramento genético das espécies do gênero.

Essas pesquisas genômicas têm facilitado, portanto, o desenvolvimento de pesquisas genéticas em espécies relacionadas aos gêneros *Vigna* e *Phaseolus*; no melhoramento assistido por marcadores, para a obtenção de linhagens com características morfoagronômicas de interesse, como resistência a fatores abióticos e a microorganismos patogênicos; na associação entre mapas genéticos e citogenéticos; bem como na análise comparativa entre os feijões *Vigna* e *Phaseolus* a outras leguminosas economicamente importantes (Iwata-Otsubo *et al*., 2016; Muñoz-Amatriaín *et al*., 2017).

2.4 SEQUENCIAMENTO DO GENOMA DE LEGUMINOSAS

Durante os últimos anos, os avanços das pesquisas genômicas suportadas pelas plataformas de bioinformática e de sequenciamento de nova geração (NGS) permitiram um progresso nos estudos citogenéticos moleculares de sintenia e evolução cromossômica em plantas (Chèvre *et al*., 2018). O sequenciamento do genoma das leguminosas-modelo *L. japonicus* (Sato *et al*., 2008), *M. truncatula* (Young *et al*., 2011; Tang *et al*., 2014) e *G. max* (Schmutz *et al*., 2010) abriu novas possibilidades para as pesquisas genéticas em leguminosas, acelerando estudos de organização genômica e evolução em espécies economicamente importantes da família Leguminosae. Esses estudos serviram como base para o conhecimento dos processos de fixação do nitrogênio atmosférico no solo, das relações simbióticas entre legumes-rizóbios, bem como para uma melhor compreensão acerca da genômica e da evolução dessa família (Dash *et al*., 2016).

Com os avanços das plataformas de sequenciamento, aliados à sua redução de custo e de tempo, atualmente, cerca de 35 espécies de leguminosas anteriormente consideradas culturas órfãs, devido à limitação de pesquisas genômicas, apresentam genoma sequenciado e disponível (revisado por Bauchet *et al*., 2019).

Dentre as espécies dos gêneros *Vigna* e *Phaseolus,* o genoma de *P. vulgaris* (~587 Mb) foi o primeiro a ser publicado, mediante abordagem combinada pelas plataformas Roche 454, Illumina e Sanger (Schmutz *et al*., 2014). Posteriormente, Lobaton *et al*. (2018) ressequenciaram o genoma inteiro de 35 variedades cultivadas e elites de *P. vulgaris* pertencentes a diferentes programas de melhoramento genético do gênero, bem como de *P. acutifolius* e *P. coccineus*. Os resultados permitiram identificar diferenças de variação genética entre e dentro espécies fornecendo, assim, informações valiosas para programas de melhoramento genético voltados para as espécies do gênero.

Dentro de *Vigna*, Kang *et al*. (2015) realizaram a montagem *de novo* do genoma de *V. angularis*, mediante plataformas Illumina HiSeq e Roche GS-FLX1, cobrindo 75% do genoma (estimado em ~591 Mb). Já Yang *et al.* (2015) realizaram um rascunho do genoma *V. angularis*, estimado em~542 Mb. Posteriormente, Sakai *et al*. (2015) reconstruíram e reestimaram o genoma de *V. angularis* (~541 Mb), com 86% de cobertura, mediante sequenciamento de molécula simples em tempo real (SMRT), suportado pelas plataformas de sequenciamento de segunda geração previamente

utilizadas. O maior conhecimento acerca do genoma de *V. angularis* e seus parentais selvagens são, assim, importantes fontes de marcadores genéticos, *loci* relacionados à pressão de seleção e genes candidatos aos programas de melhoramento genético dessa espécie.

Recentemente, Lonardi *et al*. (2019) realizaram a montagem de alta qualidade do genoma de *V. unguiculata* (IT97K-499-35), mediante sequenciamento de terceira geração PacBio de SMRT. Os autores reestimaram o tamanho do genoma com cobertura de 91x, em ~586 Mb, número correspondente à média entre as estimativas baseadas em k-mer (560 Mb) e à citometria de fluxo (640 Mb). Além disso, dois mapas ópticos (Bionano Genomics) e 10 mapas genéticos contendo SNPs únicos (Muñoz-Amatriaín *et al*., 2017), juntamente com análise de transcriptoma e dados prévios de sequências Illumina, WGS (Sequenciamento do Genoma Total) e sequências BACs, foram usados para a ancoragem, orientação e qualidade de montagem das 11 pseudomoléculas cromossômicas dessa espécie.

Ainda, Lonardi *et al*. (2019) compararam os dados de sequenciamento de *V. unguiculata* e realizaram a análise sintenia de sequência com outras leguminosas do clado Phaseoloid. Para facilitar uma maior compreensão da sintenia entre espécies, os autores padronizaram a numeração das pseudomoléculas cromossômicas de acordo com a homeologia de sequência com *P. vulgaris,* sendo identificado um alto grau de sintenia compartilhada entre o genoma de *V. unguiculata* com *P. vulgaris, V. angularis* e *V. radiata*. Essa última espécie, pertencente ao subgênero asiático *Ceratotropis*, também apresenta genoma disponível (~579 Mb) e montado (Kang *et al*., 2014), além de *V. subterranea* (subgênero *Vigna*), com tamanho do genoma estimado em ~550Mb (Chang *et al*. 2019). Para outras treze espécies selvagens de *Vigna,* o sequenciamento do genoma está em progresso, incluindo *V. aconitifolia* (Sakai *et al*., 2016).

2.5 CARACTERIZAÇÃO CITOGENÉTICA EM LEGUMINOSAS

2.5.1 Citogenética clássica

A citogenética tornou-se uma ferramenta valiosa para caracterização da diversidade dos recursos genéticos vegetais. A análise de cariótipos envolvendo o número, morfologia e tamanho dos cromossomos, presença de constrição secundária

e quantidade de heterocromatina, são informações importantes para comparar espécies ou detectar polimorfismos entre cromossomos homólogos e não homólogos de indivíduos da mesma espécie ou entre homeólogos de espécies relacionadas (Moscone *et al*., 1996). Esses dados, associados a outras características citológicas, têm se mostrado importantes para o reconhecimento de variedades, híbridos e poliploides e na compreensão das relações filogenéticas dentro e entre táxons (Guerra, 2000; Mirzaie-Nodoushan *et al*., 2006).

As leguminosas pertencentes ao clado Galegoid possuem, em geral, conjunto cromossômico básico 2*n* = 2*x* = 12, 14 ou 16, com cariótipos variáveis e tamanho genômico variando de ~470 Mb, em *L. japonicus* e *M. truncatula,* a ~13.000 Mb em *Vicia faba* L. (revisado por Iwata *et al*., 2013). Diferentemente, as leguminosas pertencentes ao clado Phaseoloid possuem, em geral, tamanhos de genoma similares (~600 Mb), com cariótipos estáveis e número cromossômico 2*n* = 2*x* = 22. Uma das exceções ocorre no gênero *Glycine* L., em que a maioria das espécies apresenta 2*n* = 4*x* = 40, fato relacionado a eventos de poliploidização na base do gênero, seguida de perda de cromossomos e diploidização do genoma dessas espécies (Schmutz *et al*., 2010; McClean *et al*., 2010; Iwata *et al*., 2013). Análises de sintenia previamente realizadas por Lin *et al.* (2010) e McClean *et al*. (2010) sugerem, por exemplo, que a soja sofreu rearranjos cromossômicos extensivos ao longo da sua evolução, seguidos de uma duplicação total do seu genoma (WGD).

Estudos citogenéticos clássicos em *Phaseolus* e *Vigna* iniciaram-se por volta de 1925 e 1955, respectivamente (Karpetschenko, 1925; Darlington e Wylie, 1955). A maioria das espécies de *Vigna* e *Phaseolus* apresenta conjunto cromossômico diploide 2*n* = 22, com cromossomos de morfologia metacêntrica e submetacêntrica, de tamanho reduzido e de difícil identificação, sendo o menor par cromossômico reportado em *V. trilobata* Chiov (0,58 µm) e o maior par cromossômico em *V. unguiculata* (4,0 µm) (Guerra *et al*., 1996; Joseph e Bouwkamp, 1978; Venora e Saccardo, 1993; Zheng *et al*., 1991).

Reduções no número cromossômico foram relatadas em três espécies relacionadas do gênero *Phaseolus*: *P. leptostachyus*, *P. micranthus* Hook. & Arn. e *P. macvaughii* A. Delgado, todos com 2*n* = 2*x* = 20 cromossomos, sendo essa redução causada por eventos de disploidia descendente (Mercado-Ruaro e Delgado-Salinas, 1998; 2000; Fonsêca *et al*., 2016). Já em *Vigna,* as espécies *V. heterophylla* A. Rich. e *V. filicaulis* Hepper apresentam 2*n* = 2*x* = 20 (Sen e Bhowal, 1960; Galasso *et al*.,

1996), enquanto duas alopoliploides naturais, *V. glabrescens* (Roxb.) Verdc. e *V. reflexo-pilosa* var. *glabra* Maréchal, possuem 2*n* = 4*x* = 44 (Madlung, 2013; Kang *et al*., 2014).

P. vulgaris, *V. angularis*, *V. aconitifolia* e *V. unguiculata* possuem 2*n* = 22, com cariótipos estáveis, cromossomos pequenos com morfologia metacêntrica e submetacêntrica. Em *P. vulgaris* (1C = 0,60 picogramas), os cromossomos variam de 1,5 a 3 µm (Mercado-Ruaro e Delgado-Sainas, 2000; revisado por Fonsêca e Pedrosa-Harand *et al*., 2017). Já em *Vigna,* o conteúdo de DNA encontra-se disponível para 16 espécies, variando de 1C = 0,43 pg, em *V. oblongifolia* (A.) Rich.*,* a 1,0 pg em *V. glabrescens* (Parida *et al*., 1990, recalibrados por Bennett & Leitch, 1995). Em *V. angularis* (1C = 0,60 pg), os cromossomos variaram de 1,19 a 2,06 µm (Joseph e Bouwkamp, 1978). *V. aconitifolia* possui 1C = 0,49 pg, sem dados prévios acerca da variação de tamanho cromossômico nessa espécie (Oliveira, 2018). Em *V. unguiculata* (1C = 0,70 pg), por sua vez, o tamanho dos cromossomos é bastante variável entre diferentes autores: Sen e Bhowal (1960) descreveram os menores e maiores pares cromossômicos como 0,96 e 2,88 µm; já Zheng *et al.* (1991) e Venora e Saccardo (1993) sugeriram uma variação cromossômica de 1,05 a 1,96 µm; enquanto Alam *et al.* (2013) identificaram o menor par como 2,0 µm e o maior como 4,0 µm.

Para Pozzobon *et al*. (2006), diferenças observadas na morfologia do par cromossômico dentro e entre as espécies podem sugerir diferenças biológicas, podem estar relacionadas ao padrão de condensação cromossômica ou ser apenas reflexo das diferenças entre as técnicas. A coloração convencional não é, portanto, um método adequado para identificar pares cromossômicos de maneira precisa e individual no cariótipo da maioria das espécies.

Segundo Guerra (2000), a análise do padrão de distribuição de heterocromatina constitutiva (HC) possibilita a verificação de bandas localizadas em regiões cromossômicas específicas, sugerindo assim um propósito funcional dessa heterocromatina, além da identificação de pares cromossômicos homólogos e seu heteromorfismo dentro de cada táxon estudado. Ainda, a quantidade de heterocromatina não é homogênea entre e dentro espécies e pode apresentar polimorfismos quanto ao número e tamanho das suas bandas (Moscone *et al.*, 2007).

Técnicas bastante utilizadas em estudos citogenéticos que detectam regiões ricas em heterocromatina são o bandeamento C e a coloração com os fluorocromos cromomicina A_3 (CMA) e 4´-6-diamidino-2-fenilindol (DAPI). Na diferenciação da heterocromatina baseada no bandeamento C em *Phaseolus* e em *Vigna*, blocos com intensidade semelhantes foram encontrados nas regiões pericentroméricas e subterminais para da maioria dos cromossomos (entre oito e 11 cromossomos) de cerca de 20 espécies de *Phaseolus* e 10 espécies de *Vigna* analisadas, todas com com 2*n* = 22 cromossomos (Lavania e Lavania, 1982; Zheng *et al.,* 1991; Galasso *et al.,* 1992; 1993; 1996). Zheng *et al.* (1991) identificaram bandas C pericentroméricas presentes em 10 dos 11 pares cromossômicos de *P. vulgaris.* sendo quatro pares com bandas C terminais adicionais. Já Galasso *et al.* (1992) identificaram bandas C pericentroméricas presentes em todos os cromossomos de *V. unguiculata*, sendo quatro pares com bandas C subterminais e terminais adicionais. Excepcionalmente, Carvalheira e Guerra (1994; 1998) e Carvalheira (2000), mediante bandeamento C-Giemsa, identificaram cromossomos politênicos em células suspensoras e células do tapete da antera em seis espécies de *Phaseolus e* cinco espécies de *Vigna,* incluindo *V. unguiculata* e *P. vulgaris,* com padrão heteropicnótico na região proximal e região terminal descondensada para a maioria dos cromossomos politênicos das espécies analisadas dos gêneros.

Os corantes fluorescentes informam, de maneira mais simples e reprodutível, a constituição da heterocromatina, detalhando o padrão de bases pelo uso dos fluorocromos CMA e DAPI, que mostram especificidade de ligação com sequências de bases de DNA GC e AT, respectivamente (Guerra,1988; 2000). Geralmente, três tipos de heterocromatina são descritos entre espécies: heterocromatina altamente rica em GC e reduzida em AT ($CMA^{++}/DAPI^{-}$); heterocromatina moderadamente rica em GC e reduzida em AT ($CMA^{+}/DAPI^{-}$); e heterocromatina moderadamente rica em GC e neutra em AT ($CMA^{+}/DAPI^{0}$). A distribuição dessas bandas pode variar, contudo, entre espécies e até mesmo dentro de diferentes acessos de uma mesma espécie (Schweizer, 1976, Schweizer *et al.,* 1990).

Nas espécies de *Phaseolus* analisadas até o momento, *P. vulgaris, P. lunatus, P. leptostachys*, *P. microcarpus* e *P. macvaughii*, possuem blocos de heterocromatina pericentromérica CMA^{+} na maioria dos seus cromossomos. Em *P. vulgaris,* esses blocos correspondem a 34% do tamanho do seu conjunto cromossômico total. Adicionalmente, pelo menos um par cromossômico com banda CMA^{+} terminal,

colocalizada com o sítio de DNA ribossomal 35S, está presente em todas as espécies analisadas (Zheng *et al.*, 1993; Fonsêca *et al*., 2010; Bonifácio *et al*., 2012; Fonsêca e Pedrosa, 2013; Fonsêca *et al*., 2014).

Dentro de *Vigna,* as bandas heterocromáticas CMA/DAPI são bastante variáveis quanto ao número, tamanho e posição nos cromossomos dos cariótipos das espécies. 18 bandas $CMA^{+}/DAPI^{0}$ foram identificadas *V. racemosa* Hutc & Dalziel (subgênero *Vigna)*, enquanto *V. aconitifolia* (subgênero *Ceratotropis*) destaca-se por apresentar heteromorfismo quanto ao padrão de bandas CMA/DAPI, sendo relatados acessos com 2-3 bandas CMA^{+} e 7-8 $DAPI^{-}$ (Galasso *et al*., 1996; Shamurailatpam *et al.*, 2015; She *et al*., 2015). Em *V. angularis*, Oliveira (2018) identificaram quatro bandas $CMA^{+}/DAPI^{-}$ no cariótipo dessa espécie. Já em *V. unguiculata*, Bortoleti *et al*. (2012) identificaram bandas CMA^{+} nos 11 cromossomos dessa espécie, sendo observados três padrões distintos de bandas: $CMA^{++}/DAPI^{0}$, colocalizadas com sítios maiores de DNAr 35S (evidenciados por FISH), presentes em dois cromossomos; $CMA^{+}/DAPI^{-}$, colocalizadas com sítios menores de DNAr 35S, presentes em três cromossomos; e $CMA^{+}/DAPI^{0}$, presentes nas regiões pericentroméricas de todos os cromossomos. Bandas $DAPI^{+}$ não foram observadas nos cromossomos de *Vigna*¸ fato que corrobora com dados prévios de Galasso *et al.* (1993; 1996) e Zheng *et al.* (1993).

2.5.2 Citogenética molecular

No início da década de 70, com o advento da técnica de FISH (Fluorescent *In Situ* Hybridization; Hibridização *In Situ* fluorescente), deu-se início a uma nova era da citogenética molecular (Gall e Pardue, 1969; Speicher et al., 1996). A FISH foi aplicada, pela primeira vez em plantas, por Schwarzacher *et al.* (1989). Essa técnica, que substituiu as sondas previamente marcadas por métodos radioativos, permitiu a utilização de sondas específicas marcadas com fluorescência para hibridizar *in situ*, isto é, no sítio de localização das regiões específicas de interesse no cromossomo (O'Connor, 2008). Atualmente, os alvos da FISH incluem os territórios dos núcleos interfásicos, cromossomos mitóticos e meióticos, além de fibras estendidas de DNA. Ainda, a FISH possibilita a integração dos marcadores de mapas genéticos a cromossomos específicos (mapas citogenéticos ou físicos), a comparação das distâncias genéticas e físicas, a análise da distribuição de sequências repetitivas no genoma de determinada espécie, bem como a determinação da origem do genoma

em híbridos interespecíficos, por meio da técnica de GISH (Genomic *In Situ* Hybridization; Hibridização Genômica *In Situ*) usando o DNA genômico dos parentais (Jiang e Gill, 2006; Omhido *et al*., 2010; Heslop-Harrison e Schwarzacher, 2011). As sequências de DNA comumente utilizadas como sondas em FISH são: DNA altamente repetitivo em tandem, como os sítios de DNA ribossomais (DNAr) 5 e 35S; sequências centroméricas; teloméricas; repetitivas dispersas, como os elementos transponíveis; e sequências repetitivas e cópia-única inseridas em vetores, como plasmídeos, cosmídeos, Cromossomos Artificiais de Leveduras (YACS) e de Bactérias (BACs) (Guerra, 2004; Jiang e Gill, 2006).

Esses avanços permitiram a identificação cromossômica de maneira precisa e individual em leguminosas, principalmente em espécies com cromossomos pequenos e de morfologia similar, como as espécies pertencentes aos gêneros *Vigna* e *Phaseolus.* Isso levou, portanto, a uma maior compreensão acerca das propriedades funcionais e estruturais dos genomas dessas espécies (Iwata *et al*., 2013). Estudos citogenéticos moleculares têm sido conduzidos em espécies dos gêneros *Vigna* e *Phaseolus,* mediante FISH utilizando como sondas sítios de DNAr (Guerra *et al*., 1996; Moscone *et al*., 1999; Pedrosa-Harand *et al*., 2006), DNA centromérico e sequências teloméricas (Galasso *et al*., 1995), retrotransposons (Galasso *et al*., 1997; Iwata-Otsubo *et al.*, 2016), DNA satélite (Ribeiro *et al.,* 2016) e BACs (Pedrosa-Harand *et al*., 2009;Fonsêca *et al*., 2010; Bonifácio *et al*., 2012; Almeida e Pedrosa-Harand, 2013; Fonsêca e Pedrosa-Harand, 2013; Vasconcelos *et al*., 2015). Recentemente, Ribeiro *et al.* (2019), mediante abordagem computacional aliada à citogenética molecular, identificaram os principais retrotransposons LTR, do tipo *Ty1-Copia* e Chromovirus, presentes no genoma de duas espécies de *Vigna* [*V. angularis* e *V. nakashimae* (Ohwi) Ohwi & H.Ohashi] e de três espécies de *Phaseolus* (*P. vulgaris, P. acutifolius e P. coccineus*). Ainda, dentro de *Phaseolus*, também foram identificados LTRs específicos do tipo Ogre, ausentes em *Vigna* e em *P. acutifolius*.

As frações repetitivas do DNA correspondem a cerca de 45% do genoma total de *P. vulgaris*, sendo 34% correspondentes a regiões pericentroméricas (Fonsêca *et al.,* 2010; Schmutz *et al.*, 2014). Variações nos números de sítios de DNAr são encontradas em diferentes acessos de *P. vulgaris*. Os dois pares de DNAr 5S são bastante conservados, conforme sugerido por Pedrosa-Harand *et al*. (2006). Por outro lado, ao analisarem 37 acessos selvagens e domesticados de *P. vulgaris* pertencentes aos *pools* gênicos Mesoamericano e Andino, os autores observaram uma ampla

variação de sítios de DNAr 35S de 2-4 a 6-9, respectivamente. Isso é, provavelmente, resultado de uma recombinação ectópica (não-homóloga) ao longo da evolução desses clados, que poderia ter favorecido a localização dos sítios de 35S nas regiões terminais cromossômicas. Fonsêca *et al*. (2010) identificaram, por sua vez, três pares cromossômicos portadores de 35S (cromossomos 6, 9 e 10) no cultivar BAT93. Apesar dos cromossomos 9 e 10 apresentarem sítios maiores, o cromossomo 6 é conservado entre as espécies previamente analisadas, *P. vulgaris, P. lunatus*, *P. microcarpus* e *P. leptostachyus,* sendo considerado o provável cromossomo ancestral do cariótipo do gênero (Almeida e Pedrosa-Harand, 2013; Fonsêca e Pedrosa-Harand, 2013; Fonsêca *et al.*, 2016).

Os centrômeros de *P. vulgaris* são compostos por sequências-satélite Cent*Pv*1 (conhecidas como Nazca) e Cent*Pv*2 *(*Iwata-Otsubo *et al.,* 2013). O DNA satélite CC4, similar à sequência intergênica espaçadora (IGS-like) do DNAr 35S, está presente em dois a quatro pares cromossômicos de *P. vulgaris* e *P. coccineus,* sendo hibridizados em espécies que não fazem parte do grupo Vulgaris e em espécies de outros gêneros. Isso sugere, portanto, que o DNAr 35S divergiu e tornou-se homogeneizado por evolução em concerto (genes parálogos de uma mesma espécie apresentam similaridade de sequência maior um ao outro quando comparados a genes ortólogos) como uma sequência CC4 distinta no grupo Vulgaris que se tornou um satélite independente (Almeida *et al*., 2012). Ainda, sequências de DNA satélite gênero-específica *khipu* (unidades de repetição de 588 pb) foram distribuídas desigualmente nas regiões subterminais dos cromossomos de *P. vulgaris*, enquanto as sequências repetitivas *PvMeso* foram restritas à região subtelomérica do cromossomo 7 em acessos Mesoamericanos. A sequência telomérica de plantas TTTAGGG foi encontrada, por sua vez, na extremidade de todos os cromossomos de *P. vulgaris* (revisado por Fonsêca e Pedrosa-Harand, 2017). Ribeiro *et al.* (2019) localizaram os retrotransposons Ogre e Chromovirus (correspondentes a 24% do genoma total), majoritariamente, nas regiões pericentroméricas de *P. vulgaris*, confirmando o acúmulo de sequências repetitivas nas regiões próximas ao centrômero dessa espécie, como proposto por Fonsêca *et al.* (2010).

Dentro de *Vigna*, variações nos números de sítios de DNAr são encontradas em diferentes espécies. Sítios de DNAr 5S mantêm-se menos variáveis (dois a seis sítios) entre espécies. Diferentemente, para o DNAr 35S, há uma variação de dois a 14 sítios reportadas em *V. aconitifolia* e *V. unguiculata*, respectivamente (Vasconcelos

et al., 2015; She *et al*., 2015). Já *V. angularis* possui dois ou quatro sítios de 5S e seis sítios de 35S (Choi *et al*., 2013; She *et al.*, 2015). Esses dados de variação de sítios DNAr fornecem, portanto, suporte acerca dos processos cromossômicos evolutivos entre as espécies de *Vigna* (Raskina *et al*., 2004; Lysak *et al*., 2006; Schubert, 2007; She *et al*., 2015).

As frações repetitivas do DNA correspondem a cerca de 43% e 50% do genoma total de *V. angularis* e *V. unguiculata*, respectivamente (Kang *et al*., 2015; Lonardi *et al*., 2019). Recentemente, Ribeiro *et al.* (2019) identificaram 8,8% do genoma de *V. angularis* correspondendo a retrotransposons LTR, sendo majoritariamente (2,2%) do tipo *Ty1-Copia.* Ainda, os autores identificaram um único DNA satélite VigSAT 174 (com 174 pb) no genoma dessa espécie. Esse DNA satélite também foi encontrado em *V. nakashimae* e *V. radiata*, e não foi encontrado nas espécies de *Phaseolus* analisadas (*P. vulgaris, P. acutifolius e P. coccineus*), sendo, portanto, gênero-específico. Trabalhos citogenéticos envolvendo a análise de sequências de DNA satélite e retroelementos são, contudo, majoritariamente descritos em *V. unguiculata*. A sequência centromérica repetida em tandem DraI, de 488 pb, foi previamente relatada em todos os cromossomos de *V. unguiculata*, não sendo identificada em outras espécies *de Vigna* e em outras leguminosas sendo, portanto, espécie-específica (Galasso *et al*., 1995). Galasso *et al*. (1997) visualizaram os retrotransposons *Ty1-copia*, estando uniformemente dispersos em todos os seus cromossomos, com exceção das regiões teloméricas, subteloméricas e das regiões organizadoras de nucléolo (RONs). Iwata-Otsubo *et al*. (2016) identificaram sequências repetitivas semelhantes à IGS de DNAr 35S nos cromossomos dessa espécie. Além disso, os autores identificaram estruturas cromossômicas exclusivas e altamente distintas em regiões pericentroméricas e teloméricas de cromossomos mitóticos e paquitênicos de *V. unguiculata*, que foram ausentes em *P. vulgaris*. Foram encontrados pelo menos dois tipos diferentes de elementos retrotransponíveis LTR (Gypsy-Ty3) com padrões semelhantes de distribuição, tanto nos *knobs* heterocromáticos como dispersos pelo centrômero dos cromossomos, além de sequências centroméricas de 455 pb repetidas em tandem encontradas em sete dos 11 pares cromossômicos. As regiões de *knobs* heterocromáticos no genoma de caupi apresentaram uma colocalização com sítios de DNAr 18S e com 5-mc (5-metilcitosina).

Esses dados permitiram, assim, um maior conhecimento sobre a organização genômica dos feijões *Vigna e Phaseolus,* acelerando o desenvolvimento de pesquisas genéticas, a associação entre mapas genéticos e físicos, bem como a análise comparativa entre os feijões e outras leguminosas economicamente importantes.

2.5.2.1 BAC-FISH e mapas citogenéticos

Estudos envolvendo a construção de mapas genéticos, citogenéticos e de sequenciamento têm sido bastante úteis na localização de genes que controlam características de importância agronômica, além de permitirem uma análise comparativa ou de sintenia entre as espécies, possibilitando uma maior compreensão acerca dos mecanismos evolutivos entre os genomas de plantas (Ha *et al*., 2012; Andargie *et al*., 2013).

Os mapas genéticos têm sido comumente integrados aos mapas citogenéticos mediante a utilização de clones de BACs, previamente selecionados a partir de marcadores moleculares localizados no mapa genético de determinada espécie de interesse, que são utilizados como sondas em FISH (Iwata-Otsubo *et al*., 2016; revisado por Jiang, 2019). Estudos BAC-FISH comparativos têm sido reportados em diversas espécies vegetais, incluindo trigo, algodão, mamão, batata, tomate, cenoura e maracujá (Zhang *et al.,* 2004; Wang *et al.,* 2006; Iovene *et al.,* 2008. 2011; Snizay *et al.,* 2012; Gaiero *et al.,* 2017; Sader *et al.,* 2019). A técnica de BAC-FISH tem sido bastante útil em estudos de organização cariotípica, evolução genômica, macrossintenia e colinearidade entre espécies proximamente relacionadas e para correlacionar determinada marca genética a regiões de eu- e heterocromatina, bem como sua localização física ao longo do cromossomo. Além disso, essa técnica permite identificar discrepâncias entre os mapas genéticos/ de sequenciamento e citogenéticos. Ainda, podem sofrer distorções por não levarem em consideração as regiões heterocromáticas, já que essas ocupam, em geral, regiões significativas nos cromossomos de espécies vegetais. Já que os mapas genéticos baseiam-se nas frequências de recombinação e indicam a distância relativa entre duas marcas gênicas (em centimorgan, cM), os mapas citogenéticos indicam a localização exata de determinada marca em um cromossomo (em µm) e, por isso, são bastante úteis em estudos de organização cariotípica e evolução genômica entre espécies relacionadas (Jiang e Gill, 2006; Jiang, 2019).

O mapa físico do feijão comum, iniciado por Pedrosa *et al.* (2009), que mapearam fisicamente 3 cromossomos dessa espécie, foi estabelecido por Fonsêca *et al*. (2010). Em seguida, a biblioteca de sondas BACs de *P. vulgaris* foi utilizada em estudos carioevolutivos dentro do gênero, como em *P. lunatus* (Bonifácio *et al*., 2012; Almeida e Pedrosa-Harand, 2013), *P. microcarpus* (Fonsêca e Pedrosa-Harand, 2013) e *P. leptostachyus* (Fonsêca *et al*., 2016). De maneira geral, foi observado um alto grau de macrossintenia compartilhada dentro do gênero, com exceção da comparação entre *P. vulgaris e P. leptostachyus* (2*n* = 20), em que foram observadas diversas translocações envolvendo oito pares cromossômicos dessas espécies, provavelmente relacionadas a eventos de disploidia descendente e instabilidade cariotípica em *P. leptostachyus.*

Em *Vigna,* o primeiro mapeamento BAC-FISH comparativo foi realizado por Vasconcelos *et al*. (2015). Os autores realizaram a análise comparativa utilizando o bacteriófago SJ19.12, relacionado a gene de resistência à antractonose, e 19 BACs de *P. vulgaris* que foram hibridizados nos 11 pares cromossomômicos metafásicos mitóticos de *V. unguiculata.* Uma conservação parcial da macrossintenia foi observada entre as duas espécies, sendo identificados rearranjos cromossômicos envolvendo cinco cromossomos de *V. unguiculata* (cromossomos 1, 2, 3, 5 e 8), como translocações, duplicações e inversões. Ainda, os autores ratificaram a viabilidade da técnica de BAC-FISH como uma abordagem promissora para estudos carioevolutivos entre espécies relacionadas. Posteriormente, Iwata-Otsubo *et al*. (2016) além de identificar estruturas heterocromáticas cromossômicas altamente distintas no genoma do feijão-caupi, também integraram os mapas genético e físico dessa espécie utilizando 22 sequências cópia-única de *V. unguiculata* como sondas em cromossomos paquitênicos, mediante BAC-FISH. É necessário, portanto, extrapolar o número de espécies estudadas, a fim de que se possa traçar uma história evolutiva mais completa dos feijões *Vigna* e *Phaseolus.*

Essas análises conjuntas fornecem, então, um conhecimento detalhado acerca da homeologia cromossômica, macrossintenia, identificação de rearranjos cromossômicos, organização e evolução genômica entre as espécies analisadas (Jiang e Gill *et al*., 2006; Belarmino *et al*., 2012). Apesar dos progressos extensivos nos estudos de organização genômica/cromossômica das espécies de *Vigna* e *Phaseolus* e da confiabilidade da técnica de FISH para a identificação de cromossomos específicos, a maioria das sondas têm se limitado a sequências

repetitivas ou a clones de DNA genômico de insertos, como os BACs (Findley *et al*., 2010). Principalmente em plantas, que possuem genomas com grande quantidade de DNA repetitivo, a identificação de cromossomos de maneira individual é ainda mais laboriosa e desafiadora (Suzuki *et al*., 2012).

2.6 PINTURA CROMOSSÔMICA EM PLANTAS

Desde o seu desenvolvimento, na década de 90, a pintura cromossômica (PC) tem sido realizada, com sucesso, em diferentes espécies animais, como aves, répteis, insetos e mamíferos, sendo aplicada, pela primeira vez, em cromossomos do cariótipo humano (Speicher *et al*., 1996). Essa técnica tem sido considerada uma ferramenta valiosa para a citogenética clínica, na identificação de rearranjos intercromossômicos, bem como em estudos detalhados de organização da cromatina e evolução genômica, pois permite a visualização de segmentos cromossômicos ou de cromossomos inteiros mediante sondas de DNA cromossomo-específica (Ferguson-Smith e Trifonov, 2007).

As sondas de PC podem ser desenvolvidas utilizando duas abordagens principais, baseadas em microdissecção cromossômica ou em citometria de fluxo. Ambas são eficazes na produção de sondas tanto em humanos como em animais, já que esses organismos apresentam o genoma amplamente eucromático. Em plantas, por outro lado, essas metodologias não são eficientes devido à alta quantidade de DNA repetitivo presente no genoma de vegetais superiores (Fuchs *et al*., 1996).

Em plantas, a PC baseada em BAC-FISH foi realizada, pela primeira vez, em *Arabidopsis thaliana* (L.) Heynh. (Lysak *et al*., 2001). Para isso, os autores utilizaram cerca de 140 BACs derivados do par cromossômico 4 dessa espécie, que foram reunidos em oito conjuntos e rearranjados em dois agrupamentos maiores, permitindo, assim, “pintar” os braços curto e longo desse cromossomo. As regiões de heterocromatina pericentromérica foram excluídas por apresentarem sequências dispersas e repetitivas que hibridizaram em outros cromossomos do cariótipo.

Posteriormente, estudos de evolução cariotípica e de organização genômica, baseados em PC multicor, foram realizados dentro da família Brassicaceae Burnett., sendo possível identificar os mecanismos relacionados à redução de número cromossômico, como inversões e translocações, além de pontos de quebra e perda

de segmentos cromossômicos em diferentes espécies dessa família (Lysak *et al*., 2005; 2006; Mandáková e Lysak, 2008; Lysak e Mandáková, 2010). Similarmente, a PC comparativa baseada em BACs também foi utilizada para reconstruir a evolução cromossômica do gênero *Brachypodium* P. Beauv. (Idziak *et al*., 2011; Betekhtin *et al*., 2014; Lusinka *et al*., 2018).

Apesar de ser uma ferramenta útil para estudos evolutivos, a PC só foi eficaz nesses trabalhos pois *A. thaliana* e *B. distachyon (*L.) P. Beauv. possuem genomas pequenos (125 Mb e 355 Mb, respectivamente) e amplamente eucromático. Além disso, a maioria dos BACs selecionados e usados continham genes cópia-única ou de baixa cópia. Ainda, os BACs continham uma mínima quantidade de DNA repetitivo que não interferiu na FISH. Em angiospermas, que possuem alta quantidade de sequências repetitivas em seus genomas, há, portanto, uma limitação da PC baseada em BACs em relação ao número e ao tamanho de cobertura dessas sondas de BACs ao longo dos seus cromossomos, bem como a interferência da quantidade de DNA repetitivo na FISH (revisado por Jiang e Gill, 2006; Jiang, 2019).

Uma outra abordagem de PC em plantas é baseada em sequências repetitivas de DNA. Kato *et al*. (2004) foram pioneiros na identificação cromossômica individual em diferentes linhagens de milho, mediante uso de diversas sondas de DNA repetitivo, como sondas teloméricas, centroméricas, DNAr e elementos repetitivos dispersos. A mesma abordagem também foi utilizada para identificação de cariótipos de milhos e teosintos proximamente relacionados (Albert *et al*., 2010). Apesar da sua aplicabilidade, a PC baseada em sequências repetitivas é limitada, sendo, muitas vezes, gênero-específica ou espécie-específica, não podendo ser extrapolada em estudos de sintenia entre espécies próxima e/ ou distintamente relacionadas.

2.6.1 Oligo-FISH em plantas

Técnicas citomoleculares avançadas associadas a ferramentas bioinformáticas têm permitido, por sua vez, a síntese de oligonucleotídeos (oligos) que são utilizados como sondas para FISH (Oligo-FISH). Beliveau *et al*. (2012) descreveram uma tecnologia de nova geração (NG) baseada na síntese *de novo* de milhares de oligos independentes, mediante plataforma de bioinformática. Os autores mostraram a eficácia das sondas de oligopinturas na identificação de regiões de 7,6 Mb no cromossomo X humano, utilizando cerca de 60.000 oligos, além de uma região de 20

Mb em cromossomos politênicos de *Drosophila*, coberta por cerca de 75.000-180.000 oligos. Essa tecnologia de FISH de NG gerou novas possibilidades para a identificação cromossômica de maneira precisa e individual em plantas, permitindo, portanto, uma nova perspectiva para o desenvolvimento de pinturas cromossomo-específicas em espécies vegetais, contornando as restrições da PC baseada em BACs ou em sequências repetitivas.

Han *et al*. (2015), pioneiros na PC em plantas, desenvolveram um *pipeline* de bioinformática para a seleção e montagem de oligos específicos a partir dos cromossomos 3 e 7 do pepino (*Cucumis sativus* L.), que foram marcados como sondas para a PC em diferentes espécies de *Cucumis* L. Assim, foi possível identificar esses cromossomos nas diferentes espécies diploides e poliploides do gênero, além de permitir a localização de cromossomos homeólogos em híbridos interespecíficos, importantes para a aplicação de germoplasma selvagem no melhoramento genético vegetal.

Após o trabalho de Han *et al*. (2015), a PC baseada em Oligo-FISH tem sido reportada em diferentes espécies vegetais, como em outras espécies de *Cucumis* (Zhao *et al.,* 2019; Bi *et al.,* 2020), morango (Qu *et al*., 2017), batata (Braz *et al*., 2018; He *et al*., 2018), arroz (Hou *et al*., 2018; Liu *et al*., 2019), espécies pertencentes ao gênero *Populus* (Xin *et al*., 2018; 2010), cana-de-açúcar (Meng *et al*., 2018, 2020), banana (Simoníková *et al.,* 2019), milho (Albert *et al*., 2019; do Vale Martins *et al*., 2019) e trigo (Song *et al.,* 2020).

Braz *et al*. (2018) desenvolveram um novo sistema de identificação cromossômica em Solanaceae Juss., através da seleção de um conjunto de 55.000 oligos cópia-única, associados a 26 regiões cromossômicas específicas do genoma de *Solanum tuberosum* L. Essas regiões foram utilizadas como um código de barras para identificar, distintamente, os $n = x = 12$ cromossomos do cariótipo de diferentes espécies selvagens diploides e poliploides cultivadas e selvagens de batatas. Esse padrão de bandeamento de código de barras mostrou-se útil e eficaz para identificar os rearranjos cromossômicos dentro de *Solanum* L., além de diferenciar os cromossomos homeólogos entre as espécies relacionadas que divergiram do gênero há 7 e 15 Ma, como o tomate e a berinjela, respectivamente.

Beliveau *et al*. (2015) utilizaram sondas de oligos baseadas em SNPs para visualizar, distintamente, cromossomos parentais animais. Os autores utilizaram oligopinturas haplótipo-específicas, com 2 a 3 SNPs de variação, para identificar os

dois cromossomos do genoma parental em metáfases de híbridos de ratos e em *Droposhila*. Recentemente, do Vale Martins *et al*. (2019) utilizaram abordagem similar de sondas haplótipo-específicas para identificar, pela primeira vez em plantas, cromossomos homeólogos em milhos híbridos. As sondas utilizadas foram baseadas em sequências PAV (Presença/Ausência de variação) e SNPs, com 1 a 5 SNPs de variação. Os cromossomos parentais de duas linhagens puras do milho, B73 e Mo17, foram identificados tanto no milho híbrido F_1, como em 58 indivíduos da geração F_2. Além disso, essas sondas permitiram localizar diferentes pontos de recombinação próximos ao centrômero de 10 indivíduos de população IBMRILs (Intermated B73 x Mo17, linhagens recombinantes endogâmicas entre B73xMo17), sugerindo acúmulo de *crossing over* e localização de potenciais alelos favoráveis nessa população.

A técnica de Oligo-FISH apresenta, portanto, eficácia, resolução e versatilidade superiores quando comparada às demais técnicas citogenéticas vegetais que utilizam sondas baseadas em BACs ou em DNA repetitivo, como sondas teloméricas e centroméricas. São sondas curtas (de 20 a 50 pares de bases), de fitas simples e fácil hibridização. Além disso, estas sondas podem ser desenhadas baseadas em sequências conservadas, sendo bastante úteis na identificação de cromossomos homeólogos em diferentes espécies ou subespécies vegetais. Essas sondas baseadas em oligos necessitam de um genoma previamente sequenciado da espécie-alvo ou espécie proximamente relacionada e podem ser desenhadas ou projetadas especificamente para cobrir o genoma inteiro, parte do cromossomo, múltiplas regiões de um cromossomo ou diferentes regiões cromossômicas, a depender do objetivo-alvo da pesquisa. Um ponto negativo é que as sondas usadas na Oligo-FISH apresentam um maior custo na produção quando comparadas às demais sondas tradicionais que precisam de sequenciamento de alta cobertura para a espécie em questão ou proximamente relacionada a ela (Han *et al*., 2015; Jiang, 2019).

4 RESULTADOS

4.1 ARTIGO 1 - BAC- AND OLIGO-FISH MAPPING REVEALS CHROMOSOME EVOLUTION AMONG *VIGNA ANGULARIS*, *V. UNGUICULATA* AND *PHASEOLUS VULGARIS*

Lívia do Vale Martins[1], Fernanda de Oliveira Bustamante[1], Ana Rafaela da Silva Oliveira[1], Antônio Félix da Costa[2], Lidiane de Lima Feitoza[3], Qihua Liang[5], Hainan Zhao[6], Ana Maria Benko-Iseppon[1], María Muñoz-Amatriaín[5], Andrea Pedrosa-Harand[4], Jiming Jiang[6,7], Ana Christina Brasileiro-Vidal[1]✉

[1]Departmento de Genética, Universidade Federal de Pernambuco, Recife, PE, Brazil
[2]Instituto Agronômico de Pernambuco, Recife, PE, Brazil
[3]Departmento de Ciências Biológicas, Universidade Federal do Piauí, Teresina, PI, Brazil
[4]Departmento de Botânica, Universidade Federal de Pernambuco, Recife, PE, Brazil
[5]Department of Soil and Crop Sciences, Colorado State University, Fort Collins, CO, USA
[6]Department of Plant Biology, Michigan State University, East Lansing, MI 48824, USA
[7]Department of Horticulture, Michigan State University, East Lansing, MI 48824, USA

✉ Corresponding author: brasileirovidal.ac@gmail.com

Lívia do Vale Martins - ORCID: 0000-0003-4645-9055
Fernanda de Oliveira Bustamante - ORCID: 0000-0002-2826-5217
Ana Rafaela da Silva Oliveira - ORCID: 0000-0002-4815-0185
Antônio Félix da Costa - ORCID: 0000-0001-9866-3504
Qihua Liang - ORCID: 0000-0003-3467-8103
Lidiane de Lima Feitoza – ORCID: 0000-0001-7884-7058
Ana Maria Benko-Iseppon - ORCID: 0000-0002-0575-3197
María Muñoz-Amatriaín - ORCID: 0000-0002-4476-1691
Andrea Pedrosa-Harand - ORCID: 0000-0001-5213-4770
Jiming Jiang – ORCID: 0000-0002-6435-6140
Ana Christina Brasileiro-Vidal - ORCID: 0000-0002-9704-5509

Artigo submetido ao periódico Chromosoma

Abstract

Cytogenomic resources have accelerated synteny and chromosome evolution studies in plant species, including legumes. Here, we established the first cytogenetic map of *V. angularis* (*Va*, subgenus *Ceratotropis*) and compared with *V. unguiculata* (*Vu*, subgenus *Vigna*) and *P. vulgaris* (*Pv*) by BAC-FISH and chromosome painting approaches. We mapped 19 *Vu* BACs and 35S rDNA probes to the 11 chromosome pairs of *Va*, *Vu* and *Pv*. *Vigna angularis* shared high degree of macrosynteny with *Vu* and *Pv*, with five conserved syntenic chromosomes. Additionally, we developed two oligo-based chromosome painting probes (*Pv*2 and *Pv*3) that were used to paint *Vigna* ortholog chromosomes. We confirmed two reciprocal translocations (chromosomes 2 and 3; 1 and 8) that have occurred after *Vigna* and *Phaseolus* divergence (~9.7 Mya). Besides, two inversions (2 and 4) and one translocation (1 and 5) have occurred after *Vigna* and *Ceratotropis* subgenera separation (~3.6 Mya). We observed distinct oligopainting patterns for chromosomes 2 and 3 of *Vigna* species, with different breakpoints confirmed for *Va*2 and *Vu*2. Both *Vigna* species shared similar major rearrangements when compared to *Pv*: one translocation (2 and 3) and one inversion (chromosome 3). The sequence synteny identified additional inversions and/or transpositions involving pericentromeric regions of chromosomes 2 and 3. We believe these chromosomes are hotspots of rearrangements within and between *Vigna* and *Phaseolus*. We propose centromere repositioning for chromosome 2 during *Vigna* evolution. Our BAC- and oligo-FISH mapping contributed to physically trace the chromosome evolution of *Vigna* and *Phaseolus* and its application in further studies of both genera.

Keywords: BAC-FISH, beans, chromosomal rearrangements, karyotype evolution, macrosynteny, oligopainting

Funding

This research was supported by CNPq (Conselho Nacional de Desenvolvimento Científico e Tecnológico) Grant no. 442019/2019-0, 421968/2018-4, 433931/2018-3, 310804/2017-5,310871/2014-0, and 313527/2017-2); and FACEPE (Fundação de Amparo à Ciência e Tecnologia do Estado de Pernambuco) APQ- 0409-2.02/16. The doctorate scholarship and a doctorate abroad scholarship were provided by CAPES (Coordenação de Aperfeiçoamento de Pessoal de Nível Superior), Finance Code 001 and Project no. 88881.189152/2018-01), respectively.

Conflicts of interest

The authors declare that they have no conflicts of interest.

Ethics approval

Not applicable.

Availability of data and material

All data generated during this study are available in this published paper and its Supplementary Information files.

Author's Contributions

LVM: performed the BAC- and oligo-FISH experiments and wrote the paper. FOB and ARSO: helped to perform the experiments. AFC: performed seed multiplication. QL: analyzed the sequence synteny data. HZ: designed the oligo-FISH probes. APH and FOB: conceived the oligo probes. MMA and TC: maintained and provided *V. unguiculata* BAC clones. JJ: provided the resources for the oligo-FISH experiments. APH, LLF, AMBI, and JJ: planed the experiments and discussed the results. ACBV: doctorate supervisor of LVM, designed and directed the research, and helped to write the paper. All authors read, discussed, and approved the final version of the paper.

Introduction

Current advances in genomics and bioinformatics, including next-generation sequencing technologies, have allowed progress on molecular cytogenetic studies of synteny and chromosome evolution in plant species (Chèvre et al. 2018). Genome sequencing of the model legumes *Lotus japonicus* (Regel) K. Larsen (Sato et al. 2008), *Medicago truncatula* Gaertn. (Young et al. 2011; Tang et al. 2014), and *Glycine max* (L.) Merr. (Schmutz et al. 2010; Valliyodan et al. 2019) opened the door for legume genome research, accelerating the study of genomic organization and evolution of Leguminosae Juss. family, which is the second and the third-largest angiosperm family in terms of economic importance and in species number, respectively (LPWG, 2017).

Phaseolus L. and *Vigna* Savi, with $2n = 2x = 22$ for most species, belong to Phaseolineae subtribe (Leguminosae family, Papilionoideae subfamily, Phaseoloid clade) and have agronomically important species distributed worldwide (Mercado-Ruaro and Delgado-Salinas 1996; Lewis 2005; Delgado-Salinas et al. 2011). The divergence time between both genera is around 9.7 million years ago (Mya) (Li et al. 2013). The reference genome of *P. vulgaris* L. (common bean) (~587 Mb) was the first to be published (Schmutz et al. 2014). For *Vigna*, the first genome assembled was for *V. angularis* (Willd.) Ohwi & Ohashi (adzuki bean, Asiatic-origin, subgenus *Ceratotropis*), which was estimated in ~540 Mb (Sakai et al. 2015). Recently, Lonardi et al. (2019) published the reference genome sequence of *V. unguiculata* (L.) Walp. (cowpea, African-origin, subgenus *Vigna*), estimated in ~640 Mb, and inferred on its synteny relationships with common bean, adzuki bean and mungo bean [*V. radiata* (L.) R. Wilczek]. Genome sequencing, supported by previous genetic and chromosome mapping (Vallejos et al. 1992; Han et al. 2005; Hougaard et al. 2008; Muchero et al. 2009; Wang et al. 2015) has accelerated the knowledge of the agronomic, genetic, and evolutionary studies in *Vigna* and *Phaseolus* beans.

Comparative cytogenetics using BACs (Bacterial Artificial Chromosomes) as FISH (Fluorescent *in situ* Hybridization) probes is a powerful approach for validating synteny, evolution and chromosomal rearrangements in related species (Jiang and Gill 2006). In *Phaseolus*, a cytogenetic map for common bean was established by Fonsêca et al. (2010). Then, *P. vulgaris* BAC library has been used for comparative mapping within the genus, as in *P. lunatus* L. (Bonifácio et al. 2012; Almeida and Pedrosa-Harand 2013) and *P. microcarpus* Mart. (Fonsêca and Pedrosa-Harand 2013), species

with 2*n* = 22, suggesting a high degree of macrosynteny among them with collinearity breaks caused by few inversions. On the other hand, in the *P. vulgaris* and *P. leptostachyus* Benth. (2*n* = 20) comparison, nested chromosome fusion and several translocations are related to the descending dysploidy of the later species (Fonsêca et al. 2016). In *Vigna*, the first BAC-based physical mapping was reported by Vasconcelos et al. (2015). The authors performed the comparative analysis by using one bacteriophage (SJ19.12) and 19 *P. vulgaris* BACs hybridized on the 11 pairs of *V. unguiculata* metaphase mitotic chromosomes. Macrosynteny breaks were observed between these two species, by identifying rearrangements involving five *V. unguiculata* chromosomes, as translocations, inversions, and duplication, with major rearrangements involving chromosomes 2 and 3. Later, Iwata-Otsubo et al. (2016) integrated the genetic and physical cowpea maps on *V. unguiculata* pachytene chromosomes by BAC-FISH. Oliveira et al. (2020) generated the first BAC-FISH map to *V. aconitifolia* (Jacq.) Maréchal (*Ceratotropis* subgenus) and compared to *V. unguiculata* and *P. vulgaris* chromosome maps, corroborating chromosomes 2 and 3 as hotspots for chromosomal changes.

BAC-FISH approach has also been used for chromosome painting (CP) research. Nevertheless, the CP based on BACs has been limited to few model plant species with small and largely euchromatic genomes, as crucifers (Lysak et al. 2001, 2005, 2006; Mandaková and Lysak 2008; Mandaková et al. 2010) and *Brachypodium* P. Beauv taxa (Idziak et al. 2014; Betekhtin et al. 2014; Lusinka et al. 2018). The recent development of *de novo* synthesis of single-copy oligonucleotides (oligos) by bioinformatic design has allowed the chromosomal identification and specific chromosomal regions in a more precise and efficient way (Beliveau et al. 2012; Han et al. 2015; reviewed by Jiang 2019). Since then, oligo-based CP and chromosome identification systems have been used for karyotype and chromosomal evolutionary studies in an increased number of socioeconomic plant species and their relatives, as cucumber (Han et al. 2015; Zhao et al. 2019; Bi et al. 2019), strawberry (Qu et al. 2017), potato (Braz et al. 2018; He et al. 2018), rice (Hou et al. 2018; Liu et al. 2019), poplar (Xin et al. 2018; 2019), sugarcane (Meng et al. 2018, 2020), banana (Šimoníková et al. 2019), maize (Albert et al. 2019; do Vale Martins et al. 2019; Braz et al. 2020), wheat (Song et al. 2020), cotton (Liu et al. 2020) and *Citrus* (He et al. 2020).

In *Vigna*, the physical BAC-FISH mapping has been performed only in *V. unguiculata* (Vasconcelos et al. 2015) and *V. aconitifolia* (Oliveira et al. 2020), not being possible to infer the wide chromosome evolution within the genus. Despite the availability of the genetic mapping and the genome assembly of *V. angularis*, there is no cytogenetic mapping established for this species yet. Here, we have established the cytogenetic map of the Asian species *V. angularis* (*Va*) and performed the first oligo-painting in legumes to: (1) improve our knowledge about synteny and chromosomal changes between and within *Vigna* and *Phaseolus*; (2) integrate BAC-FISH, oligopainting cytogenetic map and sequence-based synteny map to a deep analysis of the rearrangements involving the hotspot chromosomes 2 and 3 among *Vigna* and *Phaseolus* species. Our data contribute to a better understanding of the genetic diversity of *Vigna* and *Phaseolus* beans and to trace their chromosome/genome evolution.

Material and Methods

Plant materials

Vigna angularis accession number 1042, *V. unguiculata* cv. BR14-Mulato, and *Phaseolus vulgaris* cv. BRS Esplendor were used in the comparative FISH mapping. Seeds were obtained from IPK (Leibniz Institute of Plant Genetics and Crop Plant Research, Gatersleben, ST, Germany), Embrapa Meio-Norte (Empresa Brasileira de Pesquisa Agropecuária, Teresina, PI, Brazil), and Embrapa Arroz e Feijão (Santo Antônio de Goiás, GO, Brazil), respectively, and were multiplied at IPA (Instituto Agronômico de Pernambuco, PE, Brazil).

Chromosome preparation

For mitotic metaphase chromosome preparation, root tips harvested from germinated seeds were pretreated with 2 mM 8-hydroxyquinoline for 4 h and 30 min at 18 °C, fixed in freshly prepared fixative solution (3 methanol:1 glacial acetic acid, v/v) for 24 h at room temperature, and stored at −20 °C until use. The root tips were digested with an enzymatic solution containing 4% cellulase (Onozuka R-10, Serva), 2% pectolyase (Sigma-Aldrich) and 20% pectinase (Sigma-Aldrich) for 4 h at 37 °C. Slides were prepared according to Carvalho and Saraiva (1993), with minor modifications at the final steps: after air drying, the slides were immersed in 45 % acetic acid for 10 s and dried at 37 °C.

BAC clone library and probe labeling

Information from *V. unguiculata* BAC library anchored to linkage groups previously generated by Muchero et at. (2009) was provided by the University of California, Riverside, CA, USA. First, we selected and tested a set of 40 BACs belonging to the *V. unguiculata* BAC library, 21 of which were previously selected and mapped in the *V. unguiculata* pachytene chromosomes (Iwata-Otsubo et al. 2016). Nineteen BAC clones generated single-copy signals on *V. unguiculata* donor species, seven of them being used for the first time in this work (asterisk marks, Table 1). For genome comparisons, *V. unguiculata* BAC probes were then hybridized for the first time to identify the mitotic chromosome pairs of *V. angularis* and *P. vulgaris* chromosomes (Table 1, top panel). The remaining 21 BACs that generated repetitive or no FISH signals were excluded (Table 1, bottom panel). Besides, a 35S rDNA probe from *Arabidopsis thaliana* (L.) Heynh. (6.5 kb fragment of 18S-5.8S-25S rDNA repeat unit) was used for FISH analysis (Wanzenböck et al. 1997). DNA of individual BAC clones and 35S rDNA were extracted using the Plasmid Mini Kit (Qiagen), following the manufacturer's instructions. BAC DNA was directly labeled with Cy3-dUTP (GE Healthcare) and 35S rDNA probe was indirectly labeled with digoxigenin-11-dUTP (Roche Diagnostics), both by nick translation (ThermoFisher Scientific).

Table 1. List of the *Vigna unguiculata* BAC clones selected, tested, and used in the comparative BAC-FISH mapping among *V. unguiculata, V. angularis* and *P. vulgaris.* BAC clones were mapped and identified in their corresponding chromosome (Chr) arm and position of *V. unguiculata* (*Vu*), *V. angularis* (*Va*) and *P. vulgaris* (*Pv*) chromosomes, in addition to pseudomolecules for *V. angularis*. Top panel indicates the 19 *V. unguiculata* BACs with unique signals used for FISH analysis. Bottom panel indicates the 21 *V. unguiculata* BACs with disperse or no FISH signals that were excluded of our FISH analysis

BAC	Chr(arm)/ position in *Vu* [a]	Chr(arm)/ position in *Va* [b]/ *Va* Pseudomolecule [c]	Chr(arm)/ position in *Pv*
H004H23*	*Vu*1(L)/ Interstitial	*Va*1(L)/ Subterminal/ 7	*Pv*1(L)/ Interstitial
H074C16	*Vu*2(L)/ Proximal	*Va*2(S)/ Interstitial/ 10	*Pv*3(S)/ Terminal
M026L23	*Vu*2(L)/ Terminal	*Va*2(L)/ Terminal/ 10	Pv2(S)/ Subterminal
H031G07*	*Vu*3(S)/ Interstitial	*Va*3(S)/ Interstitial/ 1	*Pv*2(L)/ Interstitial
H050P11*	*Vu*3(L)/ Interstitial	*Va*3(L)/ Interstitial/ 1	*Pv*3(L)/ Interstitial
H049E24	*Vu*4(S)/ Terminal	*Va*4(S)/ Terminal/ 11	*Pv*4(L)/ Subterminal
H085I15	*Vu*4(L)/ Subterminal	*Va*4(S)/ Subterminal/ 11	No signal
M002E09	*Vu*5(S)/ Interstitial	*Va*5(L)/ Proximal/ 4	No signal
M050F11*	*Vu*5(L)/ Interstitial	*Va*1(S)/ Proximal/ 7	*Pv*8(S)/ Interstitial
H065G04	*Vu*6(L)/ Terminal	*Va*6(L)/ Terminal/ 5	*Pv*6(L)/ Terminal

H088A15	*Vu*7(S)/ Terminal	*Va*7(S)/ Terminal/ 8	*Pv*7(L)/ Terminal
H053I07*	*Vu*7(L)/ Terminal	*Va*7(L)/ Terminal/ 8	*Pv*7(S)/ Terminal
M057N05	*Vu*8(S)/ Interstitial	*Va*8(L)/ Interstitial/ 3	*Pv*1(S)/ Interstitial
H080A10*	*Vu*8(L)/ Interstitial	*Va*8(S)/ Interstitial/ 3	*Pv*8(L)/ Subterminal
H086N19	*Vu*9(S)/ Interstitial	*Va*9(S)/ Interstitial/ 2	*Pv*9(L)/ Subterminal
H010M18	*Vu*9(L)/ Terminal	*Va*9(L)/ Interstitial/ 2	*Pv*9(S)/ Proximal
H015M15	*Vu*10(S)/ Subterminal	*Va*10(S)/ Subterminal/ 9	*Pv*10(S)/ Terminal
H025N06	*Vu*10(L)/ Interstitial	*Va*10(L)/ Interstitial/ 9	*Pv*10(L)/ Interstitial
H092J22*	*Vu*11(S)/ Terminal	*Va*11(S)/ Terminal/ 6	*Pv*11(L)/ Terminal
M062M10	*Vu*1(S)/ Disperse	-	-
H068F14	*Vu*1(S)/ Unique signal	No signal	No signal
H031B04	*Vu*1(S)/ No signal	-	-
H029P08	*Vu*2(S)/ Disperse	-	-
H088H07	*Vu*2(Pericentromeric)/ Disperse	-	-
H094P14	*Vu*2(L)/ No signal	-	-
H019P01	*Vu*3(S)/ No signal	-	-
H037B01	*Vu*3(S)/ Disperse	-	-
M017H06	*Vu*3(Pericentromeric)/ Disperse	-	-
M021E17	*Vu*3(L)/ No signal	-	-
H094L14	*Vu*4(L)/ No signal	-	-
H014O11	*Vu*5(S)/ No signal	-	-
M040D10	*Vu*6(S)/ Disperse	-	-
M015O07	*Vu*6(L)/ Disperse	-	-
M006N15	*Vu*8(S)/ No signal	-	-
H039A20	*Vu*8(L)/ Disperse	-	-
H074C18	*Vu*9(Pericentromeric)/ Disperse	-	-
M054N15	*Vu*11(S)/ Unique signal	No signal	No signal
H075P08	*Vu*11(S)/ Disperse		
H043O18	*Vu*11(Pericentromeric)/ Disperse	-	-
M045J08	*Vu*11(L)/ Disperse	-	-

[a] Chromosomes of *V. unguiculata* are numbered according to Lonardi et al. (2019)
[b] Chromosomes of *V. angularis* are numbered according to their orthology with *V. unguiculata*
[c] *Vigna angularis* pseudomolecules numbering described by Sakai et al. (2015) and used by Lonardi et al. (2019)
* BAC-FISH new data for *V. unguiculata* chromosomes
S- Short arm; L- Long arm

Design, synthesis, and labeling of the oligo-based painting probes

Oligos were designed using *P. vulgaris* (Pvulgaris_442_v2.0) as reference genome from Phytozome v12 (https://phytozome.jgi.doe.gov/) by Chorus2

(https://github.com/zhangtaolab/Chorus2) (Han et al. 2015). Briefly, the genomic sequences were divided into 45 bp oligos in a step size of 5 bp. Chorus2 calculated the uniqueness of each probe in the genome by analyzing the frequency of 17-mers. Oligos with 17-mers that exist more than four times in the genome were discarded. The uniqueness of each oligo was further validated using genomic sequencing data (SRR837020). A total of 143,559 and 140,599 unique oligos specific to chromosomes 2 and 3 (*Pv*2 and *Pv*3) were designed, respectively. From these, we randomly selected 27,000 oligos for each chromosome to be synthesized by Arbor Biosciences company (Ann Arbor, Michigan, USA). *Pv*2 and *Pv*3 oligos were amplified and indirectly labeled by reverse transcription using universal oligonucleotide primers with dual biotin and digoxigenin (www.idtdna.com), respectively (Han et al. 2015).

Fluorescent *in situ* Hybridization

BAC-FISH was carried out according to Fonsêca et al. (2010). For oligo-FISH, we followed the same protocol with modifications: no RNAse addition and stringency washes using 1x PBS (Phosphate Buffered Saline). The hybridization mixture consisted of 50% formamide, 10% dextran sulfate, 2× saline sodium citrate (SSC) and 8 ng/μL for BAC probes or 20-30 ng/μL for oligo probes. The dsDNA (BAC and 35S rDNA labeled probes) was previously denatured for 10 min at 75 °C. For both dsDNA and ssDNA oligo probes, the hybridization mix was directly applied to the slides for 7 min at 75 °C and hybridized for 2-3 days at 37 °C. BAC probes were directly visualized with Cy3-dUTP. 35S biotin-labeled probe was detected using avidin-rhodamine antibody (Vector Laboratories) diluted in 1 % BSA. *Pv*2 and *Pv*3 oligo probes were detected with anti-biotin fluorescein (Vector Laboratories) and anti-digoxigenin rhodamine (Roche), respectively, both diluted in TNB 1x (1M Tris HCl pH 7.5, 3M NaCl, and blocking reagent, Sigma-Aldrich). Chromosomes were counterstained with 2 μg/mL DAPI (4',6-diamidino-2-phenylindole) in Vectashield (Vector Laboratories) antifade solution. For probe detection of different DNA using the same slide, the rehybridization was performed following Heslop-Harrison et al. (1992).

Microscopy, Image Processing and Data Analysis

FISH images were captured using Leica DMLB epifluorescence microscope and a Leica DFC 340FX camera with Leica CW4000 software or using a Hamamatsu CCD camera attached to an Olympus BX51 epifluorescence microscope with Meta Imaging

Series 7.5 software. Chromosomes were identified according to their BAC- and oligo-FISH signal position based on the sequence orthology with *V. unguiculata* (for BACs) and *P. vulgaris* (for oligos). The final image adjustments were optimized for brightness and contrast with the Adobe Photoshop CS3 software. Seven to ten chromosome pairs and their respective BAC- and oligo-FISH signals were measured using DRAWID (https://doi.org/10.3897/compcytogen.v11i4.20830) and Mi*cromeasure 3.3* (http://rydberg.biology.colostate.edu/MicroMeasure/, Colorado State University) supplemented by Microsoft Excel 2010. The oligopainting pattern of *V. angularis* and *V. unguiculata* chromosomes was calculated by dividing the average of the chromosomal total length (µm) by the average length of the oligopaint regions corresponding to *Pv*2 or *Pv*3 probes. Comparative idiograms between *V. unguiculata*, *V. angularis* and *P. vulgaris* were constructed using Adobe Flash CS4 Professional and Adobe Illustrator programs. *P. vulgaris* and *V. unguiculata* idiograms were assembled based on Vasconcelos et al. (2015).

Chromosome numbering identification

Since this is the first cytogenetic map report for *V. angularis* and to facilitate our comparative analysis, we standardized the chromosome numbering of *V. angularis* (*Va*) according to their chromosome orthology with *P. vulgaris* (*Pv*) and *V. unguiculata* (*Vu*) pseudomolecule numbers proposed by Lonardi et al. (2019). We did not follow the *V. angularis* pseudomolecules numbering proposed by Kang et al. (2015) and Sakai et al. (2015). The correspondence between *V. angularis* chromosome and its pseudomolecule numbers is described at Table 1. For the chromosome comparison, we used the species name abbreviations according to their initials followed by their chromosome numbering.

Sequence synteny data

Sequence-based synteny analysis between *P. vulgaris* chromosomes 2 and 3 with *V. angularis* and *V. unguiculata* orthologs were performed as in Lonardi et al. (2019) using MUMmer software package v3.23 (Kurtz et al. 2004). Alignments were generated between two sequences with a minimum length of an exact match of 100 bp and minimum total alignment length of 1 kb. The output alignments between chromosomes were visualized using Circos v0.69-3 (Krzywinski et al. 2009), in which *V. unguiculata* sequences were colored based on synteny with *Pv*2 (green) and *Pv*3 (red).

Results

Development of a chromosomal map of *V. angularis*

For the *V. angularis* (2*n* = 22) cytogenetic map construction, 19 single-copy *V. unguiculata* BACs and 35S rDNA probes were hybridized and located to its 11 metaphase chromosome pairs (Fig. 1b). We then hybridized the same set of BACs to *V. unguiculata* and *P. vulgaris* chromosomes (Fig. 1a, c). For most chromosomes, both short (S) and long (L) arms were identified, except for chromosome 11 of *V. angularis, V. unguiculata* and *P. vulgaris*, *Vu*1S (short arm of *V. unguiculata* chromosome 1), *Va*5S and *Pv*4S, with one BAC each. We were not able to identify *Pv*5 by using *V. unguiculata* probes: BAC M002E09 from *Vu*5S was not hybridized or did not present consistent FISH signal on *P. vulgaris* chromosomes, suggesting it is a *Vigna*-specific marker.

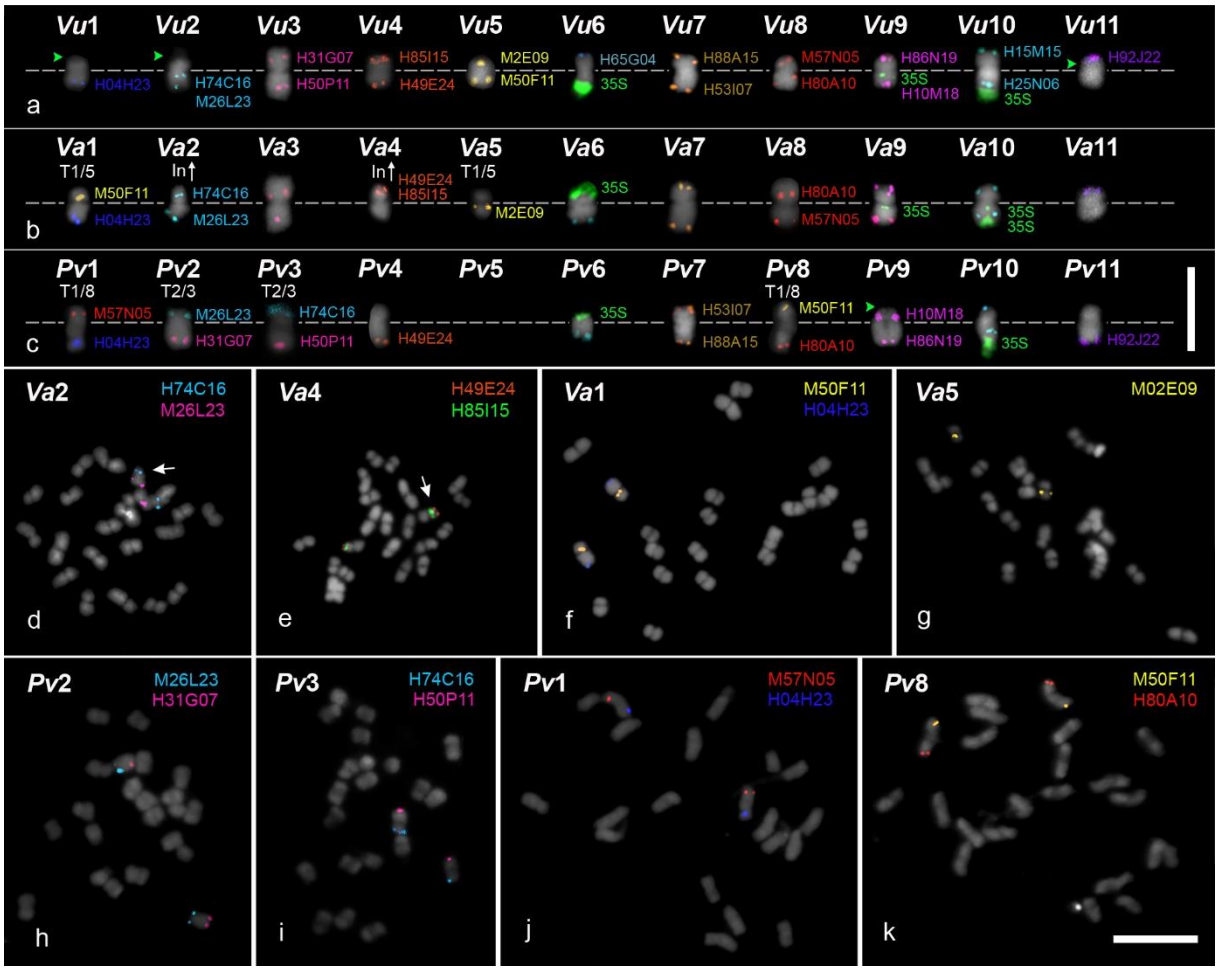

Fig. 1 *Vigna unguiculata* (*Vu*) BAC probes hybridized on the 11 metaphase chromosome pairs of *V. unguiculata* (**a**), *V. angularis* (*Va*) (**b**) and *P. vulgaris* (*Pv*) (**c**), confirming the synteny and showing chromosomal rearrangements among species. *Vigna unguiculata* BACs from the same chromosome are pseudocolored by using the same colors in the short and long arms and named in accordance with their location on *V. unguiculata* chromosomes. Chromosomes are counterstained with DAPI

(pseudocolored in gray). The 35S sites that were not mapped in this work are represented in green arrowheads in *V. unguiculata* and *P. vulgaris*, in accordance with Fonsêca et al. (2010) and Vasconcelos et al. (2015). The centromeres of the chromosomes are aligned by a dotted gray line. Bar in c = 5 µm. **d** Arrow points to the *Vu*2L markers located at the opposite arms of *Va*2 (pericentric inversion). **e** Arrow points to the *Vu* markers located at adjacent position in the *Va*4S (pericentric inversion). **f** translocation represented by M050F11 (yellow) from *Vu*5L and H004H43 (dark blue) from *Vu*1L hybridized on *Va*1. **g** Vu5S BAC located on *Va*5L. **h** M026L23 (light blue) from *Vu*2L and H031G07 (pink) from *Vu*3S hybridized on *Pv*2, indicating a reciprocal translocation in comparison to *Vigna* species. **i** H074C16 (light blue) from *Vu*2L, and H050P11 (pink) from *Vu*3L hybridized on *Pv*3, indicating a reciprocal translocation in comparison to *Vigna* species. **j** M057N05 (red) from *Vu*8S and H004H23 (dark blue) from *Vu*1L hybridized on *Pv*1, indicating a reciprocal translocation in comparison to *Vigna* species. **k** M050F11(yellow) from *Vu*5L and H080A10 (red) from *Vu*8L hybridized on *Pv*8, indicating a reciprocal translocation in comparison *Vigna* species. Bar in k = 10 µm

We identified the 35S rDNA sites distribution on *V. angularis* karyotype (Fig. 1b): one terminal site on *Va*6S, a small proximal site on *Va*9L (long arm of *V. angularis* chromosome 9), one terminal and another smaller proximal sites on *Va*10L. The comparative BAC-FISH mapping and the distribution of the 35S rDNA sites for individual *V. angularis*, *V. unguiculata* and *P. vulgaris* chromosomes was schematically represented as circular idiograms, revealing the macrosynteny relationships and the chromosomal rearrangements among the analyzed species (Fig. 2).

Macrosynteny between *Vigna* species and *P. vulgaris* by BAC-FISH

Overall, five chromosomes (6, 7, 9, 10, and 11) showed a conservation of macrosynteny across the genomes (Figs. 1, 2). However, according to the *V. unguiculata* BAC orientation and position along *P. vulgaris* chromosomes, we highlight the BAC positioning change for the type of chromosome arm for *Va*8, *Pv*4, *Pv*7, *Pv*9, and *Pv*11 when comparing to *V. unguiculata* (Figs. 1, 2). Three *V. angularis* chromosomes (*Va*7, *Va*9, and *Va*10) showed conserved synteny for all markers with their corresponding *P. vulgaris* and *V. unguiculata* chromosomes, although number or position of the 35S rDNA clusters in chromosome 9 and 10 varied between *Phaseolus* and *Vigna*. Additionally, *Va*11 (with one BAC-FISH marker) was orthologous to *Pv*11 and *Vu*11. We also used rDNA probes to the opposite *Va*11 and *Vu*11 chromosome arm identification, but only *Vu*11S carries an interstitial 35S rDNA site (Vasconcelos al. 2015). No rDNA sites were observed in *Va*11.

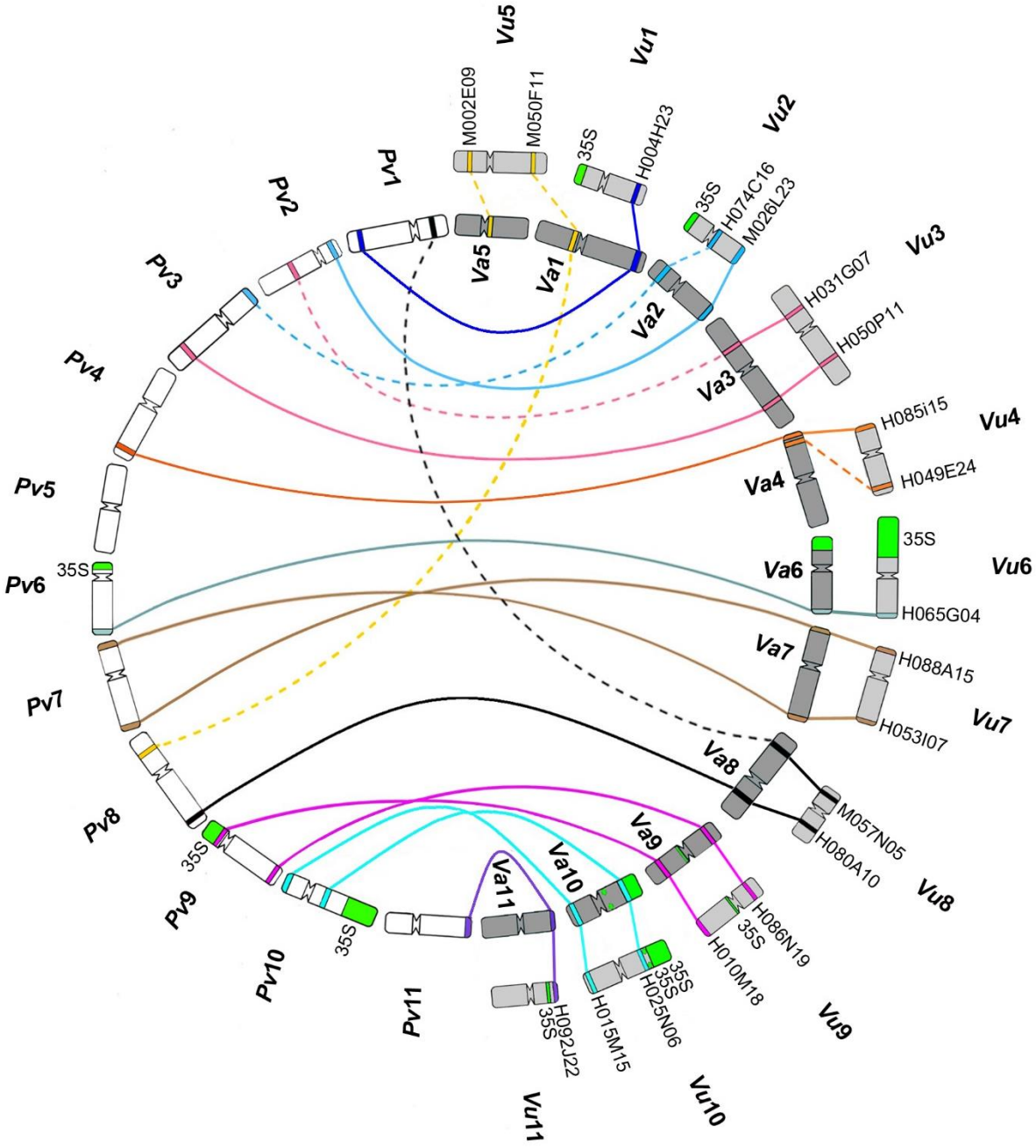

Fig. 2 Circular schematic representation of the comparative BAC-FISH mapping among *P. vulgaris* (*Pv*), *V. angularis* (*Va*) and *V. unguiculata* (*Vu*). *Vigna unguiculata* BACs (named in the right) from the same chromosome are represented by using the same colors in the short and long arms. Chromosomes *Vu*6, *Vu*10, *Va*8 and *Va*10 were inverted to their orientation. 35S rDNA sites are mapped in green. Conservation of synteny is represented by a continuous line, while chromosomal rearrangements are represented by dashed lines. For the rDNA sites location on *P. vulgaris* and *V. unguiculata,* we followed Fonsêca et al. (2010) and Vasconcelos et al. (2015)

Chromosomal translocations between *Vigna* species and *P. vulgaris* by BAC-FISH

We confirmed two translocation events between *Vigna* and *Phaseolus* (Fig. 1h-k). Between *V. angularis* and *P. vulgaris*, we were able to identify a translocation involving chromosomes 1 and 8 (Fig. 1b, c, f, j-k). Between *V. unguiculata* and *P. vulgaris*, three *V. unguiculata* chromosomes (1, 5 and 8) are involved in a complex translocation with two *P. vulgaris* chromosomes (1 and 8): *Vu*8S BAC (M057N05) and *Vu*1L BAC (H004H23) were located at short and long arms of *Pv*1, respectively, while *Vu*5L BAC (M050F11) and *Vu*8L BAC (H080A10) were located at short and long arms of *Pv*8, respectively (Fig. 1j-k). The other translocation involves chromosomes 2 and 3 of *Vigna* species and *P. vulgaris*: *Vu*2L BAC (M026L23) and *Vu*3S BAC (H031G07) were located at short and long arms of *Pv*2, respectively, while *Vu*2L BAC (H074C16) and *Vu*3L BAC (H050P11) were located at short and long arms of *Pv*3, respectively (Fig. 1h-i).

Chromosomal translocation and inversions between *V. angularis* and *V. unguiculata* by BAC-FISH

We confirmed four chromosomes involved in intra- and interchromosomal rearrangements between *V. angularis* and *V. unguiculata*, being two inversions and one translocation (Fig. 1d-g). For the first inversion, BACs from *Vu*2L (H074C16 and M026L23) were hybridized to the opposite arms of *Va*2 (Fig. 1d). We tested other BAC probes from the short and long arms of *Vu*2. Nevertheless, these probes showed dispersed signals in *V. angularis*, *V. unguiculata* and *P. vulgaris* (Table 1, bottom panel). Iwata-Otsubo et al. (2016) suggested that none or very few genetic markers exist for *Vu*2S. On the other hand, for the other inversion, the opposite BAC markers (H049E24 and H085I15) of *Vu*4 were both located at adjacent positions in *Va*4S (Fig. 1e). Also, the hybridization of *Vu*5L BAC (M050F11) and *Vu*1L BAC (H004H23) into the short and long arms of *Va*1 chromosome, respectively, and the hybridization of *Vu*5S BAC (M002E09) on *Va*5L suggest the occurrence of a translocation event between them (Fig. 1f-g) We were not able, however, to identify the short arm of *Va*5, since other *Vu*1 and *Vu*5 BAC probes showed disperse or no FISH signals on *V. unguiculata*, *V. angularis* and *P. vulgaris* chromosomes (Table 1, bottom panel). *Vu*1S BAC H068F14, which presented unique signal on *V. unguiculata*, showed no signal on

V. angularis and *P. vulgaris* (data not shown), suggesting that it is a species-specific marker for *V. unguiculata*.

Validation of translocation and inversion by oligopainting of chromosomes 2 and 3

For a further investigation of the rearrangements involving chromosomes 2 and 3 between genera, we developed oligo-based probes chromosome-specific to *Pv*2 and *Pv*3 and hybridized both on *V. angularis* and *V. unguiculata* ortholog chromosomes (Fig. 3). Probes generated strong FISH signals covering almost the whole *Pv* metaphase chromosomes, with a lack of signals in their pericentromeric regions (Fig. 3a3). Translocation complexes between *P. vulgaris*-*V. angularis* and *P. vulgaris*-*V. unguiculata* were confirmed by the CP, corroborating our BAC-FISH analysis. Additionally, we identified distinct oligopainting patterns for each *V. angularis* and *V. unguiculata* chromosomes. The oligopainting pattern of chromosomes 2 and 3 of *V. angularis* and *V. unguiculata* is represented as idiograms in Fig. 4a-c.

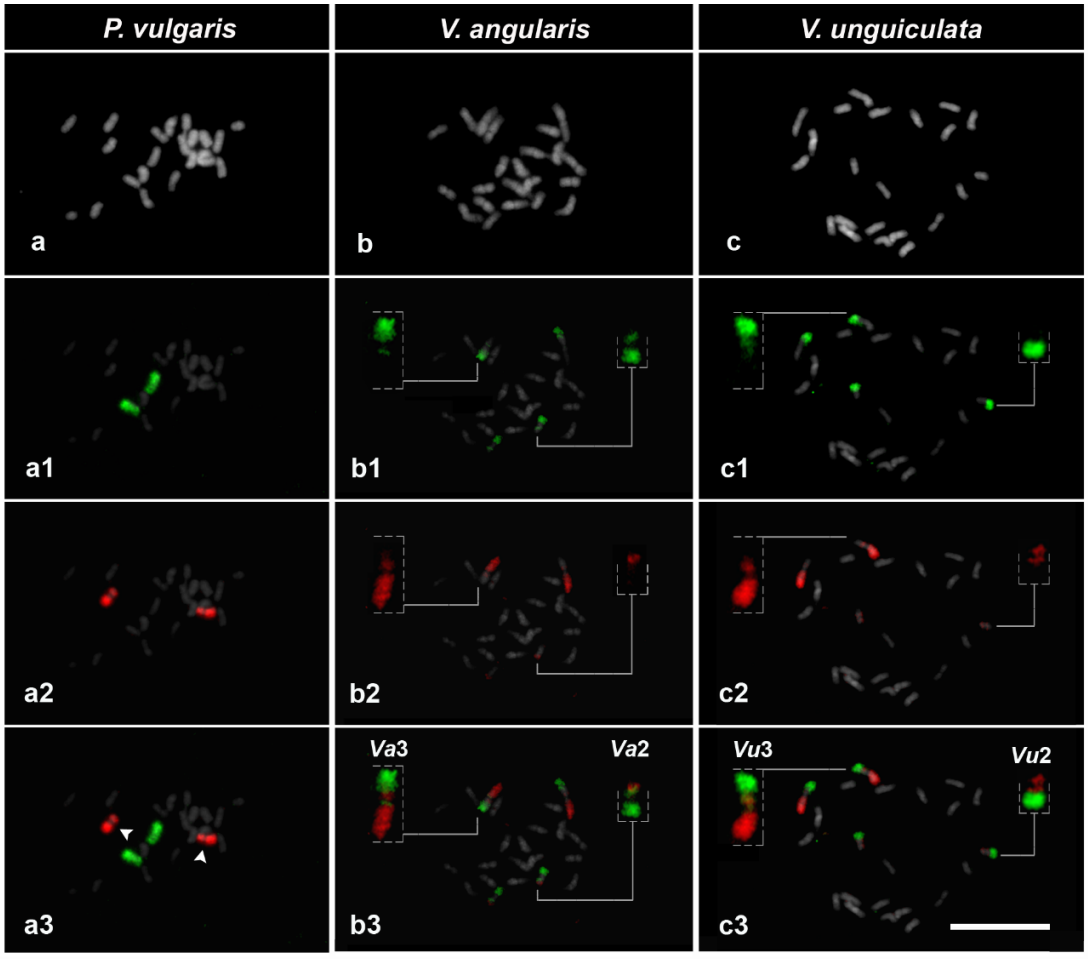

Fig. 3 Oligo-FISH chromosome painting using *Pv*2 (green) and *Pv*3 (red) probes hybridized on metaphase chromosomes 2 and 3 of *V. angularis* (*Va*) and *V. unguiculata* (*Vu*), showing distinct

patterns. Chromosomes are counterstained with DAPI (pseudocolored in gray). **a-a3** *Phaseolus vulgaris* metaphase chromosomes, with *Pv*2 (green; **a1, a3**) and *Pv*3 (red; **a2, a3**) chromosome painting on *P. vulgaris* chromosomes. Arrowheads in **a3** indicate gaps in the FISH signal of the filtered centromeric regions on *Pv*3. **b-b3** *Vigna angularis* metaphase chromosomes, with *Va*2 and *Va*3 chromosomes detailed in the inserts (**b1-b3**). **b3** Merged reciprocal translocation between chromosomes 2 and 3 of *P. vulgaris* and *V. angularis*, highlighting an inversion event on *Va*3. **c-c3** *Vigna unguiculata* metaphase chromosomes, with *Vu*2 and *Vu*3 chromosomes detailed in the inserts (**c1-c3**). **c3** Merged reciprocal translocation between chromosomes 2 and 3 of *P. vulgaris* and *V. unguiculata*, highlighting an inversion event on *Vu*3. Bar = 10 µm

Almost the entire *Va*2 chromosome was hybridized with *Pv*2 probe (green), with the half terminal region of the short arm (23.2 % of the chromosome total length) painted with *Pv*3 probe (in red) (Figs. 3b1-3, 4a). Inversely, the whole *Vu*2S arm and the proximal region of *Vu*2L were hybridized with *Pv*3 probe (red), while almost all the long arm of *Vu*2 (47.3 % of chromosomal total length) was painted with *Pv*2 (green) (Fig. 3c1-3, 4b). A breakpoint was identified at the interstitial region of *Va*2S, but at the proximal region of *Vu*2L. Despite the painting gap at pericentromeric region, the *Va*2 centromere seems to be surrounded by *Pv*2 sequences (green), while the *Vu*2 centromere is embedded in *Pv*3 sequences (red) (Figs. S1 3c, c', 4a). For *Vigna* chromosome 3, besides the 2-3 reciprocal translocation, we also identified an inversion involving a small region close to the centromere of *Va*3 and *Vu*3 chromosomes (Figs. 3b3, c3; 4c). *Va*3 and *Vu*3 seem to have similar, but not identical, painting patterns: the short arms presented a large green segment (*Pv*2) and a small proximal region in red (*Pv*3); the long arms presented a large red region covering almost the whole chromosome arm (*Pv*3), while a proximal region on *Va*3 and a small pericentromeric region on *Vu*3 correspond to *Pv*2 (green).We were not able, however, to identify the exact break point site of these chromosomes. The *Va*3 centromere seems to be surrounded by *Pv*3 sequences (red), while the *Vu*3 centromere is surrounded by *Pv*2 painting sequences (green, from ~26 to 30 Mb in the short arm and from 32 to 34 Mb in the long arm) (Fig. 3c3 and 4b', c').

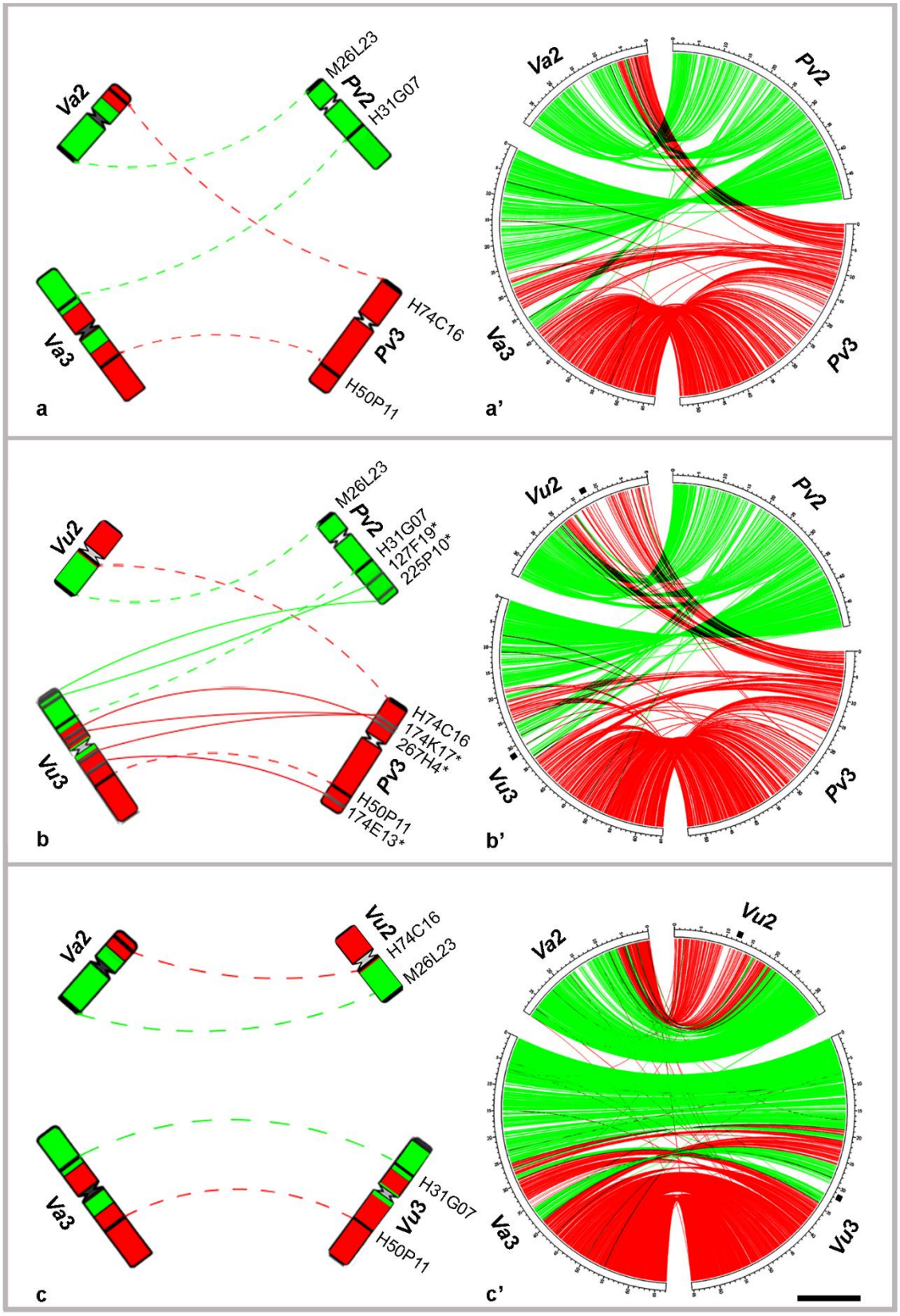

Fig. 4 Integrative FISH mapping and sequence synteny analysis between chromosomes and the pseudomolecules 2 and 3 of *V. angularis* (*Va*) and *P. vulgaris* (*Pv*), *V. unguiculata* (*Vu*) and *P. vulgaris*, and *V. angularis* and *V. unguiculata*. **a-c** Idiograms based on our integrative BAC- and Oligo-FISH mapping. Black blocks represent *Vu*2 (H074C16 and M026L23) and *Vu*3

(H031G07 and H050P11) BACs anchored on *V. angularis, V. unguiculata* and *P. vulgaris* ortholog chromosomes. Gray blocks represent *Pv*2 (127F19 and 225P10) and *Pv*3 (174K17, 267H4, and 174E13) BACs (asterisk marks) anchored on *V. unguiculata* and *P. vulgaris* chromosomes, previously identified by Vasconcelos et al. (2015). Green (*Pv*2) and red (*Pv*3) colors on chromosomes are in accordance with the chromosome painting. Green and red dashed lines represent the rearrangements detected by our cytogenetic mapping. Green and red continuous lines represent the rearrangements found by Vasconcelos et al (2015). **a', b', c'** Sequence synteny between *V. angularis* and *P. vulgaris*, *V. unguiculata* and *P. vulgaris*, and *V. angularis* and *V. unguiculata*, using *V. unguiculata* sequences but colored in accordance to *Pv*2 (green) and *Pv*3 (red) pseudomolecules. Lateral black squares in **c'** represent the centromere of *Vu*2 and *Vu*3 pseudomolecules. Bar =10 Mb

Validation of inversions and transpositions by sequence synteny of chromosomes 2 and 3

Moreover, the sequence-based synteny analysis using the sequence map confirmed the distinct distribution patterns of *Pv*2 and *Pv*3 gene regions on *V. unguiculata* and *V. angularis* chromosomes found by our CP. On *Va*3 and *Vu*3, for instance, *Pv*2 (green) proximal sequences located in the long arm represented 12.3 % and 7.5 % of the pseudochromosomal total lengths, respectively. Besides, sequence synteny data identified additional complex microrearrangements, including several inversions and transpositions mainly involving regions close to the centromere of these two chromosomes, that were not identified by oligo-FISH technique (Figs. S1, 4a', b', c'). Sequence synteny between pseudochromosomes 2 and 3 of *V. angularis* and *V. unguiculata* using *V. unguiculata* sequences showed that these two chromosomes share similar rearrangements when compared to *P. vulgaris* and are macrosyntenic between them, with a great number of micro transpositions and inversions (Figs. S1, 4c'). The chromosomal rearrangements between *Pv*2-*Pv*3 and *Va*2-*Va*3, *Pv*2-*Pv*3 and *Vu*2-*Vu*3 and between *Va*2-*Va*3 and *Vu*2-*Vu*3 were identified in detail by combining the three approaches used in this work. Idiograms representing the integrated FISH mapping (CP using *P. vulgaris* oligo-probes and *V. unguiculata* and previously *P. vulgaris* anchored BACs) were compared with their pseudomolecules using *V. unguiculata* sequences (Fig. 4). Based on the reference genome of *V. unguiculata* (Lonardi et al. 2019), the location of the *Vu*2 and *Vu*3 centromeres is represented in lateral black squares of these pseudomolecules at around 12 and 31 Mb on average, respectively (Figs. S1, 4b', c'). In turn, the *V. angularis* centromeres were not located.

Fig. S1

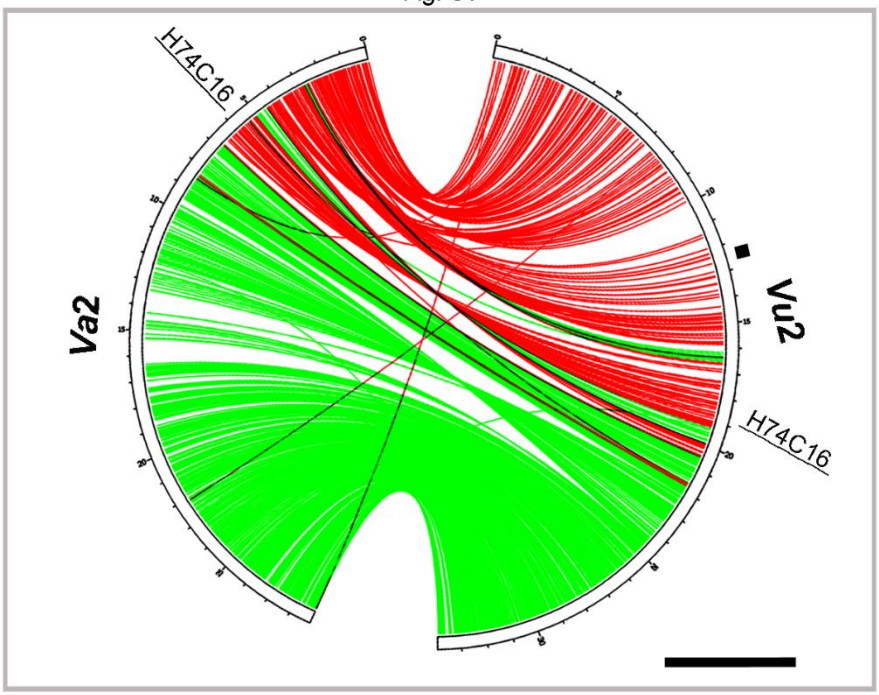

Fig. S1 Detailed sequence synteny between *Vigna angularis* (*Va*) and *V. unguiculata* (*Vu*) pseudomolecules 2 using *V. unguiculata* sequences but colored in accordance with *Pv*2 (green) and *Pv*3 (red). The pericentric inversion, previously identified by our BAC-FISH analysis, was confirmed by our sequence analysis: H074C16 *Vu* BAC is located at 5.6 Mb and 18.7 Mb region of *Va*2 and *Vu*2, respectively, that corresponds to a red region in both species. Lateral black square on *Vu*2 represents the centromere. Bar =5 Mb

Discussion

Despite recent advances in sequencing and genomic platforms in legume species, cytogenetic mapping remains an efficient approach for validating the above methods, and for cytogenomic macro comparison studies of related species. Here, we have established the first cytogenetic map of *V. angularis* and compared it with *V. unguiculata* and *P. vulgaris* for a karyoevolution analysis. Besides, we have developed, for the first time, the CP based on oligo-FISH approach in legumes. We selected *Pv*2 and *Pv*3 since they are recognized as the most rearranged chromosomes between *V. unguiculata* and *P. vulgaris* (Vasconcelos et al. 2015). By combining BAC- and oligo-FISH strategies with sequencing data, it was possible to better understand the macrosynteny and to deeply investigate the chromosomal rearrangements among the studied species.

The chromosome synteny involving five chromosomes (chromosomes 6, 7, 9, 10 and 11) has been well maintained between *Vigna* species and *P. vulgaris*, as observed in previous BAC-FISH mapping between *V. unguiculata* and *P. vulgaris* (Vasconcelos et al. 2015), *V. aconitifolia* and *P. vulgaris* (Oliveira et al. 2020), and confirmed by the sequence-based synteny analysis between cowpea and common bean and between cowpea and adzuki bean (Lonardi et al. 2019). As expected, a higher degree of synteny was observed within *Vigna* species, with seven macrosyntenic chromosomes (3, 6, 7, 8, 9, 10, and 11).

Chromosomal rearrangements are considered evolutionary events that can be used as cytogenetics evidence to trace the genome evolution among related species (Raskina et al. 2008). Structural chromosome changes can be detected by FISH mapping and could be better acknowledged when integrated with molecular and genomic studies of the evolutionary and speciation processes among related species (Wellenreuther and Bernatchez 2018). In this work, we propose that the major and minor rearrangements that led to speciation and the chromosomal evolution between *Vigna* and *Phaseolus* genera (~9.7 Mya; Li et al. 2013) and between *Vigna* and *Ceratotropis* subgenera (~3.6 Mya; Javadi et al. 2011) are: translocations, inversions and transpositions.

Three *V. unguiculata* chromosomes (1, 5, and 8) and two *P. vulgaris* chromosomes (1 and 8) are involved in a reciprocal translocation. According to the sequence synteny between cowpea and common bean, a third *P. vulgaris* chromosome (*Pv*5) is involved in this translocation event (Lonardi et al. 2019). However, we cannot extrapolate this complex translocation rearrangement to other *Vigna* species, since we were not able to physically confirm *Va*5 and *V. aconitifolia* chromosome 5 participation (Oliveira et al., 2020). Comparing *V. angularis* and *V. aconitofolia* (Oliveira et al. 2020) to *P. vulgaris,* only chromosomes 1 and 8 could be identified at the translocation event (Oliveira et al. 2020). *Phaseolus vulgaris* chromosome 5 seems to have few single-copy markers for its identification since no *Pv*5 markers were mapped to other *Phaseolus* nor closely related *Vigna* species (Bonifácio et al. 2012; Fonsêca and Pedrosa 2013; Vasconcelos et al. 2015). Thus, different markers and/or oligopainting probes for chromosome 5 are needed to investigate the karyotypic changes between *Vigna* and *Phaseolus.* Additionally, a reciprocal translocation (1 and 5) was observed within *Vigna* genus as well as in the comparative cytogenetic map for *V. aconitifolia* (Oliveira et al. 2020) and in the

sequence synteny between *V. unguiculata* - *V. angularis* and *V. unguiculata* - *V. radiata* (Lonardi et al. 2019).

The second translocation event between *V. angularis* and *P. vulgaris* involved chromosomes 2 and 3. This translocation, previously detected by Vasconcelos et al. (2015), was confirmed by Lonardi et al. (2019) and also found between *V. aconitifolia* and *P. vulgaris* (Oliveira et al. 2020). To investigate this translocation in detail, we developed oligopainting probes specific to *Pv*2 and *Pv*3 chromosomes. Our CP confirmed the reciprocal translocation between *Vigna* analyzed species and *P. vulgaris*.

For chromosome 3, a breakpoint was observed at an interstitial region of *Va*3S and *Vu*3S. Our oligo-FISH analysis revealed one macro inversion close to the centromere of these chromosomes in addition to the previous translocation. Both rearrangements may have occurred after *Vigna* and *Phaseolus* separation. Additionally, the size difference of the translocated regions/oligopainting patterns of *V. angularis* and *V. unguiculata* chromosome 3 suggests additional small chromosomal rearrangements. We identified multiple small inversions and/or transpositions mainly close to the *Va*3 and *Vu*3 centromeres, especially in the later chromosome. Lonardi et al. (2019) also identified an unrelated inversion of 4.21 Mb on *Vu*3 from 36.12 to 40.33 Mb (long arm at red *Pv*3 sequences) that is present in the reference accession 'IT97K-499-35' as well as in 9% of additional analyzed accessions, but not on *Va*3, suggesting that the cowpea reference genome is inverted in this region.

For chromosome 2, we identified a breakpoint site at the interstitial region of *Va*2S, but at the proximal region of *Vu*2L. However, *Pv*3 (red) fragment corresponds to a segment with different sizes in *Va*2 and *Vu*2, being *Pv*3 sequences more spread in *Vu*2 when compared to *Va*2. This can be related to the higher density of repetitive DNA on *Vu*2 segment, considering the reported repetitive DNA fraction of 43 % and 50 % for *V. angularis* and *V. unguiculata* genomes, respectively (Kang et al. 2015; Lonardi et at. 2019). Besides, comparing *Va*2 and *Vu*2 ortholog sequences, we also detected inversions and transpositions, mainly for *Pv*3 region (red). BAC H074C16, for instance, was observed in different chromosome arms of *Va*2S and *Vu*2L, confirming the positioning change by different spread and one of the inversion events.

We also observed differences in the position of *Vigna* centromeres. While *Va*2 centromere was embedded in *Pv*2 sequences, *Vu*2 centromere was surrounded by *Pv*3 sequences. The opposite seems to be observed for *Vigna* chromosomes 3. We

suggest at least one centromere repositioning in *Vu*2. In a recent review, Schubert (2018) proposed a positional centromere change based on chromosome rearrangements, including pericentric and posterior paracentric inversion, or based on multiple DNA double-strand breaks (DSBs). Both cases maintain the original centromere, but in a new position. However, we did not observe chromosomal rearrangements involving the probable centromere regions comparing *Va*2 and *Vu*2, despite a centromere position change. One hypothesis is related to de novo centromere/new centromere formation, which has been reported in different plant species (Shubert 2018), including barley (Nasuda et al. 2005), cucumber (Han et al. 2009), maize (Zhao et al. 2017) and different species of Arabideae tribe (Brassicaceae) (Mandaková et al. 2020). In cucurbit species, centromere activation or inactivation was associated with gain or loss of a large amount of pericentromeric heterochromatin (Han et al. 2009). In *V. unguiculata*, the whole chromosome region above BAC H074C16 in *Vu*2 pachytene (previously named chromosome 7) is constituted by moderately or highly condensed heterochromatin, which corroborates the lack of genetic markers in *Vu*2S of this entire short arm (Iwata-Outsubo et al. 2016; Lonardi et al. 2019). Due to the limited sequence information for *Vigna* centromeres, further studies are needed to fully understand their positional changes.

Based on our results, we believe the pericentromeric region of chromosomes 2 and 3 are hotspots for chromosomal rearrangements in *Vigna* species and *P. vulgaris*. As suggested by Coghlan et al. (2005), there is a strong association between breakpoints and repeat sequence abundance, which can explain the large number of rearrangements close to the heterochromatic centromere regions of these chromosomes. These hotspots may be related to adaptative effects, as observed in *Brachypodium* species (Idziak et al. 2014); to epigenetic mechanisms of gene expression, as found in the Arabideae tribe (Mandaková et al. 2020); and/ or to genomic responses to biotic stresses, as noted in *A. thaliana* population studies (Jiao and Schneeberger 2020).

Together, our integrative BAC- and oligo-FISH mapping combined with the synteny data provide a foundation for comparative cytogenetics of legumes, and helped to clarify the macrosynteny, cytogenomic organization and chromosome evolution mechanisms within and between *Vigna* and *Phaseolus.* Therefore, the continued development of the genetic/genomic diversity exploration based on the comparative analysis is essential for the comprehension of synteny and evolution of

closely and distantly related species, especially considering that most *Vigna* and *Phaseolus* species do not present genetic and physical maps, nor genome sequencing. The combined BAC- and oligo-FISH resources have the potential to trace a more complete evolutionary history of beans.

Acknowledgments

We thank Embrapa Arroz e Feijão, Embrapa Meio-Norte, and IPK for providing the seeds. We also thank Timothy Close (University of California, Riverside) for providing the *V. unguiculata* BAC clones and Claudio César Montenegro Júnior for positioning the BAC 074C16 at sequence map. We thank CNPq, CAPES and FACEPE for fellowships and financial support.

References

Albert PS, Zhang T, Semrau K, Rouillard JM, Kao YH, Wang CJR, Danilova TV, Jiang J, Birchler JA (2019) Whole-chromosome paints in maize reveal rearrangements, nuclear domains, and chromosomal relationships. Proc Natl Acad Sci 116:1679–1685. https://doi.org/10.1073/pnas.1813957116

Almeida C, Pedrosa-Harand A (2013) High macro-collinearity between lima bean (*Phaseolus lunatus* L.) and the common bean (*P. vulgaris* L.) as revealed by comparative cytogenetic mapping. Theor Appl Genet 126:1909–1916. https://doi.org/10.1007/s00122-013-2106-9

Beliveau BJ, Joyce EF, Apostolopoulos N et al (2012) Versatile design and synthesis platform for visualizing genomes with Oligopaint FISH probes. Proc Natl Acad Sci 109:21301–21306. https://doi.org/10.1073/pnas.1213818110

Betekhtin A, Jenkins G, Hasterok R (2014) Reconstructing the evolution of *Brachypodium* genomes using comparative chromosome painting. PLoS One 9:e115108. https://doi.org/10.1371/journal.pone.0115108

Bi Y, Zhao Q, Yan W et al (2019) Flexible chromosome painting based on multiplex PCR of oligonucleotides and its application for comparative chromosome analyses in *Cucumis*. Plant J. https://doi.org/10.1111/tpj.14600

Bonifácio EM, Fonsêca A, Almeida C, dos Santos KG, Pedrosa-Harand A (2012) Comparative cytogenetic mapping between the lima bean (*Phaseolus lunatus* L.)

and the common bean (*P. vulgaris* L.). Theor Appl Genet 124:1513–1520. https://doi.org/10.1007/s00122-012-1806-x

Braz GT, do Vale Martins L, Zhang T, Albert PS, Birchler JA, Jiang J (2020) A universal chromosome identification system for maize and wild *Zea* species. Chromosome Res 28:183–194. https://doi.org/10.1007/s10577-020-09630-5

Braz GT, He L, Zhao H, Zhang T, Semrau K, Rouillard JM, Torres GA, Jiang JM (2018) Comparative oligo-FISH mapping: an efficient and powerful methodology to reveal karyotypic and chromosomal evolution. Genetics 208:513–523. https://doi.org/10.1534/genetics.117.300344

Cheng ZK, Presting GG, Buell CR, Wing RA, Jiang J (2001) High-resolution pachytene chromosome mapping of bacterial artificial chromosomes anchored by genetic markers reveals the centromere location and the distribution of genetic recombination along chromosome 10 of rice. Genetics 157: 1749–1757

Chèvre AM, Mason AS, Coriton O, Grandont L, Jenczewski E, Lysak M (2018) Cytogenetics, a science linking genomics and breeding: The *Brassica* Model. In: Liu S, Snowdon R, Chalhoub B (eds) The *Brassica napus* Genome. Compendium of Plant Genomes. Springer Nature, Switzerland, pp 21–39. https://doi.org/10.1007/978-3-319-43694-4_2

Coghlan A, Eichler EE, Oliver SG, Paterson AH, Stein L (2005) Chromosome evolution in eukaryotes: a multi-kingdom perspective. Trends Genet 21:673–682. https://doi/10.1016/j.tig.2005.09.009

de Carvalho CR, Saraiva LS (1993) An air drying technique for maize chromosomes without enzymatic maceration. Biotech Histochem 68:142–145. https://doi/10.3109/10520299309104684

Delgado-Salinas A, Thulin M, Pasquet R, Weeden N, Lavin M (2011) *Vigna* (Leguminosae) sensu lato: the names and identities of the American segregate genera. Am J Bot 98:1694–715. https://doi.org/10.3732/ajb.1100069

do Vale Martins L, Yu F, Zhao H et al (2019) Meiotic crossovers characterized by haplotype-specific chromosome painting in maize. Nat Commun 10:4604. https://doi.org/10.1038/s41467-019-12646-z

Fonsêca A, Ferraz ME, Pedrosa-Harand A (2016) Speeding up chromosome evolution in *Phaseolus*: multiple rearrangements associated with a one-step descending dysploidy. Chromosoma 125:413–421. https://doi.org/10.1007/s00412-015-0548-3

Fonsêca A, Ferreira J, dos Santos TR et al (2010) Cytogenetic map of common bean (*Phaseolus vulgaris* L.). Chromosome Res 18:487–502. https://doi.org/10.1007/s10577-010-9129-8

Fonsêca A, Pedrosa-Harand A (2013) Karyotype stability in the genus *Phaseolus* evidenced by the comparative mapping of the wild species *Phaseolus microcarpus*. Genome 56:335–343. https://doi.org/10.1139/gen-2013-0025

Gaiero P, van de Belt J, Vilaró F, Schranz ME, Speranza P, de Jong H (2017) Collinearity between potato (*Solanum tuberosum* L.) and wild relatives assessed by comparative cytogenetic mapping. Genome 60:228–240. https://doi.org/10.1139/gen-2016-0150

Han OK, Kaga A, Isemura T, Wang XW, Tomooka N, Vaughan DA (2005) A genetic linkage map for azuki bean [*Vigna angularis* (Willd.) Ohwi & Ohashi]. Theor Appl Genet 111:1278–1287. https://doi.org/10.1007/s00122-005-0046-8

Han Y, Zhang T, Thammapichai P, Weng Y, Jiang J (2015) Chromosome-specific painting in *Cucumis* species using bulked oligonucleotides. Genetics 200:771–779. https://doi.org/10.1534/genetics.115.177642

Han Y, Zhang Z, Liu C, Liu J, Huang S, Jiang J, Jin W (2009) Centromere repositioning in cucurbit species: Implication of the genomic impact from centromere activation and inactivation. Proc Natl Acad Sci 106:14937–41. https://doi.org/10.1073/pnas.0904833106

He L, Braz GT, Torres GA, Jiang J (2018) Chromosome painting in meiosis reveals pairing of specific chromosomes in polyploid *Solanum* species. Chromosoma 127:505–513. https://doi.org/10.1007/s00412-018-0682-9

He L, Zhao H, He J, Yang Z, Guan B, Chen K, Hong Q, Wang J, Liu J, Jiang J (2020) Extraordinarily conserved chromosomal synteny of *Citrus* species revealed by chromosome-specific painting. Plant J. https://doi.org/10.1111/tpj.14894

Heslop-Harrison JS, Harrison GE, Leitch IJ (1992) Reprobing of DNA: DNA in situ hybridization preparations. Trends Genet 8:372–373. https://doi.org/10.1016/0168-9525(92)90287-e

Hou L, Xu M, Zhang T et al (2018) Chromosome painting and its applications in cultivated and wild rice. BMC Plant Biol 18:110. https://doi.org/10.1186/s12870-018-1325-2

Hougaard BK, Madsen LH, Sandal N et al (2008) Legume anchor markers link syntenic regions between *Phaseolus vulgaris*, *Lotus japonicus*, *Medicago truncatula* and *Arachis*. Genetics 179:2299–2312. https://doi.org/10.1534/genetics.108.090084

Idziak D, Hazuka I, Poliwczak B, Wiszynska A, Wolny E, Hasterok R (2014) Insight into the karyotype evolution of *Brachypodium* species using comparative chromosome barcoding. PLoS One 9:e93503. https://doi.org/10.1371/journal.pone.0093503

Iovene M, Cavagnaro PF, Senalik D, Buell CR, Jiang J, Simon PW (2011) Comparative FISH mapping of *Daucus* species (Apiaceae family). Chromosome Res 19:493–506. https://doi.org/10.1007/s10577-011-9202-y

Iovene M, Wielgus SM, Simon PW, Buell CR, Jiang J (2008) Chromatin structure and physical mapping of chromosome 6 of potato and comparative analyses with tomato. Genetics 180:1307–1317. https://doi.org/10.1534/genetics.108.093179

Iwata-Otsubo A, Lin JY, Gill N, Jackson SA (2016) Highly distinct chromosomal structures in cowpea (*Vigna unguiculata*), as revealed by molecular cytogenetic analysis. Chromosome Res 24:197–216. https://doi.org/10.1007/s10577-015-9515-3

Javadi F, Tun YT, Kawase M, Guan K, Yamaguchi H (2011) Molecular phylogeny of the subgenus *Ceratotropis* (genus *Vigna*, Leguminosae) reveals three eco-geographical groups and Late Pliocene-Pleistocene diversification: evidence from four plastid DNA region sequences. Ann Bot 108:367–380. https://doi.org/10.1093/aob/mcr141

Jiang J, Gill BS (2006) Current status and the future of fluorescence in situ hybridization (FISH) in plant genome research. Genome 49:1057–1068. https://doi.org/10.1139/g06-076

Jiang J (2019) Fluorescence in situ hybridization in plants: recent developments and future applications. Chromosome Res 27:153–165. https://doi.org/10.1007/s10577-019-09607-z

Jiao W, Schneeberger K (2020) Chromosome-level assemblies of multiple *Arabidopsis* genomes reveal hotspots of rearrangements with altered evolutionary dynamics. Nat Commun 11:989. https://doi.org/10.1038/s41467-020-14779

Kang YJ, Satyawan D, Shim S et al (2015) Draft genome sequence of adzuki bean, *Vigna angularis*. Sci Rep 5:8069. https://doi.org/10.1038/srep08069

Krzywinski M, Schein J, Birol I, Connors J, Gascoyne R, Horsman D, Jones SJ, Marra MA (2009) Circos: an information aesthetic for comparative genomics. Genome Res 19:1639–1645. https://doi.org/10.1101/gr.092759.109

Kurtz S, Phillippy A, Delcher AL, Smoot M, Shumway M, Antonescu C, Salzberg SL (2004) Versatile and open software for comparing large genomes. Genome Biol 5:R12. https://doi.org/10.1186/gb-2004-5-2-r12

Lewis GP (2005) Tribe Caesalpinieae. In: Lewis G, Schrire B, Mackinder B and Lock M (eds) Legumes of the world. UK, Royal Botanic Gardens, Kew

Li H, Wang W, Lin L, Zhu X, Li J, Zhu X, Chen Z (2013) Diversification of the phaseoloid legumes: effects of climate change, range expansion and habit shift. Front Plant Sci 4:386. https://doi.org/10.3389/fpls.2013.00386

Liu X, Sun S, Wu Y et al (2019) Dual-color oligo-FISH can reveal chromosomal variations and evolution in *Oryza* species. Plant J 101:112–121. https://doi.org/10.1111/tpj.14522

Liu Y, Wang X, Wei Y, Liu Z, Lu Q, Liu F, Zhang T, Peng R (2020) Chromosome painting based on bulked oligonucleotides in cotton. Front Plant Sci 11:802. https://doi.org/10.3389/fpls.2020.00802

Lonardi S, Muñoz-Amatriaín M, Liang Q et al (2019) The genome of cowpea (*Vigna unguiculata* [L.] Walp.). Plant J 98:767–782. https://doi.org/10.1111/tpj.14349

Lou QF, Iovene M, Spooner DM, Buell CR, Jiang J (2010) Evolution of chromosome 6 of *Solanum* species revealed by comparative fluorescence in situ hybridization mapping. Chromosoma 119:435–442. https://doi.org/10.1007/s00412-010-0269-6

LPWG (2017) A new subfamily classification of the Leguminosae based on a taxonomically comprehensive phylogeny: The Legume Phylogeny Working Group (LPWG). Taxon 66:44–77. https://doi.org/10.12705/661.3

Lusinska J, Majka J, Betekhtin A, Susek K, Wolny E, Hasterok R (2018) Chromosome identification and reconstruction of evolutionary rearrangements in *Brachypodium distachyon, B. stacei* and *B. hybridum*. Ann Bot 122:445–59. https://doi.org/10.1093/aob/mcy086

Lysak MA, Berr A, Pecinka A, Schmidt R, McBreen K, Schubert I (2006) Mechanisms of chromosome number reduction in *Arabidopsis thaliana* and related Brassicaceae species. Proc Natl Acad Sci 103:5224–5229. https://doi.org/10.1073/pnas.0510791103

Lysak MA, Fransz PF, Ali HB, Schubert I (2001) Chromosome painting in *Arabidopsis thaliana*. Plant J 28:689–697. https://doi.org/10.1046/j.1365-313x.2001.01194.x

Lysak MA, Koch MA, Pecinka A, Schubert I (2005) Chromosome triplication found across the tribe Brassiceae. Genome Res 15:516–525. https://doi.org/10.1101/gr.3531105

Mandáková T, Hlousková P, Koch MA, Lysak MA (2020) Genome evolution in Arabideae was marked by frequent centromere repositioning. Plant Cell 32:650–665. https://doi.org/10.1105/tpc.19.00557

Mandáková T, Joly S, Krzywinski M, Mummenhoff K, Lysak MA (2010) Fast diploidization in close mesopolyploid relatives of *Arabidopsis*. Plant Cell 22:2277–2290. https://doi.org/10.1105/tpc.110.074526

Mandáková T, Lysak MA (2008) Chromosomal phylogeny and karyotype evolution in x=7 crucifer species (Brassicaceae). Plant Cell 20:2559–2570. https://doi.org/10.1105/tpc.108.062166

Meng Z, Han J, Lin Y et al (2020) Characterization of a *Saccharum spontaneum* with a basic chromosome number of x=10 provides new insights on genome evolution in genus *Saccharum*. Theor Appl Genet 133:187–199. https://doi.org/10.1007/s00122-019-03450-w

Meng Z, Zhang Z, Yan T et al (2018) Comprehensively characterizing the cytological features of *Saccharum spontaneum* by the development of a complete set of chromosome-specific oligo probes. Front Plant Sci 9:1624. https://doi.org/10.3389/fpls.2018.01624

Mercado-Ruaro P, Delgado-Salinas A (1996) Karyological studies in several Mexican species of *Phaseolus* L. and *Vigna* Savi (Phaseolinae, Fabaceae). In: Pickersgill B, Lock. JM (eds) Advances in legumes systematics. 8: Legumes of economic importance. Royal Botanic Gardens, Kew, pp 83-87

Muchero W, Diop NN, Bhat PR et al (2009) A consensus genetic map of cowpea [*Vigna unguiculata* (L) Walp] and synteny based on EST-derived SNPs. Proc Natl Acad Sci 106:18159–18164. https://doi.org/10.1073/pnas.0905886106

Nasuda S, Hudakova S, Schubert I, Houben A, Endo TR (2005) Stable barley chromosomes without centromeric repeats. Proc Natl Acad Sci 102:9842-9847. https://doi.org/10.1073/pnas.0504235102

Oliveira ARS, Martins LV, Bustamante FO, Muñoz-Amatriaín M, Close T, Costa AF, Benko-Iseppon AM, Pedrosa-Harand A, Brasileiro-Vidal AC (2020) Breaks of

macrosynteny and collinearity among moth bean (*Vigna aconitifolia*), cowpea (*V. unguiculata*), and common bean (*Phaseolus vulgaris*). Chromosome Res. https://doi.org/10.1007/s10577-020-09635-0

Pedrosa A, Sandal N, Stougaard J, Schweizer D, Bachmair A (2002) Chromosomal map of the model legume *Lotus japonicus*. Genetics 161:1661–1672

Qu M, Li K, Han Y, Chen L, Li Z, Han Y (2017) Integrated karyotyping of woodland strawberry (*Fragaria vesca*) with oligopaint FISH probes. Cytogenet Genome Res 153:158–164. https://doi.org/10.1159/000485283

Sader MA, Dias Y, Costa ZP, Munhoz C, Penha H, Bergès H, Vieira MLC, Pedrosa-Harand H (2019) Identification of passion fruit (*Passiflora edulis*) chromosomes using BAC-FISH. Chromosome Res 27:299–311. https://doi.org/10.1007/s10577-019-09614-0

Sakai H, Naito K, Ogiso-Tanaka E et al (2015) The power of single molecule real-time sequencing technology in the *de novo* assembly of a eukaryotic genome. Sci Rep 5:16780. https://doi.org/10.1038/srep16780

Sato S, Nakamura Y, Kaneko T et al (2008) Genome structure of the legume, *Lotus japonicus*. DNA Res 15:227–239. https://doi.org/10.1093/dnares/dsn008

Schmutz J, Cannon SB, Schlueter J et al (2010) Genome sequence of the palaeopolyploid soybean. Nature 463:178–183. https://doi.org/10.1038/nature08670

Schmutz J, McClean PE, Mamidi S et al (2014) A reference genome for common bean and genome-wide analysis of dual domestications. Nat Genet 46:707–713. https://doi.org/10.1038/ng.3008

Schubert I (2018) What is behind “centromere repositioning”? Chromosoma 127:229–234. https://doi.org/10.1007/s00412-018-0672-y

Šimoníková D, Němečková A, Karafiátová M, Uwimana B, Swennen R, Doležel J, Hřibová E (2019) Chromosome painting facilitates anchoring reference genome sequence to chromosomes *in situ* and integrated karyotyping in banana (*Musa* spp.). Front Plant Sci 10:1503. https://doi.org/10.3389/fpls.2019.01503

Song X, Song R, Zhou J et al (2020) Development and application of oligonucleotide-based chromosome painting for chromosome 4D of *Triticum aestivum* L. Chromosome Res 28:171–182. https://doi.org/10.1007/s10577-020-09627-0

Szinay D, Wijnker E, van den Berg R, Visser RG, de Jong H, Bai Y (2012) Chromosome evolution in *Solanum* traced by cross-species BAC-FISH. New Phytol 195:688–698. https://doi.org/ 10.1111/j.1469-8137.2012.04195.x

Tang H, Krishnakumar V, Bidwell S et al (2014) An improved genome release (version Mt4.0) for the model legume *Medicago truncatula*. BMC Genomics 15:312. https://doi.org/10.1186/1471-2164-15-312

Vallejos CE, Sakiyama NS, Chase CD (1992) A molecular marker-based linkage map of *Phaseolus vulgaris* L. Genetics 131:733–740

Valliyodan B, Cannon SB, Bayer PE et al (2019) Construction and comparison of three reference-quality genome assemblies for soybean. Plant J 100:1066–1082. https://doi.org/10.1111/tpj.14500

Vasconcelos EV, Fonsêca AFA, Pedrosa-Harand A, Bortoleti KCA, Benko-Iseppon AM, da Costa AF, Brasileiro-Vidal AC (2015) Intra- and interchromosomal rearrangements between cowpea [*Vigna unguiculata* (L.) Walp.] and common bean (*Phaseolus vulgaris* L.) revealed by BAC-FISH. Chromosome Res 23:253–266. https://doi.org/10.1007/s10577-014-9464-2

Wang CJ, Harper L, Cande WZ (2006) High-resolution single-copy gene fluorescence in situ hybridization and its use in the construction of a cytogenetic map of maize chromosome 9. Plant Cell 18:529–544. https://doi.org/10.1105/tpc.105.037838

Wang L, Kikuchi S, Muto C, Naito K, Isemura T, Ishimoto M, Cheng X, Kaga A, Tomooka N (2015) Reciprocal translocation identified in *Vigna angularis* dominates the wild population in East Japan. J Plant Res 128:653–663. https://doi.org/10.1007/s10265-015-0720-0

Wanzenböck EM, Schöfer C, Schweizer D, Bachmair A (1997) Ribosomal transcription units integrated via T-DNA transformation associate with the nucleolus and do not require upstream repeat sequences for activity in *Arabidopsis thaliana*. Plant J 11:1007–1016. https://doi.org/10.1046/j.1365-313x.1997.11051007.x

Wellenreuther M, Bernatchez L (2018) Eco-evolutionary genomics of chromosomal inversions. Trends Ecol Evol 33:427–440. https://doi.org/10.1016/j.tree.2018.04.002

Xin H, Zhang T, Han Y, Wu Y, Shi J, Xi M, Jiang J (2018) Chromosome painting and comparative physical mapping of the sex chromosomes in *Populus tomentosa* and *Populus deltoides*. Chromosoma 127:313–321. https://doi.org/10.1007/s00412-018-0664-y

Xin H, Zhang T, Wu Y, Zhang W, Zhang P, Xi M, Jiang J (2019) An extraordinarily stable karyotype of the woody *Populus* species revealed by chromosome painting. Plant J 101:253–264. https://doi.org/10.1111/tpj.14536

Young ND, Debellé F, Oldroyd GE et al (2011) The *Medicago* genome provides insight into the evolution of rhizobial symbioses. Nature 480:520–524. https://doi.org/10.1038/nature10625

Zhao Q, Wang Y, Bi Y, Zhai Y, Yu X, Cheng C, Wang P, Li J, Lou Q, Chen J (2019) Oligo-painting and GISH reveal meiotic chromosome biases and increased meiotic stability in synthetic allotetraploid *Cucumis* ×*hytivus* with dysploid parental karyotypes. BMC Plant Biol 19:471. https://doi.org/10.1186/s12870-019-2060-z

Zhao H, Zeng Z, Koo DH, Gill BS, Birchler JA, Jiang J (2017) Recurrent establishment of de novo centromeres in the pericentromeric region of maize chromosome 3. Chromosome Res 25:299–311. https://doi.org/10.1007/s10577-017-9564-x

5 CONCLUSÕES

1. Os mapas citogenéticos comparativos fornecem informações detalhadas acerca da macrossintenia e organização/ estruturação genômica e evolução cromossômica entre leguminosas economicamente importantes dos gêneros *Vigna* e *Phaseolus.*
2. Uma conservação parcial de macrossintenia envolvendo cinco cromossomos (6, 7, 9, 10 e 11) é observada entre os genomas de *V. aconitifolia, V. angularis, V. unguiculata* e *P. vulgaris*, sugerindo uma estabilidade cariotípica entre essas espécies.
3. Os principais rearranjos identificados e relacionados à evolução cromossômica entre as espécies de *Vigna* comparativamente a *P. vulgaris* (há 9,7 milhões de anos) e entre os subgêneros *Vigna* e *Ceratotropis* (há 3,6 milhões de anos) são translocações e inversões.
4. A presença de um sítio de DNAr 35S no cromossomo 6 de todas as espécies analisadas e previamente descritas na literatura suporta a hipótese de ancestralidade e conservação desse cromossomo na subtribo Phaseolinae.

REFERÊNCIAS

ALAM S.S.; TASMIN R.I.; JAHAN I.; HABIB M.D.A.; SULTANA S.S. Fluorescent Banding and RAPD Analysis of Five Cultivars in *Vigna unguiculata* ssp. *sesquipedalis* (L.) Verdc**. Cytologia** 78: 73-79, 2013.

ALBERT P.S.; GAO Z.; DANILOVA T.V.; BIRCHLER J.A. Diversity of Chromosomal Karyotypes in Maize and Its Relatives. **Cytogenet Genome Res** 129: 6–16, 2010.

ALBERT P.S.; ZHANG T.; SEMRAU K.; ROUILLARD J.M.; KAO Y.H.; WANG C.J.R.; DANILOVA T.V.; JIANG J.; BIRCHLER J.A. Whole-chromosome paints in maize reveal rearrangements, nuclear domains, and chromosomal relationships. **Proc Natl Acad Sci** 116: 1679–1685, 2019.

ALMEIDA C.; FONSÊCA A.; DOS SANTOS K.G.B. et al. Contrasting evolution of a satellite DNA and its ancestral IGS rDNA in *Phaseolus* (Fabaceae). **Genome** 55**:** 683–689, 2013.

ALMEIDA C.; PEDROSA-HARAND A. High macro-collinearity between lima bean (*Phaseolus lunatus* L.) and the common bean (*P. vulgaris* L.) as revealed by comparative cytogenetic mapping. **Theor Appl Genet** 126: 1909–1916, 2013.

ANDARGIE M.; PASQUET R.S.; MULUVI G.M.; TIMKO M.P. Quantitative trait loci analysis of flowering time related traits identified in recombinant inbred lines of cowpea (*Vigna unguiculata*). **Genome** 56: 289–294, 2013.

APG III. An update of the Angiosperm Phylogeny Group classification for the orders and families of flowering plants: APG III. **Bot J Linn Soc** 161: 105–121, 2009.

ARIANI A.; MIER TERAN J.C.B.; GEPTS P. Spatial and Temporal Scales of Range Expansion in Wild *Phaseolus vulgaris*. **Mol Biol Evol** 35: 119–131, 2018.

BELIVEAU B.J.; JOYCE E.F.; APOSTOLOPOULOS N. et al. Versatile design and synthesis platform for visualizing genomes with oligopaint FISH probes. **Proc Natl Acad Sci** 109: 21301–6, 2012.

BELIVEAU B.J.; BOETTIGER A.N.; AVENDAÑO M.S. et al. Single-molecule super-resolution imaging of chromosomes and in situ haplotype visualization using Oligopaint FISH probes. **Nat Commun** 6: 7147, 2015.

BELARMINO L.C.; OLIVEIRA A.R.S.; BRASILEIRO-VIDAL A.C.; BORTOLETI K.C.A.; BEZERRA-NETO J.P.; ABDELNOOR R.V.; BENKO-ISEPPON A.M. Mining plant genome browsers as a mean for efficient connection of physical genetic and cytogenetic mapping: an example using soybean. **Genet Mol Biol** 35: 335-347, 2012.

BETEKHTIN A.; JENKINS G.; HASTEROK R. Reconstructing the evolution of *Brachypodium* genomes using comparative chromosome painting. **PLoS One** 9: e115108, 2014.

BITOCCHI E.; RAU D.; BELLUCI E.; RODRIGUEZ M.; MURGIA M.L.; GIOIA T.; SANTO D.; NANNI L.; ATTENE G.; PAPA R. Beans (*Phaseolus* ssp.) as a model for understanding crop evolution. **Front Plant Sci** 8: 722, 2017.

BONIFÁCIO E.M.; FONSÊCA A.; ALMEIDA C.; DOS SANTOS K.G.B.; PEDROSA-HARAND A. Comparative cytogenetic m,apping between the lima bean (*Phaseolus lunatus* L.) and the common bean (*P. vulgaris* L.). **Theor Appl Genet** 124: 1513–1520, 2012.

BORTOLETI K.C.A.; BENKO-ISEPPON A.M.; MELO N.F.; BRASILEIRO-VIDAL A.C. Chromatin differentiation between *Vigna radiata* (L.) R. Wilczek and *V. unguiculata* (L.) Walp. (Fabaceae)**. Plant Syst Evol** 298: 689-693, 2012.

BOUKAR O.; FATOKUN C.A.; HUYNH B.L.; ROBERTS P.A.; CLOSE T.J. Genomic tools in cowpea breeding programs: Status and perspectives. **Front Plant Sci** 7: 757, 2016.

BOUKAR O.; BELKO N.; CHAMARTHI S. et al. Cowpea (*Vigna unguiculata*): Genetics, genomics and breeding. **Plant Breed** 138: 415–424, 2019.

BRAZ G.T.; HE L.; ZHAO H.; ZHANG T.; SEMRAU K.; ROUILLARD J.M.; TORRES G.A.; JIANG J. Comparative oligo-FISH mapping: An efficient and powerful methodology to reveal karyotypic and chromosomal evolution. **Genetics** 208: 513–523, 2018.

CANNON S.B. The model legume genomes. **Methods Mol Biol** 1069: 1–14, 2013.

CARVALHEIRA G.; GUERRA M. The polytene chromosomes of anther tapetum of some *Phaseolus* species. **Cytologia** 59: 211-217, 1994.

CARVALHEIRA G.; GUERRA M. The polytene chromosomes of tapetal cells in the anther of some *Vigna* Savi cultivars and species. **Cytobios** 94: 161-168, 1998.

CARVALHEIRA G.M.G. Plant polytene chromosomes. **Genet Mol Biol** 23: 1043–1050, 2000.

CHANG Y.; LIU H.; LIU M. et al. The draft genomes of five agriculturally important African orphan crops. **Gigascience** 8: 1–16, 2019.

CHATIENG B.; KAGA A.; TOMOOKA N.; ISEMURA T.; KURODA Y.; VAUGHAN D.A. Development of a black gram [*Vigna mungo* (L.) Hepper] linkage map and its comparison with an azuki bean [*Vigna angularis* (Willd.) Ohwi and Ohashi] linkage map. **Theor Appl Genet** 113: 1261-1269, 2006.

CHANKAEW S.; ISEMURA T.; NAITO K. et al. QTL mapping for salt tolerance and domestication-related traits in *Vigna marina* subsp. *oblonga*, a halophytic species. **Theor Appl Genet** 127: 691-702, 2014.

CHÈVRE A.M.; MASON A.S.; CORITON O.; GRANDONT L.; JENCZEWSKI E.; LYSAK M.A. **Cytogenetics, a Science Linking Genomics and Breeding:** The

Brassica Model. pp 21–39, 2018.

CHOI H.K.; MUN J.H.; KIM D.J.et al. Estimating genome conservation between crop and model legume species. **Proc Natl Acad Sci** 101: 15289–15294, 2004.

COGHLAN A.; EICHLER E.E.; OLIVER S.G.; PATERSON A.H.; STEIN L. Chromosome evolution in eukaryotes: a multi-kingdom perspective. **Trends Genet** 21: 673–682, 2005.

DARLINGTON C.D.; WYLIE A.P. **Chromosome atlas of flowering plants.** In: George Allen and Unwin (eds) Ltd. London, 1955.

DASH S.; CAMPBELL J.D.; CANNON E.K.S. et al. Legume information system (LegumeInfo.org): A key component of a set of federated data resources for the legume family. **Nucleic Acids Res** 44: D1181–D1188, 2016.

DELGADO-SALINAS A.; BIBLER R.; LAVIN M. M Phylogeny of the Genus *Phaseolus* (Leguminosae): A Recent Diversification in an Ancient Landscape. **Syst Bot** 31: 779–791, 2006.

DELGADO-SALINAS A.; THULIN M.; PASQUET R.; WEEDEN N.; LAVIN M. *Vigna* (Leguminosae) sensu lato: The names and identities of the American segregate genera. **Am J Bot** 98: 1694–1715, 2011.

DO VALE MARTINS L.; YU F.; ZHAO H.; DENNINSON T.; LAUTER N.; WANG H.; DENG Z.; THOMPSON A.; SEMRAU K.;ROUILLARD J.M.; BIRCHLER J.A.; JIANG J. Meiotic crossovers characterized by haplotype-specific chromosome painting in maize. **Nat Commun** 10: 4604, 2019.

DOYLE J.J.; LUCKOW M.A. The rest of the iceberg. Legume diversity and evolution in a phylogenetic context. **Plant Physiol** 131: 900–910,2003.

ELLIS T.H.; TURNER L.; HELLENS R.; LEE D.; HARKER C.L.; ENARD C.; DOMONEY C.; DAVIES D.R. Linkage maps in pea. **Genetics** 130: 649–63, 1992.

FATAKOUN C.A.; BOUKAR O.; MURANAKA S. Evaluation of cowpea (*Vigna unguiculata* (L.) Walp.) germplasm lines for tolerance to drought. **Plant Genet Resour Characterisation Util** 10: 171–176, 2012.

FERGUSON-SMITH M.A.; TRIFONOV V. Mammalian karyotype evolution. **Nat Rev Genet** 8: 950–962, 2007.

FINDLEY S.D.; CANNON S.; VARALA K.; DU J.; MA J.; HUDSON M.E.; BIRCHLER J.A.; STACEY G. A fluorescence in Situ hybridization system for karyotyping soybean. **Genetics** 185: 727–744, 2010.

FONSÊNCA A.; FERREIRA J.; DOS SANTOS T.R.B. et al. Cytogenetic map of common bean (*Phaseolus vulgaris* L.). **Chromosom Res** 18: 487–502, 2010.

FONSÊCA A.; PEDROSA-HARAND A. Karyotype stability in the genus *Phaseolus* evidenced by the comparative mapping of the wild species *Phaseolus microcarpus*. **Genome** 56: 335–343, 2013.

FONSÊCA A.; RICHARD M.M.; GEFFROY V.; PEDROSA-HARAND A. Epigenetic analyses and the distribution of repetitive DNA and resistance genes reveal the complexity of common bean (*Phaseolus vulgaris* L., Fabaceae) heterochromatin. **Cytogenet Genome Res** 143: 168–178, 2014.

FONSÊCA A.; FERRAZ M.E.; PEDROSA-HARAND A. Speeding up chromosome evolution in *Phaseolus:* multiple rearrangements associated with a one-step descending dysploidy**. Chromosoma** 125: 413–421, 2016.

FONSÊCA A.; PEDROSA-HARAND A. Cytogenetics and Comparative Analysis of *Phaseolus* Species. In: Pérez de la Vega M., Santalla M., Marsolais F. (eds) **The Common Bean Genome.** Compendium of Plant Genomes, Springer, 2017.

FREIRE-FILHO F.R. et al. Feijão-caupi no Brasil: produção, melhoramento genético, avanços e desafios. **Embrapa Meio-Norte,** Teresina, 84 pp. 2011.

FUCHS J.; HOUBEN A.; BRANDES A.; SCHUBERT I. Chromosome 'painting' in plants: a feasible technique? **Chromosoma** 104: 315–320, 1996.

GAIERO P.; VAN DE BELT J.; VILARÓ F.; SCHRANZ M.E.; SPERANZA P.; DE JONG H. Collinearity between potato (*Solanum tuberosum* L.) and wild relatives assessed by comparative cytogenetic mapping. **Genome** 60: 228–240, 2017.

GALASSO I.; PIGNONE D.; PERRINO P. Cytotaxonomic studies in *Vigna*. I. General technique and *Vigna unguiculata* C-banding. **Caryologia** 45: 155-161, 1992.

GALASSO I.; PIGNONE D.; PERRINO P. Cytotaxonomic studies in *Vigna*. II. Heterochromatin characterization in *Vigna unguiculata* and three related wild species. **Caryologia** 46: 275-282, 1993.

GALASSO I.; SCHMIDT T.; PIGNONE D.; HESLOP-HARRISON J.S. The molecular cytogenetics of *Vigna unguiculata* (L.) Walp: the physical organization and characterization of 18 s-5.8 s-25 s rRNA genes, 5 s rRNA genes, telomere-like sequences, and a family of centromeric repetitive DNA sequences. **Theor Appl Genet** 91: 928–935, 1995.

GALASSO I.; SAPONETTI L.S.; PIGNONE D. Cytotaxonomic studies in *Vigna*. III. Chromosomal distribution and reacting properties of the heterochromatin in five wild species of the section *Vigna*. **Caryologia** 49: 311-319, 1996.

GALASSO I.; HARRISON G.E.; PIGNONE D.; BFRANDES A.; HESLOP-HARRISON J.S. The distribution and organization of Ty1-copia-like retrotransposable elements in the genome of *Vigna unguiculata* (L.) Walp. (Cowpea) and its relatives. **Ann Bot** 80: 327–333, 1997.

GALL J.G.; PARDUE. M.L. Formation and detection of RNA-DNA hybrid molecules in cytological preparations. **Proc Natl Acad Sci** 63: 378–383, 1969.

GEPTS P.; BEAVIS W.D.; BRUMMER E.C.; SHOEMAKER R.C.; STALKER H.T.; WEEDEN N.E.; YOUNG N.D. Legumes as a model plant family. Genomics for

food and feed report of the cross-legume advances through genomics conference. **Plant Physiology** 137: 1228–1235, 2005.

GIOIA T.; LOGOZZO G.; MARZARIO S.; ZEULI P.S.; GEPTS P. Evolution of SSR diversity from wild types to U.S. advanced cultivars in the Andean and Mesoamerican domestications of common bean (*Phaseolus vulgaris*). **Plos One** 14: e0211342, 2019.

GOHARA A.K.; DE SOUZA A.P.H.; GOMES S.T.M.; DE SOUZA N.E.; VISENTAINER J.V.; MATSUSHITA M. Nutritional and bioactive compounds of adzuki bean cultivars using chemometric approach. **Cienc e Agrotecnologia** 40: 104–113, 2016.

GUERRA M. rDNA Sites in Mitotic and Polytene Chromosomes of *Vigna unguiculata* (L.) Walp. and P*haseolus coccineus* L. revealed by in situ Hybridization. **Ann Bot** 78: 157–161, 1994.

GUERRA M. **Introdução a citogenética geral.** Rio de Janeiro: Ed. Guanabara Koogan,142p, 1988.

GUERRA M. Patterns of heterochromatin distribution in plant chromosomes. **Genet Mol Biol** 23: 1029–1041, 2000.

GUERRA M. **Hibridização In Situ:** Princípios Básicos. FISH – conceitos e aplicações na citogenética. Sociedade Brasileira de Genética, Ribeirão Preto, pp 1–33, 2004.

GUJARIA-VERMA N.; VAIL S.L.; CARRASQUILA-GARCIA N.; PENMETSA R.V.; COOK D.R.; FARMER A.D.; VANDENBER A.; BETT K.E. Genetic mapping of legume orthologs reveals high conservation of synteny between lentil species and the sequenced genomes of *Medicago* and chickpea. **Front Plant Sci** 5: 676, 2014.

GUPTA S.K.; SOUFRAMANIEN J.; GOPALAKRISHNA T. Construction of a genetic linkage map of black gram, *Vigna mungo* (L.) Hepper, based on molecular markers and comparative studies. **Genome** 51: 628–637, 2008.

GUPTA S.; NADARAJAN N.; GUPTA D.S. **Legumes in the Omic Era.** 1st edition. Springer, New York, 2014.

HA J.; ABERNATHY B.; NELSON W. et al. Integration of the Draft Sequence and Physical Map as a Framework for Genomic Research in Soybean (*Glycine max* (L.) Merr.) and Wild Soybean (*Glycine soja* Sieb. and Zucc.). **Genes, Genomes,Genetics** 2: 321–329, 2012.

HAN Y.; LI K.; HAN Y.; CHEN L.; LI Z. Integrated Karyotyping of Woodland Strawberry (*Fragaria vesc*a) with Oligopaint FISH Probes. **Cytogenet Genome Res** 153: 158–164, 2018.

HAN O.K.; KAGA A.; ISEMURA T.; WANG X.W.; TOMOOKA N.; VAUGHAN D.A. A genetic linkage map for azuki bean [*Vigna angularis* (Willd.) Ohwi & Ohashi] **Theor Appl Genet** 111: 1278-87, 2005.

HAN Y.; ZHANG T.; THAMMAPICHAI P.; WENG Y.; JIANG J. Chromosome-specific painting in *Cucumis* species using bulked oligonucleotides. **Genetics** 200: 771–779, 2015.

HAROUNA D.V.; VENKATAEAMANA P.B.; NDAKIDEMI P.A.; MATEMU A.O. Under-exploited wild *Vigna* species potentials in human and animal nutrition: A review. **Glob Food Sec** 18: 1–11, 2018.

HE Q.; CAI Z.; HU T.; BAO C.; MAO W.; JIN W. Repetitive sequence analysis and karyotyping reveals centromere-associated DNA sequences in radish (*Raphanus sativus* L.). **BMC Plant Biol** 15: 105, 2015.

HE L.; BRAZ G.T.; TORRES G.A.; JIANG J. Chromosome painting in meiosis reveals pairing of specific chromosomes in polyploid *Solanum* species. **Chromosoma** 127: 505-513, 2018.

HESLOP-HARRISON J.S.P.; SCHWARZACHER T. Organisation of the plant genome in chromosomes. **Plant J** 66: 18–33, 2011.

HO W.K.; CHAI H.H.; KENDABIE P.; AHMAD N.S.; JANI J.; MASSAWE F.; KILIAN A.; MAYES S. Integrating genetic maps in bambara groundnut [*Vigna subterranea* (L) Verdc.] and their syntenic relationships among closely related legumes. **BMC Genomics** 18: 192–200, 2017.

HOU L.; XU M.; ZHANG T. et al.Chromosome painting and its applications in cultivated and wild rice. **BMC Plant Biol** 18: 110, 2018.

IDZIAK D.; POLIWACZAK B.; WISZYNSKA A.; WOLNY E.; HASTEROCK R. Insight into the Karyotype Evolution of *Brachypodium* Species Using Comparative Chromosome Barcoding. **PLoS One** 9: e93503, 2014.

IOVENE M.; WIELGUS S.M.; SIMON P.W.; BUELL C.R.; JIANG J. Chromatin structure and physical mapping of chromosome 6 of potato and comparative analyses with tomato. **Genetics** 180: 1307–1317, 2008.

IOVENE M.; CAVAGNARO P.F.; SENALIK D.; BUELL C.R.; JIANG J.; SIMON P.W. Comparative FISH mapping of *Daucus* species (Apiaceae family). **Chromosom Res** 19: 493–506, 2011.

ISEMURA T.; KAGA A.; KONISHI S.; ANDO T.; TOMOOKA N.; HAN O.K.; VAUGHAN D.A.Genome dissection of traits related to domestication in azuki bean (*Vigna angularis*) and comparison with other warm-season legumes. **Ann Bot** 100: 1053–1071, 2007.

ISEMURA T.; KAGA A.; TOMOOKA N.; SHIMIZU T.; VAUGHAN D.A. The genetics of domestication of rice bean, *Vigna umbellata*. **Ann Bot** 106: 927–944, 2010.

IWATA-OTSUBO A.; LIN J.Y.; GILL N.; JACKSON S.A. Highly distinct chromosomal structures in cowpea (*Vigna unguiculata*), as revealed by molecular cytogenetic analysis. **Chromosom Res** 24: 197–216, 2016.

IWATA A.; GREENLAND C.M.; JACKSON S.A. Cytogenetics of legumes in the Phaseoloid clade. **Plant Genome** 6: 3, 2013.

JIANG J.; PARROT W.A.; DAWE R.K. A molecular view of plant centromeres. **Trends Plant Sci** 8: 570–575, 2003.

JIANG J.; GILL B.S. Current status and the future of fluorescence in situ hybridization (FISH) in plant genome research. **Genome** 49: 1057–1068, 2006.

JIANG J. Fluorescence in situ hybridization in plants: recent developments and future applications. **Chromosom Res** 27: 153–165, 2019.

JOSEPH L.S.; BOUWKAMP J.C. Karyomorphology of Several Species of *Phaseolus* and *Vigna.* **Cytologia** 43: 595-600, 1978.

JUDD W.S.; CAMPBELL C.S.; KELLOOGG E.A.; STEVENS P.F.; DONOGHUE M.J. **Sistemática Vegetal:** Um Enfoque Filogenético 3a ed. Porto Alegre: Artmed, pp 612, 2009.

KANG Y.J.; KIM S.K.; KIM M.Y. et al. Genome sequence of mungbean and insights into evolution within *Vigna* species. **Nat Commun** 5: 5445, 2014.

KANG Y.J.; SATYAWAN D.; SHIM S.et al. Draft genome sequence of adzuki bean, *Vigna angularis.* **Sci Rep** 5: 8069, 2015.

KARPECHENKO G.D. On the chromosomes of the Phaseolineae. **Bull Appl Bot** 14: 143–148, 1925.

KENICER G. **Legumes of the World .** Edited by LEWIS G.; SCHRIRE B.; MACKINDER B.; LOCK M. Royal Botanic Gardens, Kew. 577pp. 62: 195–196, 2005.

LAUCOU V.; HAUROGNÉ K.; ELLIS N.; RAMEAU C. Genetic mapping in pea. 1. RAPD-based genetic linkage map of *Pisum sativum*. **Theor Appl Genet** 97: 905–915, 1988.

LAVANIA U.C.; LAVANIA S. Chromosome Banding Patterns in some Indian Pulses. **Ann Bot** 49: 235-239, 1982.

LAVIN M.; HERENDEEN P.S.; WOJCIECHOWSKI M.F. Evolutionary rates analysis of Leguminosae implicates a rapid diversifycation of lineages during the Tertiary. **Systematic Biology** 54: 575-594, 2005.

LESTARI P.; KANG Y.J.; HAN K.S.; GWAG J.G.; MOON J.K.; KIM Y.H.; LEE Y.H.; LEE S.H. Genome-wide single nucleotide polymorphism discovery and validation in adzuki bean. **Mol Breed** 33: 497–501, 2014.

LIOI L.; RIERGIOVANNI A.R. Common bean cultivation in the Mediterranean Basin. **Legume Perspect** 10: 22–24, 2015.

LI H.; WAMG W.; LIN L.; ZHU X.; LI J.; ZHU X.; CHEN Z. Diversification of the phaseoloid legumes: effects of climate change, range expansion and habit shift.

Front Plant Sci 4: 386, 2013.

LIU X.; SUN S.; WU Y. et al Dual-color oligo-FISH can reveal chromosomal variations and evolution in *Oryza* species. **Plant J** 101: 112-121, 2019.

LOBATON J.D.; MILLET T.; GIL J.; ARIZA D.; DE LA HOZ J.F.; SOLER A.; BEEBE S.; DUITAMA J.; GEPTS P.; RAATZ B. Resequencing of common bean identifies regions of inter–gene pool introgression and provides comprehensive resources for molecular breeding. **Plant Genome** 11(2), 2019.

LONARDI S.; MUÑOZ-AMATRIAÍN M.; LIANG Q. et al. The genome of cowpea (*Vigna unguiculata* [L.] Walp.). **Plant J** 98: 767–782, 2019.

LPGW (The Legume Phylogeny Working Group) A new subfamily classification od the Leguminosae based on taxonomically comprehensive phylogeny. **Taxon** 66: 44-77, 2017.

LUCAS M.R.; WANAMAKER S.; EHLERS J.D.; ROBERTS P.A.; CLOSE T.J. Cowpea-soybean synteny clarified through an improved genetic map. **Plant Genome** 4: 218–225, 2011.

LUCAS M.R.; HUYNH B.L.; DA SILVA VINHOLES P.; CISSE N.; DRABO I.; EHLERS J.D.; ROBERTS P.A.; CLOSE T.J. Association Studies and Legume Synteny Reveal Haplotypes Determining Seed Size in *Vigna unguiculata*. **Front Plant Sci** 4: 95, 2013.

LYSAK M.A.; FRANSZ P.F.; ALI H.B.M.; SCHUBERT I. Chromosome painting in *Arabidopsis thaliana*. **Plant J** 28: 689–697, 2001.

LYSAK M.A.; KOCH M.A.; PECINKA A.; SCHUBERT I. Chromosome triplication found across the tribe Brassiceae. **Genome Res** 15: 516–525, 2005.

LYSAK M.A.; BERR A.; PECINKA A.; SCHMIDT R.; MCBREEN K.; SCHUBERT I. Mechanisms of chromosome number reduction in *Arabidopsis thaliana* and related Brassicaceae species. **Proc Natl Acad Sci** 103: 5224–9, 2006.

LYSAK M.A.; MANDÁKOVÁ T.; LACOMBE E. Reciprocal and multi-species chromosome bac painting in crucifers (Brassicaceae). **Cytogenet Genome Res** 129: 184–189, 2010.

MADLUNG A. Polyploidy and its effect on evolutionary success: Old questions revisited with new tools. **Heredity** 110: 99–104, 2013.

MANDAKOVÁ T.; JOLY S.; KRZYWINSKI M.; MUMMENHOFF K.; LYSAK M.A. Fast diploidization in close mesopolyploid relatives of *Arabidopsis.* **Plant Cell** 22: 2277–2290, 2010.

MANDAKOVÁ T.; LYSAK M.A. Chromosomal phylogeny and karyotype evolution in x=7 crucifer species (Brassicaceae). **Plant Cell** 20: 2559–2570, 2008.

MARUBODEE R.; OGISO-TANAKA E.; ISEMURA T.; CHANKAEW S.; KAGA A.; NAIKO K.; EHARA H.; TOMOOKA N. Construction of an SSR and RAD-marker

based molecular linkage map of *Vigna vexillata* (L.) A. Rich. **Plos One** 10: e0138942, 2015.

MCCLEAN P.E.; MAMIDI S.; MCCONNELL M.; CHIKARA S.; LEE R. Synteny mapping between common bean and soybean reveals extensive blocks of shared loci. **BMC Genomics** 11: 184, 2010.

MENÉNDEZ C.M.; HALL A.E.; GEPTS P. A genetic linkage map of cowpea (*Vigna unguiculata*) developed from a cross between two inbred, domesticated lines. **Theor Appl Genet** 95: 1210–1217, 1997.

MENG Z.; ZHANG Z.; YAN T. et al. Comprehensively characterizing the cytological features of *Saccharum spontaneum* by the development of a complete set of chromosome-specific oligo probes. **Front Plant Sci** 9: 1624, 2018.

MENG Z.; HAN J.; LIN Y. et al. Characterization of a *Saccharum spontaneum* with a basic chromosome number of x=10 provides new insights on genome evolution in genus *Saccharum*. **Theor Appl Genet** 133: 187-199, 2020.

MERCADO-RUARO P.; DELGADO-SALINAS A. Karyotypic studies on species of *Phaseolus* (Fabaceae: Phaseolinae). **Am J Bot** 85: 1, 1988.

MERCADO-RUARO P.; DELGADO-SALINAS A. Cytogenetic studies in *Phaseolus* L. (Fabaceae). **Genet Mol Biol** 23: 985–987, 2000.

MILLAN T.; WINTER P.; JUNGLING R. et al. A consensus genetic map of chickpea (*Cicer arietinum* L.) based on 10 mapping populations. **Euphytica** 175: 175–189, 2010.

MIRZAIE-NODOUSHAN H.; DEHGHANSHOAR M.; MADDAH-AREFI H.; ASADI-COROM F. Karyotypic characteristics of several *Bromus* Species. **Internation Journal of Agriculture and Biology** 8: 717–720, 2006.

MOSCONE E.A.; MATZKE M.A.; MATZKE A.J.M. Fluorescent chromosome banding in the cultivated species of *Capsicum* (Solanaceae). **Plant Systematic Evolution** 202: 37-63, 1996.

MOSCONE E.A.; KLEIN F.; LAMBROU M.; FUCHS J.; SCHWEIZER D. Quantitative karyotyping and dual-color FISH mapping of 5S and 18S-25S rDNA probes in the cultivated *Phaseolus* species (Leguminosae). **Genome** 42: 1224–1233, 1999.

MOSCONE E.A.; SCALDAFERRO M.A.; GABRIELE M.; CECCHINI N.M.; SÁNCHEZ GARCIA Y.; JARRET R.; DAVIÑA J.R.; DUCASSE D.A.; BARBOZA G.E.; EHRENDORFER F. The evolution of chili pepers (*Capsicum* Solanaceae): a cytogenetic perspective. **Acta Horticulturae** 745: 137-170, 2007.

MUCHERO W.; DIOP N.N.; BHAT P.R. et al. A consensus genetic map of cowpea [*Vigna unguiculata* (L) Walp.] and synteny based on EST-derived SNPs. **Proc Natl Acad Sci** 106: 18159–18164, 2009.

MUKAI Y.; SATO S. Polyphenol-containing azuki bean (*Vigna angularis)* seed

coats attenuate vascular oxidative stress and inflammation in spontaneously hypertensive rats. **J Nutr Biochem** 22: 16–21, 2011.

MUÑOZ-AMATRIAÍN M.; MIREBRAHIM H.; XU P. et al. Genome resources for climate-resilient cowpea, an essential crop for food security. **Plant J** 89: 1042–1054, 2017.

O'CONNOR C. Fluorescence in situ hybridization (FISH). **Nature Education** 1: 171, 2008.

OHMIDO N.; FUKUI K.; KINOSHITA T. Recent advances in rice genome and chromosome structure research by fluorescence in situ hybridization (FISH). **Proc Japan Acad Ser B Phys Biol Sci** 86: 103–106, 2010.

PARDUE M.L.; GALL J.G. Molecular hybridization of radioactive DNA to the DNA of cytological preparations. **Proc Natl Acad Sci** 64: 600–604, 1969.

PARIDA A.; RAINA S.; NARAYAN R. Quantitative DNA variation between and within chromosome complements of *Vigna* species (Fabaceae). **Genetica** 82: 125-133, 1990.

PEDROSA-HARAND A.; DE ALMEIDA C.C.S.; MOSIOLEK M.; BLAIR M.W.; SCHWEIZER D.; GUERRA M. Extensive ribosomal DNA amplification during Andean common bean (*Phaseolus vulgaris* L.) evolution. **Theor Appl Genet** 112: 924–933, 2006.

PEDROSA-HARAND A.; KAMI J.; GEFFROY V.; GEPTS P.; SCHWEIZER D. Cytogenetic mapping of common bean chromosomes reveals a less compartmentalized small-genome plant species. **Chromos Res** 17: 405-417, 2009.

POLANCO C.; SÁENZ DE MIERA L.E.; GONZÁLEZ A.I.; GARCÍA P.; FRATINI R.; VAQUERO F.; JAVIER VENCES F.; DE LA VEJA M.P. Construction of a high-density interspecific (*Lens culinaris* x *L. Odemensis*) genetic map based on functional markers for mapping morphological and agronomical traits, and QTLs affecting resistance to *Ascochyta* in lentil. **PLoS One** 14: 0214409, 2019.

QU M.; LI K.; HAN Y.; CHEN L.; LI Z.; HAN Y. Integrated karyotyping of woodland strawberry (*Fragaria vesca*) with oligopaint FISH probes. **Cytogenet Genome Res** 153: 158–164, 2017.

SACCARDO F.; DEL GIUDICE A.; GALASSO I. **Cytogenetics of cowpea.** In: Biotechnol enhancing. Res Trop Crop Africa. Ibadan, p 89–98, 1992.

RASINKA O.; BARBER J.C.; NEVO E.; BELYAYEV A. Repetitive DNA and chromosomal rearrangements: speciation-related events in plant genomes. **Cytogenet Genome Res** 120: 351–7, 2008.

RAWAL V.; NAVARRO D.K. T**he Gobal Economy of Pulses.** Rome, FAO. Available: http://www.fao.org/3/i7108en/I7108EN.pdf., 2019.

RIBEIRO T.; VASCONCELOS E.V.; DOS SANTOS K.G.B.; VAIO M.;

BRASILEIRO-VIDAL A.C.; PEDROSA-HARAND A. Diversity of repetitive sequences within compact genomes of *Phaseolus* L. beans and allied genera *Cajanus* L. and *Vigna* Savi. **Chromosom Res** 28: 139-153, 2019.

SADER M.A.; DIAS Y.; COSTA Z.P.; MUNHOZ C.; PENHA H.; BERGÈS H.; VIEIRA M.L.C.; PEDROSA-HARAND A. Identification of passion fruit (*Passiflora edulis)* chromosomes using BAC-FISH. **Chromosom Res** 27: 299-311, 2019.

SAKA J.O.; AGBELEYE O.A.; AYOOLA O.T.; LAWAL B.O.; ADETUMBI J.A.; OLEYEDE-KAMIYO Q.O. Assessment of varietal diversity and production systems of cowpea (*Vigna unguiculata* (L.) walp.) in southwest nigeria. **J Agric Rural Dev Trop Subtrop** 119: 43–52, 2018.

SAKAI H.; NAITO K.; TAKAHASHI T.; SATO T.; YAMAMOTO T.; MUTO I.; ITOH T.; TOMOOKA N. The *Vigna* Genome Server, ' *Vig* GS': A Genomic Knowledge Base of the Genus *Vigna* Based on High-Quality, Annotated Genome Sequence of the Azuki Bean, *Vigna angularis* (Willd.) Ohwi & Ohashi. **Plant Cell Physiol** 57: e2–e2, 2016.

SANDAL N.; KRUSHELL L.; RADUTOIU S. et al. A genetic linkage map of the model legume L*otus japonicus* and strategies for fast mapping of new loci. **Genetics** 161: 1673–83, 2002.

SATO S.; NAKAMURA Y.; KANEKO T. et al. Genome structure of the legume, *Lotus japonicus*. **DNA Res** 15: 227–239, 2008.

SCHMUTZ J.; CANNON S.B.; SCHLUETER J. et al. Genome sequence of the palaeopolyploid soybean. **Nature** 463: 178–183, 2010.

SCHMUTZ J.; MCCLEAN P.E.; MAMIDI S. et al. A reference genome for common bean and genome-wide analysis of dual domestications. **Nat Genet** 46: 707–713, 2014.

SCHWARZACHER T.; LEITCH A.R.; BENNET M.D.; HESLOP-HARRISON J.S. *In situ* localization of parental genome in a wide hybrid. **Ann Bot** 64: 315-324, 1989.

SCHWEIZER D. Reverse fluorescent chromosome banding with Chromomycin and DAPI. **Chromosoma** 58: 307-324, 1976.

SCHWEIZER D.; STREHL S.; HAGEMANN S. Plant repetitive DNA elements and chromosome structure. **Chromosome Today** 10: 33-43, 1990.

SHAMURAILATPAM A.; MADHAVAN L.; YADAV S.R.; BHAT K.V.; RAO S.R. Heterochromatin characterization through differential fluorophore binding pattern in some species of *Vigna* Savi. **Protoplasma** 252: 629-635, 2015.

SEN N.K.; BHOWAL J.G. Cytotaxanomy studies on *Vigna.* **Cytologia** 25: 195-207, 1960.

SHE C.W.; JIANG X.H.; OU L.J.; LIU J.; LONG K.L.; ZHANG L.H.; DUAN W.T.; ZHAO W.; HU J.C. Molecular cytogenetic characterisation and phylogenetic

analysis of the seven cultivated *Vigna* species (Fabaceae). **Plant Biology** 17: 268–280, 2015.

SHUNMUGAM A.S.K.; KANNAN U.; JIANG Y.; DABA K.A.; GORIN L.Y. Physiology based approaches for breeding of next-generation food legumes. **Plants** 7: 72, 2018.

SPEICHER M.R.; BALLARD S.G.; WARD D.C. Karyotyping human chromosomes by combinatorial multi-fluor FISH. **Nat Genet** 12: 368–375,1996.

SUZIKI G.; OGAKI Y.; HOKIMOTO N. et al. Random BAC FISH of monocot plants reveals differential distribution of repetitive DNA elements in small and large chromosome species. **Plant Cell Rep** 31: 621–628, 2012.

TANG X.; SZINAY D.; LANG C. et al. Cross-species bacterial artificial chromosome-fluorescence in situ hybridization painting of the tomato and potato chromosome 6 reveals undescribed chromosomal rearrangements. **Genetics** 180: 1319–1328, 2008.

TANG H.; KRISHNAKUMAR V.; BIDWELL S. et al. An improved genome release (version Mt4.0) for the model legume *Medicago truncatula*. **BMC Genomics** 15: 312, 2014.

TANI E.; ABRAHAM E.; CHACHALIS D.; TRAVLOS I. Molecular, genetic and agronomic approaches to utilizing pulses as cover crops and green manure into cropping systems. **Int J Mol Sci** 18: 1202, 2017.

VARSHNEY R.K.; GLASZMANN J.C.; LEUNG H.; RIBAUT J.M. More genomic resources for less-studied crops. **Trends Biotechno**l 28: 452–460, 2010.

VARSHNEY R.K.; GRANER A.; SORRELLS M.E. Genomics-assisted breeding for crop improvement. **Trends Plant Sci** 10: 621–630, 2005.

VASCONCELOS E.V.; FONSÊCA A.F.; PEDROSA-HARAND A.; DE ANDRADE BORTOLETI K.C.; BENKO-ISEPPON A.M.; DA COSTA A.F.; BRASILEIRO-VIDAL A.C. Intra- and interchromosomal rearrangements between cowpea [*Vigna unguiculata* (L.) Walp.] and common bean (*Phaseolus vulgaris* L.) revealed by BAC-FISH. **Chromosome Res** 23: 253–266, 2015.

VENORA G.; SACCARDO E. Mitotic karyotype analysis in the *Vigna* genus by means of an image analyser. **Caryologia** 46: 139-149, 1993.

WINTER P.; BENKO-ISEPPON A.M.; HUTTEL B. et al. A linkage map of the chickpea (*Cicer arietinum* L.) genome based on recombinant inbred lines from a *C. arietinum*×*C. reticulatum* cross: localization of resistance genes for fusarium wilt races 4 and 5. **Theor Appl Genet** 101: 1155–1163, 2002.

WOJCIECHWSKI M.F. Reconstructing the phylogeny of legumes (Leguminosae): an early 21st century perspective. In: B.B. Klitgaard & A. Bruneau (eds.). **Advances in Legume Systematics.** Royal Botanic Gardens, Kew,10, pp.5-35, 2003.

XIN H.; ZHANG T.; HAN Y.; WU Y.; SHI J.; XI M.; JIANG J. Chromosome painting and comparative physical mapping of the sex chromosomes in *Populus tomentosa* and *Populus deltoides*. **Chromosoma** 127: 313–321, 2018.

XIN H.; ZHANG T.; WU Y.; ZHANG W.; ZHANG P.; XI M.; JIANG J. An extraordinarily stable karyotype of the woody *Populus* species revealed by chromosome painting. **Plant J** 101: 253–264, 2020.

XU P.; WU X.; WANG B. et al. A SNP and SSR based genetic map of asparagus bean (*Vigna unguiculata* subsp. *sesquipedalis*) and comparison with the broader species. **Plos One** 6:e15952, 2011.

YANG K.; TIAN Z.; CHEN C. et al. Genome sequencing of adzuki bean (*Vigna angularis)* provides insight into high starch and low fat accumulation and domestication. **Proc Natl Acad Sci** 112: 13212-13218, 2015.

YOUNG N.D.; DEBELLÉ F.; OLDROYD G.E.D. et al. The *Medicago* genome provides insight into the evolution of rhizobial symbioses. **Nature** 480: 520–52, 2011.

YOUSIF A.M.; BATEY I.L.; LARROQUE O.R.; CURTIN B.; BEKES F.; DEETH H.C. Effect of storage of adzuki bean (*Vigna angularis*) on starch and protein properties. **Food Sci Technol** 36: 601–607, 2003.

YUNDAENG C.; SOMTA P.; AMKUL K.; KONGJAIMUN A.; KAGA A.; TOMOOKA N. Construction of genetic linkage map and genome dissection of domestication-related traits of moth bean (*Vigna aconitifolia*), a legume crop of arid areas. **Mol Genet Genomics** 294: 621-635, 2019.

ZHENG J.; NAKATA M.; UCHYAMA H.; MORIKAWA H.; TANAKA R. Giemsa C-banding Patterns in Several Species of *Phaseolus* L. and *Vigna* Savi, Fabaceae. **Cytologia 5**6: 459-466, 1991.

ZHENG J.Y.; NAKATA M.; IRIFUNE K.; TANAKA R.; MORIKAWA H. Fluorescent banding pattern analysis of eight taxa of *Phaseolus* and *Vigna* in relation to their phylogenetic relationships. **Theor Appl Genet** 87: 38-43, 1993.

Internet resources

CONAB (2016) Companhia Nacional de Abastecimento. https://www.conab.gov.br/. (accessed 18 December 2019).

EMBRAPA (2019) Empresa Brasileira de Pesquisa Agropecuária. http://www.cnpaf.embrapa.br/socioeconomia/index.htm. (accessed 10 January 2018).

FAOSTAT (2015) Statistical database of the Food and Agriculture Organization of the United Nations. http://faostat.fao.org. (accessed 30 July 2020).

FAOSTAT (2020) Statistical database of the Food and Agriculture Organization of

the United Nations. http://faostat.fao.org. (accessed 01 February 2020).

USDA (2015) United States Department of Agriculture. https://www.usda.gov/. (accessed 17 December 2019).

APÊNDICES

APÊNDICE A – ARTIGO PUBLICADO NA REVISTA CHROMOSOME RESEARCH

Chromosome Res
https://doi.org/10.1007/s10577-020-09635-0

ORIGINAL ARTICLE

Breaks of macrosynteny and collinearity among moth bean (*Vigna aconitifolia*), cowpea (*V. unguiculata*), and common bean (*Phaseolus vulgaris*)

Ana Rafaela da S. Oliveira · Lívia do Vale Martins · Fernanda de O. Bustamante · María Muñoz-Amatriaín · Timothy Close · Antônio F. da Costa · Ana Maria Benko-Iseppon · Andrea Pedrosa-Harand · Ana Christina Brasileiro-Vidal

Received: 13 April 2020 / Revised: 29 June 2020 / Accepted: 1 July 2020

Abstract Comparative cytogenetic mapping is a powerful approach to gain insights into genome organization of orphan crops, lacking a whole sequenced genome. To investigate the cytogenomic evolution of important *Vigna* and *Phaseolus* beans, we built a BAC-FISH (fluorescent in situ hybridization of bacterial artificial chromosome) map of *Vigna aconitifolia* (*Vac*, subgenus *Ceratotropis*), species with no sequenced genome, and compared with *V. unguiculata* (*Vu*, subgenus *Vigna*) and *Phaseolus vulgaris* (*Pv*) maps. Seventeen *Pv* BACs, eight *Vu* BACs, and 5S and 35S rDNA probes were hybridized in situ on the 11 *Vac* chromosome pairs. Five *Vac* chromosomes (*Vac*6, *Vac*7, *Vac*9, *Vac*10, and *Vac*11) showed conserved macrosynteny and collinearity between *V. unguiculata* and *P. vulgaris*. On the other hand, we observed collinearity breaks, identified by pericentric inversions involving *Vac*2 (*Vu*2), *Vac*4 (*Vu*4), and *Vac*3 (*Pv*3). We also detected macrosynteny breaks of translocation type involving chromosomes 1 and 8 of *V. aconitifolia* and *P. vulgaris*; 2 and 3 of *V. aconitifolia* and *P. vulgaris*; and 1 and 5 of *V. aconitifolia* and *V. unguiculata*. Considering our data and previous BAC-FISH studies, six chromosomes (1, 2, 3, 4, 5, and 8) are involved in major karyotype divergences between genera and five (1, 2, 3, 4, and 5) between *Vigna* subgenera, including mechanisms such as duplications, inversions, and translocations. Macrosynteny breaks between *Vigna* and *Phaseolus* suggest that the major chromosomal rearrangements have occurred within the *Vigna* clade. Our cytogenomic comparisons bring new light on

Key message *Vigna aconitifolia*, *V. unguiculata*, and *Phaseolus vulgaris* karyotypes share partial macrosynteny, with evidences of major chromosomal rearrangements (inversions, duplications and translocations) related to the *Vigna* and *Phaseolus* (Phaseolineae subtribe) diversification.

Responsible Editor: Andreas Houben

Electronic supplementary material The online version of this article (https://doi.org/10.1007/s10577-020-09635-0) contains supplementary material, which is available to authorized users.

A. R. d. S. Oliveira · L. d. Martins · F. d. O. Bustamante · A. M. Benko-Iseppon · A. C. Brasileiro-Vidal (✉)
Departamento de Genética, Universidade Federal de Pernambuco, Recife, Pernambuco, Brazil
e-mail: brasileirovidal.ac@gmail.com

M. Muñoz-Amatriaín
Department of Soil and Crop Sciences, Colorado State University, Fort Collins, CO, USA

T. Close
Department of Botany and Plant Sciences, University of California, Riverside, CA, USA

A. F. da Costa
Instituto Agronômico de Pernambuco, Recife, Pernambuco, Brazil

A. Pedrosa-Harand
Departamento de Botânica, Universidade Federal de Pernambuco, Recife, Pernambuco, Brazil

Published online: 11 July 2020

the degree of shared macrosynteny and mechanisms of karyotype diversification during *Vigna* and *Phaseolus* evolution.

Keywords BAC-FISH · beans · chromosome rearrangements · karyotype evolution · Phaseolineae subtribe · synteny

Abbreviations

BAC	Bacterial artificial chromosome
Chr	Chromosome
DAPI	4,6-Diamidino-2-phenylindole
FISH	Fluorescence in situ hybridization
LG	Linkage group
Mya	Million years ago
rDNA	Ribosomal DNA
Pl	*Phaseolus lunatus*
Pm	*Phaseolus microcarpus*
Pv	*Phaseolus vulgaris*
Vac	*Vigna aconitifolia*
Vm	*Vigna mungo*
Vum	*Vigna umbellata*
Vu	*Vigna unguiculata*

Introduction

Vigna Savi and *Phaseolus* L. are socioeconomic important legumes with wide distribution, mainly in the southern hemisphere. These phylogenetically related genera were separated ~ 9.7 million years ago (Mya) (Li et al. 2013) and belong to the Phaseolineae subtribe, Papilionoideae subfamily, Leguminosae family (LPWG 2017). *Phaseolus* comprises about 100 species (The Plant List 2013), with five domesticated species of American origin, including *P. vulgaris* L. (common bean), the main grain legume for human diet in the world (Broughton et al. 2003; Gepts et al. 2008). In turn, *Vigna* comprises about 120 species (The Plant List 2013) distributed in five subgenera (Delgado-Salinas et al. 2011), including several agriculturally important legumes from *Ceratotropis* (Asian group) and *Vigna* (African group) subgenera (~ 3.6 Mya divergence; Javadi et al. 2011), such as *V. aconitifolia* (Jacq.) Maréchal (moth bean; Tomooka et al. 2002; Brink and Jansen 2006) and *Vigna unguiculata* (L.) Walp. (cowpea; Maréchal et al. 1978), respectively.

Most *Phaseolus* and *Vigna* species are diploid with $2n = 2x = 22$ chromosomes (Mercado-Ruaro and Delgado-Salinas 1996, 1998; Forni-Martins 1986; Venora et al. 1999; She et al. 2015). Genetic maps based on different molecular markers have been developed for *P. vulgaris* (Vallejos et al. 1992; Freyre et al. 1998) and for several *Vigna* species, such as *V. unguiculata* (Ouédraogo et al. 2002; Muchero et al. 2009; Muñoz-Amatriaín et al. 2017) and *V. aconitifolia* (Yundaeng et al. 2019). However, whole-genome assembly is limited to few species, such as *P. vulgaris* (Schmutz et al. 2014), *V. radiata* (L.) R. Wilczek (mungbean; Kang et al. 2014), *V. angularis* (Willd.) Ohwi & H. Ohashi (adzuki bean; Kang et al. 2015; Sakai et al. 2015; Yang et al. 2015), *V. subterranea* (Chang et al. 2019), and *V. unguiculata* (Lonardi et al. 2019). For most of the remaining *Vigna* species, genetic and genomic comparisons are limited to the genetic linkage map information.

Cytogenomic comparative analysis using BACs (bacterial artificial chromosomes) as FISH (fluorescent in situ hybridization) probes has been a useful approach for comparative evolution studies in legumes, including some *Vigna* and *Phaseolus* species. In *Phaseolus*, macrosynteny studies by BAC-FISH indicated that the genus evolution mostly relies on chromosomal rearrangements of little complexity in $2n = 22$ species, with few breaks of collinearity due to inversions between *P. vulgaris* and *P. lunatus* L. (Bonifácio et al. 2012; Almeida and Pedrosa-Harand 2013), and between *P. vulgaris* and *P. microcarpus* Mart. (Fonsêca and Pedrosa-Harand 2013). For *P. leptostachyus* Benth., species with $2n = 20$, BAC-FISH revealed that the descending dysploidy was caused by a nested chromosome fusion, accompanied by several additional translocations and inversions not previously reported for the genus (Fonsêca et al. 2016). Additionally, in the intergeneric comparison using *P. vulgaris* BAC probes hybridized on the mitotic chromosomes of *V. unguiculata* (BAC-FISH), a partial conservation of macrosynteny between these species was identified, with translocations, inversions, and duplications involved in five *V. unguiculata* chromosome pairs (Vasconcelos et al. 2015). Nevertheless, it was not possible to infer about chromosome diversification and evolution within *Vigna* genus since the cytogenetics analysis was restricted to *V. unguiculata*.

The present work aimed to expand the cytogenomic comparison within *Vigna* by studying a species with no assembled genome and with distinct cytogenetic

features with respect to the number of rDNA sites (She et al. 2015): *Vigna aconitifolia*, which has only one pair of 5S rDNA and one pair of 35S rDNA. It is an Asian wild species tolerant to drought stress (as discussed by Takahashi et al. 2016), which makes it a target species for genetics studies. To better understand the chromosome evolution and genome organization within *Vigna* and between *Vigna* and *Phaseolus*, we constructed a cytogenetic map for *V. aconitifolia* and compared it with *V. unguiculata* and *P. vulgaris* maps, using *V. unguiculata* and *P. vulgaris* BACs, and 5S and 35S rDNA as FISH probes. Taken together with previous BAC-FISH studies, the present results provide evidence and help to understand the chromosome evolutionary paths and to identify the main chromosomal rearrangements that occurred during *Vigna* and *Phaseolus* divergence.

Materials and methods

Plant material

Vigna aconitifolia (*Vac*) accession VIG 1609 (Indian), *V. unguiculata* (*Vu*) cv. BR14-Mulato, *P. vulgaris* (*Pv*) cv. BRS Esplendor, and *P. vulgaris* Mesoamerican breeding line BAT93 seeds were provided by IPK (Institute of Plant Genetics and Crop Plant Research, Gatersleben, Germany), Embrapa Meio-Norte (Empresa Brasileira de Pesquisa Agropecuária Meio-Norte, Teresina, Brazil), Embrapa Arroz e Feijão (Empresa Brasileira de Pesquisa Agropecuária Arroz e Feijão, Santo Antônio de Goiás, Brazil), and CIAT (International Center for Tropical Agriculture, Cali, Colombia), respectively. All seeds were multiplied at IPA (Instituto Agronômico de Pernambuco, Recife, Brazil).

Chromosome preparation

After seed germination, root tips were collected and pretreated with 2 mM 8-hydroxyquinoline (8-HQ) for 4.5 h at 18 °C, fixed in methanol to acetic acid (3:1, v/v) from 4 to 24 h at room temperature and stored at − 20 °C until use. Then, meristems were digested for 4 h at 37 °C in 2% (w/v) cellulase "Onozuka R-10" (Serva)/20% (v/v) pectinase (Sigma). Slides were prepared according to Carvalho and Saraiva (1993), with minor modifications at the final steps: after air drying, the slides were immersed in 45% acetic acid for 10 s and dried at 37 °C.

BAC selection and probe labeling

For *V. aconitifolia* comparative BAC-FISH map, 31 BAC clones from *P. vulgaris* (Kami et al. 2006), previously selected (Pedrosa-Harand et al. 2009; Fonsêca et al. 2010) with genetically mapped markers (Vallejos et al. 1992; Hougaard et al. 2008), as well as the bacteriophage SJ19.12 related to anthracnose resistance were tested (Table 1; Online Resource 1; Fonsêca et al. 2010). Additionally, 14 *Vu* BAC clones were used, of which eight were previously mapped in situ on *Vu* pachytene chromosomes (Iwata-Otsubo et al. 2016) and six were used for the first time for in situ hybridization (Table 1; Online Resource 1). These BAC clones contain SNPs previously located on *V. unguiculata* consensus map and anchored in silico in *Pv* pseudomolecules (Muñoz-Amatriaín et al. 2017).

Moreover, the R2 probe, 6.5-kb fragment containing the 18S-5.8S-25S rDNA repeat unit from *A. thaliana* (L.) Heynh. (Wanzenböck et al. 1997) and the D2 sequence, 400-bp fragment containing two 5S rDNA repeats from *Lotus japonicus* (Regel) K.Larsen (Pedrosa et al. 2002), were used for the identification of *V. aconitifolia* chromosomes that carry rDNA. DNA extraction of *Pv* and *Vu* BACs, and plasmid containing rDNA followed the Plasmid Mini Kit protocol (Qiagen). BACs, 35S, and 5S rDNA probes were labeled with Cy3-dUTP (GE Healthcare), digoxigenin-11-dUTP (Roche Diagnostics), and biotin-16-dUTP (Sigma), respectively, via nick translation kit (Thermo Fisher Scientific).

Fluorescent in situ hybridization

The FISH procedure followed Fonsêca et al. (2010). All selected BAC probes were first hybridized on donor species (*P. vulgaris* and/or *V. unguiculata*) metaphases, confirming the presence of a single FISH signal on their chromosomes. The hybridization mixture comprised 50% formamide (v/v), 10% dextran sulfate (w/v), 2× saline sodium citrate (SSC), and 2–5 ng/μL of each probe, denatured for 10 min at 75 °C. For blocking the repetitive DNA of some BACs with disperse signals on FISH, the C_0t-100 fraction of *P. vulgaris* was isolated (Zwick et al. 1997) and added to the hybridization mix (Table 1; Online Resource 1). After the addition of the hybridization mixture, slides were denatured at 75 °C for 7 min, and kept for 2 days in humid chamber at 37 °C (stringency of 77%). The post-hybridization

Table 1 List of 17 BACs from *Phaseolus vulgaris* (*Pv*) and eight BACs from *Vigna unguiculata* (*Vu*) mapped in situ on chromosomes of *V. aconitifolia* (*Vac*), *V. unguiculata*, and *P. vulgaris* chromosomes (with or without C_0t-100 blocking DNA)

Vac	BAC	BAC chromosome position/arm		
		V. aconitifolia	*V. unguiculata*[a] *Vu*[c]/LG[d]	*P. vulgaris*[b] *Pv*[e]
*Vac*1	177I19	Interstitial/short (0×)	Terminal/long (0×) *Vu*5/*Vu*LG1	Interstitial/short (0×) *Pv*8
	38C24	Terminal/long (0×)	Subterminal/long (50×) *Vu*1/*Vu*LG4	Subterminal/long (0×) *Pv*1
*Vac*2	H074C16#	Proximal/short (0×)	Proximal/long (0×) *Vu*2/*Vu*LG7	Terminal/short (0×) *Pv*3*
	M026L23#	Terminal/long (0×)	Terminal/long (0×) *Vu*2/*Vu*LG7	Terminal/short (0×) *Pv*2*
*Vac*3	225P10	Terminal/short (0×)	Terminal/short (0×) *Vu*3/*Vu*LG3	Subterminal/long (0×) *Pv*2
	21N14	Interstitial/short (*Vac*3) and interstitial/short (small chromosome) (50×)	No signal (0×)	Interstitial/long (80×) *Pv*2
	127F19	Interstitial/short (*Vac*3) and interstitial/short (small chromosome) (50×)	Terminal/short (50×) *Vu*3/*Vu*LG3	Interstitial/long (0×) *Pv*2
	267H4	Proximal/short (0×)	Interstitial/short (50×) *Vu*3/*Vu*LG3	Interstitial/short (50×) *Pv*3
	147K17	Proximal/long (0×)	Proximal/short and long (0×) *Vu*3/*Vu*LG3	Interstitial/short (0×) *Pv*3
	95L13	Interstitial/long (0×)	Interstitial/long (0×) *Vu*3/*Vu*LG3	Subterminal/long (0×) *Pv*3
*Vac*4	221J10	Terminal/short (0×)	Terminal/short (50×) *Vu*4/*Vu*LG11	Subterminal/short (50×) *Pv*4
	190C15	Terminal/long (0×)	Subterminal/short (20×) *Vu*4/*Vu*LG11	Interstitial/long (50×) *Pv*4
*Vac*5	M002E09#	Interstitial/long (0×)	Subterminal/short (0×) *Vu*5/*Vu*LG1	Not analyzed
*Vac*6	121F5	Subterminal/long (0×)	No signal (0×)	Interstitial/long (0×) *Pv*6
	18B15	Terminal/long (0×)	Terminal/short (0×) *Vu*6/*Vu*LG6	Subterminal/long (0×) *Pv*6
*Vac*7	22I21	Terminal/short (0×)	Terminal/short (0×) *Vu*7/*Vu*LG2	Interstitial/long (50×) *Pv*7
	86I17	Terminal/long (0×)	Terminal/long (0×) *Vu*7/*Vu*LG2	Subterminal/short (50×) *Pv*7
*Vac*8	169G16	Interstitial/short (0×)	Terminal/long (50×) *Vu*8/*Vu*LG5	Subterminal/long (50×) *Pv*8
	221F15	Interstitial/long (0×)	Proximal/short (5×) *Vu*8/*Vu*LG5	Proximal/short (20×) *Pv*1
*Vac*9	H086N19#	Terminal/short (0×)	Subterminal/short (0×) *Vu*9/*Vu*LG8	Subterminal/long (0×) *Pv*9*
	H010M18#	Terminal/long (0×)	Terminal/long (0×) *Vu*9/*Vu*LG8	Proximal/short (0×) *Pv*9*
*Vac*10	H015M15#	Terminal/short (0×)	Subterminal/long (0×) *Vu*10/*Vu*LG10	Terminal/short (0×) *Pv*10*
	H025N06#	Proximal/long (0×)	Interstitial/short (0×) *Vu*10/*Vu*LG10	Proximal/long (0×) *Pv*10*
*Vac*11	H092J22#	Subterminal/short (0×)	Terminal/short (0×)	Terminal/long (0×)

Table 1 (continued)

Vac	BAC	BAC chromosome position/arm		
		V. aconitifolia	*V. unguiculata*[a] *Vu*[c]/LG[d]	*P. vulgaris*[b] *Pv*[e]
			*Vu*11*/*Vu*LG9	*Pv*11*
	179N14	Terminal/long (50×)	Terminal/long (0×) *Vu*11/*Vu*LG9	Subterminal/short (0×) *Pv*11

[a] BACs hybridized in situ in Vasconcelos et al. (2015)

[b] BACs hybridized in situ in Pedrosa-Harand et al. (2009) and Fonsêca et al. (2010)

[c] Chromosomes numbered according to Lonardi et al. (2019)

[d] Linkage groups according to Muñoz-Amatriaín et al. (2017)

[e] Chromosomes numbered according to Schmutz et al. (2014)

[#] BAC clones of *V. unguiculata*

*New data for *V. unguiculata* or *P. vulgaris*

washes were performed in 0.1× SSC at 42 °C. For BACs with no FISH signal, 40% stringency was tested (for details, see Schwarzacher and Heslop-Harrison 2000). 35S biotin-labeled probes were detected using avidin-rhodamine antibody (Vector Laboratories), and 5S digoxigenin-labeled probes were detected using sheep anti-digoxigenin primary antibody conjugated with FITC (fluorescein isothiocyanate; Roche), both antibodies diluted in 1% (w/v) BSA. All preparations were counterstained with 8 μL of DAPI (4′,6-diamidino-2-phenylindole) in Vectashield (1 μg/mL) (Vector). For different DNA sequence detection using the same cells, slides were rehybridized (Heslop-Harrison et al. 1992).

Data analysis

Images of the best mitotic metaphases were acquired using Leica DMLB epifluorescence microscope and Leica DFC 340FX camera with the Leica CW4000 software. Images were pseudocolored and optimized for brightness and contrast with Adobe Photoshop CS4 (Adobe Systems Incorporated) software. For each chromosome, five mitotic metaphases were selected. Chromosomes and BAC signal positions were measured using MicroMeasure v3.3 software (available at http://rydberg.biology.colostate.edu/MicroMeasure/, Colorado State University). The BAC positions were classified in terminal (= subtelomeric), subterminal, interstitial, and proximal. Twenty chromatids per chromosome type were measured for size, arm ratio, and BAC position.

Chromosomes were named according to the initials of *V. aconitifolia* (*Vac*), in accordance with their orthology to *V. unguiculata* (*Vu*) and *P. vulgaris* (*Pv*) chromosomes, using the numbering system proposed by Lonardi et al. (2019). Subsequently, we constructed comparative circular ideograms among *Vac*/*Vu*/*Pv* using Adobe Flash CS4 Professional program. *Pv* and *Vu* ideograms were assembled based on Vasconcelos et al. (2015). To facilitate our comparisons, *Vu* chromosome numbering described by Vasconcelos et al. (2015) was substituted by the new *Vu* numbering system (Lonardi et al. 2019), and *Vac* and *Vu* chromosomes were positioned according to Lonardi et al. (2019), independent of their morphology. A comparison of the major chromosomal changes among *Vigna* and *Phaseolus* species was performed based on the present work and on the literature data for *V. unguiculata* (Vasconcelos et al. 2015), *P. vulgaris* (Pedrosa-Harand et al. 2009; Fonsêca et al. 2010), *P. lunatus* (*Plu*) (Bonifácio et al. 2012; Almeida and Pedrosa-Harand 2013), and *P. microcarpus* (*Pm*) (Fonsêca and Pedrosa-Harand 2013). These comparisons were schematically represented in a modified phylogenetic tree based on ITS, *trnK* and *mat*K sequences (Delgado-Salinas et al. 2011).

Results

In our BAC-FISH map construction for *V. aconitifolia* (*Vac*, $2n = 22$), we identified its 11 meta- and

submetacentric mitotic chromosome pairs by using 17 *Pv* (*P. vulgaris*) BACs, eight *Vu* (*V. unguiculata*) BACs, and 35S and 5S rDNA as probes (Figs. 1 and 2, Table 1, Online Resource 1). To perform the intra- and intergeneric comparative BAC-FISH analysis, we compared our *Vac* map with *Vu* and *Pv*, as schematically represented in circular maps (Fig. 3). In the present work, at least two markers were physically mapped on each of the 11 chromosome pairs of *Vac*, *Vu*, and *Pv*, except for *Pv*5.

From the BACs tested, 14 *Pv* BACs and eight *Vu* BACs showed unique signals on *Vac* chromosomes without addition of blocking DNA (Table 1). However, SJ19.12 bacteriophage, 14 *Pv* BACs, and four *Vu* BACs showed no or disperse FISH signals on *Vac* chromosomes, being excluded from further analyses. Additionally, for three *Pv* BACs and two *Vu* BACs with disperse signals, we added the blocking DNA (50–100× C_0t-100 fraction), but only for BAC 179N14, a single-copy signal was detected on *Vac*11, while BACs 127F19 and 21N14 (*Pv*2) were mapped on *Vac*3 and on a small chromosome (Table 1; Online Resource 1).

Five of the 11 *Vac* chromosomes (*Vac*6, *Vac*7, *Vac*9, *Vac*10, and *Vac*11) showed conservation of synteny and collinearity with their corresponding *Vu* and *Pv* chromosomes (Fig. 3). Our BAC-FISH comparison identified two translocation events with macrosynteny breaks between *V. aconitifolia* and *P. vulgaris*: one involving *Vac*1 (177I19, 38C24; Fig. 1b) and *Vac*8 (169G16, 221F15; Fig. 2d), when compared with *Pv*1 (221F15, 38C24) and *Pv*8 (177I19, 169G16), and the other involving *Vac*2 (H074C16, M026L23; Fig. 1c) and *Vac*3 (225P10, 127F19, 21N14, 267H4, 147K17, 95L13; Fig. 1d–f), when compared with *Pv*2 (M026L23, 127F19, 21N14, 225P10) and *Pv*3 (H074C16, 147K17, 267H4, 95L13) (Figs. 3 and 4). Since chromosomes 2 and 3 are known to be the most involved in rearrangements between *Vu* and *Pv* (Vasconcelos et al. 2015), we increased the number of BACs in their analysis. After adding block DNA (50× C_0t-100 fraction), 127F19 and 21N14 BACs (both markers colocalized on *Pv*2) were colocalized on *Vac*3, but also mapped in a small chromosome, suggesting a duplication for these two sequences on different chromosomes (Table 1; Fig. 1d and f, respectively). The chromosome segment including BACs 147K17 and 267H4 (*Pv*3, short arm) was inverted on *Vac*3, with 267H4 at short arm and 147K17 at the long arm, suggesting a break of collinearity caused by an inversion between genera, which also involved a centromere repositioning (Figs. 1a, e and 3). As previously reported by Vasconcelos et al. (2015), we also observed a duplication of 147K17 BAC marker on *Vu*3 (Fig. 3), being considered a species-specific event since it was not observed on *Vac*3 (Fig. 1e).

Furthermore, the comparative BAC-FISH map between *Vigna* species also revealed breaks of synteny within the genus. We identified a translocation involving *Vac*1 (177I19 and 38C24; Fig. 1b) and *Vac*5 (M002E09; Fig. 1h) when compared with *Vu*1 (38C24) and *Vu*5 (M002E09 and 177I19; Fig. 3). Additionally, two collinearity breaks caused by pericentric inversions were observed between *Vigna* species, involving Chr2 (H074C16 and M026L23; Figs. 1c and 3) and Chr4 (221J10 and 190C15; Figs. 1g and 3). In the latter case, BACs located on *Vac*4 were collinear to *Pv*4, suggesting the inversion is species-specific and has occurred in *V. unguiculata* (Figs. 3 and 4).

We also compared the position and distribution of the rDNA sites among all analyzed species. The mapped *P. vulgaris* accession presented two chromosomes with 5S rDNA sites (*Pv*6, *Pv*10) and three chromosomes with 35S rDNA sites (*Pv*6, *Pv*9, *Pv*10), while *V. unguiculata* showed two chromosomes carrying 5S rDNA sites (*Vu*10, *Vu*11) and six with 35S rDNA sites (*Vu*1, *Vu*2, *Vu*6, *Vu*9, *Vu*10, *Vu*11), as previously described by Fonsêca et al. (2010) and Vasconcelos et al. (2015), respectively. In contrast, only one pair of 5S rDNA sites was located at the proximal region of the long arm of *Vac*5 (Fig. 1a, h), and one 35S rDNA pair was found covering the whole short arm of *Vac*6 (Fig. 2a, b).

To provide additional support for our comparative chromosome analysis between genera, we compared our FISH mapping with the previous literature data for *P. microcarpus* (Fonsêca and Pedrosa-Harand 2013) and *P. lunatus* (Bonifácio et al. 2012; Almeida and Pedrosa-Harand 2013). The cytogenetic comparison is schematically represented in a simplified phylogenetic tree (adapted of Delgado-Salinas et al. 2011), which helped us to understand the macrosynteny, collinearity, and chromosome alterations among *Vigna* and *Phaseolus* species (Fig. 4). Inversions were the only rearrangement type found in *Phaseolus* genus. One paracentric and one pericentric inversion were identified between clades A and B. Within clade B (*P. vulgaris* and *P. lunatus*), three pericentric inversions were previously described. Altogether, the results described above associated with these previous BAC-FISH studies identified the main chromosomes and the major rearrangements among these

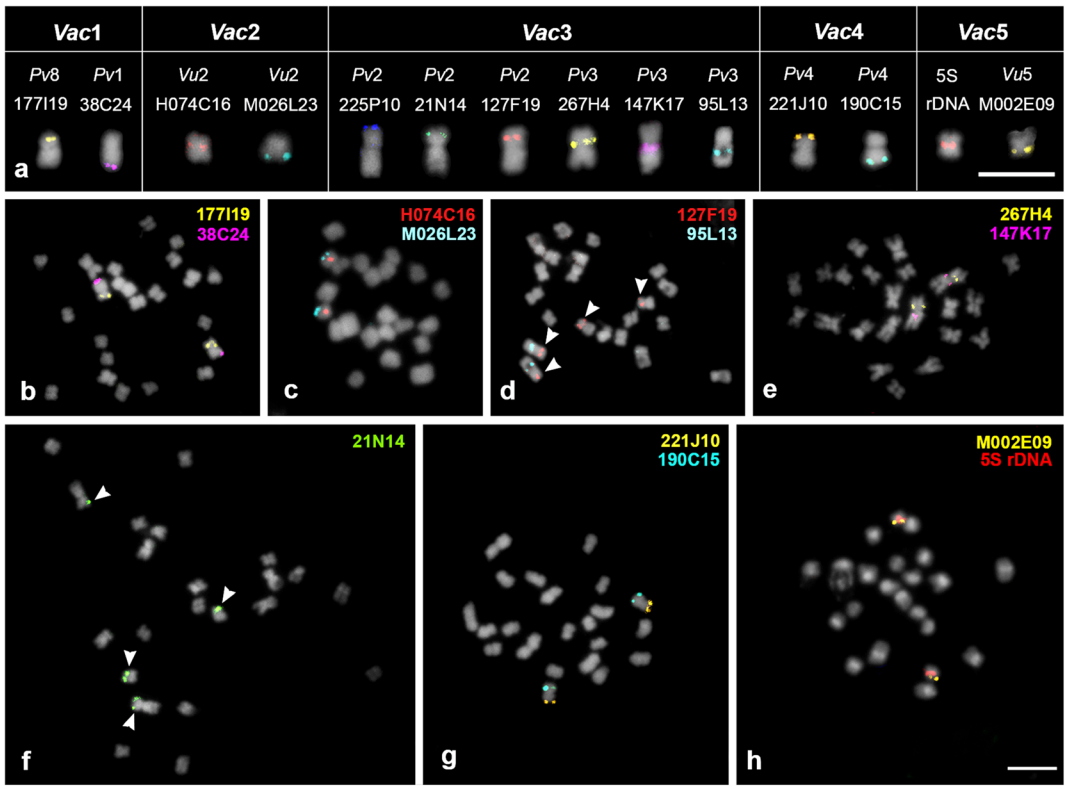

Fig. 1 Fluorescent in situ hybridization of ten genetically assigned BACs of *Phaseolus vulgaris* (*Pv*) and three BACs of *Vigna unguiculata* (*Vu*), as well as 5S rDNA, in *V. aconitifolia* (*Vac*) mitotic chromosomes counterstained with DAPI (pseudocolored in gray). **a** *Vigna aconitifolia* chromosomes (*Vac*1, *Vac*2, *Vac*3, *Vac*4, and *Vac*5) hybridized with 5S rDNA, BACs from five *P. vulgaris* chromosomes (*Pv*1, *Pv*2, *Pv*3, *Pv*4, and *Pv*8) and two *V. unguiculata* chromosomes (*Vu*2 and *Vu*5). BACs were labeled with Cy3-dUTP and different pseudocolors were applied. Chromosomes were orientated according to their morphology. **b** BACs 177I19 (*Pv*8) and 38C24 (*Pv*1) in situ located in *Vac*1. **c** BACs H074C16 (*Vu*2) and M026L23 (*Vu*2) mapped in *Vac*2. **d** BACs 127F19 (*Pv*2, arrowhead and in an unidentified second pair) and 95L13 (*Pv*3) in *Vac*3. **e** BACs 267H4 (*Pv*3) and 147K17 (*Pv*3) mapped in *Vac*3. **f** BAC 21N14 (*Pv*2, arrowhead and in an unidentified second pair) hybridized on chromosome *Vac*3. **g** BACs 221J10 (*Pv*4) and 190C15 (*Pv*4) in *Vac*4. **h** 5S rDNA and BAC M002E09 (*Vu*5) in *Vac*5. Bars in **a** and **h** represent 5 μm

species. Chromosomes 1, 2, 3, 4, 5, and 8 were involved in translocations, inversions, and duplications related to the divergence and evolution between and within *Vigna* and/or *Phaseolus* genera.

Discussion

To increase the knowledge of the global macrosynteny and karyoevolutionary mechanisms in *Vigna* and *Phaseolus*, we constructed a comparative FISH map among *V. aconitifolia*, *V. unguiculata*, and *P. vulgaris* (Pedrosa-Harand et al. 2009; Fonsêca et al. 2010; Vasconcelos et al. 2015) (Fig. 3). Partial conservation of synteny was observed among *Vigna* and *Phaseolus* species. Five chromosomes (6, 7, 9, 10, and 11) were highly syntenic and collinear among *V. aconitifolia* (present work), *V. unguiculata* (Vasconcelos et al. 2015; Muñoz-Amatriaín et al. 2017; Lonardi et al. 2019), and *P. vulgaris* (Pedrosa-Harand et al. 2009; Fonsêca et al. 2010). Additionally, despite its involvement in chromosomal rearrangement between both genera, chromosome 8 was syntenic within *Vigna*, as observed in our *Vu* and *Vac* comparison, and from genomic data in other two species from *Ceratotropis* subgenus, *V. angularis* (*Va*) and *V. radiata* (*Vr*) (Lonardi et al. 2019). Overall, breaks of macrosynteny and collinearity due to translocations, inversions, and duplications were detected in the other six or five chromosomes that are involved in the major karyotype divergences between both genera or between *Vigna* and *Ceratotropis* subgenera, respectively.

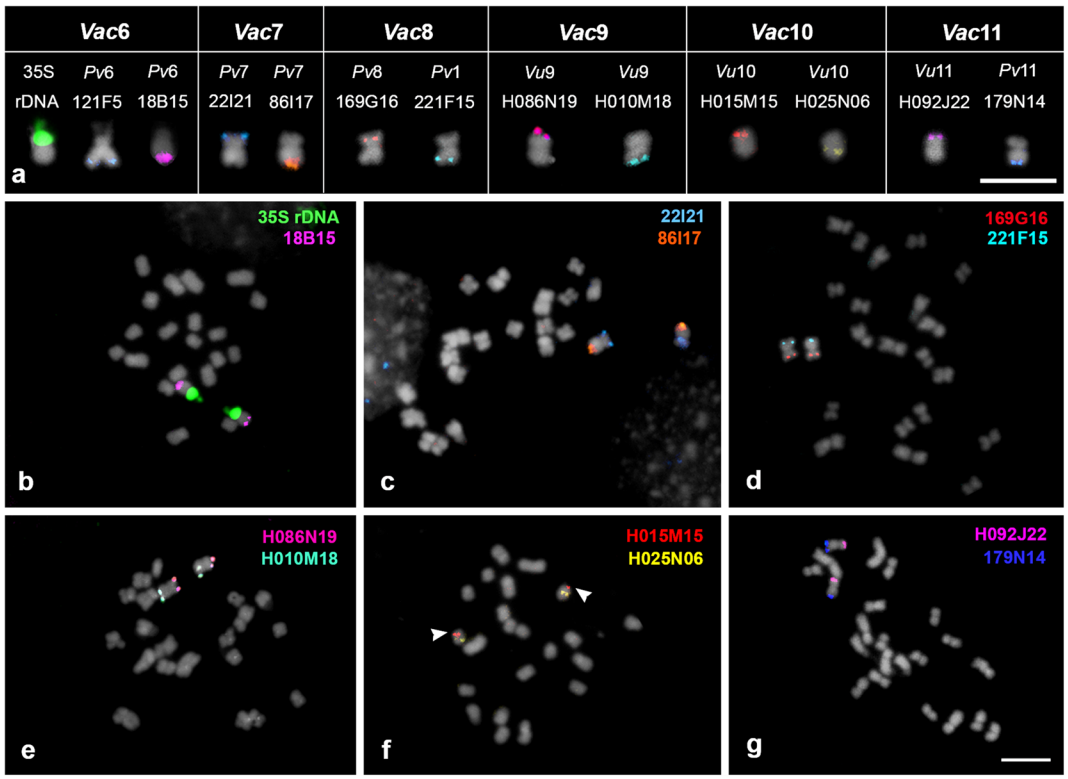

Fig. 2 Fluorescent in situ hybridization of seven genetically assigned BACs of *Phaseolus vulgaris* (*Pv*) and five BACs of *Vigna unguiculata* (*Vu*), as well as 35S rDNA, in *Vigna aconitifolia* (*Vac*) mitotic chromosomes counterstained with DAPI (pseudocolored in gray). **a** *V. aconitifolia* chromosomes (*Vac*6, *Vac*7, *Vac*8, *Vac*9, *Vac*10, and *Vac*11) hybridized with 35S rDNA and BACs from five *P. vulgaris* chromosomes (*Pv*1, *Pv*6, *Pv*7, *Pv*8, and *Pv*11) and three *V. unguiculata* chromosomes (*Vu*9, *Vu*10, and *Vu*11). BACs were labeled with Cy3-dUTP and different pseudocolors were applied. Chromosomes were orientated according to their morphology. **b** 35S rDNA and BAC 18B15 (*Pv*6) mapped in *Vac*6. **c** BACs 22I21 (*Pv*7) and 86I17 (*Pv*7) in *Vac*7. **d** BACs 169G16 (*Pv*8) and 221F15 (*Pv*1) mapped in *Vac*8. **e** BACs H086N19 (*Vu*9) and H010M18 (*Vu*9) identified in *Vac*9. **f** BACs H015M15 (*Vu*10) and H025N06 (*Vu*10) located in *Vac*10. **g** BACs H092J22 (*Vu*11) and 179N14 (*Pv*11) hybridized in *Vac*11. Bars in **a** and **g** represent 5 μm

We also expanded our comparison to the literature data for *P. lunatus* (Bonifácio et al. 2012; Almeida and Pedrosa-Harand 2013) and *P. microcarpus* (Fonsêca and Pedrosa-Harand 2013), including the chromosomes involved in rearrangements (Fig. 4). In *Phaseolus*, *P. vulgaris*, *P. lunatus*, and *P. microcarpus* showed conserved synteny, being identified by BAC-FISH only inversions involving four chromosomes (3, 6, 9, and 10, but only Chr3 is represented in Fig. 4) resulting in breaks of collinearity, in addition to one duplication involving *Pm*3 and *Pm*6 (*Pv*3 marker) (Fonsêca et al. 2010; Bonifácio et al. 2012; Fonsêca and Pedrosa-Harand 2013).

Between *Vigna* and *Phaseolus*, major synteny breaks were found within *Vigna*, suggesting that most of the chromosomal rearrangements must have occurred during its genus diversification. For instance, pericentric inversions, as observed for Chr2 and Chr4, indicate collinearity breaks within *Vigna*. Regarding synteny, while chromosomes 1 and 8 are syntenic among *Phaseolus* species with 22 chromosomes (Fonsêca et al. 2010; Bonifácio et al. 2012; Fonsêca and Pedrosa-Harand 2013), only Chr8 was syntenic within *Vigna* (present work; Lonardi et al. 2019). Comparing *Vigna-Phaseolus*, we identified a *Pv*1-*Pv*8 BAC translocation for Chr8 of both *Vigna* species. However, in *Vu-Pv* comparison, Chr1 and Chr8 are involved in a complex translocation with a third chromosome (Vasconcelos et al. 2015), which was identified in the present work as *Vu*5, corroborating Lonardi et al. (2019). Our results indicate that a translocation between Chr1 and Chr8 occurred after *Phaseolus-Vigna* divergence (9.7 Mya, Li et al. 2013), followed by an additional translocation with Chr5 observed in the *V. unguiculata* lineage.

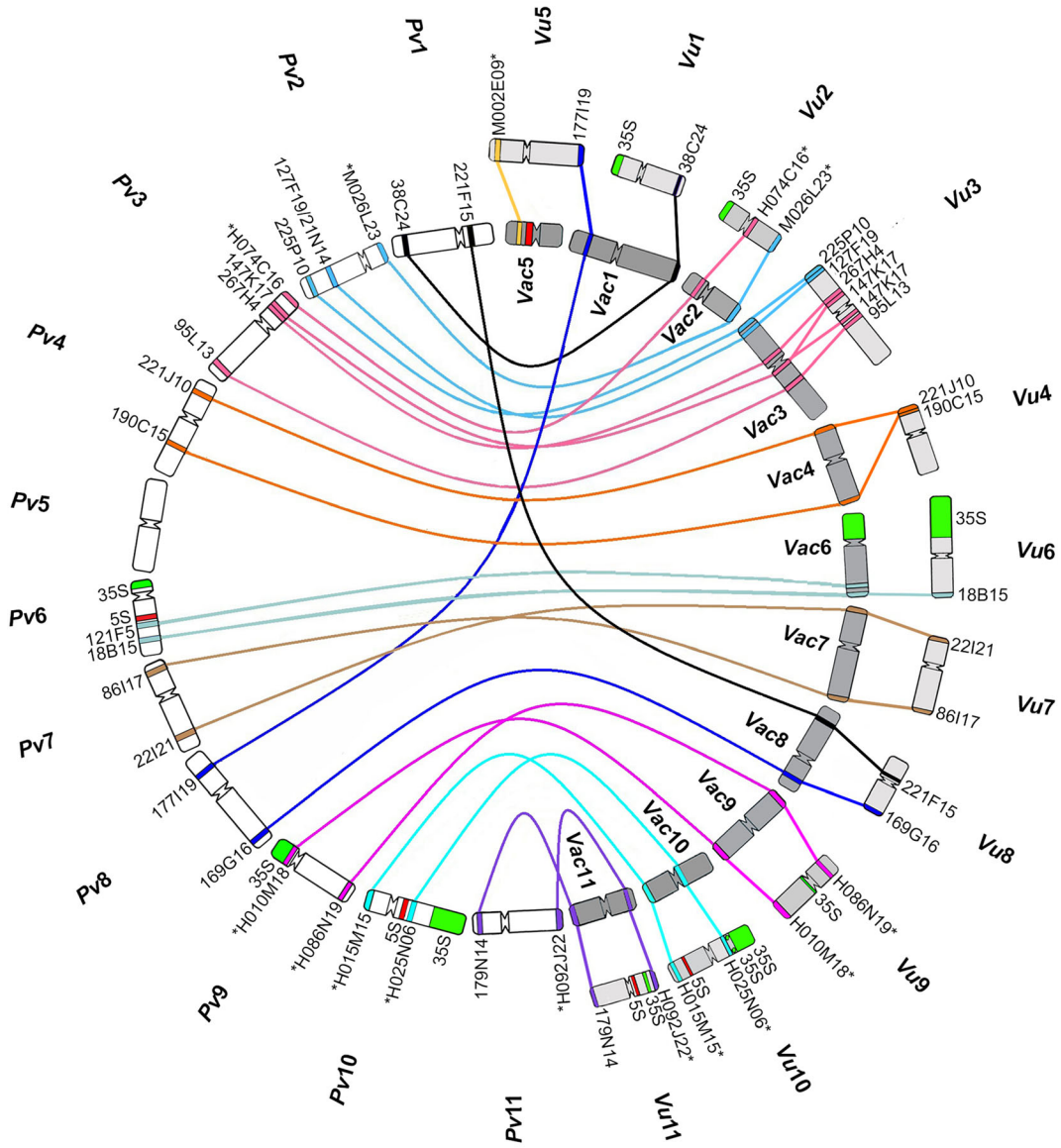

Fig. 3 Schematic representation of comparative cytogenetic maps of *Vigna aconitifolia* (*Vac*), *V. unguiculata* (*Vu*), and *Phaseolus vulgaris* (*Pv*), showing chromosomal localization of 17 *Pv* BACs, eight *Vu* BACs, and 35S and 5S rDNA clones. BACs 21N14 and 127F19 (both localized at the same position in the *Pv2* cytogenetic map) were colocalized in *Vac*3. #BAC 86I17 was not mapped as a single copy in *P. vulgaris*, but as repetitive subtelomeric sites. Here, it was positioned as single site, according to their reported genetic position and location in *P. lunatus* (Almeida and Pedrosa-Harand 2013). Same BACs are connected by lines colored according to *P. vulgaris* chromosome number. *New data for *V. unguiculata* and *P. vulgaris*. Chromosome numbering and positioning followed the new *V. unguiculata* numbering system (Lonardi et al. 2019), and *V. aconitifolia* chromosomes were orientated according to *V. unguiculata* chromosome orthology, independent of their morphology

Between genera, BACs from *Pv*2 and *Pv*3 are involved in at least one reciprocal translocation and a complex inversion or transposition when compared with *Vac* and *Vu* chromosomes (present work; Vasconcelos et al. 2015; Lonardi et al. 2019), suggesting that this event must have occurred after *Vigna* and *Phaseolus* divergence and before diversification of the genus in which it occurred. Within *Vigna* species analyzed in our work, as well as in previous *V. unguiculata*-*V. radiata* and *V. unguiculata*-*V. angularis* comparisons, both chromosomes are mainly syntenic, with breaks of collinearity identified (Lonardi et al. 2019). We observed a

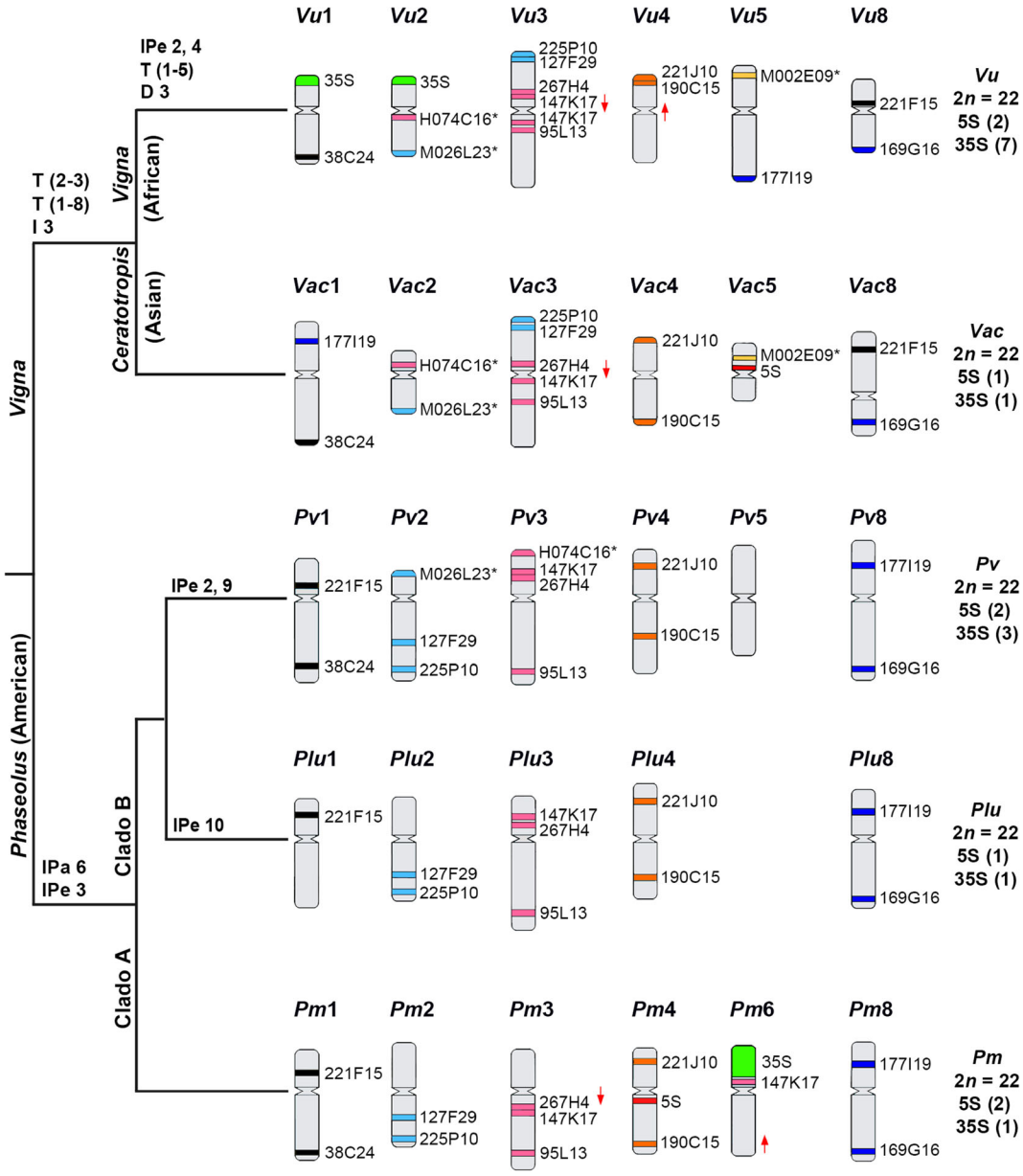

Fig. 4 Schematic BAC-FISH comparative analysis, using BACs from *P. vulgaris* and *Vigna unguiculata* (*), for six chromosomes of *V. aconitifolia* (*Vac*; present work) and *V. unguiculata* (*Vu*; Vasconcelos et al. 2015), *Phaseolus vulgaris* (*Pv*; Pedrosa-Harand et al. 2009; Fonsêca et al. 2010), *P. lunatus* (*Plu*; Bonifácio et al. 2012; Almeida and Pedrosa-Harand 2013), and *P. microcarpus* (*Pm*; Fonsêca and Pedrosa-Harand 2013), involved in the major rearrangements in relation to *P. vulgaris*, considering the proposed phylogeny for the genera *Vigna* and *Phaseolus* (adapted from Delgado-Salinas et al. 2011). T, translocation; D, duplication; I, inversion; IPe, pericentric inversion; IPa, paracentric inversion. Arrows in red indicate inversions in comparison with *P. vulgaris* chromosomes. *Vigna unguiculata* chromosome numbering and positioning followed the new numbering system (Lonardi et al. 2019), and *V. aconitifolia* chromosomes were orientated according to *V. unguiculata* chromosome orthology, independent of their morphology

pericentric inversion for Chr2 besides a species-specific duplication of BAC 147K17 (*Pv*3) for Chr3 in *V. unguiculata* (Vasconcelos et al. 2015), but not in *V. aconitifolia*. Comparing different accessions of *V. unguiculata*, Lonardi et al. (2019) also identified a 4.2-Mb inversion at the long arm of *Vu*3 for 33 out of

368 analyzed accessions. Most accessions that carry the inversion were breeding materials (98.8%), indicating the breeding selection can act to maintain the inversion as an advantageous feature. In *V. aconitifolia* and *V. unguiculata*, stress factors can be related to their growing condition, mostly in hot and/or drought regions (Singh 2005; Brink and Jansen 2006). Since translocation, inversions, and duplication were identified for Chr2 and Chr3, we believe these chromosomes are hotspots for chromosomal rearrangements, which contributed to the karyotype divergence between *Vigna* and *Phaseolus*.

Genetic linkage groups and/or sequenced pseudochromosomes of Asian *Vigna* species, such as *V. aconitifolia*, *V. angularis*, *V. mungo* (L.) Hepper (*Vm*), *V. radiata*, and *V. umbellata* (Thunb.) Ohwi & H.Ohashi (*Vum*), were previously compared by several authors. In general, conserved synteny was observed among these five *Ceratotropis* species, except for some inversions, deletions, and few translocations (Chaitieng et al. 2006; Gupta et al. 2008; Isemura et al. 2010; Yundaeng et al. 2019). Between *V. mungo* and *V. angularis*, only one translocation was detected. A linkage block with three RFLP markers located on the *Vm* LG10 was positioned in the distal end region of the *Va* LG1 (Chaitieng et al. 2006), which in our nomenclature corresponds to the most rearranged Chr2 and Chr3, respectively (see Lonardi et al. 2019 and Figs. 3 and 4). The comparison of the species with sequenced genomes, such as *V. angularis* and *V. radiata* (https://legumeinfo.org/genomes/gbrowse/Va3.0), indicated few major and several minor translocation events between them.

We detected differences regarding the centromere relative position and arm sizes for *Vac*6, *Vac*8, and *Vac*10 when compared with their *Vu* orthologs. Differences in *Vac*6 and *Vac*10 are probably related to the 35S rDNA block size or to its absence, respectively, while *Vac*8 could vary due to other repetitive sequences or chromosome rearrangements such as pericentric inversion and deletion. Number variation of rDNA sites is commonly found in plant species, and in some families as Leguminosae, the preferential position of the sites in a chromosome can vary according to the studied genus (revised by Roa and Guerra 2012). Between *P. vulgaris* and *V. unguiculata*, changes regarding the number or location of rDNA *loci* seem to be related to transposition events (Iwata et al. 2013), or to the activity of transposable elements associated to cooptation of rDNA or rRNA (Kalendar et al. 2008). In both genera, the number of 5S rDNA is less variable with one or two pairs of carrier chromosomes (Moscone et al. 1999; Almeida and Pedrosa-Harand 2011; She et al. 2015). In *Phaseolus*, Chr10 is considered the ancestral chromosome condition for the 5S rDNA site (Fonsêca et al. 2016), which was conserved on its *V. unguiculata* ortholog chromosome, besides an additional site at *Vu*11 (Vasconcelos et al. 2015). However, in *V. aconitifolia*, the 5S rDNA site was not conserved at Chr10, which presented only one site at *Vac*5. Regarding the 35 rDNA sites, *V. aconitifolia* presented one pair located on *Vac*6 that was syntenic to *Vu*6 and *Pv*6. On the other hand, six additional sites (five chromosome pairs) were present in *V. unguiculata* (Vasconcelos et al. 2015). In other *Vigna* species, at least two and three pairs of 35 rDNA were reported in both *Ceratotropis* and *Vigna* subgenera, respectively (She et al. 2015). In *Phaseolus*, *Pm*6, *Plu*6, and Chr6 of *P. leptostachyus* also presented the 35S rDNA site (Fonsêca et al. 2010; Bonifácio et al. 2012; Fonsêca and Pedrosa-Harand 2013; Fonsêca et al. 2016). The presence of the 35S rDNA site on Chr6 of all species analyzed so far supports the idea of its ancestral condition not only in the genus *Phaseolus*, as suggested by Fonsêca et al. (2016), but also in the Phaseolineae subtribe species. Nevertheless, comparative analyses, including other clades, would be necessary to propose the chromosome ancestry for the subtribe.

Here, we presented the first physical map of *V. aconitifolia* and expanded the chromosome comparison to other *Vigna* and *Phaseolus* species. Macrosynteny analyses demonstrated highly syntenic relationships between and within both genera, indicating the conservation and ancestry of the 35S rDNA site on Chr6 for both genera. At least two translocations (Chr1-Chr8 and Chr2-Chr3) and a complex inversion or transposition (Chr3) have probably occurred after *Vigna*-*Phaseolus* separation (9.7 Mya; Li et al. 2013), with additional rearrangements involving these chromosomes within each genus. We believe that Chr2 and Chr3 are hotspots for chromosomal rearrangements in these and other species of the subtribe Phaseolinae. Our data, together with previous reports, suggest that major rearrangements have occurred within *Vigna* genus. Within *Vigna*, at least one translocation (Chr1 and Chr5), two pericentric inversions (Chr2 and Chr4) and duplications (Chr3 markers) occurred after *V. unguiculata* (subgenus *Vigna*) and *V. aconitifolia*

(subgenus *Ceratotropis*, age of the clade ~3.6 Mya; Javadi et al. 2011) diversification. The new *V. aconitifolia* map provided new insights to the *Vigna* comparative cytogenomic analyses, helping to elucidate the chromosomal changes related to the evolution and karyotype diversification of these economically important legume crops.

Acknowledgments The authors thank Embrapa Meio-Norte (Teresina, Brazil), Embrapa Arroz e Feijão (Santo Antônio de Goiás, Brazil), and IPK (Institute of Plant Genetics and Crop Plant Research, Gatersleben, Germany) for supplying the seeds; Paul Gepts (University of California, Davis, United States) for supplying the BAC clones from *P. vulgaris*; and Valérie Geffroy (Université Paris-Sud, Orsay Cedex, France) for the bacteriophage SJ19.12 from *P. vulgaris*.

Author contribution ARSO: performed BAC-FISH, constructed comparative maps and figures, and wrote the manuscript. LVM: performed BAC-FISH and helped to write the manuscript. FOB: helped to carry out the experiments and to write the manuscript. APH: doctorate co-supervisor of ARSO, discussed the experiments and results, maintained and provided *P. vulgaris* BAC clones. MMA: maintained and provided *V. unguiculata* BAC clones. TC: maintained and provided *V. unguiculata* BAC clones. AMBI: doctorate co-supervisor of ARSO and discussed the results. AFC: performed seed multiplication. ACBV: doctorate supervisor of ARSO, designed and directed the research, and corrected the manuscript. All authors read, discussed, and approved the final version of the manuscript.

Funding information This study received financial support and fellowships from CNPq (Conselho Nacional de Desenvolvimento Científico e Tecnológico), CAPES (Coordenação de Pessoal de Nível Superior: Finance Code001; InterSys Network, BioComputational Program), and FACEPE (Fundação de Amparo a Ciência e Tecnologia do Estado de Pernambuco).

Compliance with ethical standards

Conflict of interest The authors declare that they have no conflict of interest.

References

Almeida C, Pedrosa-Harand A (2011) Contrasting rDNA evolution in lima bean (*Phaseolus lunatus* L.) and common bean (*P. vulgaris* L. Fabaceae). Cytogenet Genome Res 132:212–217. https://doi.org/10.1159/000321677

Almeida C, Pedrosa-Harand A (2013) High macro-collinearity between lima bean (*Phaseolus lunatus* L.) and the common bean (*P. vulgaris* L.) as revealed by comparative cytogenetic mapping. Theor Appl Genet 126:1909–1916. https://doi.org/10.1007/s00122-013-2106-9

Bonifácio EM, Fonsêca A, Almeida C, Santos KGB, Pedrosa-Harand A (2012) Comparative cytogenetic mapping between the lima bean (*Phaseolus lunatus* L.) and the common bean (*P. vulgaris* L.). Theor Appl Genet 124:1513–1520. https://doi.org/10.1007/s00122-012-1806-x

Brink M, Jansen PCM (2006) *Vigna aconitifolia* (Jacq.) Maréchal. In: Brink M, Belay G (eds) PROTA 1: cereals and pulses/ Céréales et Légumes Secs. Wageningen, Netherlands, pp 1–5

Broughton WJ, Hernandez G, Blair M, Beebe S, Gepts P, Vanderleyden J (2003) Beans (*Phaseolus* spp.): model food legumes. Plant Soil 252:55–128. https://doi.org/10.1023/A:1024146710611

Carvalho CR, Saraiva LS (1993) An air drying technique for maize chromosomes without enzymatic maceration. Biotech Histochem 68:142–145. https://doi.org/10.3109/10520299309104684

Chaitieng B, Kaga A, Tomooka N, Isemura T, Kuroda Y, Vaughan DA (2006) Development of a black gram [*Vigna mungo* (L.) Hepper] linkage map and its comparison with an azuki bean [*Vigna angularis* (Wild.) Ohwi and Ohashi] linkage map. Theor Appl Genet 113:1261–1269. https://doi.org/10.1007/s00122-006-0380-5

Chang Y, Liu H, Liu M, Liao X, Sahu SK, Fu Y, Song B, Cheng S, Kariba R, Muthemba S, Hendre PS, Mayes S, Ho WK, Yssel AEJ, Kendabie P, Wang S, Li L, Muchugi A, Jamnadass R, Lu H, Peng S, van Deynze A, Simons A, Yana-Shapiro H, van de Peer Y, Xu X, Yang H, Wang J, Liu X (2019) The draft genomes of five agriculturally important African orphan crops. GigaScience 8:1–16. https://doi.org/10.1093/gigascience/giy152

Delgado-Salinas A, Thulin M, Pasquet R, Weeden LM (2011) *Vigna* (Leguminosae) *sensu lato*: the names and identities of the American segregate genera. Am J Bot 98:1694–1715. https://doi.org/10.3732/ajb.1100069

Fonsêca AFA, Pedrosa-Harand A (2013) Karyotype stability in the genus *Phaseolus* evidenced by the comparative mapping of the wild species *Phaseolus microcarpus*. Genome 56:335–343. https://doi.org/10.1139/gen-2013-0025

Fonsêca AFA, Ferreira J, Santos TRB et al (2010) Cytogenetic map of common bean (*Phaseolus vulgaris* L.). Chromosom Res 18:487–502. https://doi.org/10.1007/s10577-010-9129-8

Fonsêca AFA, Ferraz ME, Pedrosa-Harand A (2016) Speeding up chromosome evolution in *Phaseolus*: multiple rearrangements associated with a one-step descending dysploidy. Chromosoma. 125:413–421. https://doi.org/10.1007/s00412-015-0548-3

Forni-Martins ER (1986) New chromosome number in the genus *Vigna* Savi (Leguminosae-Papilionoideae). Bull Jardin Bot Nat Belgique 56:129–133

Freyre R, Skroch PW, Geffroy V, Adam-Blondon AF, Shirmohamadali A, Johnson WC, Llaca V, Nodari RO, Pereira PA, Tsai SM, Tohme J, Dron M, Nienhuis J, Vallejos CE, Gepts P (1998) Towards an integrated linkage map of common bean 4: development of a core linkage map and alignment of RFLP maps. Theor Appl Genet 97:847–856. https://doi.org/10.1007/s001220050964

Gepts P, Aragão FJL, Barros E et al (2008) Genomics of *Phaseolus* beans, a major source of dietary protein and

micronutrients in the tropics. In: Moore PH, Ming R (eds) Genomics of tropical crop plants. Springer, New York, pp 113–143

Gupta SK, Souframanien J, Gopalakrishna T (2008) Construction of a genetic linkage map of black gram, *Vigna mungo* (L.) Hepper, based on molecular markers and comparative studies. Genome 51:628–637. https://doi.org/10.1139/G08-050

Heslop-Harrison JS, Harrison GE, Leitch IJ (1992) Reprobing of DNA: DNA in situ hybridization preparations. Trends Genet 8:372–373. https://doi.org/10.1016/0168-9525(92)90287-E

Hougaard BK, Madsen LH, Sandal N, de Carvalho Moretzsohn M, Fredslund J, Schauser L, Nielsen AM, Rohde T, Sato S, Tabata S, Bertioli DJ, Stougaard J (2008) Legume anchor markers link syntenic regions between *Phaseolus vulgaris*, *Lotus japonicus*, *Medicago truncatula* and *Arachis*. Genetics 179:2299–2312. https://doi.org/10.1534/genetics.108.090084

Isemura T, Kaga A, Tomooka N, Shimizu T, Vaughan DA (2010) The genetics of domestication of rice bean, *Vigna umbellata*. Ann Bot 106:927–944. https://doi.org/10.1093/aob/mcq188

Iwata A, Greenland CM, Jackson AS (2013) Cytogenetics of legumes in the Phaseoloid clade. Plant Genome 6:1–8. https://doi.org/10.3835/plantgenome2013.03.0004

Iwata-Otsubo A, Jer-Young L, Gill N, Jackson SA (2016) Highly distinct chromosomal structures in cowpea (*Vigna unguiculata*), as revealed by molecular cytogenetic analysis. Chromosom Res 24:197–216. https://doi.org/10.1007/s10577-015-9515-3

Javadi F, Tun YT, Kawase M, Guan K, Yamaguchi H (2011) Molecular phylogeny of the subgenus *Ceratotropis* (genus *Vigna*, Leguminosae) reveals three eco-geographical groups and Late Pliocene-Pleistocene diversification: evidence from four plastid DNA region sequences. Ann Bot 8:367–380. https://doi.org/10.1093/aob/mcr141

Kalendar R, Tanskanen J, Chang W, Antonius K, Sela H, Peleg O, Schulman AH (2008) *Cassandra* retrotransposons carry independently transcribed 5S RNA. PNAS 105:5833–5838. https://doi.org/10.1073/pnas.0709698105

Kami J, Poncet V, Geffroy V, Gepts P (2006) Development of four phylogenetically-arrayed BAC libraries and sequence of the APA locus in *Phaseolus vulgaris*. Theor Appl Genet 112:987–998. https://doi.org/10.1007/s00122-005-0201-2

Kang YJ, Kim SK, Kim MY, Lestari P, Kim KH, Ha BK, Jun TH, Hwang WJ, Lee T, Lee J, Shim S, Yoon MY, Jang YE, Han KS, Taeprayoon P, Yoon N, Somta P, Tanya P, Kim KS, Gwag JG, Moon JK, Lee YH, Park BS, Bombarely A, Doyle JJ, Jackson SA, Schafleitner R, Srinives P, Varshney RK, Lee SH (2014) Genome sequence of mungbean and insights into evolution within *Vigna* species. Nat Commun 5:5443–5452. https://doi.org/10.1038/ncomms6443

Kang YJ, Satyawan D, Shim S, Lee T, Lee J, Hwang WJ, Kim SK, Lestari P, Laosatit K, Kim KH, Ha TJ, Chitikineni A, Kim MY, Ko JM, Gwag JG, Moon JK, Lee YH, Park BS, Varshney RK, Lee SH (2015) Draft genome sequence of adzuki bean, *Vigna angularis*. Sci Rep 5:8069–8077. https://doi.org/10.1038/srep08069

Li H, Wang W, Lin L, Zhu X, Li J, Zhu X, Chen Z (2013) Diversification of the phaseoloid legumes: effects of climate change, range expansion and habit shift. Front Plant Sci 4:386. https://doi.org/10.3389/fpls.2013.00386

Lonardi S, Muñoz-Amatriaín M, Liang Q, Shu S, Wanamaker SI, Lo S, Tanskanen J, Schulman AH, Zhu T, Luo MC, Alhakami H, Ounit R, Hasan AM, Verdier J, Roberts PA, Santos JRP, Ndeve A, Doležel J, Vrána J, Hokin SA, Farmer AD, Cannon SB, Close TJ (2019) The genome of cowpea (*Vigna unguiculata* [L.] Walp.). Plant J 98:767–782. https://doi.org/10.1111/tpj.14349

LPWG (2017) A new subfamily classification of the Leguminosae based on a taxonomically comprehensive phylogeny. The Legume Phylogeny Working Group (LPWG). Taxon 66:44–77. https://doi.org/10.12705/661.3

Maréchal R, Mascherpa JM, Stainier F (1978) Étude taxonomique d'un groupe complexe d'espèces de genres *Phaseolus* et *Vigna* (Papilionaceae) sur la base de donneés morphologiques et polliniques, traitées par l'analyse informatique. Conservatoire et jardin botaniques, Genève. Boissiera 28:1–273

Mercado-Ruaro P, Delgado-Salinas A (1996) Karyological studies in several Mexican species of *Phaseolus* L. and *Vigna* Savi (Phaseolinae, Fabaceae). In: Pickersgill B, Lock JM (eds) Advances in legumes systematics. 8: legumes of economic importance. Royal Botanic Gardens, Kew, pp 83–87

Mercado-Ruaro P, Delgado-Salinas A (1998) Karyotypic studies on species of *Phaseolus* (Fabaceae: Phaseolinae). Am J Bot 85:1–9. https://doi.org/10.2307/2446547

Moscone EA, Klein F, Lambrou M, Fuchs J, Schweizer D (1999) Quantitative karyotyping and dual-color FISH mapping of 5S and 18S-25S rDNA probes in the cultivated *Phaseolus* species (Leguminosae). Genome 42:1224–1233. https://doi.org/10.1139/g99-070

Muchero W, Diopb NN, Bhat PR et al (2009) A consensus genetic map of cowpea [*Vigna unguiculata* (L.) Walp] and synteny based on EST-derived SNPs. PNAS 106:18159–18164. https://doi.org/10.1073/pnas.0905886106

Muñoz-Amatriaín M, Mirebrahim H, Xu P, Wanamaker SI, Luo MC, Alhakami H, Alpert M, Atokple I, Batieno BJ, Boukar O, Bozdag S, Cisse N, Drabo I, Ehlers JD, Farmer A, Fatokun C, Gu YQ, Guo YN, Huynh BL, Jackson SA, Kusi F, Lawley CT, Lucas MR, Ma Y, Timko MP, Wu J, You F, Barkley NA, Roberts PA, Lonardi S, Close TJ (2017) Genome resources for climate-resilient cowpea, an essential crop for food security. Plant J 89:1042–1054. https://doi.org/10.1111/tpj.13404

Ouédraogo JT, Gowda BS, Jean M, Close TJ, Ehlers JD, Hall AE, Gillaspie AG, Roberts PA, Ismail AM, Bruening G, Gepts P, Timko MP, Belzile FJ (2002) An improved genetic linkage map for cowpea (*Vigna unguiculata* L.) combining AFLP, RFLP, RAPD, biochemical markers, and biological resistance traits. Genome 45:175–188. https://doi.org/10.1139/g01-102

Pedrosa A, Sandal N, Stougaard J, Schweizer D, Bachmair A (2002) Chromosomal map of the model legume *Lotus japonicus*. Genetics 161:1661–1672

Pedrosa-Harand A, Kami J, Geffroy V, Gepts P, Schweizer D (2009) Cytogenetic mapping of common bean chromosomes reveals a less compartmentalized small-genome plant species. Chromosom Res 17:405–417. https://doi.org/10.1007/s10577-009-9031-4

Roa F, Guerra M (2012) Non-random distribution of 5S rDNA sites and its association with 45S rDNA in plant

chromosomes. Cytogenet Genome Res 146(3):243–249. https://doi.org/10.1159/000440930

Sakai H, Naito K, Ogiso-Tanaka E, Takahashi Y, Iseki K, Muto C, Satou K, Teruya K, Shiroma A, Shimoji M, Hirano T, Itoh T, Kaga A, Tomooka N (2015) The power of single molecule real-time sequencing technology in the de novo assembly of a eukaryotic genome. Sci Rep 5:16780. https://doi.org/10.1038/srep16780

Schmutz J, McClean PE, Mamidi S et al (2014) A reference genome for common bean and genome-wide analysis of dual domestications. Nature 46:707–713. https://doi.org/10.1038/ng.3008

Schwarzacher T, Heslop-Harrison P (2000) Practical *in situ* hybridization, 1st edn. BIOS Scientific, Oxford, pp 1–203

She CW, Jiang XH, Ou LJ, Liu J, Long KL, Zhang LH, Duan WT, Zhao W, Hu JC (2015) Molecular cytogenetic characterisation and phylogenetic analysis of the seven cultivated *Vigna* species (Fabaceae). Plant Biol 17:268–280. https://doi.org/10.1111/plb.12174

Singh BB (2005) Cowpea [*Vigna unguiculata* (L.) Walp]. In: Singh RJ, Jauhar PP (eds) Genetic resources. Chromosome Engineering and Crop Improvement. CRC Press, Boca Raton, pp 117–162

Takahashi Y, Somta P, Muto C, Iseki K, Naito K, Pandiyan M, Natesan S, Tomooka N (2016) Novel genetic resources in the genus *Vigna* unveiled from Gene Bank accessions. PLoS One 11:e0147568. https://doi.org/10.1371/journal.pone.0147568

The Plant List (2013) Version 1.1. Available: http://www.theplantlist.org/tpl1.1/search?q=Vigna; http://www.theplantlist.org/tpl1.1/search?q=Phaseolus. Accessed 28 November 2019

Tomooka N, Vaughan DA, Moss H, Maxted N (2002) The Asian *Vigna*: genus *Vigna* subgenus *Ceratotropis* genetic resources. Kluwer Academic Publishers, Dordrecht, pp 1–270

Vallejos CE, Sakiyama NS, Chase CD (1992) A molecular marker-based linkage map of *Phaseolus vulgaris* L. Genetics 131:733–740

Vasconcelos EV, Fonsêca AFA, Pedrosa-Harand A, Bortoleti KCA, Benko-Iseppon AM, Costa AF, Brasileiro-Vidal AC (2015) Intra- and interchromosomal rearrangements between cowpea [*Vigna unguiculata* (L.) Walp.] and common bean (*Phaseolus vulgaris* L.) revealed by BAC-FISH. Chromosom Res 23:253–266. https://doi.org/10.1007/s10577-014-9464-2

Venora G, Blangiforti S, Cremonini R (1999) Karyotype analysis of twelve species belonging to genus *Vigna*. Cytologia 64: 117–127. https://doi.org/10.1508/cytologia.64.117

Wanzenböck EM, Schöfer C, Schweizer D, Bachmair A (1997) Ribosomal transcription units integrated via T-DNA transformation associate with the nucleolus and do not require upstream repeat sequences for activity in *Arabidopsis thaliana*. Plant J 11:1007–1016. https://doi.org/10.1046/j.1365-313x.1997.11051007.x

Yang K, Tian Z, Chen C, Luo L, Zhao B, Wang Z, Yu L, Li Y, Sun Y, Li W, Chen Y, Li Y, Zhang Y, Ai D, Zhao J, Shang C, Ma Y, Wu B, Wang M, Gao L, Sun D, Zhang P, Guo F, Wang W, Li Y, Wang J, Varshney RK, Wang J, Ling HQ, Wan P (2015) Genome sequencing of adzuki bean (*Vigna angularis*) provides insight into high starch and low fat accumulation and domestication. PNAS 112:13213–13218. https://doi.org/10.1073/pnas.1420949112

Yundaeng C, Somta P, Amkul K, Kongjaimun A, Kaga A, Tomooka N (2019) Construction of genetic linkage map and genome dissection of domestication-related traits of moth bean (*Vigna aconitifolia*), a legume crop of arid areas. Mol Gen Genomics 294:621–635. https://doi.org/10.1007/s00438-019-01536-0

Zwick MS, Hanson RR, Mcknight TD et al (1997) A rapid procedure for the isolation of C0t-1 DNA from plants. Genome 40:138–142 https://legumeinfo.org/genomes/gbrowse/vigun.IT97K-499-35. Accessed 12 December 2019 http://rydberg.biology.colostate.edu/MicroMeasure/. Accessed 12 December 2019

APÊNDICE B – ARTIGO PUBLICADO NA REVISTA NATURE COMMUNICATION

nature COMMUNICATIONS

ARTICLE

https://doi.org/10.1038/s41467-019-12646-z OPEN

Meiotic crossovers characterized by haplotype-specific chromosome painting in maize

Lívia do Vale Martins[1,2,12], Fan Yu[1,2,3,12], Hainan Zhao[1,2,12], Tesia Dennison[4], Nick Lauter[4,5], Haiyan Wang[1,2], Zuhu Deng[3], Addie Thompson[6,7], Kassandra Semrau[8,11], Jean-Marie Rouillard[8,9], James A. Birchler[10] & Jiming Jiang[1,2,7*]

Meiotic crossovers (COs) play a critical role in generating genetic variation and maintaining faithful segregation of homologous chromosomes during meiosis. We develop a haplotype-specific fluorescence in situ hybridization (FISH) technique that allows visualization of COs directly on metaphase chromosomes. Oligonucleotides (oligos) specific to chromosome 10 of maize inbreds B73 and Mo17, respectively, are synthesized and labeled as FISH probes. The parental and recombinant chromosome 10 in B73 x Mo17 F_1 hybrids and F_2 progenies can be unambiguously identified by haplotype-specific FISH. Analysis of 58 F_2 plants reveals lack of COs in the entire proximal half of chromosome 10. However, we detect COs located in regions very close to the centromere in recombinant inbred lines from an intermated B73 x Mo17 population, suggesting effective accumulation of COs in recombination-suppressed chromosomal regions through intermating and the potential to generate favorable allelic combinations of genes residing in these regions.

[1] Department of Plant Biology, Michigan State University, East Lansing, MI 48824, USA. [2] Department of Horticulture, Michigan State University, East Lansing, MI 48824, USA. [3] National Engineering Research Center for Sugarcane, Fujian Agriculture and Forestry University, Fuzhou, China. [4] Genetics and Genomics Graduate Program, Iowa State University, Ames, IA 50011, USA. [5] USDA-ARS Corn Insects and Crop Genetics Research Unit, Iowa State University, Ames, IA 50011, USA. [6] Department of Plant, Soil and Microbial Sciences, Michigan State University, East Lansing, MI 48824, USA. [7] Michigan State University AgBioResearch, East Lansing, MI 48824, USA. [8] Arbor Biosciences, Ann Arbor, MI 48103, USA. [9] Department of Chemical Engineering, University of Michigan, Ann Arbor, MI 48109, USA. [10] Division of Biological Sciences, University of Missouri, Columbia, MO 65211, USA. [11] Present address: Department of Natural Sciences, University of Michigan-Dearborn, Dearborn, MI 48128, USA. [12] These authors contributed equally: Lívia do Vale Martins, Fan Yu, Hainan Zhao. *email: jiangjm@msu.edu

Meiotic recombination, which generates genetic variation via exchange of DNA between homologous parental chromosomes, is essential for plant and animal breeding. Breeders rely on meiotic recombination to create new and favorable combinations of parental alleles. Meiotic recombination is initiated from the formation of double-strand breaks (DSBs) of DNA molecules[1]. DSBs are then repaired through the double Holliday junction or synthesis-dependent strand annealing pathways, which result in meiotic crossovers (COs) or non-crossovers (NCOs), respectively[2]. COs, which create a physical connection of the homologous chromosome pairs, are also essential for faithful chromosome segregation in meiosis. Thus, essentially every chromosome at the first metaphase of meiosis acquires at least one CO, which is known as the obligatory CO rule[3,4]. The frequency of zero-CO chromosomes is extremely low and is usually much less than 1% in different organisms[4,5].

Meiotic COs can be mapped on chromosomes using different methods. COs can be indicated based on the locations of late recombination nodules (RNs) or protein markers associated with COs, such as MLH1, on synaptonemal complexes (SCs)[6,7]. However, it is often difficult or impossible to distinguish individual SCs in the same plant species, which would prevent to map each RN on a specific chromosome. Physical mapping of genetically anchored DNA markers can be used to predict the locations of COs on chromosomes. Physical mapping in plants can be achieved by using cytogenetic stocks[8,9], or by fluorescence in situ hybridization (FISH) of DNA markers directly on chromosomes[10–14]. However, physical mapping can unveil the relationship between genetical and chromosomal distances of the DNA markers, but does not reveal the exact positions of individual COs. Lastly, genomic in situ hybridization (GISH) can be used to visualize COs derived from homoeologous chromosomes[15–17]. GISH, however, relies on presence of dispersed repeats specific to each chromosone, thus, it can not be used to detect COs from homologous chromosomes.

We develop a FISH technique that allows us to visualize meiotic COs derived from homologous plant chromosomes. We computationally identify large sets of oligonucleotides (oligos) that are specific to chromosome 10 of either maize inbred B73 or Mo17, two highly utilized inbreds that belong to two important opposing heterotic groups[18] and have been used extensively as parental lines for genetic mapping and heterosis studies[19–21]. The identified oligos are based on presence-absence variation (PAV), single nucleotide polymorphisms (SNPs), and/or insertions and deletions (indels) in chromosome 10 sequences derived from the two inbreds. These oligos are then massively synthesized and labeled as FISH probes. We are able to differentially paint the two copies of parental chromosome 10 in a B73 × Mo17 hybrid using these haplotype-specific FISH probes. We intend to use this FISH technique to detect and quantify meiotic COs derived from the two homologous chromosome 10 in different maize populations.

Results

Identification of haplotype-specific oligos. Chromosome 10 of maize consists of 150.98 megabases (Mb) of DNA sequences[22,23]. To develop oligo-FISH probes that can be used differentially paint the chromosome 10 from maize inbreds B73 and Mo17, respectively, we used Chorus (https://github.com/forrestzhang/Chorus) to generate single copy oligos (45 nucleotides (nt)) from the pseudomolecules of chromosome 10 of B73[24] and Mo17[23]. We obtained a total of 175,437 and 174,728 oligos for B73 (B73 oligos) and Mo17 (Mo17 oligos), respectively. We then identified B73 oligos that are absent in the Mo17 genome and vice versa (see Methods section), which were named PAV oligos. B73 oligos that contain mismatches and/or indels to the Mo17 chromosome 10 sequence, and vice versa, were defined as SNP oligos. We only retained oligos with mismatches and/or indels located between 10–35 bp within each oligo. SNP oligos were identified in pairs (see Methods section), one for B73 and one for Mo17. We calculated the ΔTm between the B73 and Mo17 oligos of each pair using primer3[25,26]. Oligo pairs with ΔTm > 5 °C were discarded to avoid hybridization bias towards one variant.

Chromosome painting using haplotype-specific oligo probes. We identified 6251 and 5506 PAV oligos specific to B73 and Mo17, respectively. These two sets of oligos were synthesized as two oligo pools. The two synthesized pools of oligos were then amplified, labeled, and hybridized to the metaphase chromosomes prepared from a B73 × Mo17 hybrid plant. Each pool of oligos generated distinct FISH signals highly specific to the chromosome 10 derived from B73 (red) or Mo17 (green) (Fig. 1a). The B73 PAV probe generated only minimal cross hybridization to chromosome 10 from Mo17, and vice versa. However, the Mo17 probe hybridized to the 45S ribosomal RNA gene region on chromosome 6 from both inbreds (Fig. 1a). This cross hybridization was found to be caused by three oligos that shared 79–88% sequence similarity with the 45S rRNA genes. These three oligos were not detected by the oligo selection software.

We identified 4353 pairs of oligos that are differentiated by 5 or more SNPs between the B73 and Mo17 chromosome 10 sequences. These two sets of oligos generated strong signals on the respective chromosome 10 from B73 or Mo17. We observed weak but visible cross hybridization of the B73 probe to the Mo17 chromosome, and vice versa (Fig. 1b). Similarly, we identified 3894, 6506, and 19,885 pairs of oligos that are differentiated by 3–4 SNPs, 2 SNPs, and 1 SNP, respectively, between the B73 and Mo17 chromosome 10 sequences. Each SNP probe generated stronger signals on the respective chromosome 10 than on the other copy of chromosome 10 in the hybrid. However, the cross hybridization signals became stronger as the number of SNP decreased (Fig. 1). We then used different combinations of these five pairs of oligo pools. The combined pools of oligos with PAV, ≥5 SNPs, and 3–4 SNPs produced the best contrast of haplotype-specific FISH signals (Fig. 2b, c). These two probe pools, thereafter named hapB (haplotype B73, red) and hapM (haplotype Mo17, green), and were used in all future FISH experiments.

Probes hapB and hapM contain 14,498 and 13,753 oligos, respectively. These oligos are not uniformly distributed on chromosome 10 (Fig. 2a). The chromosomal region spanning 42–54 Mb, which includes the centromere[27], contained only 27 and 39 oligos in B73 and Mo17, respectively. Similarly, only 74 (115) oligos were identified in the first 2 Mb on the short arm and 19 (0) oligos identified in the final 1 Mb on the long arm of B73 (Mo17) (Supplementary Data 1). Thus, these regions showed weak or undetectable FISH signals (Fig. 2c).

Meiotic COs revealed by chromosome painting. We wanted to exploit the potential of oligo-FISH using hapB and hapM to detect meiotic COs derived from the homologous chromosome 10 from B73 and Mo17. We produced F_2 seeds by pollinating sibling B73 × Mo17 hybrid plants. Each F_2 plant contains two copies of chromosome 10, with each homolog classified as parental or recombinant (Fig. 3). We performed oligo-FISH experiments on somatic metaphase chromosomes from 58 F_2 plants (BM1-BM58), resulting in the analysis of 116 copies of chromosome 10. These chromosomes can be cataloged as eight different types based on the positions of chromosomal exchanges (Fig. 3c). We identified at least one unambiguous B73-Mo17

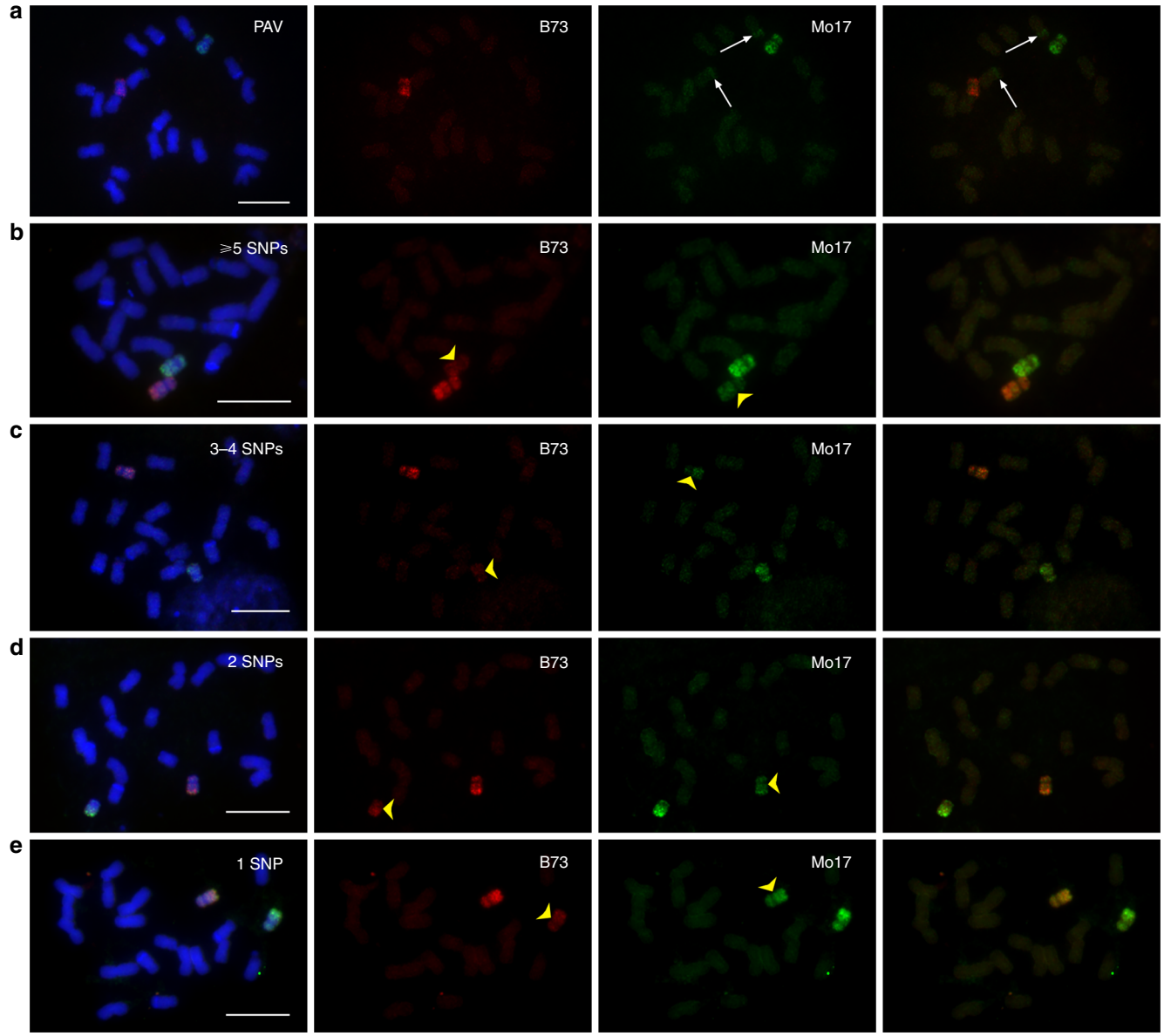

Fig. 1 Development of maize chromosome 10 oligo-FISH probes specific to inbreds B73 or Mo17. **a** Two oligo-FISH probes based on presence-absence variation. **b** Two oligo-FISH probes based on 5 or more single nucleotide polymorphisms (SNPs). **c** Two oligo-FISH probes based on 3 or 4 SNPs. **d** Two oligo-FISH probes based on 2 SNPs. **e** Two oligo-FISH probes based on 1 SNP. Oligo-FISH probes specific to the B73 haplotype were detected in red color. Oligo-FISH probes specific to the Mo17 haplotype were detected in green color. Images in first column: Complete metaphase cells hybridized with the two FISH probes; Images in the second column: digitally separated red FISH signals derived from the B73-specific probes; Images in the third column: digitally separated green FISH signals derived from the Mo17-specific probes; Images in the forth column: merged FISH signals derived from both B73 and Mo17. Arrows indicate the cross-hybridization signals at the 45 rDNA region associated with chromosome 6. Yellow arrowheads indicate the cross-hybridization signals from B73-specific probes to Mo17 chromosome 10, and vice versa. Bars = 10 μm. The original gray-scale images used to generate the five color images in the first column of all panels of Fig. 1 are provided as a Source Data file

chromosomal exchange on 50 (43%) of the 116 chromosomes (Supplementary Data 2), including 6 chromosomes with an exchange on both arms (Fig. 3a). A chromosome 10 with three or more COs was not identified in the analysis.

We measured the distance (μm) from each homologous chromosome exchange position (EP) to the telomere of the respective chromosome arm. This distance was divided by the total length of the respective chromosome arm to calculate the FLA (Fractional Length of the Arm) (see Methods section), which was used to map the position of each EP on the arm (Fig. 4). For example, if the FLA of an EP is 42.5 on the long arm, the distance from this EP to the telomere is 42.5% of the long arm. We divided the short and long arms of the chromosome into 100 intervals, from 0 at the telomere to 100 at the centromere. Each EP was then mapped to one of these intervals (Fig. 4). Most EPs were located within intervals 20–40 on the short arm and intervals 10–55 on the long arm (Fig. 4). Thus, no EP was observed within nearly half of the chromosome 10 flanking the centromere (Fig. 4). In addition, double COs in the same arm were rare and were found only in one of the 116 copies of chromosome 10 analyzed (Fig. 3b).

Validation of crossovers by genomic sequencing. Recombinant or parental copies of chromosome 10 were unambiguously

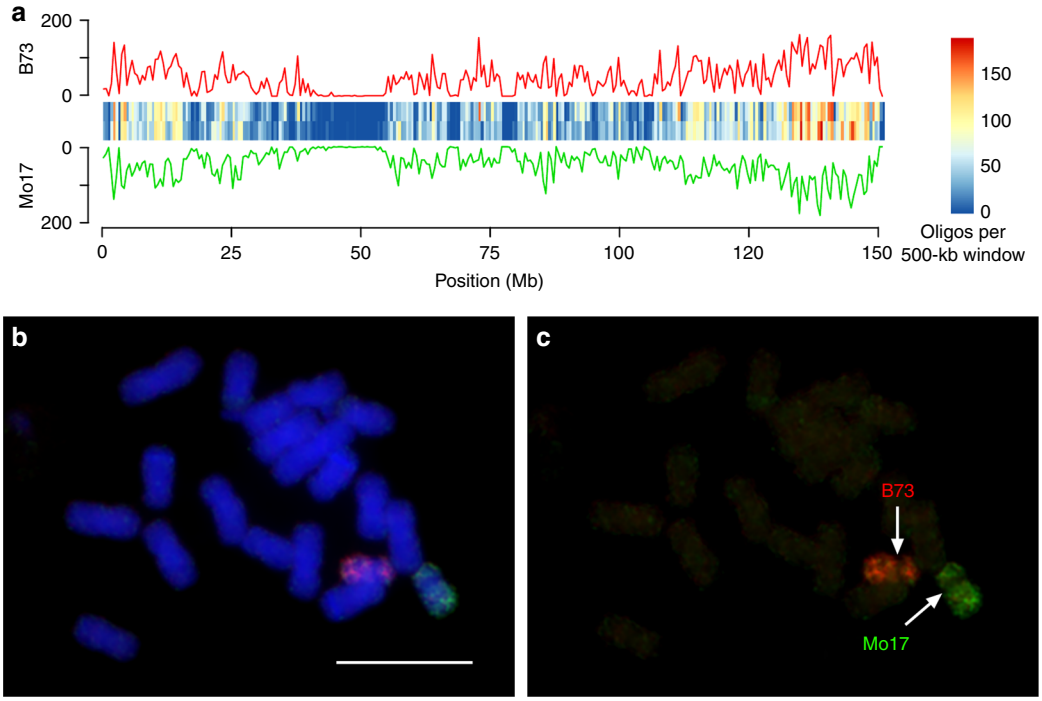

Fig. 2 Development of hapB and hapM probes. **a** Distribution of 14,498 oligos (red) of probe hapB and 13,753 oligos (green) of probe hapM on maize chromosome 10. The chromosome was divided into 500-kb windows and number of oligos was calculated for each window. The distribution of the number of oligos is shown in the line plot and heatmap. *y*-axis is the number of oligos in each 500-kb window. **b** Oligo-FISH on metaphase chromosomes from a B73 × Mo17 hybrid using hapB (red) and hapM (green). Bar = 10 μm. **c** The oligo-FISH signals were digitally separated from panel (**b**). The original gray-scale images used to generate the color image in Fig. 2b are provided as a Source Data file

identified in 54 of the 58 F_2 plants analyzed. In the remaining four F_2 plants (BM5, BM33, BM34, BM48) (Supplementary Data 2), we observed putative recombinant chromosome(s) with faint FISH signals that were inconsistently observed in the metaphase cells analyzed (Fig. 5). We conducted genomic sequencing of these four plants to validate the inconsistent identification of the COs. In addition, no COs were identified in 18 of 58 (31%) F_2 plants. We suspected that CO(s) may occur at the distal regions on chromosome 10 in these plants. These COs may not be detectable by FISH due to the lack of a sufficient number of oligos selected from the distal regions (Fig. 2a, Supplementary Data 1). Therefore, we also included six F_2 plants (BM8, BM12, BM19, BM21, BM31, BM42), which did not have visible COs, in the sequencing analysis. These 10 plants included 13 copies of chromosome 10 without a visible CO. We generated an average of 2.41× coverage of 150 bp paired-end Illumina sequences from each of the 10 plants for the analysis.

BM5 contained two copies of Mo17-derived chromosome 10. A CO was detected on the short arm of one chromosome 10 in 8 of 25 (32%) metaphase cells analyzed (Fig. 5). Sequencing analysis showed that one chromosome 10 has a CO at 5.04 Mb (Fig. 5). Thus, the oligo-FISH result was supported by the sequencing data. Similarly, BM33 also contained two copies of Mo17-derived chromosome 10. FISH detected a CO on the short arm of one chromosome 10 in 11 of 19 (58%) metaphase cells analyzed. Sequencing analysis revealed a CO at 6.45 Mb on the short arm of one chromosome (Fig. 5), thereby supporting the CO observed with oligo-FISH.

BM34 contained two copies of Mo17-derived chromosome 10. We observed hapB FISH signals at the distal regions of the long arms of both chromosome 10 homologs in 6 of 29 (21%) metaphase cells analyzed (Fig. 5). Sequencing analysis revealed a single CO on the long arm of each chromosome 10 homolog: at 145.73 Mb (5.25 Mb away from the end of the long arm telomere) and 148.93 Mb (2.06 Mb away from the long arm telomere), respectively (Fig. 5). Thus, the sequencing data confirmed the locations of COs on the long arms of both chromosomes.

BM48 contained one B73-derived and one Mo17-derived chromosome 10. We observed weak hapB FISH signals on the Mo17-derived chromosome 10, and weak hapM FISH signals on the B73-derived chromosome 10, but only in 35% (9/26) and 8% (2/26) of the metaphase cells, respectively. Sequencing analysis identified a duplicated B73 fragment between 3.86 Mb and 5.42 Mb on the short arm (Fig. 5). This fragment was possibly resulted from a putative double COs occurred at 3.86 Mb and 5.42 Mb, respectively, or two single COs, one at 3.86 Mb on the B73-derived chromosome 10, and one at 5.42 Mb on the Mo17-derived chromosome 10 (Fig. 5).

COs were not detected by oligo-FISH in BM8, BM12, BM19, and BM21. However, a single CO was discovered on one copy of chromosome 10 in each of these four lines by sequence analysis. The EPs of these four COs were 5.53 Mb, 2.37 Mb, 1.69 Mb, and 1.74 Mb away from the end of the chromosome, respectively (Fig. 5). COs were not detected in BM31 and BM42 using oligo-FISH or sequencing analysis (Fig. 5).

In summary, genomic sequencing of 10 F_2 plants revealed COs in 9 of the 20 copies of chromosome 10, including 4 copies of recombinant chromosome 10 that were FISH negative. No COs were detected in BM31 and BM42 (Fig. 5). The comparative analysis showed that COs cannot be reliably detected by the hapB and hapM probes if the EP is located <5 Mb away from the telomere of a chromosome arm, which contain only ~600 oligos within each probe (Supplementary Data 1).

Characterization of recombinant inbred lines. B73 and Mo17 have been popular parental lines used in genetic mapping of maize. An intermated B73 × Mo17 recombinant inbred line

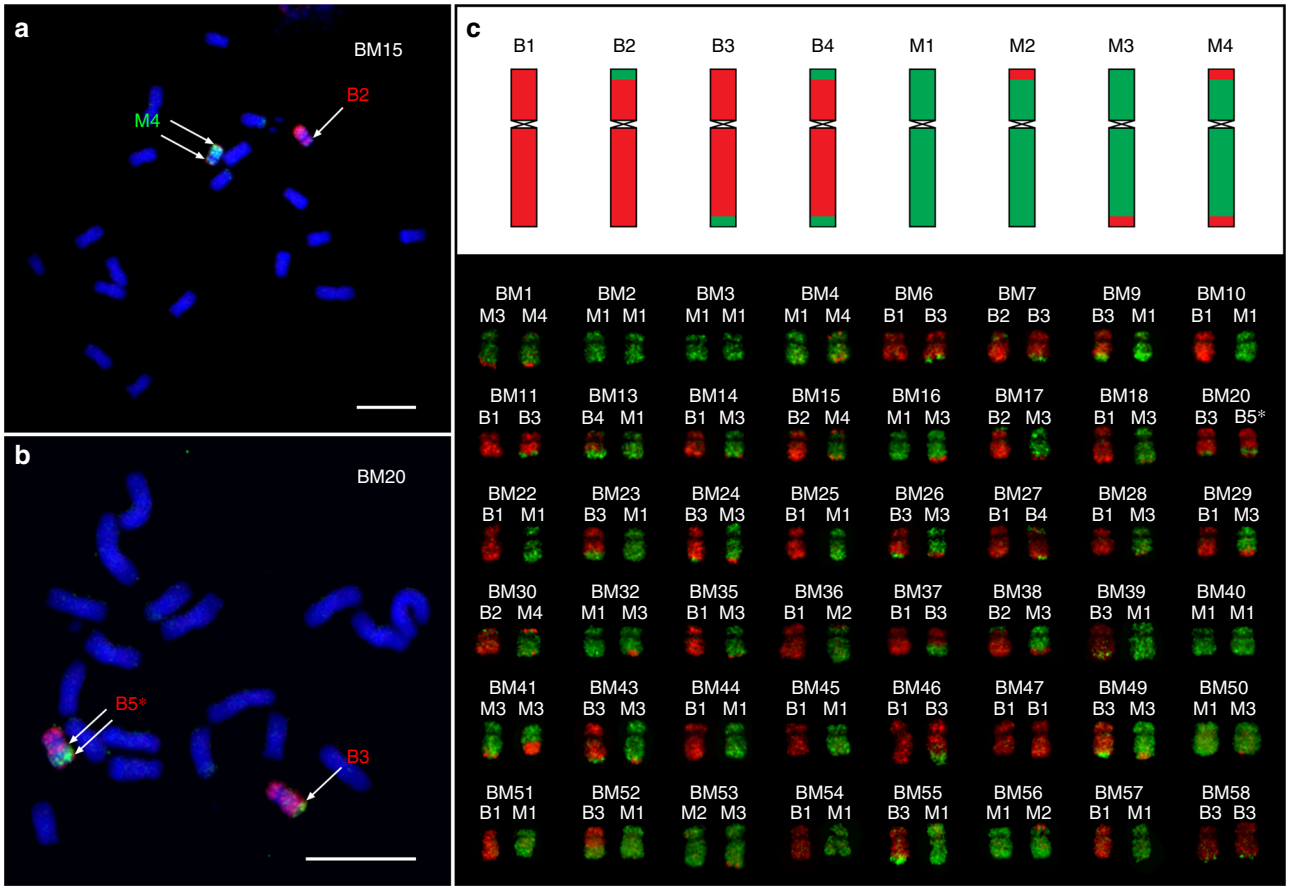

Fig. 3 Crossovers between B73 and Mo17 chromosome 10 revealed by oligo-FISH mapping using probes hapB and hapM. **a** Oligo-FISH mapping of B73 × Mo17 F_2 plant BM15. Probes hapB and hapM are shown in red and green, respectively. The single arrow identifies a single chromosomal exchange position (EP) on the B2-classified chromosome. Double arrows point to the two chromosomal EPs on the M4-classified chromosome. Bar = 10 μm. **b** Oligo-FISH mapping of B73 × Mo17 F_2 plant BM20. The single arrow points a single EP on the B3-classified chromosome. Double arrows point to the two EPs of double crossovers (COs) on the B5*-classified chromosome. Bar = 10 μm. **c** Upper panel: diagrams of the 8 types of parental or recombinant chromosomes identified in F_2 plants. B indicates B73; M indicates Mo17. Lower panel, representative images of the two copies of chromosomes 10 in 48 F_2 plants. One copy of chromosome 10 in BM20 is marked as B5*, which is the only chromosome that does not belong to any of the eight types listed in the upper panel. The original gray-scale images used to generate the color images in Figs. 3a, b are provided as a Source Data file

(IBMRIL) population was developed by randomly intermating plants for four generations following the F_2 generation[28]. The increased recombination in this population has resulted in a nearly 4-fold increase in the genetic map distance compared with conventional nonintermated RIL populations[29]. Thus, chromosomes in IBMRIL are expected to contain four times of more COs compared to the F_2 plants from the B73 × Mo17 hybrids. We intended to use oligo-FISH to cytologically characterize the multiple COs on chromosome 10, which were delineated by genotype and genome sequence data[30,31].

We re-analyzed the chromosome 10 genotyping data of the IBMRIL population (see Methods section) and chose 10 IBMRILs for oligo-FISH analysis. A total of 45 genetically immortalized CO events were identified across the 10 IBMRILs using genotypic data sets[30,31] (Supplementary Table 1). The genotypic data indicated that these 10 IBMRILs contain multiple COs located throughout chromosome 10 (Fig. 6). Several of these IBMRILs contain putative COs located in the pericentromeric regions. FISH using the hapB and hapM probes revealed that nearly all of the recombination events predicted by the genotypic data were associated with a visible CO. For example, line Mo189 was predicted to contain a proximal B73 chromosome segment, including the centromere, and a distal B73 segment on the long arm (Fig. 6, Supplementary Data 3). Oligo-FISH mapping revealed that chromosome 10 of Mo189 contains two chromosomal segments, including the centromere, from B73 and two segments from Mo17 (Figs. 6 and 7a, b). Similarly, both genotyping and oligo-FISH data showed that chromosome 10 of Mo270 contains two segments from Mo17, including the centromere, and two segments from B73 (Figs. 6 and 7c, d). However, we were not able to detect the putative small chromosomal fragments, which were indicated by a single or few DNA markers, such as those associated with lines Mo270 and Mo346 (Fig. 6). These regions may represent small chromosomal segments from B73 or Mo17, but cannot be visualized by oligo-FISH using the hapB and hapM probes.

COs close to the centromere of chromosome 10 were detected in several IBMRILs. For example, an EP on chromosome 10 of Mo189 was mapped at FLA 68.8 on the long arm (Figs. 6 and 7b). The EP that is most close to the centromere was mapped at FLA 84.6 on the long arm of chromosome 10 of Mo029 (Fig. 6). Marker analysis on 209 IBMRILs showed that 11 additional lines (in addition to the five lines in Fig. 6) contain a CO with a breakpoint at the same position as Mo189 or more close to the centromere of chromosome 10. Therefore, the intermating process is highly effective to recover and accumulate the rare CO events occurred in the pericentromeric regions.

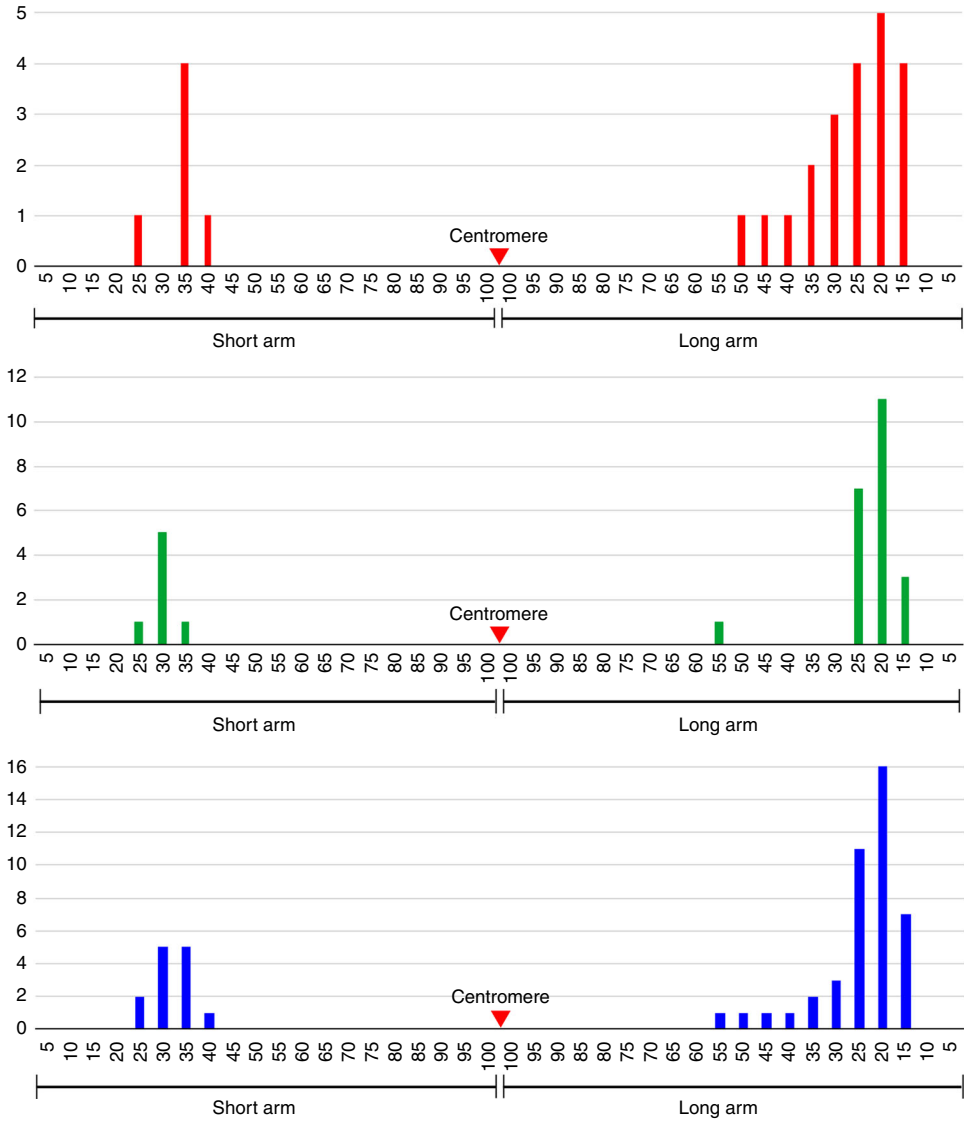

Fig. 4 Distribution of chromosomal exchange positions on chromosome 10. Upper panel, middle panel, and lower panel show exchange positions (EPs) on chromosome 10 of B73, Mo17, and combined chromosome 10, respectively. Each interval on the *x*-axes represents 5% of the length of the short or long arm. *y*-axes indicate the number of EPs within a particular 5% of the short arm or long arm. The red triangles point to the centromere position on the chromosome

Discussion

COs are not evenly distributed along the chromosomes in most plant species studied so far. Suppression of genetic recombination in the pericentromeric regions has been well documented in a number of plant species[8,9,13]. Physical mapping of a large number of RNs indicated the lack of recombination in the pericentromeric regions of maize chromosomes, although such analysis was conducted only in a single inbred line KYS[32]. The RN-based analysis showed that the pericentromeric regions, which account approximately half of the length of each chromosome, were nearly free of RNs[32]. Recombination suppression in the pericentromeric regions was also supported by physical mapping of genetically achored DNA markers on maize chromosomes[33–35]. We demonstrate that several IBMRILs contain COs close to the centromere of chromosome 10 (Fig. 6), which were not detected in the 58 F_2 plants (Fig. 4). Thus, the intermating process was effective to accumulate COs in recombination-suppressed chromosomal regions, which can be used to generate favorable allelic combinations of genes residing in these regions.

If a single CO is associated with chromosome 10 during meiosis of the B73 × Mo17 hybrid, two of the four chromatids will be involved in this CO event. Therefore, 50% of the progeny chromosome 10 will become a recombinant chromosome that may be detected by FISH. Our FISH analysis of 58 F_2 BM plants indicated that 60 of the 116 copies of chromosome 10 are not recombinant chromosomes (Supplementary Data 2). We sequenced 10 F_2 BM plants, including 13 copies of chromosome 10 that were FISH negative (Fig. 5). Sequence analysis showed that 69% (9/13) of these FISH-negative chromosome 10 were confirmed as non-recombinant chromosomes. Therefore, the percentage of chromosome 10 without CO is estimated to be 36% (69% × 60/116) in the F_2 population. Luo et al. (2019)[36] have recently developed a technique to sequence individual gametophyte using a maize hybrid derived from a cross between inbreds Zheng58 and SK. They reported that 18% male gametes and 31% female gametes from this hybrid do not contain a CO on chromosome 10[36], which would result in 25% of chromosome 10 without CO in F_2 population. Thus, our data

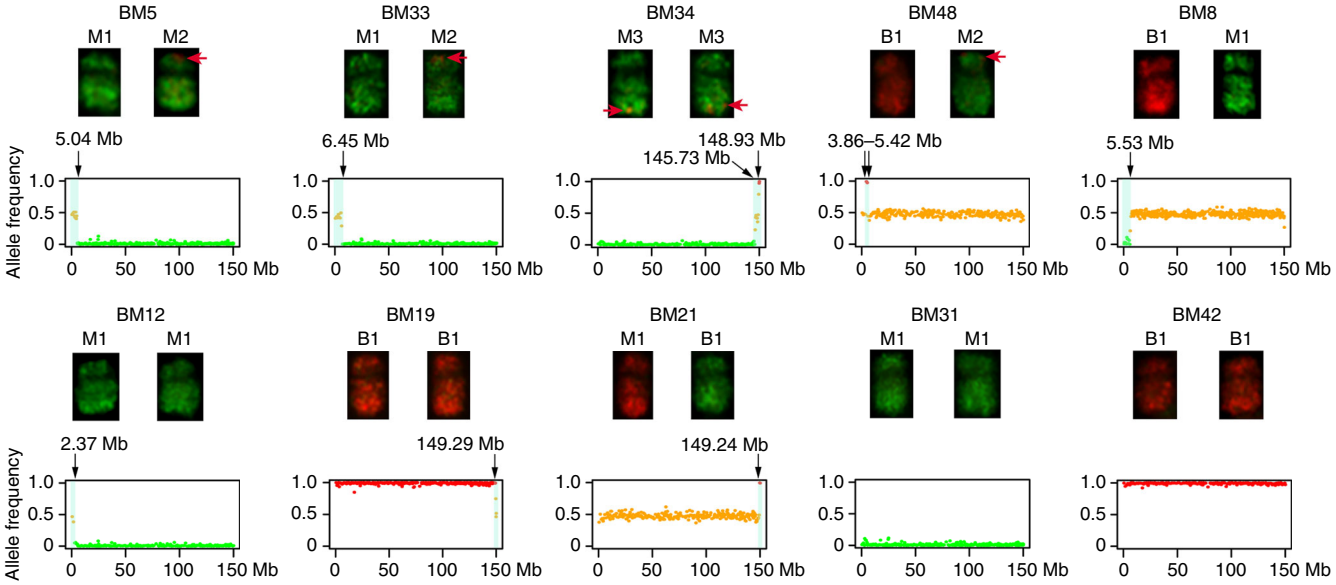

Fig. 5 Oligo-FISH and sequencing analyses of 10 F_2 plants. Red arrows indicate the B73 FISH signals located on Mo17-derived chromosome 10 in BM5, BM33, BM34, and BM48. These crossovers (COs) were inconsistently detected in different metaphase cells in each line. Black arrows mark the chromosomal exchange position on chromosome 10. No CO was detected in any of the chromosome 10 in BM31 and BM42. The *y*-axis of each sequencing profile represents the allele frequency of B73 (red) or Mo17 (green). The *x*-axis represents the sequence position of chromosome 10 (150.98 Mb). Orange dots indicate the mix of red (B73 allele) and green (Mo17 allele) dots

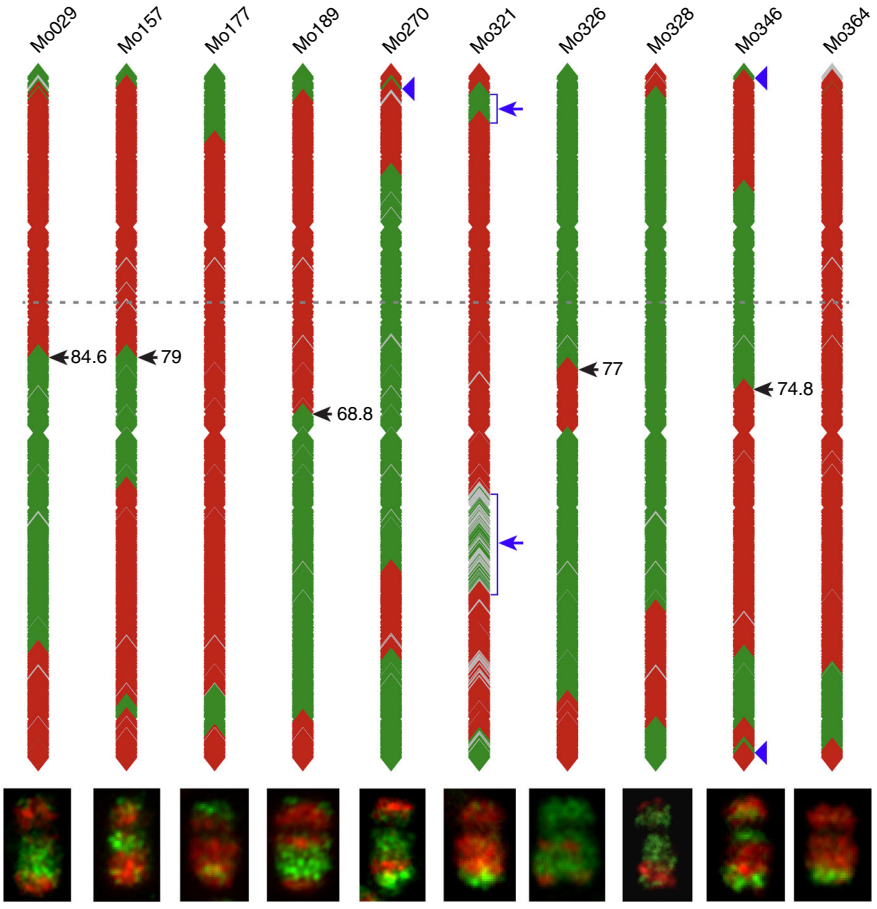

Fig. 6 Schematic illustration of genotyping data and oligo-FISH results of 10 lines from the IBMRIL population. The genotyping data is illustrated by location of markers from B73 (red) and Mo17 (green), respectively. Gray indicates missing genotyping data. A dashed line marks the putative position of the centromere on each of the marker-based diagrams. The regions indicated by blue arrows on Mo321 were not consistently visualized by oligo-FISH. Blue arrowheads on Mo270 and Mo346 point to small regions that were not identified by oligo-FISH. Black arrows point to the chromosomal exchange positions (EPs) and their fractional length of the arm (FLA), all on the long arm

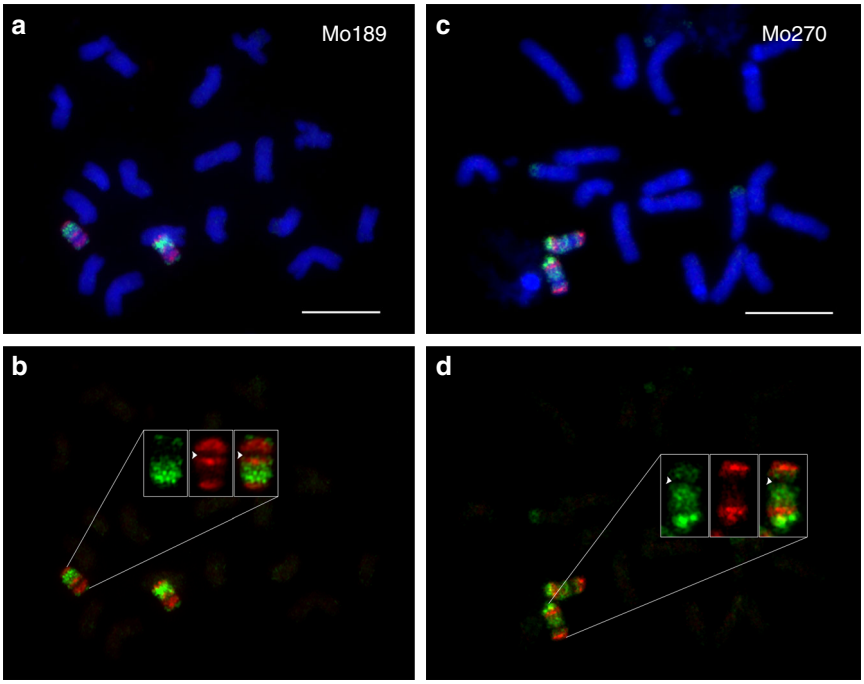

Fig. 7 Oligo-FISH characterization of two lines from the IBMRIL population. **a** Oligo-FISH analysis of Mo189. Bar = 10 μm. **b** The oligo-FISH signals of the two chromosome 10 were digitally separated from panel (**a**). Signals from one copy of chromosome 10 are exemplified. Two B73 chromosomal blocks (red), including the centromere, and two Mo17 blocks (green) are identified on chromosome 10. Arrowheads indicate the centromeric region that shows weak signals due to few oligos available. **c** Oligo-FISH mapping of Mo270. Bar = 10 μm. **d** The oligo-FISH signals of the two chromosome 10 were digitally separated from panel (**c**). Signals from one copy of chromosome 10 are exemplified. Two Mo17 blocks (green), including the centromere and two B73 blocks (red) are identified on chromosome 10. Arrowheads indicate the centromeric region that shows weak signals due to few oligos available. The original gray-scale images used to generate the color images in Fig. 7a and c are provided as a Source Data file

of 36% chromosome 10 without CO in the B73 × Mo17 F_2 population is higher than the predicted 25% in the Zheng58 × SK F_2 population. This variation may be caused by the different maize inbreds used in the F_1 hybrids. In Arabidopsis, meiotic COs on chromosome 4, the smallest chromosome, were analyzed by genotyping F_2 plants resulting from a cross between ecotypes Columbia and Landsberg[37]. Approximately 30% (423 of 1404) chromosome 4 do not contain a CO[37], which is close to 36% of non-recombinant maize chromosome 10 in our study.

A major recent advance of FISH is the application of probes based on synthetic oligos[38–40]. Oligo-based chromosome painting probes have been developed in several plant species and applied in various types of chromosomal studies[41–47]. We demonstrate that haplotype-specific oligo-FISH can be to visualize meiotic COs derived from homologous chromosomes derived from different maize inbreds. Although COs can be mapped using RNs or protein markers[7,32], these traditional methods can only predict the positions of COs on SCs in a specific maize line. In contrast, haplotype-specific FISH maps the chromosomal breakpoints derived from historical COs, including breakpoints derived from multiple COs on recombinant inbred lines from the intermated B73 × Mo17 population (Fig. 7), which can not be analyzed by the traditional methods. The haplotype-specific FISH probes will have unique applications in tracking specific chromosomes derived from a single genotype (Supplementary Note 1). For example, such probes can be used to examine the extent of somatic recombination reported in several plant species[48,49]. Haplotype-specific probes can potentially be used to distinguish true homologous chromosome pairing from pairing of homoeologous chromosome with minor structural variation in polyploid species.

Methods

Plant materials and associated genomic data sets. Hybrids between B73 and Mo17 were developed and sibling F_1 plants were pollinated to generate F_2 seeds. IBMRIL seed was originally obtained from the Maize Genetics Cooperative Stock Center and was bulked and quality-controlled as described[50]. This ensured correspondence with the genotype data used to construct the original IBM2 map[30], which are available at MaizeGDB[51]. To add genetic detail for the chromosome 10 investigation, data for 1761 SNPs genotyped for the IBMRILs[31] was merged with the 64 markers available in the IBM2:chromosome 10 data set. Physical genomic coordinates of the markers corresponding to the Zm00001d genome[24] were obtained using resources available at MaizeGDB[51].

Development of haplotype-specific oligo-FISH probes. Chorus software (https://github.com/forrestzhang/Chorus) was used to generate single copy 45-nt oligos from chromosome 10 of B73[24] and Mo17[23], respectively, with a parameter of Chorus "-l 45 –homology 75 –step 5". B73 reference genome Zm-B73-REFERENCE-GRAMENE-4.0[24] and Mo17 genome Zm-Mo17-REFERENCE-CAU-1.0[23] were download from NCBI under project PRJNA10769 and PRJNA358298, respectively. To validate the repetitiveness of each oligo, we generated the frequency distribution of 17-mers from B73 (SRR407544 and SRR407504, JGI) and Mo17 (SRR5826129,[23]) genomic sequencing data. Any 17-mers with a frequency more than 100 in the genome was defined as a repetitive 17-mer. Oligos containing 2 or more repetitive 17-mers were discarded.

In total, 175,437 and 174,728 oligos from B73 and Mo17 chromosome 10 were generated, respectively (Supplementary Note 1). To identify oligos that distinguish the chromosome 10 sequences from the two inbreds, we mapped B73 (Mo17) oligos to Mo17 (B73) reference genome using BWA ALN[52] with default parameters and blastn in BLAST[53] with parameter "-task blastn". B73 (Mo17) oligos that were not identified on Mo17 (B73) chromosome 10 were defined as PAV oligos. B73 (Mo17) oligos containing mismatches and/or indels to Mo17 (B73) chromosome 10 were defined as SNP probe. We only retained SNP oligos with mismatches and/or indels located between 10 and 35 bp within each oligo. For each B73 oligo, the B73 sequences at SNPs and/or indels were replaced by the Mo17 sequences, and vice versa. Therefore, SNP oligos are in pairs, in which one oligo set is homologous to the B73 genome but showed mismatches and/or indels to Mo17 genome and vice versa. We then calculated the ΔTm (difference of melting temperature) between B73 oligo and Mo17 oligo of each oligo pair using primer3[25,26]. We discarded oligo pairs with ΔTm > 5 °C to avoid hybridization bias toward one

variant. The SNP oligo pairs were divided into four different classes: oligos with 1 SNP, 2 SNPs, 3–4 SNPs, and 5 or more SNPs. The two probes used for CO characterization, hapB and hapM, included all PAV oligos and oligos with 3–4 SNPs, and 5 or more SNPs. These two probes contained 14,498 and 13,753 oligos, respectively (Supplementary Data 4).

Oligo-FISH. All seeds were germinated in the laboratory and plants were transferred to the greenhouse. Root tips were collected from the plants and were treated with nitrous oxide at a pressure of 160 psi (~10.9 atm) for 2 h. Root tips were harvested from plants growing in greenhouses. Chromosome preparation from root tips followed published protocols[42]. We synthesized 10 different oligo pools (five for B73, five for Mo17), including two PAV oligo pools, and four paired (i.e., eight total) oligo pools with 1 SNP, 2 SNPs, 3–4 SNPs, or ≥5 SNPs. The B73 oligo probes were labeled with digoxigenin and Mo17 probes were labeled with biotin. Amplification and labeling of the oligo-based probes were according to published protocols[41]. All biotin-labeled probes were detected by anti-biotin fluorescein (Vector Laboratories, Burlingame, California) and digoxigenin-labeled probes were detected by anti-digoxigenin rhodamine (Roche Diagnostics, Indianapolis, Indiana). DAPI (4',6-diamidino-2-phenylindole) was used to counterstain chromosomes in the Vecta-Shield antifade solution (Vector Laboratories). FISH images were captured using a QImaging Retiga EXi Fast 1394 CCD. The original gray scale images were processed with Meta Imaging Series 7.5 software. The contrast of the gray scale images was adjusted and merged using Adobe Photoshop CS3 software.

For each unambiguously identified meiotic CO we measured the distance, or length (μm), from the chromosomal exchange point (EP) to the telomere of the respective chromosome arm. The length (μm) of the respective chromosome arm bearing the CO was also measured. The chromosomal position of each EP is presented as a FLA (Fractional Length of the Arm) by dividing the measured distance by the total length of the chromosome arm. DRAWID (https://doi.org/10.3897/compcytogen.v11i4.20830) was used to measure the distance from the FISH signal to the telomere of the corresponding arm, as well as the length of the entire arm.

Sequencing and analysis. Genomic DNA was isolated from 10 F_2 plants (BM5, BM33, BM34, BM48, BM8, BM12, BM19, BM21, BM31, BM42) for Illumina sequencing. We generated an average of 2.41× coverage of 150 bp pair-end sequences from these plants. The sequence data was mapped to the B73 RefGen_v4[24] by BWA MEM software with default parameters[52]. Reads with mapping quality more than 50 were retained for SNP calling. SNPs were detected using freebayes with parameter "-C 1 –m 50 –q 30"[54]. Raw SNPs were further filtered using vcffilter in freebayes package by "DP < 40" and "QUAL/DP > 10". The bin map was constructed using a sliding window approach[55] with minor modification. SNPs were scanned in 300-SNP-windows and the genotype of each window defined by the percentage of B73 and Mo17 SNPs: the windows were called homozygous B73 genotype when SNP_{B73} is more than 80% in the window, homozygous Mo17 genotype when SNP_{Mo17} is more than 80% in the window and heterozygous genotype when SNP_{B73} was between 20 and 80%.

Reporting summary. Further information on research design is available in the Nature Research Reporting Summary linked to this article.

Data availability

Data supporting the findings of this work are available within the paper and its Supplementary Information files. A reporting summary for this article is available as a Supplementary Information file. The datasets generated and analyzed during the current study are available from the corresponding author upon request. Genomic sequencing data of the 10 maize lines have been deposited to NCBI Sequence Read Archive (SRA) under project PRJNA540894 (https://www.ncbi.nlm.nih.gov/bioproject/?term=PRJNA540894). The source data underlying Figs. 1, 2b, 3a, 3b, 7a, and c are provided as a Source Data file.

Received: 27 April 2019; Accepted: 20 September 2019;
Published online: 10 October 2019

References

1. Keeney, S., Giroux, C. N. & Kleckner, N. Meiosis-specific DNA double-strand breaks are catalyzed by Spo11, a member of a widely conserved protein family. *Cell* **88**, 375–384 (1997).
2. Gray, S. & Cohen, P. E. Control of meiotic crossovers: from double-strand break formation to designation. *Annu. Rev. Genet.* **50**, 175–210 (2016).
3. Jones, G. H. & Franklin, F. C. H. Meiotic crossing-over: obligation and interference. *Cell* **126**, 246–248 (2006).
4. Wang, S. X., Zickler, D., Kleckner, N. & Zhang, L. R. Meiotic crossover patterns: obligatory crossover, interference and homeostasis in a single process. *Cell Cycle* **14**, 305–314 (2015).
5. Zickler, D. & Kleckner, N. Recombination, pairing, and synapsis of homologs during meiosis. *Cold Spring Harb. Persp. Biol.* **7**, a016626 (2015).
6. Carpenter, A. T. C. Electron microscopy of meiosis in *Drosophila melanogaster* females: II: the recombination nodule—a recombination-associated structure at pachytene. *Proc. Natl Acad. Sci. USA* **72**, 3186–3189 (1975).
7. Lhuissier, F. G. P., Offenberg, H. H., Wittich, P. E., Vischer, N. O. E. & Heyting, C. The mismatch repair protein MLH1 marks a subset of strongly interfering crossovers in tomato. *Plant Cell* **19**, 862–876 (2007).
8. Gill, K. S., Gill, B. S., Endo, T. R. & Taylor, T. Identification and high-density mapping of gene-rich regions in chromosome group 1 of wheat. *Genetics* **144**, 1883–1891 (1996).
9. Kunzel, G., Korzun, L. & Meister, A. Cytologically integrated physical restriction fragment length polymorphism maps for the barley genome based on translocation breakpoints. *Genetics* **154**, 397–412 (2000).
10. Cheng, Z., Presting, G. G., Buell, C. R., Wing, R. A. & Jiang, J. M. High-resolution pachytene chromosome mapping of bacterial artificial chromosomes anchored by genetic markers reveals the centromere location and the distribution of genetic recombination along chromosome 10 of rice. *Genetics* **157**, 1749–1757 (2001).
11. Lamb, J. C. et al. Single-gene detection and karyotyping using small-target fluorescence in situ hybridization on maize somatic chromosomes. *Genetics* **175**, 1047–1058 (2007).
12. Danilova, T. V. & Birchler, J. A. Integrated cytogenetic map of mitotic metaphase chromosome 9 of maize: resolution, sensitivity, and banding paint development. *Chromosoma* **117**, 345–356 (2008).
13. Iovene, M., Wielgus, S. M., Simon, P. W., Buell, C. R. & Jiang, J. M. Chromatin structure and physical mapping of chromosome 6 of potato and comparative analyses with tomato. *Genetics* **180**, 1307–1317 (2008).
14. Tang, X. M. et al. Cross-species bacterial artificial chromosome-fluorescence in situ hybridization painting of the tomato and potato chromosome 6 reveals undescribed chromosomal rearrangements. *Genetics* **180**, 1319–1328 (2008).
15. King, J. et al. Physical and genetic mapping in the grasses *Lolium perenne* and *Festuca pratensis*. *Genetics* **161**, 315–324 (2002).
16. Khrustaleva, L. I., de Melo, P. E., van Heusden, A. W. & Kik, C. The integration of recombination and physical maps in a large-genome monocot using haploid genome analysis in a trihybrid Allium population. *Genetics* **169**, 1673–1685 (2005).
17. Zhang, W. et al. Meiotic homoeologous recombination-based mapping of wheat chromosome 2B and its homoeologues in *Aegilops speltoides* and *Thinopyrum elongatum*. *Theor. Appl. Genet.* **131**, 2381–2395 (2018).
18. Mikel, M. A. & Dudley, J. W. Evolution of North American dent corn from public to proprietary germplasm. *Crop Sci.* **46**, 1193–1205 (2006).
19. Swanson-Wagner, R. A. et al. All possible modes of gene action are observed in a global comparison of gene expression in a maize F1 hybrid and its inbred parents. *Proc. Natl Acad. Sci. USA* **103**, 6805–6810 (2006).
20. Stupar, R. M. & Springer, N. M. Cis-transcriptional variation in maize inbred lines B73 and Mo17 leads to additive expression patterns in the F1 hybrid. *Genetics* **173**, 2199–2210 (2006).
21. Swanson-Wagner, R. A. et al. Paternal dominance of trans-eQTL influences gene expression patterns in maize hybrids. *Science* **326**, 1118–1120 (2009).
22. Schnable, P. S. et al. The B73 maize genome: complexity, diversity, and dynamics. *Science* **326**, 1112–1115 (2009).
23. Sun, S. L. et al. Extensive intraspecific gene order and gene structural variations between Mo17 and other maize genomes. *Nat. Genet.* **50**, 1289–1295 (2018).
24. Jiao, Y. P. et al. Improved maize reference genome with single-molecule technologies. *Nature* **546**, 524–527 (2017).
25. Koressaar, T. & Remm, M. Enhancements and modifications of primer design program Primer3. *Bioinformatics* **23**, 1289–1291 (2007).
26. Untergasser, A. et al. Primer3-new capabilities and interfaces. *Nucleic Acids Res.* **40**, e115 (2012).
27. Zhao, H. N. et al. Gene expression and chromatin modifications associated with maize centromeres. *G3* **6**, 183–192 (2016).
28. Lee, M. et al. Expanding the genetic map of maize with the intermated B73 x Mo17 (IBM) population. *Plant Mol. Biol.* **48**, 453–461 (2002).
29. Zhang, N. Y. et al. Fine quantitative trait loci mapping of carbon and nitrogen metabolism enzyme activities and seedling biomass in the maize IBM mapping population. *Plant Physiol.* **154**, 1753–1765 7 (2010).
30. Sharopova, N. et al. Development and mapping of SSR markers for maize. *Plant Mol. Biol.* **48**, 463–481 (2002).
31. Ganal, M. W. et al. A large maize (*Zea mays* L.) SNP genotyping array: development and germplasm genotyping, and genetic mapping to compare with the B73 reference genome. *PLoS ONE* **6**, e28334 (2011).
32. Anderson, L. K. et al. High-resolution crossover maps for each bivalent of Zea mays using recombination nodules. *Genetics* **165**, 849–865 (2003).
33. Koumbaris, G. L. & Bass, H. W. A new single-locus cytogenetic mapping system for maize (*Zea mays* L.): overcoming FISH detection limits with marker-selected sorghum (*S. propinquum* L.) BAC clones. *Plant J.* **35**, 647–659 (2003).

34. Wang, C. J. R., Harper, L. & Cande, W. Z. High-resolution single-copy gene fluorescence in situ hybridization and its use in the construction of a cytogenetic map of maize chromosome 9. *Plant Cell* **18**, 529–544 (2006).
35. Figueroa, D. M. & Bass, H. W. Development of pachytene FISH maps for six maize chromosomes and their integration with other maize maps for insights into genome structure variation. *Chromosome Res.* **20**, 363–380 (2012).
36. Luo, C., Li, X., Zhang, Q. H. & Yan, J. B. Single gametophyte sequencing reveals that crossover events differ between sexes in maize. *Nat. Commun.* **10**, 785 (2019).
37. Drouaud, J. et al. Variation in crossing-over rates across chromosome 4 of *Arabidopsis thaliana* reveals the presence of meiotic recombination "hot spots". *Genome Res.* **16**, 106–114 (2006).
38. Beliveau, B. J. et al. Versatile design and synthesis platform for visualizing genomes with Oligopaint FISH probes. *Proc. Natl Acad. Sci. USA* **109**, 21301–21306 (2012).
39. Beliveau, B. J. et al. Single-molecule super-resolution imaging of chromosomes and in situ haplotype visualization using Oligopaint FISH probes. *Nat. Commun.* **6**, 7147 (2015).
40. Jiang, J. M. Fluorescence in situ hybridization in plants: recent developments and future applications. *Chromosome Res.* **27**, 153–165 (2019).
41. Han, Y. H., Zhang, T., Thammapichai, P., Weng, Y. Q. & Jiang, J. M. Chromosome-specific painting in cucumis species using bulked oligonucleotides. *Genetics* **200**, 771–779 (2015).
42. Braz, G. T. et al. Comparative Oligo-FISH mapping: an efficient and powerful methodology to reveal karyotypic and chromosomal evolution. *Genetics* **208**, 513–523 (2018).
43. He, L., Braz, G. T., Torres, G. A. & Jiang, J. M. Chromosome painting in meiosis reveals pairing of specific chromosomes in polyploid Solanum species. *Chromosoma* **127**, 505–513 (2018).
44. Hou, L. L. et al. Chromosome painting and its applications in cultivated and wild rice. *BMC Plant Biol.* **18**, 110 (2018).
45. Meng, Z. et al. Comprehensively characterizing the cytological features of *Saccharum spontaneum* by the development of a complete set of chromosome-specific oligo probes. *Front. Plant Sci.* **9**, 1624 (2018).
46. Xin, H. et al. Chromosome painting and comparative physical mapping of the sex chromosomes in *Populus tomentosa* and *Populus deltoides*. *Chromosoma* **127**, 313–321 (2018).
47. Albert, P. S. et al. Whole-chromosome paints in maize reveal rearrangements, nuclear domains, and chromosomal relationships. *Proc. Natl Acad. Sci. USA* **116**, 1679–1685 (2019).
48. Vig, B. K. Somatic crossing over in *Glycine max* (L) Merrill: effect of some inhibitors of DNA synthesis on induction of somatic crossing over and point mutations. *Genetics* **73**, 583–596 (1973).
49. Carlson, P. S. Mitotic crossing-over in a higher plant. *Genet. Res.* **24**, 109–112 (1974).
50. Lauter, N., Moscou, M. J., Habiger, J. & Moose, S. P. Quantitative genetic dissection of shoot architecture traits in maize: Towards a functional genomics approach. *Plant Genome* **1**, 99–110 (2008).
51. Andorf, C. M. et al. MaizeGDB update: new tools, data and interface for the maize model organism database. *Nucleic Acids Res.* **44**, D1195–D1201 (2016).
52. Li, H. & Durbin, R. Fast and accurate short read alignment with Burrows-Wheeler transform. *Bioinformatics* **25**, 1754–1760 (2009).
53. Altschul, S. F. et al. Gapped BLAST and PSI-BLAST: a new generation of protein database search programs. *Nucleic Acids Res.* **25**, 3389–3402 (1997).
54. Garrison, E. & Marth, G. Haplotype-based variant detection from short-read sequencing. Preprint at https://arxiv.org/abs/1207.3907 (2012).
55. Song, W. B. et al. Genetic dissection of maize seedling root system architecture traits using an ultra-high density bin-map and a recombinant inbred line population. *J. Integr. Plant Biol.* **58**, 266–279 (2016).

Acknowledgements

We thank the Maize Genetics Cooperative Stock Center for the original provision of seed stocks and MaizeGDB for genetic and genomic data curation. We thank Kyle King and Colton McNinch for bioinformatics efforts to attach physical genome coordinates to the genetic markers used in this study. F.Y. and Z.D. are supported by grant 31571730 from the National Natural Science Foundation of China and from the National Education Ministry, Key Laboratory of Plant Genetic Improvement and Comprehensive Utilization, Fujian Agriculture and Forestry University. This research is supported by NSF grant IOS-1444514 and MSU startup funds to J.J.

Author contributions

J.J. conceived the project; L.d.V.M., F.Y., and H.W. conducted the oligo-FISH experiments; H.Z. designed the oligo-FISH probes; T.D. and N.L. analyzed the genotyping data of the IBMRILs; K.S. and J.M.-R. synthesized probes and provided reagents; Z.D., A.T. and J.A.B. developed and provided the resources; H.Z., J.A.B., and J.J. wrote the paper.

Competing interests

K.S. and J.M.-R. are employed by Arbor Biosciences. J.M.-R. has personal financial interest in Arbor Biosciences. The remaining authors declare no competing interests.

Additional information

Supplementary information is available for this paper at https://doi.org/10.1038/s41467-019-12646-z.

Correspondence and requests for materials should be addressed to J.J.

Peer review information *Nature Communications* thanks Trude Schwarzacher, Jianbing Yan and the other, anonymous, reviewer(s) for their contribution to the peer review of this work. Peer reviewer reports are available.

Reprints and permission information is available at http://www.nature.com/reprints

Publisher's note Springer Nature remains neutral with regard to jurisdictional claims in published maps and institutional affiliations.

APÊNDICE C – ARTIGO PUBLICADO NA REVISTA CHROMOSOMA RESEARCH

Chromosome Res
https://doi.org/10.1007/s10577-020-09630-5

ORIGINAL ARTICLE

A universal chromosome identification system for maize and wild *Zea* species

Guilherme T. Braz · Lívia do Vale Martins · Tao Zhang · Patrice S. Albert · James A. Birchler · Jiming Jiang

Received: 4 February 2020 / Revised: 16 March 2020 / Accepted: 17 March 2020

Abstract Maize was one of the first eukaryotic species in which individual chromosomes can be identified cytologically, which made maize one of the oldest models for genetics and cytogenetics research. Nevertheless, consistent identification of all 10 chromosomes from different maize lines as well as from wild *Zea* species remains a challenge. We developed a new technique for maize chromosome identification based on fluorescence in situ hybridization (FISH). We developed two oligonucleotide-based probes that hybridize to 24 chromosomal regions. Individual maize chromosomes show distinct FISH signal patterns, which allow universal identification of all chromosomes from different *Zea* species. We developed karyotypes from three *Zea mays* subspecies and two additional wild *Zea* species based on individually identified chromosomes. A paracentric inversion was discovered on the long arm of chromosome 4 in *Z. nicaraguensis* and *Z. luxurians* based on modifications of the FISH signal patterns. Chromosomes from these two species also showed distinct distribution patterns of terminal knobs compared with other *Zea* species. These results support that *Z. nicaraguensis* and *Z. luxurians* are closely related species.

Keywords FISH · Oligo-FISH · Chromosome identification · Karyotype · Maize

Responsible Editor: Andreas Houben

Electronic supplementary material The online version of this article (https://doi.org/10.1007/s10577-020-09630-5) contains supplementary material, which is available to authorized users.

G. T. Braz · L. do Vale Martins · J. Jiang (✉)
Department of Plant Biology, Michigan State University, East Lansing, MI 48824, USA
e-mail: jiangjm@msu.edu

T. Zhang
Jiangsu Key Laboratory of Crop Genomics and Molecular Breeding/Key Laboratory of Plant Functional Genomics of Ministry of Education, Yangzhou University, Yangzhou 225009, China

P. S. Albert · J. A. Birchler
Division of Biological Sciences, University of Missouri, Columbia, MO 65211, USA

J. Jiang
Department of Horticulture, Michigan State University, East Lansing, MI 48824, USA

J. Jiang
AgBioResearch, Michigan State University, East Lansing, MI 48824, USA

Abbreviations

BAC	Bacterial artificial chromosome
DAPI	4,6-Diamidino-2-phenylindole
FISH	Fluorescence in situ hybridization
Mb	Megabase
MY	Million years
Oligo	Oligonucleotide

Introduction

A reliable and efficient system for chromosome identification is the foundation for cytogenetic research.

Published online: 26 March 2020

Maize (*Zea mays*) and common fruit fly (*Drosophila melanogaster*) became the most important model species for genetic and cytogenetic research in early twentieth century because individual chromosomes could be readily identified in both species (Bridges 1935; McClintock 1929). However, the identification of individual chromosomes relied on meiotic pachytene chromosomes in maize and salivary polytene chromosomes in *Drosophila*. Thus, the chromosome identification methodologies developed in these two model species were not applicable in most of the other eukaryotes. Preparation and identification of pachytene chromosomes is technically demanding; thus, cytogenetic research in most plant species relies on mitotic metaphase chromosomes. Most of the chromosome identification systems based on mitotic metaphase chromosomes were developed after 1970s using either chromosome banding or DNA in situ hybridization techniques (Jiang and Gill 1994).

Although maize chromosomes can be individually identified based on their morphology (McClintock 1929), there are ambiguities. Chromosome banding techniques were developed in 1980s and 1990s for maize chromosome identification (de Carvalho and Saraiva 1993, 1997; Deaguiarperecin and Vosa 1985; Jewell and Islam-Faridi 1994; Kakeda et al. 1990; Rayburn et al. 1985; Ward 1980). C-banding, the most popular banding technique applied in plants, revealed mostly the knob-related regions on maize chromosomes (Deaguiarperecin and Vosa 1985; Jewell and Islam-Faridi 1994; Rayburn et al. 1985). Thus, maize chromosomes showed a limited number of C-bands that are also highly polymorphic among different maize varieties. It was not possible to establish a standard banding pattern for maize chromosome identification.

Fluorescence in situ hybridization (FISH) gradually replaced chromosome banding to become the most popular technique for chromosome identification in plants (Jiang and Gill 2006). Repetitive DNA sequences and large-insert DNA clones, such as bacterial artificial chromosome (BAC) clones, have been most commonly used as FISH probes in maize (Amarillo and Bass 2007; Chen et al. 2000; Figueroa and Bass 2012; Koumbaris and Bass 2003; Lamb et al. 2007b; Sadder and Weber 2001; Wang et al. 2006). Kato et al. (2004) used a combination of several repetitive DNA sequences as FISH probes to identify all 10 maize chromosomes in the same metaphase cells. This repeat-based FISH method was successfully used to identify chromosomes in various maize lines as well as wild *Zea* species and subspecies (Albert et al. 2010; Kato et al. 2004). The FISH signal patterns of some repeats, however, are highly polymorphic among different maize lines, which may cause difficulties or errors in chromosome identification.

Recently, a new class of FISH probes was developed based on pooled single-copy oligonucleotides (oligo) (Jiang 2019). If the genomic sequence is available from a target species, oligos, typically 40–50 bp long, specific to a chromosomal region or to an entire chromosome can be synthesized in parallel and labeled as a FISH probe (Han et al. 2015). Oligo-FISH probes have been successfully developed in several plant species for various types of cytogenetic studies (Albert et al. 2019; Bi et al. 2020; He et al. 2018; Hou et al. 2018; Martins et al. 2019; Meng et al. 2018; Qu et al. 2017; Simonikova et al. 2019; Song et al. 2020; Xin et al. 2018; Xin et al. 2020). A FISH probe can include oligos derived from multiple regions from multiple chromosomes (Braz et al. 2018). Such oligo-FISH probes generate specific hybridization patterns on individual chromosomes, which resemble distinct barcodes on different chromosomes. This chromosome identification strategy has been successfully demonstrated in potato (Braz et al. 2018), rice (Liu et al. 2020), and sugarcane (Meng et al. 2020). Here, we report the development of similar barcode FISH probe in maize. We demonstrate that barcode FISH can be used as a universal chromosome identification system for maize and all wild *Zea* species. The FISH signal pattern is not affected by the DNA polymorphisms existing among different maize varieties or even among different species. Using this system, we were able to establish karyotypes of several different *Zea* species and subspecies and to discover a paracentric inversion specific to two wild *Zea* species.

Materials and methods

Plant materials

We included the following *Zea* species and subspecies in chromosome identification and karyotyping studies: *Z. mays* (inbred B73), *Z. mays* ssp. *parviglumis* (Ames 21826), *Z. mays* ssp. *mexicana* (Ames 21851), *Z. mays* ssp. *huehuetenangensis* (PI 441934), *Z. diploperennis* (PI 462368), *Z. nicaraguensis* (PI 615697), and *Z. luxurians* (PI 422162). Additional species included

in the study were the tetraploid species *Z. perennis* (Ames 21874), *Tripsacum dactyloides* (PI 421612), and *Sorghum bicolor* (PI 564163). Seeds of all wild species were originally from the Germplasm Resources Information Network (GRIN) and the National Genetics Resource Program (Ames, Iowa).

Oligo-FISH probe design

The two oligo-based barcode probes were designed following our published procedure (Albert et al. 2019) using Chorus software (https://github.com/forrestzhang/Chorus). Briefly, the maize genome sequence was divided into 45-nt long oligos in step size of 3 nt. The short sequence reads were mapped back to the genome using BWA (Burrows-Wheeler Alignment tool) (Li and Durbin 2009). Oligos mapped to two or more locations (with 70% homology) were eliminated. All repetitive sequences related oligos were filtered out from the oligo set using *k*-mer method (Albert et al. 2019). We selected oligos from 24 chromosomal regions to create a barcode for all 10 maize chromosomes (Fig. 1a). Each selected region contains approximately 2000 oligos. We selected the chromosomal regions that are relatively enriched with single copy sequences. Each of the 24 selected regions spans 1.3–3.3 Mb (Table S1). If two regions are designed from the same chromosomal arm, we then intended to separate the two regions as far as possible. The two regions on eight different chromosomal arms (Fig. 1a) are separated 28.2–66.4 Mb (Table S1).

Oligo-FISH

Root tips harvested from plants grown in greenhouse were treated with nitrous oxide at a pressure of 160 psi (~ 10.9 atm) for 2 h and 20 min (Kato 1999), fixed in fixative solution (3 ethanol:1 acetic acid) and kept at − 20 °C. Root tips were digested using an enzymatic solution composed by 4% cellulase (Yakult Pharmaceutical, Japan), 2% pectinase (Sigma-Aldrich Co., USA) and 2% pectolyase (Plant Media, USA) for 2 h at 37 °C and slides were prepared using the stirring method (Ross et al. 1996).

Two oligo-based FISH probes were labeled according to published protocols (Han et al. 2015) and hybridized to metaphase chromosomes (Cheng et al. 2002). Biotin- and digoxygenin-labeled probes were detected by anti-biotin fluorescein (Vector Laboratories, Burlingame, California) and anti-digoxygenin rhodamine (Roche Diagnostics, Indianapolis, Indiana), respectively. Chromosomes were counterstained with 4,6-diamidino-2-phenylindole (DAPI) in VectaShield antifade solution (Vector Laboratories). FISH images were captured using a QImaging Retiga EXi Fast 1394 CCD camera attached to an Olympus BX51 epifluorescence microscope. Images were processed with Meta Imaging Series 7.5 software. The final contrast of the images was processed using Adobe Photoshop software.

Karyotyping

We used 7–10 complete metaphase cells of *Z. mays* and its relatives (*Z. mays* ssp. *parviglumis*, *Z. mays* ssp. *mexicana*, *Z. mays* ssp. *huehuetenangensis*, *Z. nicaraguensis*, *Z. luxurians*) to measure the short (S) and long (L) arms of individual chromosomes using DRAWID software version 0.26 (Kirov et al. 2017). The measurements were used to determine the total length of each chromosome ($tl = S + L$), total length of entire set of chromosomes ($TL = \sum tl$), arm ratio ($AR = L/S$) of each chromosome, and relative length of each chromosome ($RL = tl/TL \times 100$). Chromosomal knobs were identified as DAPI-positive bands. Chromosomes were classified based on arm ratio following Levan et al. (1964).

Results

Development of oligo-FISH probes for maize chromosome identification

We developed two oligo-based FISH probes to facilitate simultaneous identification of all 10 maize chromosomes in the same metaphase cells. These two probes contained a total of 50,082 oligos (45 nt) designed from single copy sequences in the maize genome (Schnable et al. 2009). The oligos were selected from 24 chromosomal regions (Fig. 1a), each containing 1978–2282 oligos and spanning 1.3–3.3 megabase (Mb) of DNA sequences (Table S1). The oligos were synthesized as two separate pools, containing 25,059 (red probe) and 25,023 (green probe) oligos, respectively. FISH using these two probes generated 24 distinct signals on metaphase chromosomes prepared from maize inbred B73 (Fig. 1b). The chromosomal positions of the FISH signals matched with predicted positions on the 10

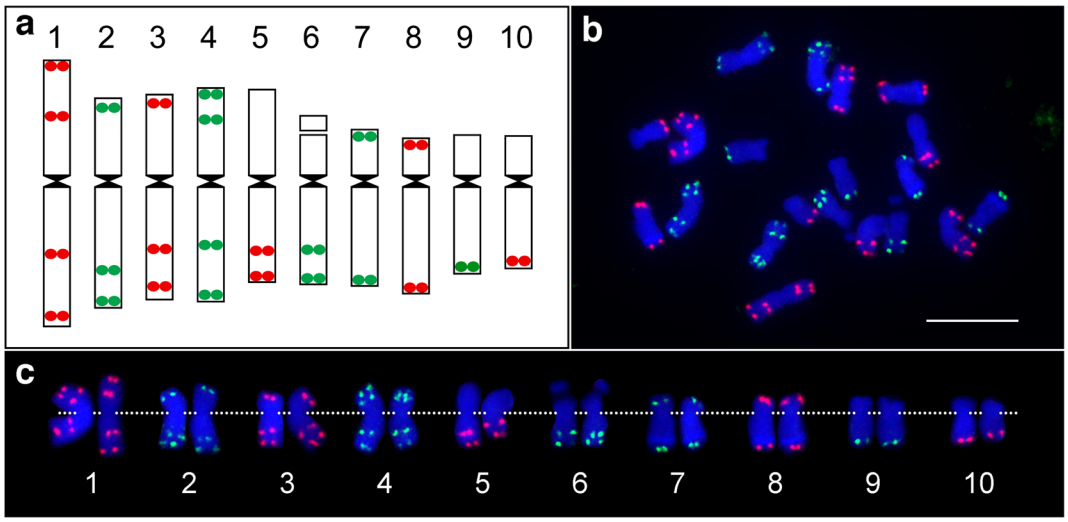

Fig. 1 Development of barcode oligo-FISH probes for maize chromosome identification. **a** Predicted locations of the oligo-FISH signals on 10 maize chromosomes. Oligos were selected from a total of 24 chromosomal regions (12 red regions and 12 green regions). The 10 chromosomes can be distinguished from each other based on number and location of the red/green signals. The centromere positions on the 10 chromosomes in the maize reference genome were based on the locations of sequences associated with CENH3 nucleosomes (Zhao et al. 2016). **b** FISH mapping of the two oligo-FISH probes on metaphase chromosomes prepared from maize inbred B73. Bar = 10 μm. **c** Homologous chromosomes were digitally excised from (**b**) and paired. The centromeres of the chromosomes are aligned by a dotted line

pseudomolecules, which allowed us to readily distinguish 10 individual chromosomes in the same metaphase cell (Fig. 1c). Several chromosomal arms contained two signals, which were well separated on metaphase chromosomes. The two signals designed on the short arm of chromosome 4 were separated by 28.2 Mb, representing the shortest distance among the paired signals (Table S1). These two signals appeared to be fused only on some highly condensed metaphase chromosomes.

Chromosome identification in different *Zea* species

The two oligo-FISH probes were used to identify chromosomes from several *Z. mays* subspecies and wild *Zea* species known as "teosintes", including *Z. mays* ssp. *parviglumis* (Fig. 2a), *Z. mays* ssp. *mexicana* (Fig. 2b), *Z. mays* ssp. *huehuetenangensis* (Fig. 2c), *Z. diploperennis* (Fig. 2d), *Z. nicaraguensis* (Fig. 2e), and *Z. luxurians* (Fig. 2f). We observed a nearly identical FISH signal pattern on chromosomes from all *Zea* species and subspecies (Fig. 3). We also performed oligo-FISH analysis in the tetraploid species *Z. perennis* ($2n = 4x = 40$). Similarly, the conserved FISH signal pattern was observed on all 10 sets of homologous chromosomes (Fig. 4). Thus, these two probes allowed us to identify all chromosomes from all *Zea* taxa.

A putative inversion detected on long arm of chromosome 4

We detected some noticeable chromosome level differences based on the signal patterns of oligo-FISH. One distinct FISH signal pattern change was observed on the long arm of chromosome 4 from *Z. nicaraguensis* and *Z. luxurians* (Fig. 3). One green signal was designed from the distal end on the long arm of chromosome 4 (at 234–236 Mb of chromosome 4, which is 242 Mb long). This signal was detected at the end of the long arm of maize chromosome 4 (Fig. 1c). However, chromosome 4 of *Z. nicaraguensis* and *Z. luxurians* did not contain this terminal signal. It instead contains two interstitial green signals on the long arm (Fig. 3). Thus, a paracentric inversion may have occurred in the long arm, which would relocate the terminal signal into an interstitial position.

Chromosomal difference revealed by oligo-FISH

The number, size, and distribution of metaphase-visible "knobs" were the most prominent factor resulting in the

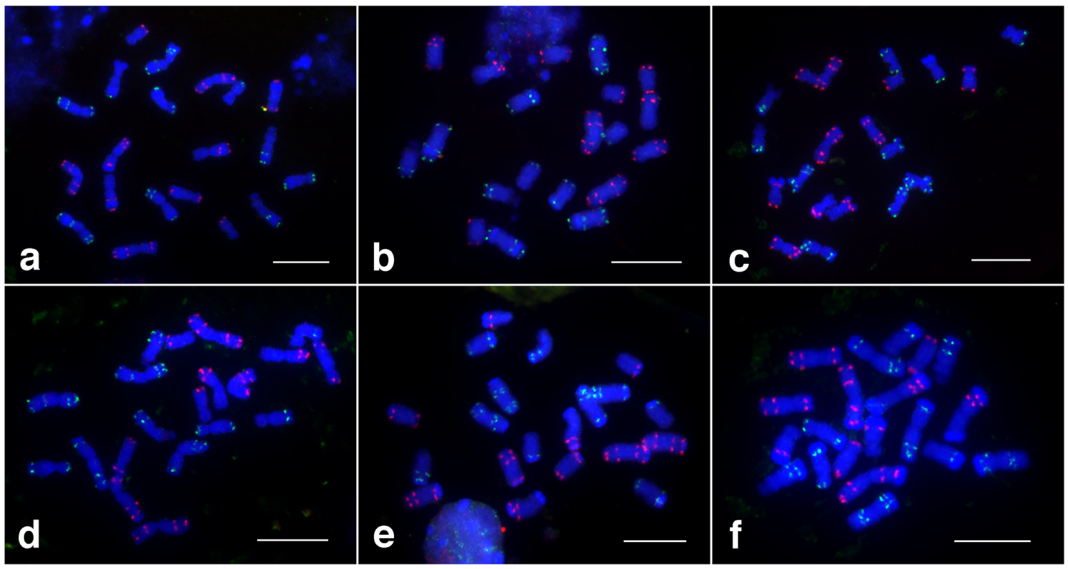

Fig. 2 FISH mapping of the two oligo-FISH probes on metaphase chromosomes prepared from **a** *Z. mays* ssp. *parviglumis*, **b** *Z. mays* ssp. *mexicana*, **c** *Z. mays* ssp. *huehuetenangensis*, **d** *Z. diploperennis*, **e** *Z. nicaraguensis*, and **f** *Z. luxurians*. Bars = 10 μm

difference observed on the same chromosome from different species (Fig. 3). Although the polymorphism of knob distribution among different maize lines is well known (Adawy et al. 2004; Albert et al. 2010), distinct knob distribution patterns were observed in some species. For example, a knob was detected between the two red signals on the long arm of chromosome 5 in *Z. mays* ssp. *parviglumis*. By contrast, a knob was observed at the distal end of the long arm of chromosome 5 in *Z. nicaraguensis* and *Z. luxurians* (Fig. 3, yellow arrowheads). A similar difference of FISH signal position among species, caused by the presence of a terminal vs. subterminal knob, was observed on the distal regions of several other chromosomal arms, including the short arm of chromosome 2, and long arm of chromosomes 1, 2, 3, 6, 7, 8, and 9 (Fig. 3). Interestingly, most of the terminal knobs in *Z. nicaraguensis* and *Z. luxurians* were located distal to the FISH signals, suggesting a close structural similarity of these two species (Fig. 3).

In several cases, a major knob was observed only on one copy of a pair of homologous chromosomes. For example, the long arm of chromosome 3 contained two red signals (Fig. 1a). The two red signals were separated by a major knob in one copy of chromosome 3 in *Z. mays* ssp. *parviglumis*. This knob was not visible in the second copy of chromosome 3 (Fig. 3). The distance between the two red signals appeared to be significantly different on the two chromosomes due to the presence of this heterozygous knob. A similar heterozygous knob was observed on several other chromosomes among different species (Fig. 3, red arrowheads).

The size of a knob can also be visibly different on two homologous chromosomes. For example, a terminal knob was observed on the long arm of chromosome 10 in several species. The size of this knob appeared to be distinctly different on the two copies of chromosome 10 in *Z. nicaraguensis* (Fig. 3, white arrowheads). Both presence/absence and size polymorphism of major knobs can result in a significant difference of the size of the homologous chromosomes.

The karyotypes of different *Zea* species and subspecies

Unambiguous identification of all chromosomes in the same metaphase cells allowed us to develop karyotypes based on individually identified chromosomes from all *Zea* species and subspecies (Tables 1 and 2). Each karyotype was developed based on measurements of all chromosomes in 7–10 complete metaphase cells. Not surprisingly, all *Zea* species and subspecies shared a highly similar karyotype with similar relative length and arm ratio of all 10 chromosomes (Tables 1 and 2). Chromosomes 1, 4, 5, and 10 are morphologically conserved, and are metacentric (Chr. 1, 4, and 5) or submetacentric (Chr. 10) in all species (Table 2). The other chromosomes are also similar but with minor variations

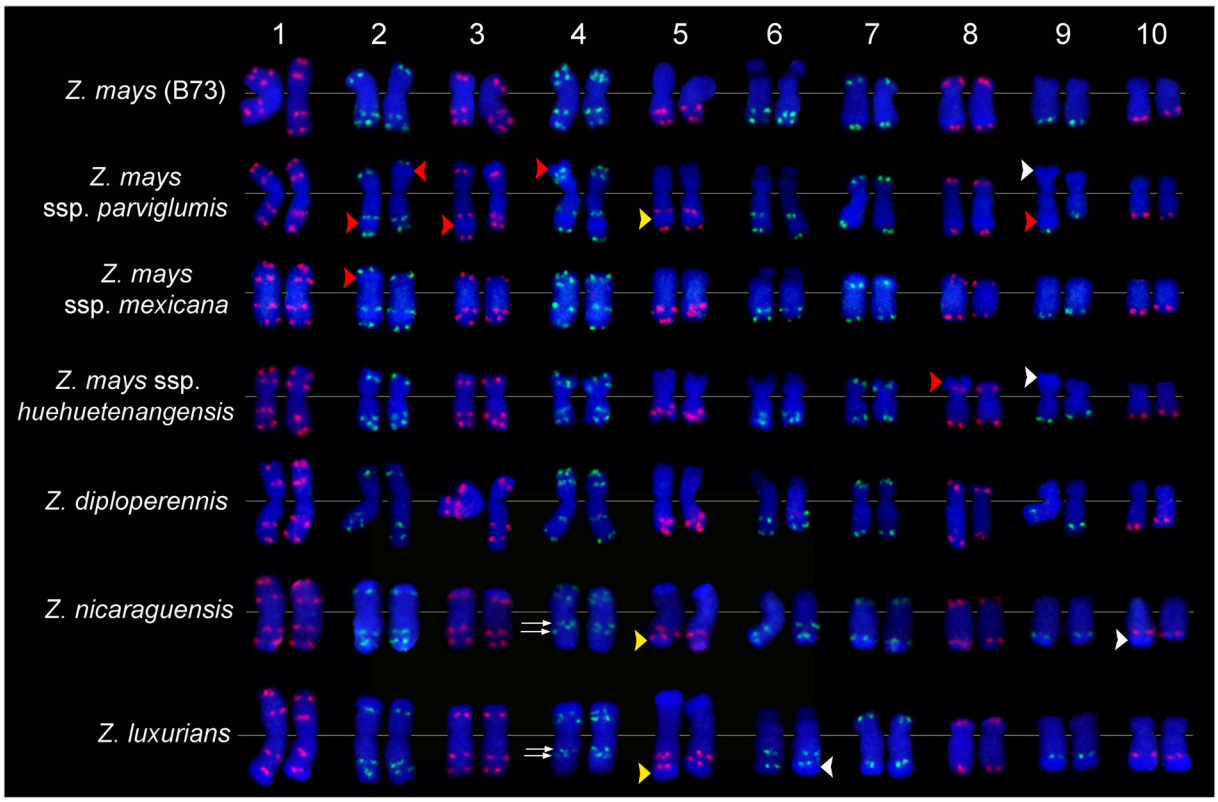

Fig. 3 Comparative karyotyping of seven *Zea* species and subspecies. Chromosomes 1–10 from each species/subspecies are arranged from left to right. The karyotypes were developed from the same metaphase cells in Fig. 1b for maize and Fig. 2 for other species/subspecies. Double arrows point to the two green signals on the long arm of chromosome 4 of *Z. nicaraguensis* and *Z. luxurians*. Both signals are located in the interstitial regions. Yellow arrowheads point to a knob on the long arm of chromosome 5, which is located in the subterminal region in *Z. mays* ssp. *parviglumis*, but at the distal end in *Z. nicaraguensis* and *Z. luxurians*. Red arrowheads point to knobs observed only on one of the two homologous chromosomes. White arrowheads point to knobs that show visibly different sizes on homologous chromosomes

among different species. Chromosomes 2 and 3 are metacentric in all species, except in *Zea mays* ssp. *mexicana* (submetacentric). Chromosome 7 is submetacentric in all species, except *Z. mays* ssp. *mexicana* (metacentric). Chromosome 8 is submetacentric in all the species, except in *Z. mays* ssp. *huehuetenangensis* (metacentric). Chromosome 9 is submetacentric in all the species, except *Z. mays* ssp. *parviglumis* and *Z. mays* ssp. *huehuetenangensis* (metacentric). Chromosome 6 is the only satellite chromosomes in all species.

Application of the oligo probes in distantly related species

We explored the potential of the barcode probes for chromosome identification in species that are more distantly related to maize. We first tested the two maize probes in hybridization to metaphase chromosomes prepared from *Tripsacum dactyloides* ($2n = 2x = 36$), a species from a sister genus related to *Zea* and diverged from maize about 4.5 million years (MYs) (Hilton and Gaut 1998). The two oligo-FISH probes produced punctuated signals on most of chromosomes, which allowed to identify few putative homoeologous chromosomes (Fig. 5a). However, most of the signals were not as strong as those on maize chromosomes. In addition, strong background signals were observed on most chromosomes. Several *T. dactyloides* chromosomes lacked unambiguous signals (Fig. 5a). Thus, the maize oligo probes were not useful to identify individual *T. dactyloides* chromosomes.

Sorghum (*Sorghum bicolor*) and maize diverged for about 12 MYs (Swigonova et al. 2004). The two maize probes produced background signals on all sorghum chromosomes (Fig. 5b). Only few of the 10 sorghum chromosomes generated consistent and distinct FISH

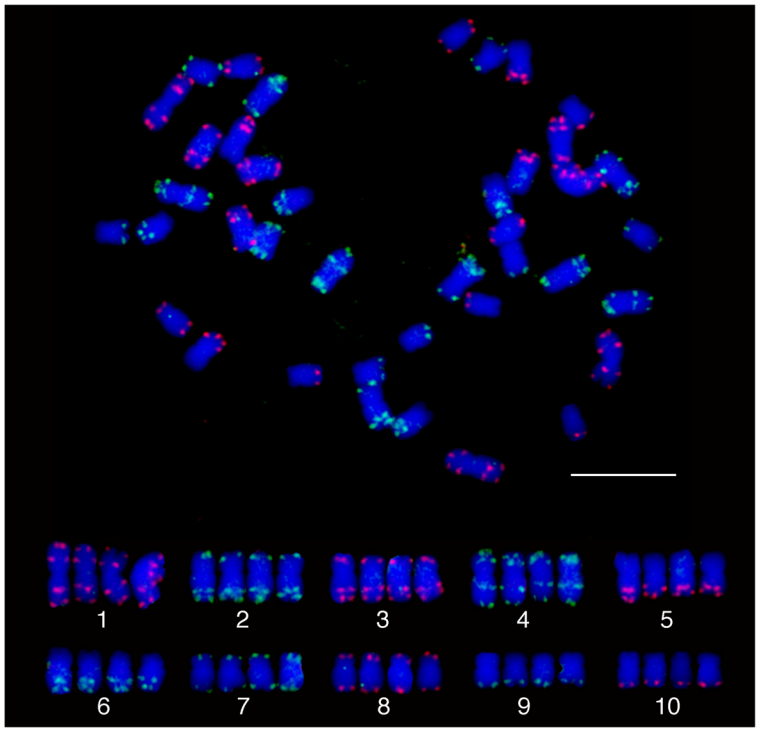

Fig. 4 Chromosome identification in a tetraploid species *Z. perennis*. The top panel shows a complete metaphase cell hybridized with the two oligo-FISH probes. The bottom panel shows the 4 homologous chromosomes of each of the 10 *Z. perennis* chromosomes digitally excised from the same cell. Bar = 10 μm

signal patterns. Thus, the maize probes were not useful to identify individual sorghum chromosomes.

Discussion

FISH has become the most popular methodology for chromosome identification in plants (Jiang and Gill 2006). Different FISH methodologies have different advantages and drawbacks. BACs and repetitive DNA sequences are the two most common types of FISH probes used in chromosome identification. Unfortunately, BACs are not ideal probes for plant species with large genomes because of the presence of large percentages of repetitive DNA sequences in the clones (Janda et al. 2006; Zhang et al. 2004). Repeat-based chromosome identification systems have been established in several plant species (Findley et al. 2010; Fradkin et al. 2013;

Table 1 Relative length of individual chromosomes of maize and its wild relatives

Chr.	*Z. mays*	*Z. mays* ssp. *parviglumis*	*Z. mays* ssp. *mexicana*	*Z. mays* ssp. *huehuetenangensis*	*Z. nicaraguensis*	*Z. luxurians*
1	14.26 ± 1.22	12.56 ± 0.41	13.26 ± 0.50	13.66 ± 0.50	13.16 ± 0.62	13.41 ± 0.76
2	11.19 ± 0.28	11.56 ± 0.30	12.89 ± 0.68	12.11 ± 0.72	12.26 ± 0.94	11.75 ± 0.61
3	10.76 ± 0.54	11.49 ± 0.38	10.23 ± 0.49	11.22 ± 0.32	10.66 ± 0.46	10.41 ± 0.45
4	11.28 ± 0.53	12.10 ± 0.39	12.12 ± 0.41	11.04 ± 0.55	11.14 ± 0.52	11.14 ± 0.63
5	10.36 ± 0.22	10.67 ± 0.36	10.34 ± 0.55	10.65 ± 0.43	11.46 ± 0.42	12.25 ± 0.56
6	8.51 ± 0.34	9.04 ± 0.42	8.06 ± 0.48	10.03 ± 0.18	8.10 ± 0.57	8.58 ± 0.74
7	9.44 ± 0.50	8.90 ± 0.42	9.40 ± 0.46	10.44 ± 1.13	9.21 ± 0.27	8.49 ± 0.32
8	9.18 ± 0.33	8.87 ± 0.37	8.79 ± 0.42	10.26 ± 1.05	8.69 ± 0.42	7.89 ± 0.50
9	8.03 ± 0.36	8.56 ± 0.61	8.00 ± 0.31	9.94 ± 0.96	7.78 ± 0.41	8.19 ± 0.40
10	6.99 ± 0.46	6.29 ± 0.33	6.91 ± 0.37	8.49 ± 1.28	7.53 ± 0.66	7.90 ± 0.30

Each chromosomal arm was measured in 10 metaphase cells of maize and its wild relatives, except for *Z. mays* ssp. *parviglumis* with only 7 metaphase cells

Table 2 Arm ratio of individual chromosomes of maize and its wild relatives

Chr.	*Z. mays*	*Z. mays* ssp. *parviglumis*	*Z. mays* ssp. *mexicana*	*Z. mays* ssp. *huehuetenangensis*	*Z. nicaraguensis*	*Z. luxurians*
1	1.26 ± 0.14 m	1.22 ± 0.16 m	1.25 ± 0.11 m	1.26 ± 0.27 m	1.11 ± 0.12 m	1.16 ± 0.12 m
2	1.52 ± 0.18 m	1.49 ± 0.36 m	1.83 ± 0.32 sm	1.43 ± 0.21 m	1.38 ± 0.23 m	1.27 ± 0.17 m
3	1.65 ± 0.28 m	1.61 ± 0.27 m	1.89 ± 0.34 sm	1.53 ± 0.19 m	1.44 ± 0.18 m	1.59 ± 0.19 m
4	1.34 ± 0.17 m	1.51 ± 0.32 m	1.60 ± 0.30 m	1.26 ± 0.17 m	1.55 ± 0.21 m	1.23 ± 0.17 m
5	1.54 ± 0.45 m	1.59 ± 0.25 m	1.68 ± 0.32 m	1.31 ± 0.35 m	1.34 ± 0.27 m	1.16 ± 0.16 m
6	2.40 ± 0.46 sm	3.31 ± 0.90 a	2.74 ± 0.63 sm	2.39 ± 0.39 sm	3.32 ± 1.06 a	3.56 ± 0.60 a
7	2.11 ± 0.46 sm	2.53 ± 0.58 sm	1.51 ± 0.37 m	1.86 ± 0.22 sm	2.58 ± 0.65 sm	2.39 ± 0.35 sm
8	2.13 ± 0.48 sm	2.78 ± 0.75 sm	1.97 ± 0.47 sm	1.69 ± 0.33 m	1.99 ± 0.48 sm	2.29 ± 0.32 sm
9	1.80 ± 0.34 sm	1.58 ± 0.29 m	1.88 ± 0.35 sm	1.41 ± 0.34 m	2.77 ± 0.58 sm	2.89 ± 0.63 sm
10	1.78 ± 0.40 sm	1.99 ± 0.20 sm	1.83 ± 0.37 sm	1.99 ± 0.36 sm	2.53 ± 0.38 sm	2.81 ± 0.39 sm

Each chromosomal arm was measured in 10 metaphase cells of maize and its wild relatives, except for *Z. mays* ssp. *parviglumis* with only 7 metaphase cells

m metacentric, *sm* submetacentric, *a* acrocentric

Kato et al. 2004; Lengerova et al. 2004; Li et al. 2014; Mukai et al. 1993; Xiong and Pires 2011). Repeat-based systems reveal polymorphisms for the constituent sequences but are not genotype independent. By contrast, single-gene karyotyping probes are genotype independent (Danilova and Birchler 2008; Danilova et al. 2014; Lamb et al. 2007a). Similarly, the FISH signal patterns derived from barcode probes are not polymorphic among different varieties in the same species. A modified pattern would indicate a potential chromosomal rearrangement associated with a cultivar. In addition, barcode probes can also be used for chromosome identification in genetically related species (Braz et al. 2018; Liu et al. 2020) (Fig. 2). Most importantly, barcode FISH probes can be developed readily in any plant species with a sequenced genome.

We have recently demonstrated that barcode FISH probes developed based on potato sequences were useful to identify individual homoeologous chromosomes from distantly related species, including tomato (*Solanum lycopersicum*), which diverged from potato for 5–8 MYs (Sarkinen et al. 2013; Wang et al. 2008). The potato barcode probes also generated punctuate signals but with a visible background on chromosomes from eggplant (*Solanum melongena*), which diverged from potato for 15.5 MYs (Wu and Tanksley 2010). A total of 54,672 oligos were used in the two potato barcode probes, including 16,489 oligos (30%) designed from coding sequences of potato genes. In contrast, among the 50,082 maize oligos, only 5525 oligos (11%) are associated with coding sequences. This may explain the fact that the maize barcode probes generate strong background signals on chromosomes of *T. dactyloides*, which diverged from maize for only 4.5 MYs (Hilton and Gaut 1998). Therefore, the percentage of oligos designed from highly conserved DNA sequences is critical to extend the value of barcode FISH probes for chromosome identification in distantly related species.

One of the key factors for developing successful barcode probes is to restrict the oligos within a chromosomal region as narrow as possible. A bright FISH signal can be generated from 1000 to 2000 oligos. However, these oligos need to be distributed within a few Mb. Each of the 24 regions of our maize barcode spans 1.3–3.3 Mb of DNA sequences (Table S1). It can be challenging to identify 1000–2000 unique oligos within repetitive chromosomal regions, especially in plant species with very large and complex genomes. Thus, it may become necessary to develop as many oligos as possible within the small islands of genic or single copy sequences in largely repetitive regions. For example, oligos, or overlapping oligos, can be designed from both strands of the DNA sequences within the single copy sequences.

It is not surprising that all *Zea* species and subspecies share a highly conserved karyotype (Tables 1 and 2) since these species have diverged for only ~ 150,000 years (Ross-Ibarra et al. 2009). Phylogenetic studies based on microsatellite markers indicated that *Z. nicaraguensis* and *Z. luxurians* are closely related

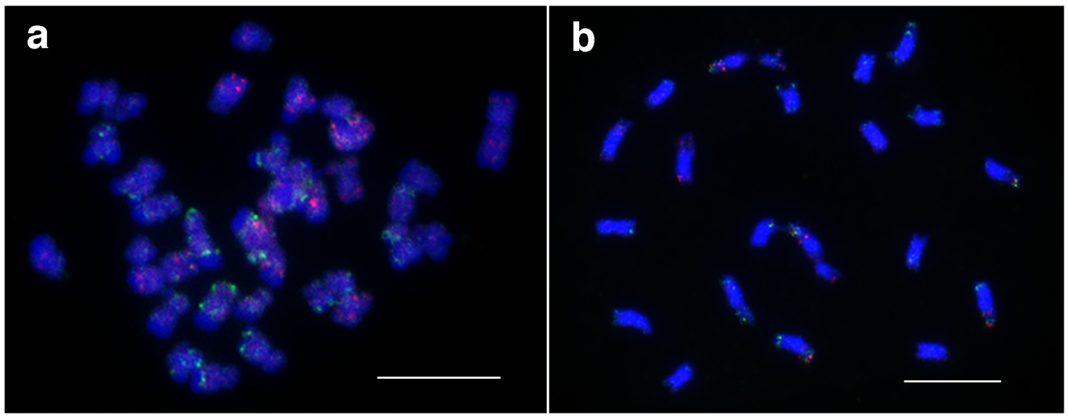

Fig. 5 FISH mapping of the two oligo-FISH probes on metaphase chromosomes prepared from **a** *Tripsacum dactyloides* ($2n = 2x = 36$); and **b** *Sorghum bicolor* ($2n = 2x = 20$). Bars = 10 μm

species and *Z. nicaraguensis* could be treated as a subspecies of *Z. luxurians* (Fukunaga et al. 2005). This conclusion was supported by our barcode FISH and karyotyping data. Terminal knobs, which are distal to the terminal FISH signals, were identified on several chromosome arms, including the long arms of chromosomes 2, 5, 6, 7, 9, and 10 in both *Z. nicaraguensis* and *Z. luxurians* (see also Albert et al. 2010). Interestingly, these terminal knobs were not observed at the same chromosomal positions in other species/subspecies (Fig. 3). In contrast, subterminal knobs, which are proximal to the terminal FISH signals, were observed on the long arms of chromosomes 2, 5, 6, 7, and 9 (Fig. 3) in several species/subspecies, but not in *Z. nicaraguensis* and *Z. luxurians*. Thus, *Z. nicaraguensis* and *Z. luxurians* share a highly similar knob distribution pattern.

A putative paracentric inversion was detected in the long arm of chromosome 4 in both *Z. nicaraguensis* and *Z. luxurians*. Poggio et al. (2005) developed hybrids between *Z. luxurians* and three subspecies of *Z. mays* (*Z. mays* ssp. *parviglumis*, *Z. mays* ssp. *mexicana*, *Z. mays* ssp. *mays*) and analyzed meiotic chromosome pairing in the hybrids. Interestingly, the most frequent chromosome pairing configuration at metaphase I of meiosis in those hybrids was eight bivalents and four univalents (Poggio et al. 2005), suggesting that major structural changes could be associated potentially with two *Z. luxurians* chromosomes relative to their homoeologous maize chromosomes. In addition, bridges and broken chromosome fragments were observed at anaphase I and II (Poggio et al. 2005), which are typical products associated with heterozygous paracentric inversions (Sybenga 1972). Genetic linkage mapping data showed that chromosome 4 from *Z. nicaraguensis* and *Z. luxurians* share the synteny, but they contain a large inversion relative to maize chromosome 4 (Mano and Omori 2013). These results support a paracentric inversion associated with the long arm of chromosome 4. It is likely that additional *Z. nicaraguensis*/*Z. luxurians* chromosomes are involved in major structural changes compared with others in the *Zea* lineage. An inversion was found on the long arm of chromosome 3 based on pachytene chromosome analysis (Fang et al. 2012; Ting 1965), although chromosome 3 shares an identical barcode FISH pattern across all *Zea* species and subspecies (Fig. 3). Indeed, because the barcode uses only a few well-spaced landmarks per chromosome, chromosomal aberrations, especially those restricted in regions proximal to the landmarks, will go undetected. Barcodes with more dense landmarks and in combination with whole chromosome paints (Albert et al. 2019) will be powerful tools to identify and characterize chromosomal rearrangements occurred during the evolution of *Zea* species.

Funding information This research is supported by NSF grant IOS-1444514 and MSU startup funds to J.J.

References

Adawy SSM, Stupar RM, Jiang J (2004) Fluorescence in situ hybridization of knob-associated DNA elements analysis reveals multiple loci in one-knob and knobless maize lines. J Histochem Cytochem 52:1113–1116

Albert PS, Gao Z, Danilova TV, Birchler JA (2010) Diversity of chromosomal karyotypes in maize and its relatives. Cytogenet Genome Res 129:6–16

Albert PS, Zhang T, Semrau K, Rouillard JM, Kao YH, Wang CJR, Danilova TV, Jiang JM, Birchler JA (2019) Whole-chromosome paints in maize reveal rearrangements, nuclear domains, and chromosomal relationships. Proc Natl Acad Sci U S A 116:1679–1685

Amarillo FIE, Bass HW (2007) A transgenomic cytogenetic sorghum (*Sorghum propinquum*) bacterial artificial chromosome fluorescence in situ hybridization map of maize (*Zea mays* L.) pachytene chromosome 9, evidence for regions of genome hyperexpansion. Genetics 177:1509–1526

Bi YF, Zhao QZ, Yan WK, Li MX, Liu YX, Cheng CY, Zhang L, Yu XQ, Li J, Qian CT, Wu YF, Chen JF, Lou QF (2020) Flexible chromosome painting based on multiplex PCR of oligonucleotides and its application for comparative chromosome analyses in *Cucumis*. Plant J. https://doi.org/10.1111/tpj.14600

Braz GT, He L, Zhao HN, Zhang T, Semrau K, Rouillard JM, Torres GA, Jiang JM (2018) Comparative Oligo-FISH mapping: an efficient and powerful methodology to reveal karyotypic and chromosomal evolution. Genetics 208:513–523

Bridges CB (1935) Salivary chromosome maps with a key to the banding of the chromosomes of *Drosophila melanogaster*. J Hered 26:60–64

Chen CC, Chen CM, Hsu FC, Wang CJ, Yang JT, Kao YY (2000) The pachytene chromosomes of maize as revealed by fluorescence in situ hybridization with repetitive DNA sequences. Theor Appl Genet 101:30–36

Cheng ZK, Buell CR, Wing RA, Jiang JM (2002) Resolution of fluorescence in-situ hybridization mapping on rice mitotic prometaphase chromosomes, meiotic pachytene chromosomes and extended DNA fibers. Chromosom Res 10:379–387

Danilova TV, Birchler JA (2008) Integrated cytogenetic map of mitotic metaphase chromosome 9 of maize: resolution, sensitivity, and banding paint development. Chromosoma 117:345–356

Danilova TV, Friebe B, Gill BS (2014) Development of a wheat single gene FISH map for analyzing homoeologous relationship and chromosomal rearrangements within the Triticeae. Theor Appl Genet 127:715–730

de Carvalho CR, Saraiva LS (1993) A new heterochromatin banding pattern revealed by modified HKG banding technique in maize chromosomes. Heredity 70:515–519

de Carvalho CR, Saraiva LS (1997) High-resolution HKG-banding in maize mitotic chromosomes. J Plant Res 110:417–420

Deaguiarperecin MLR, Vosa CG (1985) C-banding in maize II. Identification of somatic chromosomes. Heredity 54:37–42

Fang Z, Pyhajarvi T, Weber AL, Dawe RK, Glaubitz JC, Gonzalez JDS, Ross-Ibarra C, Doebley J, Morrell PL, Ross-Ibarra J (2012) Megabase-scale inversion polymorphism in the wild ancestor of maize. Genetics 191:883–U426

Figueroa DM, Bass HW (2012) Development of pachytene FISH maps for six maize chromosomes and their integration with other maize maps for insights into genome structure variation. Chromosom Res 20:363–380

Findley SD, Cannon S, Varala K, Du JC, Ma JX, Hudson ME, Birchler JA, Stacey G (2010) A fluorescence in situ hybridization system for karyotyping soybean. Genetics 185:727–744

Fradkin M, Ferrari MR, Espert SM, Ferreira V, Grassi E, Greizerstein EJ, Poggio L (2013) Differentiation of triticale cultivars through FISH karyotyping of their rye chromosomes. Genome 56:267–272

Fukunaga K, Hill J, Vigouroux Y, Matsuoka Y, Sanchez J, Liu KJ, Buckler ES, Doebley J (2005) Genetic diversity and population structure of teosinte. Genetics 169:2241–2254

Han YH, Zhang T, Thammapichai P, Weng YQ, Jiang JM (2015) Chromosome-specific painting in cucumis species using bulked oligonucleotides. Genetics 200:771–779

He L, Braz GT, Torres GA, Jiang JM (2018) Chromosome painting in meiosis reveals pairing of specific chromosomes in polyploid Solanum species. Chromosoma 127:505–513

Hilton H, Gaut BS (1998) Speciation and domestication in maize and its wild relatives: evidence from the globulin-1 gene. Genetics 150:863–872

Hou LL, Xu M, Zhang T, Xu ZH, Wang WY, Zhang JX, Yu MM, Ji W, Zhu CW, Gong ZY, Gu MH, Jiang JM, Yu HX (2018) Chromosome painting and its applications in cultivated and wild rice. BMC Plant Biol 18:110

Janda J, Safar J, Kubalakova M, Bartos J, Kovarova P, Suchankova P, Pateyron S, Cihalikova J, Sourdille P, Simkova H, Faivre-Rampant P, Hribova E, Bernard M, Lukaszewski A, Dolezel J, Chalhoub B (2006) Advanced resources for plant genomics: a BAC library specific for the short arm of wheat chromosome 1B. Plant J 47:977–986

Jewell DC, Islam-Faridi N (1994) A technique for somatic chromosome preparation and C-banding of maize. In: Freeling M, Walbot V (eds) The maize handbook. Springer-Verlag, New York, Inc, pp 484–493

Jiang JM (2019) Fluorescence in situ hybridization in plants: recent developments and future applications. Chromosom Res 27:153–165

Jiang JM, Gill BS (1994) Nonisotopic in situ hybridization and plant genome mapping: the first 10 years. Genome 37:717–725

Jiang JM, Gill BS (2006) Current status and the future of fluorescence in situ hybridization (FISH) in plant genome research. Genome 49:1057–1068

Kakeda K, Yamagata H, Fukui K, Ohno M, Fukui K, Wei ZZ, Zhu FS (1990) High resolution bands in maize chromosomes by G-banding methods. Theor Appl Genet 80:265–272

Kato A (1999) Air drying method using nitrous oxide for chromosome counting in maize. Biotech Histochem 74:160–166

Kato A, Lamb JC, Birchler JA (2004) Chromosome painting using repetitive DNA sequences as probes for somatic chromosome identification in maize. Proc Natl Acad Sci U S A 101:13554–13559

Kirov I, Khrustaleva L, Laere KV, Soloviev A, Sofie M, Romanov D, Fesenko I (2017) DRAWID: user-friendly java software for chromosome measurements and idiogram drawing. Comp Cytogenet 11:747–757

Koumbaris GL, Bass HW (2003) A new single-locus cytogenetic mapping system for maize (*Zea mays* L.): overcoming FISH detection limits with marker-selected sorghum (*S. propinquum* L.) BAC clones. Plant J 35:647–659

Lamb JC, Danilova T, Bauer MJ, Meyer JM, Holland JJ, Jensen MD, Birchler JA (2007a) Single-gene detection and karyotyping using small-target fluorescence in situ

hybridization on maize somatic chromosomes. Genetics 175: 1047–1058

Lamb JC, Meyer JM, Corcoran B, Kato A, Han FP, Birchler JA (2007b) Distinct chromosomal distributions of highly repetitive sequences in maize. Chromosom Res 15:33–49

Lengerova M, Kejnovsky E, Hobza R, Macas J, Grant SR, Vyskot B (2004) Multicolor FISH mapping of the dioecious model plant, *Silene latifolia*. Theor Appl Genet 108:1193–1199

Levan A, Fredga K, Sandberg AA (1964) Nomenclature for centromeric position on chromosomes. Hereditas-Genetisk A 52:201–220

Li H, Durbin R (2009) Fast and accurate short read alignment with burrows-wheeler transform. Bioinformatics 25:1754–1760

Li H, Wang CY, Fu SL, Guo X, Yang BJ, Chen CH, Zhang H, Wang YJ, Liu XL, Han FP, Ji WQ (2014) Development and discrimination of 12 double ditelosomics in tetraploid wheat cultivar DR147. Genome 57:89–95

Liu XY, Sun S, Wu Y, Zhou Y, Gu SW, Yu HX, Yi CD, Gu MH, Jiang JM, Liu B, Zhang T, Gong ZY (2020) Dual-color oligo-FISH can reveal chromosomal variations and evolution in Oryza species. Plant J 101:112–121

Mano Y, Omori F (2013) Flooding tolerance in interspecific introgression lines containing chromosome segments from teosinte (Zea nicaraguensis) in maize (Zea mays subsp mays). Ann Bot-London 112:1125–1139

Martins LD, Yu F, Zhao HN, Dennison T, Lauter N, Wang HY, Deng ZH, Thompson A, Semrau K, Rouillard JM, Birchler JA, Jiang JM (2019) Meiotic crossovers characterized by haplotype-specific chromosome painting in maize. Nat Commun 10:4604

McClintock B (1929) Chromosome morphology in *Zea mays*. Science 69:629–629

Meng Z, Zhang ZL, Yan TY, Lin QF, Wang Y, Huang WY, Huang YJ, Li ZJ, Yu QY, Wang JP, Wang K (2018) Comprehensively characterizing the cytological features of *Saccharum spontaneum* by the development of a complete set of chromosome-specific oligo probes. Front Plant Sci 9: 1624

Meng Z, Han J, Lin Y, Zhao Y, Lin Q, Ma X, Wang J, Zhang M, Zhang L, Yang Q, Wang K (2020) Characterization of a *Saccharum spontaneum* with a basic chromosome number of x = 10 provides new insights on genome evolution in genus Saccharum. Theor Appl Genet 133:187–199

Mukai Y, Nakahara Y, Yamamoto M (1993) Simultaneous discrimination of the three genomes in hexaploid wheat by multicolor fluorescence insitu hybridization using total genomic and highly repeated DNA probes. Genome 36:489–494

Poggio L, Gonzalez G, Confalonieri V, Comas C, Naranjo CA (2005) The genome organization and diversification of maize and its allied species revisited: evidences from classical and FISH-GISH cytogenetic analysis. Cytogenet Genome Res 109:259–267

Qu MM, Li KP, Han YL, Chen L, Li ZY, Han YH (2017) Integrated karyotyping of woodland strawberry (Fragaria vesca) with oligopaint FISH probes. Cytogenet Genome Res 153:158–164

Rayburn AL, Price HJ, Smith JD, Gold JR (1985) C-band heterochromatin and DNA content in *Zea mays*. Am J Bot 72: 1610–1617

Ross KJ, Fransz P, Jones GH (1996) A light microscopic atlas of meiosis in *Arabidopsis thaliana*. Chromosom Res 4:507–516

Ross-Ibarra J, Tenaillon M, Gaut BS (2009) Historical divergence and gene flow in the genus Zea. Genetics 181:1397–1409

Sadder MT, Weber G (2001) Karyotype of maize (*Zea mays* L.) mitotic metaphase chromosomes as revealed by fluorescence in situ hybridization (FISH) with cytogenetic DNA markers. Plant Mol Biol Rep 19:117–123

Sarkinen T, Bohs L, Olmstead RG, Knapp S (2013) A phylogenetic framework for evolutionary study of the nightshades (Solanaceae): a dated 1000-tip tree. BMC Evol Biol 13:214

Schnable PS, Ware D, Fulton RS, Stein JC, Wei FS, Pasternak S, Liang CZ, Zhang JW, Fulton L, Graves TA, Minx P, Reily AD, Courtney L, Kruchowski SS, Tomlinson C, Strong C, Delehaunty K, Fronick C, Courtney B, Rock SM, Belter E, du F, Kim K, Abbott RM, Cotton M, Levy A, Marchetto P, Ochoa K, Jackson SM, Gillam B, Chen W, Yan L, Higginbotham J, Cardenas M, Waligorski J, Applebaum E, Phelps L, Falcone J, Kanchi K, Thane T, Scimone A, Thane N, Henke J, Wang T, Ruppert J, Shah N, Rotter K, Hodges J, Ingenthron E, Cordes M, Kohlberg S, Sgro J, Delgado B, Mead K, Chinwalla A, Leonard S, Crouse K, Collura K, Kudrna D, Currie J, He R, Angelova A, Rajasekar S, Mueller T, Lomeli R, Scara G, Ko A, Delaney K, Wissotski M, Lopez G, Campos D, Braidotti M, Ashley E, Golser W, Kim H, Lee S, Lin J, Dujmic Z, Kim W, Talag J, Zuccolo A, Fan C, Sebastian A, Kramer M, Spiegel L, Nascimento L, Zutavern T, Miller B, Ambroise C, Muller S, Spooner W, Narechania A, Ren L, Wei S, Kumari S, Faga B, Levy MJ, McMahan L, van Buren P, Vaughn MW, Ying K, Yeh CT, Emrich SJ, Jia Y, Kalyanaraman A, Hsia AP, Barbazuk WB, Baucom RS, Brutnell TP, Carpita NC, Chaparro C, Chia JM, Deragon JM, Estill JC, Fu Y, Jeddeloh JA, Han Y, Lee H, Li P, Lisch DR, Liu S, Liu Z, Nagel DH, McCann M, SanMiguel P, Myers AM, Nettleton D, Nguyen J, Penning BW, Ponnala L, Schneider KL, Schwartz DC, Sharma A, Soderlund C, Springer NM, Sun Q, Wang H, Waterman M, Westerman R, Wolfgruber TK, Yang L, Yu Y, Zhang L, Zhou S, Zhu Q, Bennetzen JL, Dawe RK, Jiang J, Jiang N, Presting GG, Wessler SR, Aluru S, Martienssen RA, Clifton SW, McCombie W, Wing RA, Wilson RK (2009) The B73 maize genome: complexity, diversity, and dynamics. Science 326: 1112–1115

Simonikova D, Nemeckova A, Karafiatova M, Uwimana B, Swennen R, Dolezel J, Hribova E (2019) Chromosome painting facilitates anchoring reference genome sequence to chromosomes in situ and integrated karyotyping in Banana (Musa Spp.). Front Plant Sci 10:1503

Song XY, Song RR, Zhou JW, Yan WK, Zhang T, Sun HJ, Xiao J, Wu YF, Xi ML, Lou QF, Wang HY, Wang X (2020) Development and application of oligonucleotide-based chromosome painting for chromosome 4D of Triticum aestivum L. Chromosome Res. https://doi.org/10.1007/s10577-10020-09627-10570

Swigonova Z, Lai JS, Ma JX, Ramakrishna W, Llaca V, Bennetzen JL, Messing J (2004) Close split of sorghum and maize genome progenitors. Genome Res 14:1916–1923

Sybenga J (1972) General Cytogenetics. American Elsevier Publishing Co., INC, New York

Ting YC (1965) Spontaneous chromosome inversions of Guatemalan teosintes (*Zea mexicana*). Genetica 36:229–242

Wang CJR, Harper L, Cande WZ (2006) High-resolution single-copy gene fluorescence in situ hybridization and its use in the

construction of a cytogenetic map of maize chromosome 9. Plant Cell 18:529–544

Wang Y, Diehl A, Wu FN, Vrebalov J, Giovannoni J, Siepel A, Tanksley SD (2008) Sequencing and comparative analysis of a conserved syntenic segment in the solanaceae. Genetics 180:391–408

Ward EJ (1980) Banding patterns in maize mitotic chromosomes. Can J Genet Cytol 22:61–67

Wu FN, Tanksley SD (2010) Chromosomal evolution in the plant family Solanaceae. BMC Genomics 11:182

Xin HY, Zhang T, Han YH, Wu YF, Shi JS, Xi ML, Jiang JM (2018) Chromosome painting and comparative physical mapping of the sex chromosomes in *Populus tomentosa* and *Populus deltoides*. Chromosoma 127:313–321

Xin HY, Zhang T, Wu YF, Zhang WL, Zhang PD, Xi ML, Jiang JM (2020) An extraordinarily stable karyotype of the woody Populus species revealed by chromosome painting. Plant J 101:253–264

Xiong ZY, Pires JC (2011) Karyotype and identification of all homoeologous chromosomes of allopolyploid Brassica napus and its diploid progenitors. Genetics 187:37–49

Zhang P, Li WL, Fellers J, Friebe B, Gill BS (2004) BAC-FISH in wheat identifies chromosome landmarks consisting of different types of transposable elements. Chromosoma 112:288–299

Zhao HN, Zhu XB, Wang K, Gent JI, Zhang WL, Dawe RK, Jiang JM (2016) Gene expression and chromatin modifications associated with maize centromeres. G3-Genes Genom Genet 6:183–192

APÊNDICE D – CAPÍTULO PUBLICADO NO LIVRO METHODS IN MOLECULAR BIOLOGY

Chapter 4

Fluorescent In Situ Hybridization Using Oligonucleotide-Based Probes

Guilherme T. Braz, Fan Yu, Lívia do Vale Martins, and Jiming Jiang

Abstract

Efficient and consistent chromosome identification is the foundation for successful cytogenetic studies. Fluorescent in situ hybridization (FISH) has been the most popular technique for chromosome identification in plants. Large insert genomic DNA clones, such as bacterial artificial chromosome (BAC) clones, and repetitive DNA sequences have been the most commonly used DNA probes for FISH. However, most of such traditional probes can only be used to identify a single chromosome or are too polymorphic to consistently identify the same chromosome in the target species. In contrast, FISH using oligonucleotide (oligo)-based probes is highly versatile. In this procedure, a large number of oligos specific to a chromosomal region, to an entire chromosome, or to multiple chromosomes are computationally identified, synthesized in parallel, and labeled as probes. In addition, each oligo probe can be used for thousands of FISH experiments and represents an infinite resource. In this chapter we describe a detailed protocol for amplification and labeling of oligo-based probes, relevant chromosome preparation, and FISH procedures.

Key words Chromosome identification, Chromosome painting, FISH, Oligo-FISH, Oligonucleotide probes

1 Introduction

Chromosome identification is the fundamental attribute for the success of cytogenetics studies [1]. Barbara McClintock used a combination of chromosomal features such as centromeric position, secondary constriction, and heterochromatic knobs to identify individual maize chromosomes [2]. For many years plant cytogeneticists used a similar approach for chromosome identification. Although a number of new techniques, such as chromosome banding, were developed over the years, most of these techniques were used only in few plant species. The advent of fluorescent in situ hybridization (FISH) has made chromosome identification possible in most plant species [1]. Different types of DNA sequences, including BAC clones [3, 4], repetitive DNA elements [5, 6], and single-copy genes [7, 8], have been used as FISH probes.

Boye Schnack Nielsen and Julia Jones (eds.), *In Situ Hybridization Protocols*, Methods in Molecular Biology, vol. 2148, https://doi.org/10.1007/978-1-0716-0623-0_4,

Unfortunately, development of these probes is often labor intensive and time consuming. FISH-based chromosome identification systems have not been developed in most plant species, especially in non-model species with limited genomic resources.

Recently, bulked synthetic oligonucleotides (oligos) were used as probes for FISH [9, 10]. Oligos specific to a chromosomal region or to an entire chromosome are computationally identified, synthesized as a pool, and then labeled for FISH [11]. Oligo probe design is highly versatile. Oligos from multiple chromosomes or from multiple regions of the same chromosome can be included in the same probe [12]. These probes have been developed in an increased number of plant species [10, 12–17]. Oligo-FISH is expected to become a cornerstone methodology in chromosome identification and cytogenetics studies in plants [11].

The oligo-based FISH technique can be divided into three main steps: (1) probe design and synthesis, (2) probe amplification and labeling, and (3) FISH. Oligo probes can be designed using Chorus2 software (https://github.com/zhangtaolab/Chorus2). Briefly, the pseudomolecule of a target chromosome or the entire reference genome of a target species is computationally divided into 45 nt oligos. Single-copy oligos with dTm > 10 °C are selected for probe design. All selected oligos are synthesized as a pool [10], typically in 300 ng of DNA, which can be amplified and labeled for a million FISH experiments [10]. Two steps are used for amplification: (1) MYcroarray Debubbling PCR and (2) in vitro transcription. A reverse transcription reaction is then used for probe labeling.

In this chapter we provide a detailed protocol for amplification and labeling process of oligo-based FISH probes adapted from Murgha et al. [18] and Han et al. [10]. We also describe a chromosome preparation and FISH procedures adapted for oligo-FISH.

2 Materials

Prepare all solutions using ultrapure water.

2.1 MYtags Immortal Oligonucleotide Library

1. MYtags immortal oligonucleotide library (approximately 300 ng of library, lyophilizate) is synthesized and shipped by Arbor Biosciences™ company, formerly MYcroarray®. As soon as it is received, resuspend the oligo library in nuclease-free water or 10 mM Tris–HCl pH 7.5 at 1 ng/μL as a stock solution and store at −80 °C.
2. Prepare the MYtags immortal oligonucleotide library working solution by adding 2 μL of stock solution in 26 μL of nuclease-free water and store at −20 °C.

3. Arbor Biosciences also provides the MYtags PCR Primer mix used in the MYcroarray Debubbling PCR reaction, which must be stored at −20 °C.

2.2 MYcroarray Debubbling PCR

1. KAPA HiFi HotStart ReadyMix (KAPA Biosystems).
2. Qiagen Qiaquick PCR purification Kit (Qiagen).
3. Sodium acetate solution (3 M), pH 5.2: Dissolve 246.1 g of sodium acetate in 500 mL of deionized water and adjust the pH to 5.2 with glacial acetic acid. Adjust the final volume to 1 L with ddH_2O and filter-sterilize.

2.3 In Vitro Transcription

1. MEGAshortscript™ T7 Kit (Invitrogen).
2. RNeasy Mini Kit (Qiagen).
3. 100% Ethanol.

2.4 Reverse Transcription

1. Order the universal dye-labeled primer as the provided sequence: 5′dye-CGTGGTCGCGTCTCA3′ (*see* **Note 1**). Resuspend at 1 mM.
2. 10 mM dNTP solution mix.
3. SUPERase• In™ RNase Inhibitor (20 U/μL) (Invitrogen).
4. SuperScript™ IV Reverse Transcriptase (200 U/μL) (Invitrogen).
5. Exonuclease I enzyme (20 U/μL) (New England Biolabs).
6. 0.5 M EDTA pH 8.0.
7. Quick-RNA MiniPrep Kit (Zymo Research).
8. 100% Ethanol.

2.5 Removal of RNA

1. RNase H (5 U/μL) (New England Biolabs).
2. RNase A (10 mg/mL) (Thermo Fisher Scientific).
3. Quick-RNA MiniPrep Kit (Zymo Research).
4. 100% Ethanol.

2.6 Chromosome Spread Preparation

1. Gas-pressure chamber [16], regulated at 160 psi (~10.9 atm).
2. Nitrous oxide (N_2O) gas.
3. Fine forceps and razor blade.
4. Microscope slides and cover slides.
5. Fixative solution: 3 volumes of 100% ethanol and 1 volume of glacial acetic acid.
6. Enzyme mix: 2% Pectolyase (Sigma Chemical), 4% cellulase (Yakult Pharmaceutical), and 2% pectinase (Plant Media). Store at −20 °C.
7. Moist box.

2.7 Fluorescent In Situ Hybridization (FISH)

1. Pepsin stock solution (1 mg/mL): 0.001 g of pepsin in 1 mL of ddH_2O. Aliquot and store at −20 °C.
2. HCl 0.01 N: 100 μL of HCl 1 N in 9.9 mL of ddH_2O. Store at room temperature (RT).
3. Pepsin working solution (10 μg/mL): 1 μL of pepsin stock solution in 99 μL of HCl 0.01 N. Use freshly prepared solution.
4. 20× Saline sodium citrate (SSC) buffer, pH 7.0: 175.3 g of NaCl, 88.2 g of sodium citrate in 1 L of ddH_2O. Store at RT.
5. 4× SSC buffer: 100 mL of 20× SSC, 500 μL of Tween-20, adjust to 500 mL of ddH_2O.
6. 2× SSC buffer: 100 mL of 20× SSC in 900 mL of ddH_2O.
7. 0.1× SSC buffer: 500 μL of 20× SSC in 100 mL of ddH_2O.
8. 10× Phosphate-buffered saline (PBS) buffer, pH 7.4: 80 g of NaCl, 2 g of KCl, 14.4 g of Na_2HPO_4, 2.4 g of KH_2PO_4 in 1 L of ddH_2O. Store at RT.
9. 1× PBS buffer: 100 mL of 10× PBS in 900 mL of ddH_2O.
10. 4% Paraformaldehyde: 4 g of paraformaldehyde, 100 mL of 1× PBS (60 °C), 1 mL of 1 N NaOH. Aliquot and store at 4 °C.
11. 70% Ethanol.
12. 90% Ethanol.
13. 100% Ethanol.
14. 100% Deionized formamide.
15. 70% Formamide: 2 mL of ddH_20, 7 mL of 100% deionized formamide, and 1 mL of 20× SSC. Keep wrapped in aluminum foil and store at 4 °C.
16. 50% Dextran sulfate: 2.5 g of dextran sulfate in 5 mL of ddH_2O. Aliquot and store at −20 °C. One aliquot may be stored at 4 °C for use. Cut the end of the pipet tip and pipette slowly as this solution is quite viscous.
17. Rubber cement.
18. Iron sheet.
19. 5× TNB buffer: 5 mL of 1 M Tris (pH 7.5), 2.5 mL of 3 M NaCl, 0.25 g of blocking reagent. Adjust to 10 mL. Heating the solution to 50 °C will significantly decrease the time to dissolve the blocking reagent. Store at −20 °C.
20. 1× TNB buffer: 1 mL of 5× TNB buffer in 4 mL of ddH_2O. Store at 4 °C. Vortex before use.
21. Anti-biotin antibody, conjugated to fluorescein (1 μg/mL).

22. Anti-digoxigenin antibody, conjugated to rhodamine (200 μg/mL).
23. Antifade mounting media with 4′,6-diamidino-2-phenylindole (DAPI).

3 Methods

3.1 MYcroarray Debubbling PCR: First Step of Amplification

1. Prepare the template master mix (on ice): Mix 24.75 μL of nuclease-free water, 0.25 μL of MYtags PCR primer mix, and 25 μL of KAPA HiFi HotStart ReadyMix. Vortex for 5 s and spin down for 5 s.
2. Transfer 5 μL of the template master mix to a separate 0.2 mL tube as a negative control.
3. Add 2.5 μL of MYtags immortal oligonucleotide library working solution to the template master mix. Vortex for 5 s and spin down for 5 s.
4. Incubate the PCR mix and the negative control in a thermocycler under the following cycling conditions: 95 °C/3 min + 4 cycles (98 °C/20 s, 54 °C/15 s, and 72 °C/30 s) + 14 cycles (98 °C/20 s, 56 °C/15 s + 72 °C/30 s), keep at 24 °C until the next step.
5. In a separate tube, prepare the Debubbling mix (on ice): Mix 8.8 μL of nuclease-free water, 1.2 μL of MYtags PCR primer mix, and 10 μL of KAPA HiFi HotStart ReadyMix. Vortex for 5 s and spin down for 5 s.
6. Add the Debubbling mix to the PCR mix.
7. Incubate the reaction in a thermocycler under the following cycling conditions: 95 °C/3 min + 1 cycle (98 °C/20 s, 56 °C/15 s, and 72 °C/30 s), keep at 24 °C until the PCR purification step.

3.1.1 PCR Purification

We use the Qiagen QIAquick PCR purification Kit, following the manufacturer's instructions.

1. Add 32.5 μL of nuclease-free water to bring the PCR product to 100 μL.
2. Add 5 μL of 3 M sodium acetate solution.
3. Add 500 μL of Qiagen Buffer PB to the PCR product and vortex for 5 s.
4. Apply the entire sample to the QIAquick column in a 2 mL collection tube (supplied). Centrifuge for 1 min at 16,000 × *g* (RCF). Discard flow-through and place the QIAquick column back into the same collection tube.

5. Add 700 μL of Qiagen Buffer PE to the QIAquick column. Centrifuge for 1 min at 16,000 × *g* (RCF). Discard flow-through and place the QIAquick column back into the same collection tube.
6. Centrifuge the QIAquick column for an additional 2 min at 16,000 × *g* (RCF).
7. Place the QIAquick column in a clean 1.5 mL tube.
8. For DNA elution, add 30 μL of Qiagen Buffer EB to the center of the QIAquick column membrane. Let the column stand for 4 min. Centrifuge for 1 min at 16,000 × *g* (RCF).
9. Quantify the DNA product (ng/μL) with spectrophotometer or 2.5% agarose gel (*see* **Note 2**). Store the DNA at −20 °C.

3.2 In Vitro Transcription: Second Step of Amplification

We use the MEGAshortscript™ T7 Kit, following the manufacturer's instructions.

1. Prepare the in vitro transcription mix (on ice): Mix X μL of DNA (480 ng), 4 μL of 10× T7 reaction buffer, 16 μL of the rNTP pool (includes ATP, CTP, GTP, and UTP solution), and 4 μL of T7 enzyme mix, and complete up to 40 μL of nuclease-free water. Vortex for 10 s and spin down for 10 s.
2. Incubate the reaction in a thermocycler for 4 h at 37 °C (hot lid: 42 °C).

3.2.1 RNA Purification

We use the Qiagen RNeasy Mini Kit, following the manufacturer's instructions.

1. Put the in vitro transcription reaction product directly on ice, transfer to a 1.5 mL tube, add 260 μL of RNase-free water, and mix by pipetting. Proceed with RNeasy purification.
2. Add 350 μL of Qiagen Buffer RLT and vortex for 5 s.
3. Add 250 μL of 100% ethanol and vortex for 5 s.
4. Apply 650 μL of the sample to the RNeasy mini spin column in a 2 mL collection tube (supplied). Centrifuge for 1 min at 13,500 × *g* (RCF). Discard the flow-through and place the RNeasy mini spin column back into the same collection tube. Repeat this step once such that the entire sample has been loaded into the column.
5. Add 500 μL of Qiagen Buffer RPE to the RNeasy mini spin column. Centrifuge for 1 min at 13,500 × *g* (RCF). Discard the flow-through and place the RNeasy mini spin column back into the same collection tube.
6. Repeat the previous step once.
7. Centrifuge the RNeasy mini spin column for an additional 3 min at 13,500 × *g* (RCF).
8. Place the RNeasy mini spin column in a clean 1.5 mL tube.

9. For RNA elution, add 50 µL of RNase-free water to the center of the RNeasy mini spin column membrane. Let the column stand for 4 min and centrifuge for 1 min at 13,500 × *g* (RCF).
10. Quantify the RNA product (ng/µL) with spectrophotometer (*see* **Note 3**). Store the RNA at −80 °C.

3.3 Reverse Transcription: Labeling Step

1. Prepare the reverse transcription mix (on ice): Mix X µL of RNA (42 µg), 2.4 µL of 1 mM (1 nmol/µL) dye-labeled RT primer, 15 µL of 10 mM dNTP, and 1 µL of 20 U/µL SUPERase-In, and complete up to 60 µL of nuclease-free water. Vortex for 5 s and spin down for 5 s.
2. Incubate the reaction in a thermocycler for 5 min at 65 °C (hot lid: 75 °C). Leave on ice for 5 min.
3. In a separate 0.2 mL tube, mix (on ice) 4 µL of nuclease-free water, 20 µL of 5× RT buffer, 10 µL of 0.1 M DTT, and 1 µL of 20 U/µL SUPERase-In. Add the mixture to the reverse transcription mix. Vortex for 5 s and spin down for 5 s.
4. Incubate the reaction for 5 min at 55 °C (hot lid: 55 °C). Do not place the reaction on ice.
5. Add 2.5 µL of 200 U/µL SuperScript IV Reverse Transcriptase. Vortex for 5 s and spin down for 5 s.
6. Incubate the reaction for 1 h at 55 °C (hot lid: 55 °C). Do not place the reaction on ice.
7. To remove unincorporated primers add 11 µL of exonuclease I buffer and 2 µL of exonuclease I enzyme. Vortex for 5 s and spin down for 5 s.
8. Incubate the reaction for 15 min at 37 °C (hot lid: 105 °C). Do not place the reaction on ice.
9. Add 12 µL of 0.5 M EDTA pH 8.0. Vortex for 5 s and spin down for 5 s.
10. Incubate the reaction directly in the thermocycler for 20 min at 80 °C (hot lid: 105 °C) (no temperature ramp-up). Transfer the tube directly on ice.

3.3.1 RNA:DNA Hybrid Purification

We use the Zymo Quick-RNA MiniPrep Kit, following the manufacturer's instructions.

1. Add 500 µL of Zymo RNA lysis buffer. Vortex for 5 s.
2. Add 625 µL of 100% ethanol. Vortex for 5 s.
3. Apply 500 µL of the sample to the Zymo-Spin column in a 2 mL collection tube (supplied). Centrifuge for 30 s at 16,000 × *g* (RCF). Discard the flow-through and place the Zymo-Spin column back into the same collection tube. Repeat this step once such that the entire sample has been loaded into the column.

4. Add 400 μL of Zymo RNA Prep Buffer to the Zymo-Spin column. Centrifuge for 30 s at 16,000 × *g* (RCF). Discard the flow-through and place the Zymo-Spin column back into the same collection tube.
5. Add 700 μL of Zymo RNA wash buffer to the Zymo-Spin column. Centrifuge for 30 s at 16,000 × *g* (RCF). Discard the flow-through and place the Zymo-Spin column back into the same collection tube.
6. Add 400 μL of Zymo RNA wash buffer to the Zymo-Spin column. Centrifuge for 30 s at 16,000 × *g* (RCF). Discard the flow-through and place the Zymo-Spin column back into the same collection tube.
7. Centrifuge the Zymo-Spin column for an additional 3 min at 16,000 × *g* (RCF).
8. Place the Zymo-Spin column in a clean 1.5 mL tube.
9. For reverse transcription product elution, add 42 μL of nuclease-free water to the center of the Zymo-Spin column membrane. Let the column stand for 4 min. Centrifuge for 1 min at 16,000 × *g* (RCF). Repeat the previous step by adding 42 μL of nuclease-free water to the center of the same Zymo-Spin column membrane. Let the column stand for 4 min. Centrifuge for 1 min at 16,000 × *g* (RCF) (*see* **Note 4**). Store the reverse transcription product at −80 °C until the next step.

3.4 Removal of RNA

1. Prepare the enzymatic RNA removal mix (on ice): Mix 6 μL of nuclease-free water, 10 μL of 10× RNase H buffer, and 4 μL of RNase H (5 U/μL).
2. Add the RNA removal mix to the purified reverse transcription product. Vortex gently for 5 s and spin down for 5 s.
3. Incubate the reaction in a thermocycler for 2 h at 37 °C (hot lid: 105 °C). Do not place the reaction on ice.
4. Add 4 μL of RNase A (10 mg/mL). Vortex gently for 5 s and spin down for 5 s.
5. Incubate the reaction in a thermocycler under the following cycling conditions: 60 min at 37 °C, 20 min at 70 °C, 60 min at 50 °C, 5 min at 95 °C (ramp down 95 °C to 50 °C–0.1 °C/s), and 60 min at 50 °C, and keep at 4 °C until the purification step.

3.4.1 Single-Strand DNA Probe Purification

We use the Zymo Quick-RNA MiniPrep Kit, following the manufacturer's instructions.

1. Add 400 μL of Zymo RNA lysis buffer. Vortex for 5 s.
2. Add 500 μL of 100% ethanol. Vortex for 5 s.

3. Apply 650 μL of the sample to the Zymo-Spin column in a 2 mL collection tube (supplied). Centrifuge for 30 s at 16,000 × *g* (RCF). Discard the flow-through and place the Zymo-Spin column back into the same collection tube. Repeat this step once such that the entire sample has been loaded into the column.
4. Add 400 μL of Zymo RNA prep buffer to the column. Centrifuge for 30 s at 16,000 × *g* (RCF). Discard the flow-through and place the Zymo-Spin column back into the same collection tube.
5. Add 700 μL of Zymo RNA wash buffer to the column. Centrifuge for 30 s at 16,000 × *g* (RCF). Discard the flow-through and place the Zymo-Spin column back into the same collection tube.
6. Add 400 μL of Zymo RNA wash buffer to the column. Centrifuge for 30 s at 16,000 × *g* (RCF). Discard the flow-through and place the Zymo-Spin column back into the same collection tube.
7. Centrifuge the Zymo-Spin column for an additional 3 min at 16,000 × *g* (RCF).
8. Place the Zymo-Spin column in a clean 1.5 mL tube.
9. For ssDNA probe elution, add 50 μL of warm (65 °C) nuclease-free water to the center of the Zymo-Spin column membrane. Let the column stand for 4 min. Centrifuge for 1 min at 16,000 × *g* (RCF). Repeat the previous step by adding 50 μL of warm (65 °C) to the center of the same Zymo-Spin column membrane. Let the column stand for 4 min. Centrifuge for 1 min at 16,000 × *g* (RCF).
10. Quantify the ssDNA probe (ng/μL) with spectrophotometer (*see* **Note 5**). Store the ssDNA probe at −20 °C.

3.5 Chromosome Spread Preparation

1. Harvest young root tips from healthy plants or directly from seeds germinated in a Petri dish and keep them in distilled water.
2. Transfer the root tips to a new 1.5 mL tube keeping them moist.
3. Place the root tips in the gas-pressure chamber and treat with N_2O at 160 psi (~10.9 atm) (*see* **Note 6**).
4. After treatment, place the root tips in fixative solution for 24 h at RT. Keep at −20 °C until next step.
5. Wash the roots 3× with distilled water, 5 min each time.
6. With razor blade or fine forceps, select the meristematic region.
7. Drain the excess of water.

8. Cover the meristematic tissue with the enzyme mix. Incubate for 1–3 h at 37 °C in a moist box (*see* **Note 7**).
9. Remove the enzymatic solution.
10. Wash the meristematic tissue 2× with distilled water, 5 min each time.
11. The slides can be prepared using different methodologies. We use air-dry [19], stirring [20, 21], and dropping [6] methods for mitotic and/or meiosis preparation, with minor modifications.
12. Select the best slides for FISH using the phase contrast. The slides can be stored at −20 °C until the next step.

3.6 FISH

3.6.1 Slide Pretreatment

1. Add 100 μL of pepsin working solution (10 μg/mL)/slide and cover with a cover slide.
2. Place the slide in a moist box for 30 min at 37 °C.
3. Wash the slide 3× with 2× SSC buffer, 5 min each time.
4. Add 100 μL of 4% paraformaldehyde/slide, cover with a cover slide, and leave for 10 min at RT (in the fume hood).
5. Wash the slide 3× with 2× SSC buffer, 5 min each time.
6. Immerse the slide in 70%, 90%, and 100% ethanol, 3 min each time.
7. Dry the slide at RT (for at least 1 h).

3.6.2 Chromosome Denaturation

1. Add 100 μL of 70% formamide/slide and cover with a cover slide.
2. Place the slide directly in contact with the hot plate surface for 2 min and 30 s at 70 °C.
3. Remove the cover slide by shaking the slide vertically and immerse the slide immediately in 70% ethanol (pre-cooled at −20 °C) for 5 min.
4. Immerse the slide in 90% ethanol (pre-cooled at −20 °C) for 5 min.
5. Immerse the slide in 100% ethanol (pre-cooled at −20 °C) for 5 min.
6. Dry the slide at RT until the ethanol completely evaporates.

3.6.3 Probe Hybridization

1. Prepare the hybridization mix: Mix 10 μL of 100% deionized formamide, 2 μL of 20× SSC, and 4 μL of 50% dextran sulfate. Vortex for 10 s and spin down for 10 s.
2. Prepare the probe master mix: Add 400 ng of digoxigenin-labeled ssDNA probe and 400 ng of biotin-labeled DNA probe to the hybridization mix (*see* **Note 8**).
3. Add the probe master mix in the slide. Cover with a cover slide and seal with a rubber cement.

4. Place the slide in the hot plate on the top of an iron sheet for 3 min at 70 °C (*see* **Note 9**).
5. Place the slide in a moist box for 24–48 h at 37 °C.

3.6.4 Stringency Washes

1. Peel the rubber cement of the slide away, without moving the cover slide.
2. Place the slide in 2× SSC buffer and gently shake until the cover slide falls off.
3. Wash the slide 1× with 2× SSC buffer for 5 min at RT (shaking).
4. Wash the slide 1× with 2× SSC buffer for 10 min at 42 °C (shaking).
5. Wash the slide 1× with 1× PBS buffer for 5 min at RT (shaking).

3.6.5 Optional Higher Stringency Washes

1. Wash the slide 2× with 2× SSC buffer at 42 °C, 5 min each time.
2. Wash the slide 2× with 0.1× SSC buffer at 42 °C, 5 min each time.
3. Wash the slide 2× with 2× SSC buffer at 42 °C, 5 min each time.
4. Wash the slide 1× with 2× SSC buffer for 10 min at RT.

3.6.6 Probe Detection

Always protect fluorophores from light.

1. Prepare the antibody mix: Mix 1.5 μL of anti-digoxigenin-rhodamine (200 μg/mL) and 1.5 μL of anti-biotin-fluorescein (1 μg/mL) in 97 μL of 1× TNB buffer.
2. Drain (never dry) the slide on a paper towel. Add 100 μL of the antibody mix and cover with a cover slide.
3. Place the slide in a moist box for 1 h at 37 °C.
4. Remove the cover slide by shaking the slide vertically.
5. Wash the slide 3× with 1× PBS buffer, 5 min each time.
6. Dry the slide at RT.
7. Mount the slide in VectaShield medium with DAPI.
8. Store the slide at 4 °C until fluorescence microscopy analysis.

3.6.7 Slide Cleaning for Re-probing

1. Wash the slide 3× with 4× SSC buffer at RT, 10 min each time.
2. Wash the slide 2× with 2× SSC buffer at RT, 5 min each time.
3. Wash the slide 1× with 70% ethanol for 5 min.
4. Wash the slide 1× with 100% ethanol for 5 min.
5. Return to "Chromosome Denaturation" step.

4 Notes

1. Each labeled universal primer will be used in one reverse transcription reaction for the oligo library labeling procedure. These primers can be synthesized from commercial oligo companies such as IDT-DNA, Operon, and TriLink Biotechnologies. The companies offer a large variety of oligo modifications, such as a fluorophore conjugate nucleotide, as Cy, Alexa Fluor, and ATTO dyes (for direct labeling). We use biotin and digoxigenin nucleotide-conjugated haptens (for indirect labeling).
2. The expected yield of the MYcroarray Debubbling PCR reaction is 2–4 μg. We use 480 ng in the in vitro transcription step.
3. The expected amount of RNA product is >80 μg. At least 42 μg of RNA is necessary for the reverse transcription procedure. If the reverse transcription will be performed within 1–2 h, leave the RNA on ice.
4. The final volume of the reverse transcription product is 82 μL. The quantification is not required in this step.
5. The expected final concentration of the ssDNA probe is >150 ng/μL.
6. The treatment of the root tips with nitrous oxide is essential to provide a desired chromosome condensation. The time of this treatment varies according to the species. For example, in potato it takes about 20 min and for maize it takes about 2 h.
7. The time for meristem digestion depends on the diameter and age of the tissue and it is species related. But generally, for example, we digest the potato and maize root tips for 1 h and 2–3 h, respectively.
8. The final volume of the probe master mix is 20 μL.
9. At this time, the slide is placed on the top of iron sheet and do not directly touch the hot plate surface.

Acknowledgments

This work was supported by National Science Foundation (NSF) grants MCB-1412948 and IOS-1444514 to J.J.

References

1. Jiang JM, Gill BS (2006) Current status and the future of fluorescence in situ hybridization (FISH) in plant genome research. Genome 49:1057–1068
2. McClintock B (1929) Chromosome morphology in *Zea mays*. Science 69:629
3. Jiang JM, Gill BS, Wang GL et al (1995) Metaphase and interphase fluorescence in situ hybridization mapping of the rice genome with bacterial artificial chromosomes. Proc Natl Acad Sci U S A 92(10):4487–4491

4. Lysak MA, Fransz PF, Ali HBM et al (2001) Chromosome painting in *Arabidopsis thaliana*. Plant J 28:689–697
5. Mukai Y, Yumiko N, Maki Y (1993) Simultaneous discrimination of the three genomes in hexaploid wheat by multicolor fluorescence in situ hybridization using total genomic and highly repeated DNA probes. Genome 36:489–494
6. Kato A, Lamb JC, Birchler JA (2004) Chromosome painting using repetitive DNA sequences as probes for somatic chromosome identification in maize. Proc Natl Acad Sci U S A 101:13554–13559
7. Lamb JC, Danilova T, Bauer MJ et al (2007) Single-gene detection and karyotyping using small-target fluorescence in situ hybridization on maize somatic chromosomes. Genetics 175:1047–1058
8. Danilova TV, Friebe B, Gill BS (2012) Single-copy gene fluorescence in situ hybridization and genome analysis: Acc-2 loci mark evolutionary chromosomal rearrangements in wheat. Chromosoma 121(6):597–611
9. Beliveau BJ, Joyce EF, Apostolopoulos N et al (2012) Versatile design and synthesis platform for visualizing genomes with oligopaint FISH probes. Proc Natl Acad Sci U S A 109:21301–21306
10. Han YH, Zhang T, Thammapichai P et al (2015) Chromosome-specific painting in Cucumis species using bulked oligonucleotides. Genetics 200:771–779
11. Jiang JM (2019) Fluorescence in situ hybridization in plants: recent developments and future applications. Chromosome Res 27. https://doi.org/10.1007/s10577-019-09607-z
12. Braz GT, He L, Zhao H et al (2018) Comparative Oligo-FISH mapping: an efficient and powerful methodology to reveal karyotypic and chromosomal evolution. Genetics 208:513–523
13. He L, Braz GT, Torres GA et al (2018) Chromosome painting in meiosis reveals pairing of specific chromosomes in polyploid Solanum species. Chromosoma 127:505–513
14. Qu MM, Li K, Han Y et al (2017) Integrated karyotyping of woodland strawberry (*Fragaria vesca*) with oligopaint FISH probes. Cytogenet Genome Res 153:158–164
15. Hou LL, Xu M, Zhang T et al (2018) Chromosome painting and its applications in cultivated and wild rice. BMC Plant Biol 18:110
16. Meng Z, Zhang Z, Yan T et al (2018) Comprehensively characterizing the cytological features of *Saccharum spontaneum* by the development of a complete set of chromosome-specific oligo probes. Front Plant Sci 9:1624
17. Albert PS, Zhang T, Semrau K et al (2019) Whole-chromosome paints in maize reveal rearrangements, nuclear domains, and chromosomal relationships. Proc Natl Acad Sci U S A 116:1679–1685
18. Murgha YE, Rouillard J-M, Gulari E (2014) Methods for the preparation of large quantities of complex single-stranded oligonucleotide libraries. PLoS One 9:e94752
19. De Carvalho CR, Saraiva LS (1993) An Air Drying Technique for Maize Chromosomes without Enzymatic Maceration. Biotech Histochem 68:142–145
20. Schubert I, Fransz PF, Fuchs J, de Jong JH (2001) Chromosome painting in plants. Methods Cell Sci 23:57–69
21. Ross KJ, Fransz P, Jones GH (1996) A light microscopic atlas of meiosis in Arabidopsis thaliana. Chromosom Res 4:507–516